

Development of Injectable Anhydrous Hydrogels for the Controlled Release of Therapeutic Proteins

Dissertation to obtain the Degree of Doctor of Natural Sciences

(Dr. rer. nat.)

From the Faculty of Chemistry and Pharmacy

University of Regensburg



Presented by

Christian Ziegler

March 2022

Christian Ziegler

**Development of Injectable Anhydrous Hydrogels for the
Controlled Release of Therapeutic Proteins**

Development of Injectable Anhydrous Hydrogels for the Controlled Release of Therapeutic Proteins

Dissertation to obtain the Degree of Doctor of Natural Sciences

(Dr. rer. nat.)

From the Faculty of Chemistry and Pharmacy

University of Regensburg



Presented by

Christian Ziegler

from Sulzbach-Rosenberg

March 2022

This work was carried out from May 2017 until June 2021 at the Department of Pharmaceutical Technology of the University of Regensburg.

The thesis was prepared under supervision of Prof. Dr. Achim Göpferich.

Doctoral application submitted on: 11.03.2022

Date of examination: 05.05.2022

Examination board:

Prof. Dr. Sigurd Elz (Chairman)

Prof. Dr. Achim Göpferich (1st Expert)

Prof. Dr. Miriam Breunig (2nd Expert)

Prof. Dr. Rainer Müller (3rd Examiner)

To my family

*If you thought that science was certain –
well, that is just an error on your part.*

Richard Feynman

Table of contents

Chapter 1	Introduction Challenges of covalently cross-linked hydrogels and how to overcome them	9
Chapter 2	Goals of the thesis	65
Chapter 3	A novel anhydrous preparation of PEG hydrogels enables high drug loading with biologics for controlled release applications	71
Chapter 4	In situ forming iEDDA hydrogels with tunable gelation time release high molecular weight proteins in a controlled manner over an extended time.....	101
Chapter 5	Investigation of the impact of hydrolytically cleavable groups on the stability of PEG-based iEDDA hydrogels	145
Chapter 6	Injectable anhydrous PEG polymer liquids form protein depot for extended controlled release applications via rapid in situ gelation	187
Chapter 7	Summary and conclusion	217
Appendix	Abbreviations	227
	Symbols.....	231
	Curriculum Vitae.....	233
	List of publications.....	235
	Acknowledgements	237
	Declaration in lieu of an oath	239

Chapter 1

Challenges of covalently cross-linked hydrogels and how to overcome them

Abstract

Hardly any other biomedical material is as versatile as hydrogels. In addition to everyday applications such as in personal hygiene or visual support, hydrogels are used for wound dressings, as biosensors, or in tissue engineering and drug delivery. While their adaptability shown by the huge number of various compositions is a major factor that has contributed to their success, it complicates the selection of the appropriate type of hydrogel for a given application. In this review, we will present the key aspects of the usage of hydrogels, their limitations and how to overcome them. The main focus will lie on covalently cross-linked hydrogels, and a discussion of tuning their properties, such as gelation time, mechanical strength, biodegradation, functional group stability, off-target interaction, and release. Furthermore, more general points such as toxicity, synthesis, and sterilization will be briefly addressed. This review is intended to introduce the reader to covalently cross-linked hydrogels and provide decision support for the particular challenges of their application.

1 Introduction

Over the last few decades, hydrogels have played an important role in the field of biomedical research due to a wide range of application options. Besides classical utilization such as personal hygiene [1] or contact lenses [2], hydrogels have been established as versatile medical materials for tissue engineering [3], drug delivery [4], cell carriers [5], wound dressing [6], biosensors [7], and tissue-adhesive glue [8]. The reason why they represent such an attractive material is evident from their definition. Hydrogels are three-dimensional polymeric matrices, which are able to absorb water up to hundreds of times their initial weight [9,10]. Thereby, the network facilitates the creation of various desired shapes with adjustable properties, and three-dimensionality enables the embedding of bioactive molecules and cells [11]. The hydrogel backbone usually consists of macromolecules, which are divided into natural, semisynthetic, and synthetic polymers [12]. Prominent examples of naturally derived polymers for hydrogel preparation are alginate [13], cellulose [14], chitosan [15], hyaluronic acid [16], dextran [17], and starch [18]. Although natural polymers are usually non-toxic and biodegradable, they often show adverse variabilities in molecular weight and poor mechanical properties [19]. With synthetic alternatives, on the other side, more accurate prediction of the molecular weight is possible, leading to facilitated tailoring of mechanical properties [12]. Poly(ethylene glycol) (PEG) [20], poly(vinyl alcohol) (PVA) [21], poly(vinyl pyrrolidone) (PVP) [22], and siloxane [23] are just a few of many synthetic polymers usable for hydrogel preparation. A third option, semisynthetic polymers, should also be mentioned in this context, which are attained from natural polymers by different chemical processes [19,24].

To create a hydrogel, the individual macromonomers have to interact with each other, either physically or chemically. Physical interactions include molecular entanglements, ionic interactions, hydrogen bonds, hydrophobic interactions, or complexation [12,17]. Triggers for gelation are changes in temperature, pH value, ionic strength, or the addition of excipients [11]. On the other hand, chemical cross-linking is the generation of covalent bonds between complementary groups, which is the subject of this review. Chemically cross-linked hydrogels are usually characterized by higher stability and more beneficial mechanical properties than physically cross-linked hydrogels [25]. Furthermore, they demonstrate flexibility regarding gelation time, pore size, and degradation [25]. To enable chemical cross-linking, the polymeric macromonomers need to be modified with complementary functional groups. Cross-linking reactions, commonly used, can be taken from Table 1. Usually, cross-linking and, therefore, the hydrogel preparation takes place in water. This is beneficial as the high water content of the polymeric structure mimics the extracellular matrix of tissues and provides a three-dimensional microenvironment for bioactive substances such as cells [26,27].

While hydrogels, in general, have been subject of research for decades, certain limitations still need to be taken into account for biomedical applications [28,29]. For example, gelation time, stability of

functional polymeric groups, and off-target interactions between polymers and bioactive molecules influence the preparation as they can lead to changes in viscosity and complicate injection of hydrogels. If the hydrogel is used for drug delivery, the amount and nature of the drug to be released must be kept in mind because they are crucial for duration and loading capacity. Furthermore, stability and possible degradation of such systems determine the time span of drug administration. All these points, in turn, impact the release kinetics. In addition, features such as mechanical strength, toxicity, and sterility of the respective hydrogel are pivotal for a successful application in the living tissue.

In this review, we will provide an overview of aspects that need to be considered in the development of chemically cross-linked hydrogels to increase the chances of success for new systems, especially in the field of biomedical applications. We will highlight gelation time, hydrogel stability and mechanical strength, biodegradation, functional group stability, off-target interactions, loading capacity, and release kinetics. Moreover, general limitations in toxicity, syntheses, and sterilization will be reviewed. For each hurdle, ways for overcoming are presented, which should facilitate hydrogel preparation.

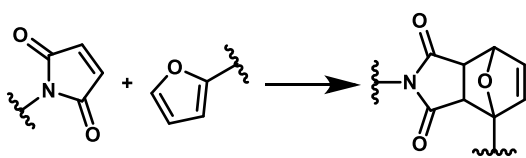
2 Gelation time

2.1 *In situ* gelation

One of the most important features of hydrogels is their gelation time. A common method that allows comparison of the time of hydrogel formation for different systems is to determine the time at which the storage modulus (G'), representative of the elastic properties of the material, intersects the loss modulus (G''), representative of the viscous properties. This time coincides with the gel point (t_{gel}) and indicates the transition from a liquid-like to a solid-like behavior [30,31].

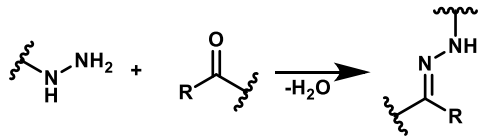
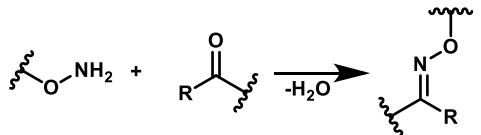
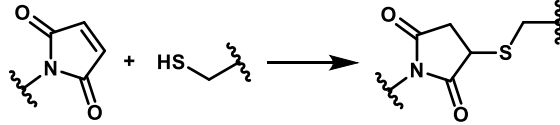
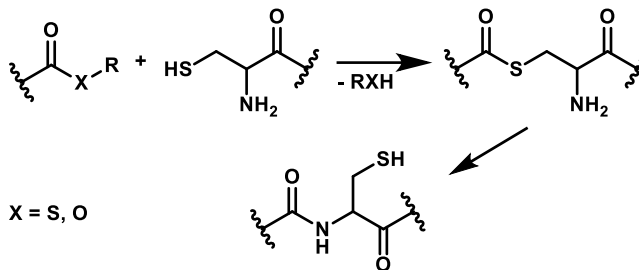
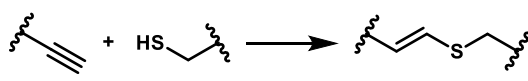
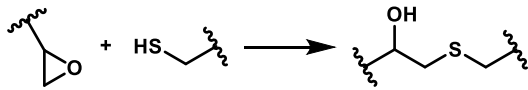
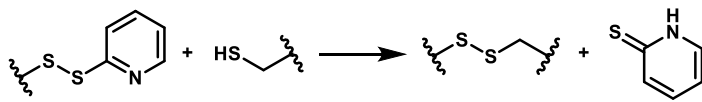
However, it should be noted that this t_{gel} is only an approximation and the true t_{gel} is described by the Winter-Chambon criterion, at which scale of G' and G'' are identical with frequency ($G' \sim G'' \sim \omega^A$) [32]. Nevertheless, t_{gel} at the cross-over of G' and G'' is close to the true t_{gel} and simplifies the characterization of gelation kinetics. Therefore, it is commonly used as t_{gel} for hydrogel characterization.

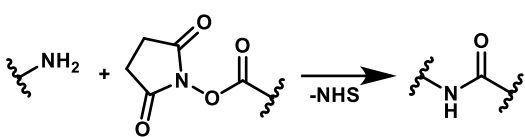
Table 1: Examples of cross-linking reactions used for hydrogel preparation.

Cross-linking reaction with mechanism example	Benefits & Limitations	Refs
Diels-Alder cycloaddition 	<ul style="list-style-type: none">+ Biodegradability- Slow gelation- Off-target reactions	[33–42]

Genipin coupling		+ Easy synthesis access [43–45]
		<ul style="list-style-type: none"> - Slow gelation - Off-target reactions
Cu(I)-free Huisgen cycloaddition		+ Bioorthogonality [46]
		- Slow gelation
Cu(I)-catalyzed azide-alkyne cycloaddition		+ <i>In situ</i> gelation [47–52]
		+ Bioorthogonality
		- Toxic catalyst
Strain-promoted azide-alkyne cycloaddition		+ <i>In situ</i> gelation [53–58]
		+ Bioorthogonality
		<ul style="list-style-type: none"> - Laborious cyclooctyne syntheses
Nitrile oxide-norbornene cycloaddition		+ <i>In situ</i> gelation [59,60]
		+ Bioorthogonality
		<ul style="list-style-type: none"> - Low nitrile oxide stability
inverse electron Diels-Alder cycloaddition		+ <i>In situ</i> gelation [61–65]
		+ Bioorthogonality
		- Nitrogen formation
Imine formation		+ Biodegradability [66–71]
		+ <i>In situ</i> gelation
		- Off-target reactions

Chapter 1: Challenges of covalently cross-linked hydrogels

Hydrazone formation		<ul style="list-style-type: none"> + Biodegradability [72–74] + <i>In situ</i> gelation - Off-target reactions
Oxime formation		<ul style="list-style-type: none"> + Biodegradability [75,76] - Off-target reactions - Slow gelation
Michael-type addition		<ul style="list-style-type: none"> + <i>In situ</i> gelation [77–90] - Off-target reactions - Thiol oxidation
Native chemical ligation	 <p>X = S, O</p>	<ul style="list-style-type: none"> + <i>In situ</i> gelation for oxo-ester mediated variation [91–93] - Side-products - Thiol oxidation
Thiol-yne click chemistry		<ul style="list-style-type: none"> + <i>In situ</i> gelation [94] - Off-target reactions - Thiol oxidation
Thiol-epoxy reaction		<ul style="list-style-type: none"> + <i>In situ</i> gelation [95] - Off-target reactions - Thiol oxidation
Disulfide exchange		<ul style="list-style-type: none"> + <i>In situ</i> gelation [96–98] + Biodegradability - Off-target reactions - Side-products - Thiol oxidation

Succinimidyl carbonate and amine	+ <i>In situ</i> gelation + Biodegradability	[99– 104]
	- Off-target reactions - Side-products	
Enzymes catalyzing cross-linking reactions:	Depending on respective enzyme. In general:	[105– 112]
<ul style="list-style-type: none"> - Tyrosinase - Horseradish peroxidase - Transglutaminase - Sortase A - Phosphopantetheinyl transferase - Lysyl oxidase 	+ <i>In situ</i> gelation + Bioorthogonality	
	- Reduced loading capacity - Stability of enzymes - Low mechanical properties	

The lower the time at which t_{gel} is reached, the faster the gelation takes place. This is particularly important for injection into the organism. The injected solution must form a network as quickly as possible to avoid material loss by diffusion into the surrounding tissue [113,114]. For chemically cross-linked hydrogels, the gelation time depends on the cross-linking reaction. A variety of chemical reactions have been suggested for *in situ* hydrogel preparation (Table 1). However, reactions such as Diels-Alder (DA) reaction between furan and maleimide, oxime bond formation, genipin coupling, and Cu(I)-free Huisgen cycloaddition are in general too slow for *in situ* gelation. For example, hydrogels cross-linked via a catalyst-free Huisgen cycloaddition between azide-functionalized polymers and dialkyne cross-linkers showed gel points of above 12 h [46]. In contrast, DA reaction led to faster gelation, but due to t_{gel} of 36 min for a hyaluronic acid-based system and 14 min for a PEG-based hydrogel, cross-linking still takes too much time [33,34]. Also for genipin coupling, low reaction kinetics ($t_{gel} > 18$ min) were reported [43,44].

However, in general acceleration of cross-linking reactions is possible by variation of temperature, pH value, and the numbers of functional groups. For example, increased number of functional groups is obtained by higher polymer concentration, higher degree of functionalization, or usage of smaller macromonomers. Kirchoff et al. showed that a decrease of the molecular weight of eight-armed PEG precursors from 20 to 10 kDa at a constant polymer concentration resulted in a higher number of functional groups and a decrease of t_{gel} from 34 to 14 min [34]. Moreover, increase of polymer concentration and functionalization degree further accelerated the gelation time [35].

Some cross-linking reaction rates depend on the pH value. For example, Boekhoven et al. showed that the formation of hydrazone bonds is preferred at lower pH values. Reaching t_{gel} after 275 min at pH 7, t_{gel} was reduced to below 8 min at pH 5 [72]. This behavior can also be seen for hydrogels formed via oxime bond formation. Acid catalyzes the oxime bond formation by aldehyde activation through

protonation and acceleration of the dehydration step [75,76]. Working at a pH in the range between 1.5–2.5 the gelation time of PEG-based hydrogels was not detectable due to very fast gelation, whereas at pH 7.4 the system reached t_{gel} only after 5 h [76].

Another way to increase the gelation kinetics is to exploit the temperature dependence of chemical reactions. Temperature increase from 37 to 50 °C almost halved t_{gel} from 13 to 7 h for genipin-cross-linked hydrogels [43]. Decrease in the gelation time was also reported for hydrogels cross-linked via DA reaction when heated above 37 °C [36].

At this point, however, it must be mentioned that these variations are not always practicable. Due to an increase in polymer concentration, cross-linking density of hydrogels increases, which in turn affects other properties such as mesh size, stability, or release kinetics. High temperatures or solutions with too acidic or basic pH are not eligible for *in vivo* use. Hence, switching to chemical reactions with higher reaction kinetics is often the simplest approach.

While photoinitiated cross-linking reactions can be used for the preparation of *in situ* forming hydrogels [113,115], only cross-linking reactions that do not need an external trigger are mentioned in this section. For this, several reactions have been suggested. A prominent example is the Cu(I)-catalyzed azide-alkyne cycloaddition (CuAAC) introduced in 2002 [116,117]. This Cu(I)-catalyzed cycloaddition of azides to alkynes to form 1,2,3-triazoles represents a regioselective version of the Huisgen cycloaddition. In 2006, Ossipov et al. were the first to develop a hydrogel cross-linked via CuAAC [47]. The reaction between alkyne- and azide-modified PVA was initialized by Cu(I) and the gelation was observed within 1 min. Since then, a high number of CuAAC-hydrogels were developed, showing fast gelation already at room temperature [48,49]. At 37 °C, even higher reaction rates can be achieved [50]. Besides temperature variations, changes in Cu(I)-concentrations impact the gelation time. For example, increasing the Cu(I) concentration from 5 to 10 mmol/l resulted in a decrease of t_{gel} from 1594 to 78 s for cellulose-based hydrogels [51]. However, usage of Cu(I) poses an obstacle as it is toxic towards tissues and cells already at low quantities [118,119].

To overcome this, the metal-free strain-promoted azide-alkyne cycloaddition (SPAAC) was introduced [120]. In this reaction, the triple bond of the alkyne is destabilized by ring strain, leading to a catalyst-free activation of the alkyne and fast reaction rates with azide groups [121]. Alkynes commonly used are 4-dibenzocyclooctynol, oxanorbornadiene, and cyclooctyne [122]. With SPAAC gelation times below 2 min are possible [53,54]. Furthermore, the reaction rate can be raised by substitution of alkynes with electron-withdrawing groups such as fluorine [53].

A further way to increase the reaction kinetics of the classical Huisgen 1,3-cycloaddition is the exchange of the azide group with nitrile oxide and the use of norbornene as complementary group for the nitrile oxide-norbornene cycloaddition [123]. For hydrogel formation, the unstable nitrile oxide can be generated *in situ* from a hydroximoyl chloride under physiological conditions (pH 7.4) [59]. Only then cross-linking with norbornene is possible. In this way, Truong et al. were able to develop a variety of PEG- and gelatin-based hydrogels, of which the fastest gelling formulation reached t_{gel} after 10 s [59,60].

Reversing the electron distribution between the two reactants of the classical DA reaction, which usually takes place between an electron-rich diene and an electron-poor dienophile, leads to the so-called inverse electron DA (iEDDA) reaction between an electron-poor diene and an electron-rich dienophile [124]. Tetrazine is commonly used as diene, whereas different counterparts are possible for the dienophile such as norbornene and *trans*-cyclooctene [125]. While t_{gel} was found to be within a range of 15 to 144 s for a multitude of hydrogels cross-linked via iEDDA reaction between tetrazine and norbornene [61,65], the reaction of tetrazine with *trans*-cyclooctene led to an even faster second-order rate and complete gel formation only after seconds [63,64].

A further cross-linking strategy for *in situ* forming hydrogels represents the Schiff base formation, which is obtained by the reaction of aldehyde or ketone groups with amines, hydrazides, or hydroxylamines. Thereby, imines, hydrazones, or oximes are formed [126]. As mentioned before, the formation of oxime bonds is too slow for a fast *in situ* gelation at physiological conditions. In contrast, Kageyama et al. achieved complete gelation below 3 min via hydrazone formation [73]. Similarly, injectable hydrogels were prepared with amine-functionalized chitosan and aldehyde-functionalized hyaluronic acid within 3 min [66,67].

The Michael-type addition, which is a 1,4-addition of nucleophiles to an α,β -unsaturated carbonyl compound, is a very prominent cross-linking reaction example for *in situ* forming hydrogels. In 2001, Elbert et al. introduced the reaction between multi-armed PEG-acrylates and PEG-dithiol for the preparation of *in situ* forming hydrogels [77]. Yet, the Michael-type addition is not limited to thiols; amines can also be used as donors. With the so-called aza-Michael-type addition, polyamidoamine dendrimer hydrogels were completely solidified within 1 to 2.5 min [78]. Additionally, acrylates can be replaced by maleimide and vinyl sulfone groups, leading both to gelation times with thiol-modified hydrogel precursors below 1 min [79,80].

Another approach for gelation is the native chemical ligation (NCL) between thiol groups of cysteine and thioesters, which was developed as chemo- and regioselective reaction for chemical ligation of peptides. The underlying mechanism includes two steps. First, the thiol group of cysteine reacts with a thioester to form a new thioester. Subsequently, this intermediate rearranges via an *S*-to-*N*-acyl migration with the amine group of the cysteine to an amide bond [91]. While hydrogels cross-linked via NCL take several hours to be completely formed, the exchange of the thioester with an oxo-ester dramatically accelerates the hydrogel formation and results in gelation times of less than 1 min [92].

Moreover, several other chemical reactions were successfully used for the preparation of *in situ* forming hydrogels and should be mentioned briefly. For example, thiol-yne click chemistry was introduced in a PEG-based system for the *in situ* gelation [94]. Under physiological conditions, the base-catalyzed reaction reached t_{gel} after 87 s. As a different thiol-mediated strategy for *in situ* gelation, the thiol-epoxy reaction was introduced by Gao et al. [95]. With epoxy-modified poly(*N,N*-dimethylacrylamide-co-glycidyl methacrylate) copolymers and thiol-modified poly[oligo(ethylene glycol)mercaptosuccinate], gelation times between 27 and 98 s were achieved. The disulfide exchange reaction represents a further

thiol-based cross-linking reaction for the preparation of *in situ* hydrogels. Navath et al., for example, succeeded to develop hydrogels that gelled within 30 s by mixing solutions containing thiopyridyl-terminated poly(amidoamine) dendrimers and thiol-modified eight-armed PEGs [98]. Furthermore, a well-known cross-linking reaction for hydrogel formation represents the reaction between *N*-hydroxysuccinimide (NHS)-activated esters and amines to form a carbamate linkage [100]. While this reaction was developed for the modification of peptides, it can also be used for cross-linking of hydrogels. As an example, Buwalda et al. developed PEG-poly(amidoamine) hydrogels cross-linked via this reaction with very fast gelation kinetics allowing the use as *in situ* forming material [101].

Enzymatic reactions represent a special, biological method for *in situ* gelation. Thereby, the formation of covalent bonds between different functionalized hydrogel precursors is catalyzed by a variety of enzymes. The advantage of this cross-linking strategy is that usually mild reaction conditions are required such as neutral pH, aqueous milieu, and mild temperature, making this approach promising for cell- and protein-based applications [127]. Enzymes that were successfully established for rapid gelation of hydrogels are tyrosinase [106], horseradish peroxidase [107], transglutaminase [109], and sortase A [110] to name only a few.

As last point, the opportunity of dual gelation should be mentioned. This method is a combination of various cross-linking mechanisms. In addition to the combination of physical and chemical cross-linking such as thermo- or pH-dependent gelation accompanied by covalent cross-linking [40,128], the simultaneous use of two chemical reactions to form an interpenetrating polymer network (IPN) was successfully introduced to decrease the gelation time [129].

2.1 Tuning of gelation time

In the previous section, the possibilities to achieve fast gelation kinetics were shown. In this part, tuning of the gelation time for *in situ* gelling systems is the subject of the discussion. As already mentioned, t_{gel} is the decisive criterion for evaluating the gelation time. However, this point also reflects a certain threshold. Once a system has reached its t_{gel} , it should no longer be subjected to shear forces that could damage the network already formed. Otherwise, inhomogeneous areas could form and change the three-dimensional integrity, impacting mechanical properties and release kinetics [81]. To avoid this for *in situ* gelling systems, fast mixing and injection are required, which complicates the administration process. In addition, too high reaction kinetics could cause clogging the needle due to the premature hydrogel formation during injection, resulting in incomplete administration [113,114]. Therefore, it is desirable to tune the gelation kinetics depending on the respective application.

One method to slow the reaction kinetics is to lower the number of functional groups present at the hydrogel precursors. In this way, the likelihood for one group to find its counterpart is reduced, so the system needs more time for sufficient hydrogel formation. Besides decreasing polymer concentration, increasing molecular weight or reducing the modification degree of the used hydrogel precursors are

possible approaches for a reduced number of functional groups and, therefore, an extended gelation time [130]. However, all these changes have in common that they lead to a lower cross-linking density that influences mechanical strength, stability, and, in the case of drug delivery systems, release kinetics. Therefore, different ways for tuning the gelation time are required.

Since covalent hydrogel bonds are created by chemical reactions that usually depend on temperature, hydrogel preparation at lower temperatures seems to be a promising approach. For example, Famili et al. showed that the gelation time of a hyaluronic acid-based system cross-linked via the iEDDA reaction between norbornene and tetrazine increased from 0.3 min at 37 °C to 3.1 min at 20 °C [131]. A further temperature decrease caused an even longer gelation time. Therefore, sufficient time should be available to mix and inject the hydrogel liquid at 20 °C. After injection, the reaction rate is accelerated due to the heat transfer from the surrounding tissue, leading to an increase in the reaction rate and a rapid hydrogel formation at the operating site. Besides hydrogels cross-linked via iEDDA reaction, lower temperatures were also exploited for systems using other cross-linking reactions [50,77]. Nevertheless, this tuning method is limited since the occurrence of pain at the injection site due to low temperatures affects patient compliance.

A more promising approach that does not require changes in number of functional groups or temperature is chemical modification of the functional groups. Usually, chemical modifications are used to accelerate reaction kinetics for faster gelation but the exact opposite, slowing the reaction rate, is also possible in this way. The underlying mechanism is the frontier molecular orbital theory. The reactivity and, hence, the reaction time can be approximated by the gap size of the highest occupied molecular orbital (HOMO) of one reaction partner and the lowest unoccupied molecular orbital (LUMO) of the complementary partner. Reducing the HOMO-LUMO energy gap increases the reaction kinetics, whereas a larger gap causes slower reaction rates. For example, smaller HOMO-LUMO energy gaps and, therefore, faster reaction rates are achieved via methyl substitution of furan for the DA reaction and substitution of electron-withdrawing groups (EWG) on the dipolarophile for the 1,3-Huisgen cycloaddition [46,132,133]. However, the underlying principle can also be used to slow down the reaction rate. For the iEDDA reaction, electron-donating substituents on the tetrazine ring raise the LUMO, and incorporation of EWGs lowers the HOMO of the dienophile. Previously, we showed that methyl substitution of tetrazine and oxygen incorporation in norbornene led both to a tenfold longer gelation time of eight-armed PEG-based hydrogels cross-linked via the iEDDA reaction [65]. T_{gel} was reached after 31 s for an unmodified hydrogel system, whereas usage of methyl-tetrazine or 7-oxanorbornene increased t_{gel} significantly to approximately 300 s.

Bi et al. showed that the gelation time of hydrogels cross-linked via Michael-type addition is dramatically affected by the electron density of the alkenyl groups [80]. The higher alkene electron density, the slower the cross-linking rate. Vinyl sulfone groups with a higher electron density were found to gel slower (gelation after 30 s) than maleimide groups (gelation after 8 s), facilitating the hydrogel handling.

Similar to the Michael-type addition, a higher electron density and, thus, a higher LUMO of the alkyne moiety results in slower reaction kinetics for the SPAAC [134]. Additional to the electron density, ring-strain stability of the cyclooctynes influences the reaction rate as mentioned above. The large number of alkynes, which show different reactivity [121], allows the SPAAC to meet the most diverse requirements.

A side effect of the functional group substitution is the steric hindrance of the cross-linking reaction. In general, the longer or more bulky the substitution group, the more the reaction is interfered and the higher is the distortion energy, which leads to a decrease in the reaction rate [135].

In the case of enzymatically cross-linked hydrogels, labor-intensive functional group modifications can be avoided. Here, it is sufficient to add less enzymes to reduce the reaction rate [106,107,111,136]. For example, gelation via a strain-promoted oxidation-controlled cyclooctyne-1,2-quinone cycloaddition (SPOQC) could be tuned by the concentration of mushroom tyrosinase [105]. With an enzyme concentration of 2000 units/ml mushroom tyrosinase, gel formation was achieved already after approximately 1 min, whereas 100 units/ml increased the time of gel formation to 20 min.

3 Mechanical properties

Due to their high water content, hydrogels often show reduced mechanical properties. Therefore, even low forces can affect their integrity and nature, resulting in unusable materials. This represents a significant disadvantage for various applications. In the field of drug delivery, for example, accelerated release and even dose dumping can occur when the hydrogel matrix is damaged. For tissue engineering, hydrogels should have similar high mechanical properties as the surrounding tissues [137]. Additionally, low mechanical strength complicates the characterization of these hydrogels. Hence, mechanical properties are decisive criteria for the production and use of hydrogels.

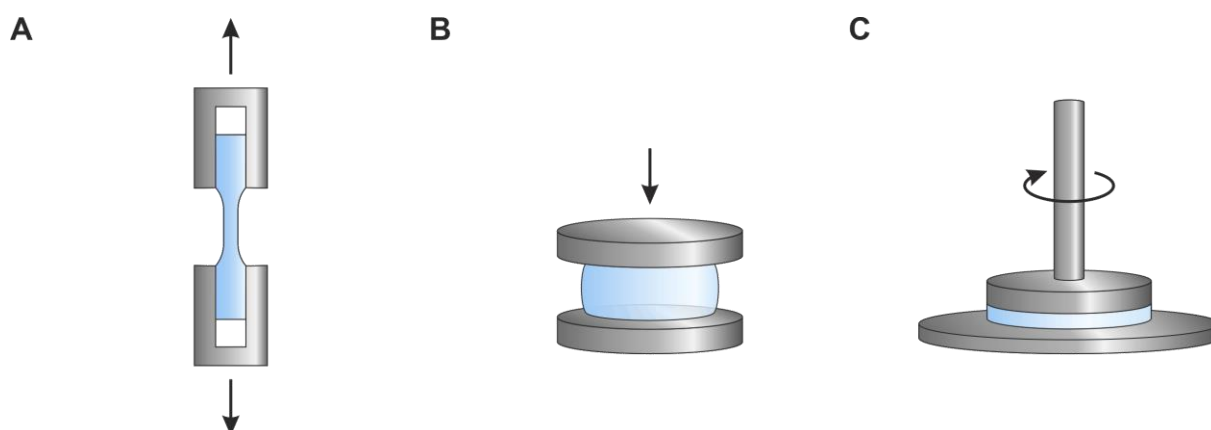


Figure 1: Common test methods to examine the mechanical properties of hydrogels. Tensile (A) and compressive testing (B) for determination of the tensile and the compressive modulus and oscillatory rheology (C) for measurements of the complex shear modulus.

To examine mechanical properties, various mechanical test methods have been suggested, including tensile and compression testing, local indentation, and frequency-based tests such as shear rheometry or dynamic mechanical analysis [138]. In this review, we will focus on tensile and compression testing as well as oscillatory shear experiments since they represent the standard test methods (Figure 1).

Tensile and compression testing are performed in opposite directions. For tensile testing, dog bone-shaped samples are stretched [139]. By the ratio of tensile strain to tensile stress, Young's modulus (tensile modulus) is obtained. On the other hand, the ratio of compressive strain to compressive stress determined by uniaxial compression of the sample is used to calculate Young's modulus of compression (compressive modulus) [139]. Tensile and compressive moduli indicate both the stiffness of a hydrogel and can be taken as the resistance of an elastic body against the deflection of an applied force [139]. Furthermore, tensile or compressive strength are defined as the maximal tensile or compressive stress that a material is able to withstand [138].

To investigate the viscoelastic behavior of hydrogels, oscillatory shear experiments are performed. Thereby, the viscous ("liquid-like") and elastic ("solid-like") parts of the polymeric material are measured [140]. After applying shear stress (σ^*) or shear strain (γ^*), the complex shear modulus (G^*) can be measured as a function of various parameters such as time, temperature, or frequency according to equation (1):

$$G^* = G' + iG'' = \frac{\sigma^*}{\gamma^*} \quad (1)$$

The storage modulus (G') is the real part of G^* , whereas the loss modulus (G'') is the imaginary part [141,142]. G' indicates the energy of the hydrogel that restores after applying a force. On the contrary, G'' represents the energy loss due to viscous flow [143]. By measuring G^* , the course of a system's stiffness and strength during cross-linking can be determined. When hydrogel polymerization is considered complete, the absolute value of G^* ($|G^*|$) shows the final strength and stiffness of the system. Often only G' is reported to assess stiffness. The reason for this is that with advanced polymerization G^* is mainly described by G' , which exceeds G'' by several decades for hydrogels with high stiffness. To enhance the chances for biomedical use, it is advantageous if the mechanical properties of a hydrogel can be adapted to the respective task. Thereby, tensile and compressive modulus as well as the complex shear modulus can be controlled via cross-linking density and polymer chain length [27]. This can be explained by the number of elastically active chains, which is related to the moduli in the classical theory of rubber elasticity [34,144]. The more elastically active chains are present in the system, the higher the mechanical stiffness and strength of the hydrogel. One way to obtain a higher cross-linking density is to increase the polymer concentration, leading to more available functional groups and a higher likelihood of forming cross-links. This was shown for a variety of systems for the tensile and the compressive

modulus [38,65,73,145,146] as well as for the complex shear modulus [34,65,68,82,95]. Another option to change the number of elastically active chains is a shift of the molecular mass between cross-links, which is achieved by varying the chain length of the polymer backbone between the cross-links. For example, by using PEG macromonomers with lower molecular weight at a constant polymer concentration, mechanical properties are increased [146,147]. Higher functionalization degree of the macromonomers used also resulted in smaller polymeric chain length between the cross-links and, therefore, improved mechanical strength [35,54,148].

A special way to tune the chain length between the cross-links are redox-responsive protein-based hydrogels, as described by Kong et al. [144]. Due to an engineered disulfide bond, the used protein can switch its conformation between folded and unfolded, leading to different chain lengths and, hence, differences in mechanical strength. For the folded conformation caused by the oxidizing condition, the chain length between the cross-links decreased and the tensile modulus was found to be 40 kPa. Under the reducing condition, the protein unfolded, resulting in an increase of the chain length and a lower tensile modulus of 10 kPa.

Further hydrogels with mechanical properties responsive to external stimuli like temperature, light, pH, or ions have been developed [149–151]. However, changes in physiological temperature or pH represent an obstacle for the *in vivo* use [152]. Moreover, external stimuli, in general, complicate the use of such systems as they require additional treatment.

A promising approach to obtain stiff hydrogels that can be formed *in situ* are IPNs. Those systems are formed by two or more networks that are interlaced but not covalently connected [153]. In this way, hydrogels with low mechanical properties can be combined to increase stiffness and strength. IPNs are generated by simultaneous cross-linking strategies that do not interact with each other. For example, via orthogonal proceeding iEDDA reaction and thiol-yne click chemistry the formation of a double network consisting of a loose and a dense network was possible [129]. Thereby, the tensile and the compressive modulus were increased approximately fivefold from 2.49 MPa and 44 kPa to 15.56 MPa and 220 kPa for the IPN compared to the single dense network cross-linked singularly via thiol-yne click chemistry. Semi-interpenetrating polymer networks (SIPNs) have to be distinguished from IPNs since per definition linear or branched macromolecules can be separated from the consisting polymer network without breaking chemical bonds [153]. SIPNs can be prepared by the simple addition of a second polymeric material. In this manner, cellulose nanocrystals or unfunctionalized hyaluronic acid-enhanced mechanical strength of physically and chemically cross-linked hydrogels significantly [71,154].

A similar approach to improve the mechanical performance is the incorporation of particles into hydrogels. In 2002, Haraguchi and Takehisa developed the first so-called nanocomposite hydrogel composed of water-swelling inorganic clay and specific polymers [155]. Due to the nanoscale of the clay particles, an increased interface for the interaction between polymer and particles is created [137]. By tuning this interaction, mechanical properties can be adjusted to the various requirements [156]. Based on this principle, nanocomposite hydrogels with very high mechanical strength can be formed by

using graphene oxide nanosheets [157]. For example, the compressive moduli of poly(acrylic acid)/gelatin composite hydrogels were found to be in the range of 6 to 16 MPa as a function of the amount of graphene oxide.

At the end of this section, it has to be mentioned that for the preparation of hydrogels with well-defined network architecture and tunable mechanical properties, synthetic polymers are preferred [12]. Natural polymers, on the other hand, often show variabilities in molecular weight and reduced mechanical strength, complicating tuning of mechanical properties.

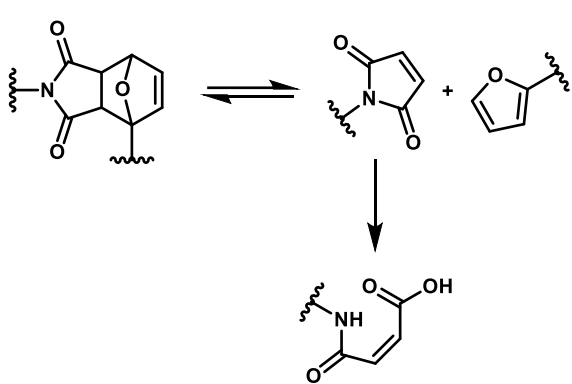
4 Degradation

Mechanical properties of hydrogels are the essential criterion for sufficient stability of hydrogels during application. Adversely, degradation limits the timeframe, in which the hydrogel can be used. Thereby, it is desirable if the material does not have to be surgically explanted at the end of therapy, which detrimentally affects patient compliance and causes further personnel costs. Instead, degradation and erosion without remaining matrix residues would be beneficial. Here, it should be noted that degradation refers to the actual bond cleavage reaction, whereas erosion designates the loss of mass from the polymer matrix [158]. In this section, we will elucidate how biodegradation and erosion can be achieved for chemically cross-linked hydrogels.

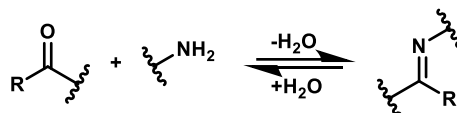
4.1 Cross-links

Erosion of chemically cross-linked hydrogels requires a target for various chemical degradation processes in the polymer matrix. Two common possibilities can be mentioned here. For the first degradation pathway, the cross-links are regarded as the vulnerable point (Table 2).

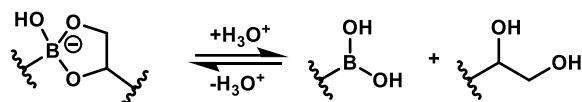
Table 2: Examples of reversible cross-linking reactions used for preparation of biodegradable hydrogels.

Reversible cross-linking reaction	Possible degradation mechanism
DA reaction	

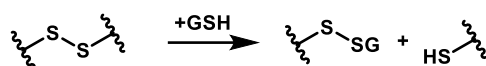
Schiff base formation



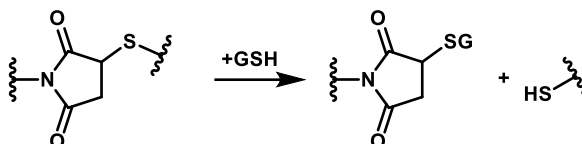
Borate ester formation



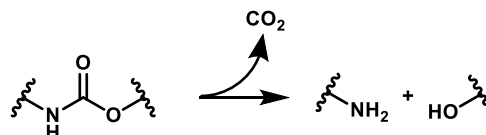
Disulfide exchange



Michael-type addition



Carbamate formation



Chemical reactions with a kinetically reversible nature can be used to make the cross-links cleavable [159]. The reaction must therefore exhibit dynamic covalent chemistry. After polymerization, the initially free complementary functional groups of the macromonomers have reacted, shifting the dynamic reaction equilibrium to the side of the product. However, some groups remain free and unreacted in the hydrogel network. In addition, the dynamic equilibrium causes the cross-linking reaction to proceed in the opposite direction on a small scale, increasing the number of free functional groups. This allows macromonomers that are no longer linked to the hydrogel network to diffuse out of the hydrogel matrix into the surrounding tissue, continuously removing functional groups from the equilibrium [84]. In this way, based on Le Châtelier's principle, the reaction equilibrium shifts further to the educt side. Additionally released macromonomers accelerate this process, and the hydrogel erosion increases until it finally dissolves completely.

The DA reaction between furan and maleimide and its counterpart the retro-Diels-Alder (rDA) reaction are connected via dynamic equilibrium [160]. The possibility of degradation of hydrogels cross-linked via DA reaction was initially described for physiologically irrelevant areas [161]. For example, rDA reaction was assumed to occur significantly only at temperatures above 37 °C [84]. To achieve rDA reaction at lower temperatures, the solvent had to be changed to *N,N*-dimethylformamide, which represents an obstacle for *in vivo* use. However, hydrogels prepared from multi-armed PEGs

functionalized with furan and maleimide were described by our group to dissolve under physiological conditions after 1 to 63 days depending on polymer concentration, branching factor, and molecular weight [34]. The underlying mechanism was found to be the hydrolysis of free maleimide groups, which leads via ring-opening to unreactive maleamic acid [39]. These groups were thus irreversibly removed from the reaction equilibrium, making the hydrogel biodegradable. Since then, various biodegradable systems have been prepared via DA reaction [35,37,38,40]. As a benefit, the stability of DA hydrogels could be controlled by the number of elastically active chains. The more cross-links present in a system, the longer they take to be cleaved and the higher the stability of the hydrogels.

Beside the DA reaction, there are more cross-linking reactions known, showing dynamic covalent chemistry. Especially in the field of self-healing materials, these cross-linking reactions can be found. Here, it is important that the hydrogel network regenerates after it is disrupted to form covalent bonds again [162]. These self-healing materials are also usually biodegradable. A prominent example are hydrogels cross-linked via dynamic Schiff base reactions [162]. After the reaction of aldehyde or ketone groups with amines, hydrazides, or hydroxylamines, an equilibrium is established that can be shifted back toward the reactant side by removing individual macromonomers and functional groups, thereby generating a biodegradable polymer [69,70]. While Schiff base cleavage takes place faster at low pH [163], complete dissolution occurs also under physiological conditions [70].

A further cross-linking reaction that is used for self-healing hydrogels is the boronate ester formation [164,165]. Exploiting this chemistry, 50% of a hyaluronic acid-based hydrogel eroded within two weeks [166]. Increasing the polymer concentration led to more elastically active chains and, therefore, higher stability. In contrast, faster erosion was achieved via additional added H_2O_2 , causing C–B bond breakage and irreversible hydrogel damage.

Disulfide exchange is also a member of dynamic covalent cross-linking reactions. This reaction forms redox-responsive disulfide bonds, representing a target for hydrogel erosion. A method to synthesize hydrogel precursors for disulfide exchange reaction is to use thiopyridyl functionalization [96]. After contact to thiol-functionalized moieties, a hydrogel can be formed by the thiol-disulfide exchange reaction [126]. These disulfide bonds can dissociate in a reductive environment, making the hydrogel biodegradable [167]. For example, due to the presence of free thiol groups such as glutathione (GSH), which ubiquitously exists in the human organism, new disulfide bonds are created, and the hydrogel starts to erode [97].

Similar to the disulfide exchange formation, the succinimide thioether formed via a Michael-type reaction between maleimide and thiol moieties can be cleaved in a reducing environment [161]. The degradation mechanism includes a covalent bond exchange in the presence of additional thiol compounds under physiological conditions [83,168]. Succinimide thioethers were found to be broken by GSH as well. The rate of the degradation could be tuned by the Michael donor reactivity, e.g., higher reactive aromatic thiols degraded faster than aliphatic thiols [168]. However, controlled degradation requires an exact concentration of free thiol groups at the operation site to maintain uniform degradation

of both cross-links, disulfide, and thiol-maleimide adduct. This represents a drawback since this does not seem practicable *in vivo*.

In addition, some cross-links can be directly cleaved by water. These include the reaction of NHS-activated esters with amines to form carbamates [102]. These carbamates undergo hydrolysis, which is triggered by the presence of large water amounts. The underlying mechanism of the carbamate degradation is an E1cB elimination reaction during which an unstable isocyanate is formed [169,170]. This intermediate reacts with water to disintegrate into a primary amine and carbon dioxide, which accelerates degradation by its removal. The erosion time can be controlled by using different leaving groups. Thereby, resonance stabilized groups such as phenols speed up the degradation kinetics [169], whereas aliphatic alcohols lead to higher stability [99]. Considering the amine component, an increase of the steric hindrance leads to a decrease in the carbamate stability, while a higher pK_a value results in higher stability [171].

4.2 Hydrogel backbone

The second opportunity to design biodegradation into hydrogels offers the hydrogel backbone itself. This is achieved in a labor-saving manner by selecting polymers that are enzymatically cleavable. Dextran, chitin, chitosan, hyaluronic acid, collagen, fibrin, gelatin, keratin, or starch represent a multitude of natural polymers for the preparation of enzymatically degradable hydrogels [41,45,172–176]. Besides relying on endogenous enzymes at the operation site such as collagenase, hyaluronidase, or lysozyme, embedding of exogenous enzymes into the hydrogel matrix in advance is possible to achieve erosion [177]. In the case of assessment of endogenous enzyme decomposition, hydrogels are incubated in enzyme solutions for *in vitro* experiments to simulate physiological conditions.

In contrast, if enzyme-stable polymers are used for hydrogel preparation, peptide sequences sensitive to specific enzymes can be synthesized into the hydrogel backbone. As a benefit, thiol or amine groups of these peptides are possible reactants for cross-linking reactions such as Michael-type addition or carbamate formation. For example, Lutolf et al. incorporated peptide substrates for matrix metalloproteinase into four-armed PEG macromonomers [85]. The thiol groups of these peptide sequences cross-linked with vinyl sulfone-functionalized four-armed PEGs via a Michael-type addition to form hydrogels as matrices for *in situ* bone regeneration. Incubated in buffer, the hydrogels degraded after addition of matrix metalloproteinase.

Similarly, branched PEG was functionalized with a collagenase substrate [100]. Hydrogel formation was achieved between substrate amine group and PEG macromonomers bearing succinimidyl carbonate functionalities. Hydrogel incubation in phosphate buffer containing collagenase resulted in complete dissolution after 10 to 19 days.

However, the limitation of hydrogels cleavable via endogenous enzymes is their reproducible degradation, which depends on the amount of enzyme present. Due to varying enzyme concentration

among patients and body parts, degradation, erosion, and associated properties such as release kinetics are challenging to predict [177]. Considering enzymes that are embedded during hydrogel formation, the already low loading capacity of hydrogels is further decreased for drug delivery applications [28]. To overcome this, hydrolytically cleavable groups can be incorporated into the hydrogel backbone (Table 3). In a labor-saving way, this can be done during the functionalization of the hydrogel precursors. For this hydrolysis-prone groups are used to link macromonomers to the functional group needed for the cross-linking reaction.

Table 3: Examples of hydrolytically cleavable groups used for preparation of biodegradable hydrogels.

Hydrolytically cleavable groups	Hydrolysis mechanism
Amide	
Carboxylate ester	
Carbamate	
Carbonate ester	

Very common coupling groups are amides. For this, well-known coupling reagents such as *N,N'*-dicyclohexylcarbodiimide, *N,N'*-diisopropylcarbodiimide, or 1-ethyl-3-(3-dimethylaminopropyl)carbodiimide, which were developed for peptide synthesis, are used [46,62,115]. However, amides are highly stable under physiological conditions and degrade faster only after shifting the pH to the acidic or basic [55]. Switching to carboxylate esters, which can be incorporated with similar coupling reagents, leads to a much higher susceptibility to hydrolysis at physiological conditions. For example, PEG-based hydrogels with ester groups showed a fivefold increase in hydrogel mass and complete dissolution after about 60 days, while amide groups lead to hydrogels without swelling and high stability for at least 150 days [115]. Modifying four-armed PEG macromonomers via amidation and esterification, a SPAAC cross-linked hydrogel platform with a predictable disintegration time was developed by Xu et al. based on the stability differences of amide and ester groups [56]. Changing the ratio of non-labile

amide linkages to labile ester-linkages in hydrogels, the decomposition time at pH 7.4 ranged from 18 days to no hydrogel dissolution by 250 days. However, the stability of carboxylate ester groups depends on the hydrogel formulation that can be seen for a multitude of hydrogels degradable through ester linkers. For example, high stability was found for a PEG-based system cross-linked via iEDDA reaction with complete dissolution only after 186 to 560 days [65], whereas hydrogels using nitrile oxide-norbornene click reaction disintegrated within 25 days [60]. The reason for this is that degradation time depends on the specific position of the linkage and the chemical nature of the leaving group [56]. If the leaving groups are stabilized, for example, by resonance, inductive, and steric factors, the ester hydrolyzes usually faster [178–180]. Destabilizing effects, on the other hand, lead to higher pK_a values, reducing the stability of the leaving group and, thus, stabilizing the ester bond.

These stabilizing and destabilizing effects of neighboring groups can also be found for hydrolytically cleavable carbonate ester and carbamate linkages. For example, Ricipato et al. prepared dihydroxyacetone-based hydrogels that contained two types of carbonate ester linkages, each with different neighboring groups: those that were connected to two PEG chains and those that connected only one PEG chain to dihydroxyacetone [181]. The ketone present on the dihydroxyacetone was found to lead to complete degradation of the carbonate linkage due to an intramolecular nucleophilic attack on the carbonate ester linker after 7 h, whereas the carbonate linker connecting two PEG chains remained stable [182]. The introduction of an additional carbon unit between the carbonate ester linkages and the ketone group caused higher stability, indicating ketones supporting effect on degradation. This was confirmed by the preparation of hydrogels containing no ketone group that showed the significantly highest stability.

More stable carbonate ester linkages were successfully introduced in dextran via carbonylimidazole-activated hydroxyethyl methacrylate [183]. After radical polymerization, a hydrogel was formed with carbonate ester linkers for hydrolytic cleavage. These hydrogels showed complete dissolution after 30 days.

However, the introduction of carbonate ester groups as hydrolytically cleavable linkages requires usually toxic phosgene derivatives during synthesis. Therefore, utmost care must be taken, and purification must guarantee complete decontamination.

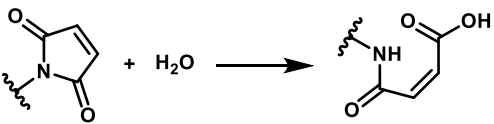
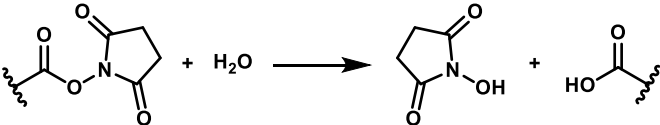
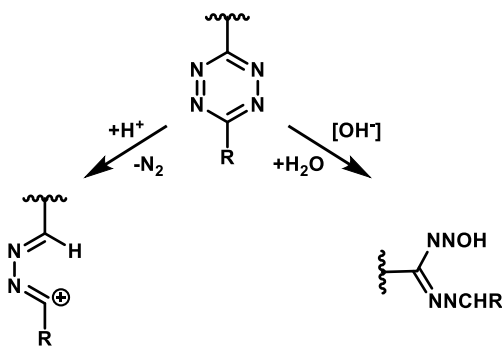
Carbamates can also be introduced into the hydrogel backbone as cleavable linkages [184]. The decomposition mechanism as well as neighboring groups affecting stability are the same as for hydrogels cross-linked via carbamate formation (section 4.1).

For sake of completeness, the possibility of incorporating photolabile linkers such as nitrobenzyl or coumarin derivatives into hydrogels should be mentioned [55,159]. However, an external light source is required for complete degradation. This method is usually applied to allow the remaining hydrogel matrix to degrade rapidly only at the end of the therapy, instead of the hydrogel eroding slowly over time.

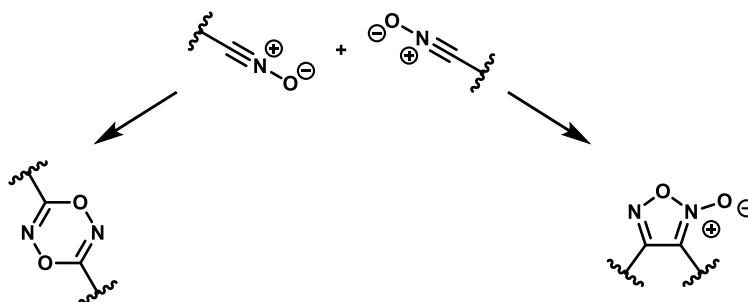
5 Functional group stability

First estimations of the hydrogel performance can be made by knowing the number of available functional groups of the hydrogel precursors. The more functional groups present, the more likely the formation of a higher number of elastically active chains, resulting in a denser polymeric network. This has an impact on different hydrogel features. As discussed in section 3, mechanical properties are enhanced by a higher cross-linking density. Moreover, a denser network generates smaller meshes. This in turn influences the release kinetics for drug delivery [185]. Therefore, to make accurate statements about hydrogel properties and to achieve high preparation reproducibility, the number of functional groups has to remain as constant as possible from synthesis through storage to preparation. However, there are various chemical processes during storage and preparation that can affect the nature of the functional groups and, in the worst case, completely inactivate them for polymerization (Table 4), making preparation of reproducible hydrogels difficult. In the following, functional groups prone to deactivation are presented and methods to protect them are outlined.

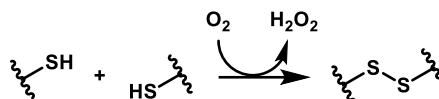
Table 4: Examples of functional groups that show stability issues.

Functional group	Example of impairment
Maleimide	
Succinimidyl carbonate	
Tetrazine	

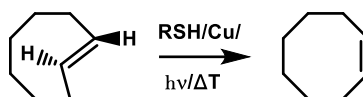
Nitrile oxide



Thiol



trans-Cyclooctene



Cyclooctyne

Trimerization

Maleimide is used for hydrogel preparation via DA reaction or Michael-type addition. It is well known that maleimide groups hydrolyze under physiological conditions via a nucleophile attack of OH^- , causing ring opening to maleamic acid [39]. While this sensitivity to hydrolysis is advantageous considering biodegradation of DA hydrogels, it leads to complications during hydrogel preparation. To avoid hydrolysis and, therefore, loss of maleimide moieties, maleimide-functionalized macromonomers must be dissolved in aqueous solution only right before preparation. Moreover, gelation time is important. The faster gelation, the fewer maleimide groups are subject to hydrolysis in solution. To address this shortcoming of the slow DA reaction, several strategies have been suggested. The most straightforward way is to lower the pH since maleimide exhibits high stability in acidic environment [39,186]. However, this is less feasible regarding patient compliance. A more suitable approach is to introduce neighbor groups with stabilizing nature such as steric and inductive effects. Knowing that additional hydrophobic alkyl groups connected to maleimide have resulted in increased hydrolytic stability [187], 6-aminohexanoic acid and 12-aminododecanoic acid were incorporated between each arm of an eight-armed PEG macromonomer and maleimide [35,38]. Besides an inductive electron-donating effect, that stabilizes the C–N–C bond of maleimide, this caused an accelerated enolization of the carbonyl group, increasing the electron density [188]. Both effects slowed down the nucleophile attack of OH^- , leading to increased stability. While the maleimide groups of maleimide-functionalized eight-armed PEGs showed a half-life of 170 min in phosphate buffer (pH 7.4) at 37 °C, half-lives were more than doubled

with the incorporation of the 6-aminohexanoic acid and even more than tripled with 12-aminododecanoic acid.

A different concept represents the anhydrous hydrogel preparation. To protect maleimide groups from hydrolysis, polymerization of an eight-armed PEG-based system was carried out at temperatures leading to melting of the hydrogel precursors (i.e., above 40 °C) under anhydrous environment, unlike the conventional hydrogel preparation that takes place in water [37]. Only after incubation did this polymer take up water and swell to become a hydrogel. Compared to the conventional hydrogel preparation, no loss of functional groups could be detected.

The reaction between liquid succinimidyl carbonate- and amine-functionalized four-armed PEGs has also been used for the preparation of water-free hydrogels [102–104]. Although the authors did not compare functional group stability between the anhydrous and the conventional hydrogel preparation, the water-free environment should protect succinimidyl groups from hydrolysis and rearrangements, which are known to occur in basic buffer [189]. Nevertheless, these hydrogel precursors should not be stored in liquid but in solid state at temperatures below -20 °C. Otherwise, mobility is sufficiently high for self-cross-linking between succinimidyl carbonate moieties and unfunctionalized hydroxy groups, which are still present after synthesis [102]. Even though water-free hydrogel preparation has so far been achieved only via DA reaction and carbamate or carbonate formation, anhydrous preparation should also be suitable for other cross-linking reactions that involve hydrolysis-sensitive groups.

Another moiety prone to hydrolysis is tetrazine, used as a diene in the iEDDA reaction. Tetrazine decomposes in basic as well as acidic milieu [190]. Due to the fast reaction rate of the iEDDA reaction, hydrolysis during gelation can be neglected. However, preparation is still an obstacle. Tetrazine-functionalized precursors should be dissolved in water only for a short time and, thus, cannot be stored in solution for an extended period without major loss. To examine stabilizing effects of substituents on tetrazine, Karver et al. performed stability tests with differently modified tetrazine in fetal bovine serum at 37 °C [191]. 60% of a monosubstituted tetrazine was found to degrade after 10 h. The second substitution with a methyl group protected tetrazine from disintegration almost completely, whereas an electron-withdrawing substituent enhanced decomposition. Hence, the substitution of electron-donating groups stabilized the tetrazine ring but lead to reduced reaction kinetics. However, if improved tetrazine stability is required, a high reaction rate can be retained by using a dienophile with an increased reactivity such as *trans*-cyclooctene.

The reaction between nitrile oxide and norbornene is a member of the 1,3-dipolar cycloadditions [123]. In contrast to stable azides commonly used as 1,3-dipoles, the majority of nitrile oxides are chemically unstable [192]. They show dimerization to furoxanes and 1,4,2,5-dioxadiazines [192,193]. To avoid nitrile oxide loss, Truong et al. presented the *in situ* generation of nitrile oxides for the preparation of hydrogels [59,60]. In this approach, the more stable hydroximoyl chloride was used as a precursor. After administration and combination with norbornene moieties, hydroximoyl chloride reacted at the operating site to nitrile oxide without requiring any catalyst to form the hydrogel.

The SPOQC is based on a similar principle. Here, catechol moieties are oxidized to 1,2-quinone functionalities by the addition of, e.g., sodium periodate or mushroom tyrosinase [105]. These additional components are a prerequisite for the proceeding of the cross-linking reaction with alkynes. Even though this reaction was developed to achieve spatiotemporally controlled gel formation [105,194], this provides additional beneficial protection of reduction-sensitive 1,2-quinones [195].

Other redox-sensitive groups used for hydrogel preparation are thiols. They tend to form disulfides, especially with increasing pH and temperature [196]. For example, thiol-functionalized PEG macromonomers showed low stability over only a few minutes after dissolving in 0.3 M triethanolamine (pH 8), impacting storage and hydrogel preparation negatively [86]. Therefore, it is often necessary to treat them with a reducing agent such as dithiothreitol to ensure no present disulfides. Usually, this is done before use to reduce any disulfides, which is extremely cumbersome and costly. To avoid these steps and to provide necessary protection against moisture and oxygen, thiol-modified macromonomers have to be stored under inert gas at low temperatures [86].

A different type of reactivity impairment of functional groups shows *trans*-cyclooctene, which reacts with tetrazine via iEDDA reaction. Here, isomerization to the more stable *cis*-derivative can occur [197]. This has a negative impact on the gelation time because the *cis*-isomer exhibits a 106-fold lower rate constant compared to the *trans*-isomer [198]. Triggers of this isomerization are of different nature. Besides the presence of thiols, copper-containing proteins can be the reason [199,200]. Temperature and light sources can also cause the reactive *trans*-cyclooctene to become a *cis*-isomer [201,202]. Rossin et al. found that a *trans*-cyclooctene tag could be deactivated *in vivo* by interaction with copper-containing proteins [200]. Shortening the distance of a linker between *trans*-cyclooctene and a lysine residue increased the steric hindrance. This in turn interfered with the interaction between *trans*-cyclooctene and serum proteins and, hence, stabilized *trans*-cyclooctene.

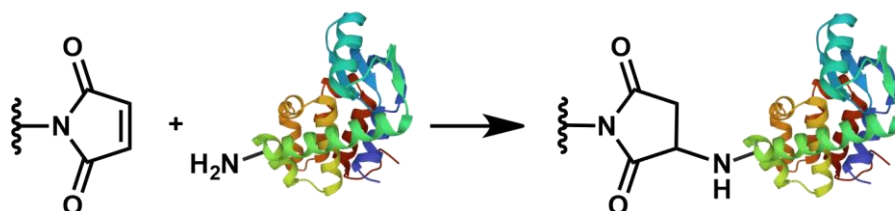
A further way to improve *trans*-cyclooctene's stability was to design conformationally strained *trans*-cyclooctene derivatives, as described by Darko et al. [203]. By synthesizing a *cis*-dioxolane-fused *trans*-cyclooctene, electron density decreased, stabilizing *trans*-cyclooctene against isomerization. Additionally, increased hydrophilicity of *trans*-cyclooctenes due to functionalization with dioxolane is advantageous regarding the use for aqueous systems such as hydrogels [204].

The introduction of ring strain-promoted dipolarophiles was a major achievement for the stride of CuAAC to SPAAC, as reaction rate was maintained while avoiding toxic copper catalysts. However, due to destabilization via ring strain, cyclooctynes are very reactive. They are air-sensitive and can polymerize or rearrange to more stable isomeric hydrocarbons [205,206]. To store cyclooctynes, complexation with β -cyclodextrin has been described [207]. For this, difluorobenzocyclooctyne was trapped in a stable inclusion complex with β -cyclodextrin, which could be stored as lyophilized powder. However, prior to use, β -cyclodextrin had to be removed by organic solvents, being very cumbersome regarding hydrogel preparation with cyclooctyne-functionalized macromonomers.

A more promising way to stabilize cyclooctynes is to replace a carbon atom with larger sulfur, leading to thiacyclooctynes [208]. In this way, the destabilizing ring strain is relieved via ring expansion. In comparison, unmodified cyclooctyne oligomerized during concentration and storage, whereas thiacyclooctyne was stable. However, lowering the ring strain decreases the reaction kinetics. In contrast, the incorporation of nitrogen causes an increased ring expansion due to the shorter carbon-nitrogen bond. Different than expected it was possible to store aza-dibenzocyclooctyne over months at room temperature without polymerization [209].

6 Off-target interaction

Chemically cross-linked hydrogels are often used for the delivery of cargo including small and large molecules as well as cells. Thereby, during *in situ* encapsulation, the cross-linking reaction should be inert towards the cargo unless it is requested. Otherwise, interaction could result in covalent bonds between the hydrogel matrix and the embedded substances [210]. This in turn can cause changes in activity up to complete inactivation of the cargo [87,211]. Furthermore, release kinetics depend on the possibility to diffuse freely out of the matrix. An unwanted tethering to the network leads to a delayed or even incomplete release and, hence, compromises the therapy [28,212]. At worst, conjugates of hydrogel residues and cargo can cause immunogenic response [211].



Scheme 1: Example of an off-target reaction between maleimide moieties and a protein's amine groups. Image from the RCSB PDB (www.rcsb.org) of PDB ID 6LZM [213] was created with Mol* viewer [214].

Cross-linking reactions are sensitive towards various functionalities (Scheme 1). For example, genipin coupling, Schiff-base formation, and carbamate formation involve amine groups [99,126]. DA reaction, Michael-type addition, thiol-yne click chemistry, radical polymerizations, and disulfide exchange show reactivity to nucleophile groups (e.g., thiol and amine groups) [126]. Since thiol and amine groups are present for many molecules used as cargo, especially proteins, side reactions occur. To verify this, the degree of side reactions during different cross-linking reactions was measured for lysozyme [210]. Only 38.9, 70.3, and 29.3% of lysozyme were found unreacted for the DA reaction, Michael-type addition, and a radical polymerization, respectively.

One way to circumvent unwanted interactions is the bioorthogonal cross-linking strategy. The key feature of this approach is the use of cross-linking reactions, whose functional groups show high reactivity and selectivity to the respective counterpart as well as inertness to biological

functionalities [47]. CuAAC, SPAAC, SPOQC, nitrile oxide-norbornene cycloaddition, and iEDDA reaction are all postulated to be bioorthogonal [47,54,59,105,124]. However, caution is necessary because side reactions in the presence of biomolecules, especially proteins, are not completely excluded [177]. For example, during the iEDDA reaction between tetrazine- and norbornene-modified PEG macromonomers, approximately 11% of the model protein lysozyme were modified [65]. Side reactions between nucleophile thiol groups and electrophile tetrazines were indicated as the reason [215]. Interaction with nucleophiles was also described for cyclooctynes, 1,2-quinones, and nitrile oxides [209,216,217]. Nevertheless, only a very small amount of the cargo should react with these cross-linking reactions, leaving the main part unmodified. Additionally, by increasing the molar ratio of the functional groups towards the less reactive moiety, off-target reactions are further reduced.

The reactivity of cargo's amines and thiols can also be lowered by pH changes. Acidic environment leads to protonation of amines to ammonium groups and prevents thiolation of thiols, decreasing the nucleophilicity of both, amines and thiols [177,218]. For example, reduced side reactions at pH 4 have been shown for the DA reaction and Michael-type addition [212]. In contrast, an increase to pH 9 caused a very high amount of modification. While working at lower pH is advantageous against off-target reactions, patient compliance does not allow injection of solutions with too low pH value as mentioned before. In addition, unphysiological pH may influence the stability of the cargo such as proteins [219]. A completely different approach represents hydrogel loading after gelation via post-fabrication equilibrium partitioning [211]. Thereby, the cross-linked hydrogel network is incubated in a concentrated solution containing the cargo [12]. In this way, the hydrogel gets loaded. Since almost all functional groups have reacted, interaction with the cargo is reduced to a minimum, and cargo integrity is ensured. However, this method can only be used if the cargo can diffuse into the network, which requires a smaller hydrodynamic diameter of the active substance than the mesh size of the hydrogel. Moreover, control of the quantities loaded into the hydrogel represents an obstacle [211], and loading after gelation is not feasible for *in situ* gelation. Therefore, different approaches are required.

Considering protein-polymer interaction, the human growth hormone was precipitated by adding zinc ions or linear PEG before gelation to protect it from side reactions during cross-linking via Michael-type addition [88]. Thereby, precipitates prepared with zinc ions additionally dissolved more slowly, leading to a more controlled release. However, precipitation might cause protein degradation and denaturation [210].

As an approach based on solvation, Censi et al. exploited hydrophilic and hydrophobic areas in a hydrogel to prevent proteins from modification during photopolymerization [220]. An ABA triblock copolymer consisting of thermosensitive methacrylated poly(*N*-(2-hydroxypropyl)methacrylamide lactate)s (A-blocks) and hydrophilic PEG (B-block) was used as hydrogel backbone. Dual cross-linking was carried out via thermogelation and UV polymerization of the methacrylate groups with Irgacure 2959 in the hydrophobic domains of the hydrogel. Thereby, proteins preferred to reside in hydrophilic chemically non-cross-linkable areas, preserving their activity during cross-linking.

Suppressing side reactions between hydrogel precursors and proteins can be achieved via “shielding” of proteins [90,210]. Different polyanions were investigated for their ability to reduce side reactions. The ionic interaction between polyanions and proteins resulted in the formation of colloidal particles and protected them from unwanted protein-polymer conjugation. In this way, dextran sulfate completely prevented side reactions during DA reaction. This “shielding” mechanism was also successfully used for other cross-linking reactions and polyanions. For example, approximately 71% of lysozyme incubated with vinyl sulfone- and thiol-functionalized methoxy PEG at pH 7.4 and 37 °C for 1 day were PEGylated. The addition of poly(acrylic acid) significantly decreased the PEGylated lysozyme amount to 29%. However, poly(acrylic acid) was not able to decrease lysozyme PEGylation during a radical polymerization. Furthermore, as the authors stated, protein-polyanion complexation might affect the chemical integrity and activity of the protein. Before using polyanions for “shielding” of proteins, the right polyanion-protein formulation must be evaluated to ensure preservation of protein activity.

Besides maintaining functional group stability, as mentioned in section 5, we showed that the anhydrous hydrogel preparation prevented also proteins from interacting with functional groups of hydrogel precursors [37]. For this, we prepared a powder blend consisting of a 1:1 mixture of furan- and maleimide-functionalized eight-armed PEGs and the model protein lysozyme. After heating above the melting point of the PEG derivatives, a three-dimensional network was formed via DA reaction in the molten state. The protein did not dissolve in the PEG melt and remained in solid state during the whole polymerization process. Hence, no interaction between the enzyme and PEG macromonomers was possible. This was confirmed via SDS-PAGE and activity assessment. However, after incubation in water, the remaining free functional groups might react with lysozyme, which dissolved after water contact. To check this, the release of the model protein from the hydrogels was analyzed. Lysozyme was found to freely diffuse out of the hydrogel matrix without activity impairment, indicating no subsequent side reactions. This water-free encapsulation of solid material is similar to the hot-melt extrusion with poly(lactic-co-glycolic acid) (PLGA) that was already used to embed proteins in polymeric implants [221].

7 Release

Since hydrogels represent a very crucial and important tool in the field of drug delivery, this topic will be examined in more detail. The fact that hydrogels are able to deliver a wide range of drugs from small molecules over large proteins up to cells distinguishes them as a very versatile technology. Their three-dimensional structure, which serves as transport vehicle for embedded bioactive molecules, is the reason why drug delivery is possible at all. Due to the high amounts of water (up to 99%), hydrogels provide a microenvironment similar to tissues, which is beneficial for the stability of sensitive substances such as biopharmaceuticals. Furthermore, hydrogels can protect biopharmaceuticals from degradation via inwardly diffusing substrates such as enzymes, cytokines, T-lymphocytes, and antibodies. For example,

Su et al. embedded cells that secreted insulin to achieve glucose-stimulated release into PEG-based hydrogels cross-linked via NCL [93]. The incorporation of a cytokine-inhibitory peptide preserved the bioactive cargo from damage induced via cytokines and increased cell viability. Moreover, these drug delivery systems can prolong half-lives of biologics, which usually vary between days to weeks after administration, making repeated injections necessary to maintain therapeutic levels for long-term treatment [185]. To address this, hydrogels are able to release therapeutic proteins in a controlled manner over the desired timescale [222]. Thereby, the requirement of only a single injection increases patient compliance and reduces health expenditure.

In general, release from hydrogels depends on factors concerning both the hydrogel network and the drug itself. These include swelling and degradation of the network, drug diffusivity, hydrodynamic diameter of the drug, and hydrogel mesh size [223–225].

Swelling and degradation of the hydrogel network impact the mesh size present in the hydrogel. Thereby, mesh size increases by cleavage of linkages (degradation) and network expansion due to the inwardly diffusing water (swelling) [223]. The more proceeded swelling and degradation the larger the mesh sizes. Therefore, both factors directly impact the release kinetics of drugs from the hydrogel network. As degradation was already the subject in section 4, we will focus on the remaining issues.

The diffusivity of a drug is a physicochemical parameter that affects passive diffusion through barriers [226]. In the case of drug release from hydrogels, diffusivity describes the extent to which the hydrogel network influences diffusion and, therefore, can be used for the prediction of release kinetics. For the determination of drug diffusivity, the drug diffusion coefficient in pure solvent (D_0) is calculated according to the Stokes-Einstein equation (2):

$$D_0 = \frac{kT}{6\pi\eta r_H} \quad (2)$$

wherein k is the Boltzmann constant, T the temperature, η the viscosity of the solvent, and r_H the hydrodynamic radius of the drug.

Thereby, r_H of the drug can be determined via several methods such as dynamic light scattering [227], electrophoresis [228], pulsed field gradient NMR spectroscopy [229], viscometry [230], and size exclusion chromatography [231].

However, in hydrogels, the presence of a cross-linked network leads to steric hindrance and frictional drag [223,232], whose extent is described by polymer concentration and composition. All these factors impact drug diffusivity. To take this into account, the network structure can be related to the drug diffusivity in hydrogels (D_g) by a free-volume approach suggested by Lustig and Peppas [224,233]:

$$\frac{D_g}{D_0} = \left(1 - \frac{r_H}{\xi}\right) e^{-\left(Y\left(\frac{v_{2s}}{1-v_{2s}}\right)\right)} \quad (3)$$

In this equation (3), ξ is the average mesh size in the hydrogel network, Y is the ratio of the critical volume required for a successful translational movement of the solute molecule and the average free volume per solvent molecule [232], and v_{2s} is the polymer fraction in swollen state.

The last point affecting the release kinetics is the average mesh size present in a hydrogel network. To examine the mesh size of hydrogels, various methods have been suggested. Techniques that allow the determination of the mesh size and its distribution include small-angle X-ray scattering [234], small-angle neutron scattering [22], NMR spectroscopy [42], neutron spin-echo spectroscopy [22], differential scanning calorimetry [235], rheology [79], and swelling studies [99]. The latter is the most common method to get information about the average mesh size. It is based on the equilibrium swelling theory. By using a modified Flory-Rehner equation (4) the number of moles of elastically active chains in the hydrogel network (v_e) can be calculated [77,236,237]:

$$v_e = -\frac{V_p}{V_1 v_{2c}} \cdot \frac{[\ln(1 - v_{2s}) + v_{2s} + \chi_1 v_{2s}^2]}{\left[\left(\frac{v_{2s}}{v_{2c}}\right)^{\frac{1}{3}} - \frac{2}{f} \left(\frac{v_{2s}}{v_{2c}}\right)\right]} \quad (4)$$

V_p is the volume of dry polymer, V_1 is the molar volume of the swelling agent, χ_1 is the Flory-Huggins interaction parameter of the used polymer in water, and f is the functionality number of the macromonomers. The polymer fraction of the hydrogel after cross-linking (v_{2c}) and the polymer fraction in swollen state (v_{2s}) are experimentally determined based on Archimedes' principle of buoyancy. Finally, the average network mesh size (ξ) is obtained by equation (5) [38,238]:

$$\xi = v_{2s}^{-\frac{1}{3}} l \left(\frac{2m_p}{v_e M_r}\right)^{\frac{1}{2}} C_n^{\frac{1}{2}} \quad (5)$$

wherein l is the average bond length along the polymer backbone, m_p is the total mass of polymer in the hydrogel, M_r is the molecular mass of polymer's repeating unit, and C_n is the Flory characteristic ratio.

Since swelling, degradation, and diffusivity in the hydrogel network are connected to the average mesh size, we will focus on the relation between mesh size and the hydrodynamic diameter of the cargo.

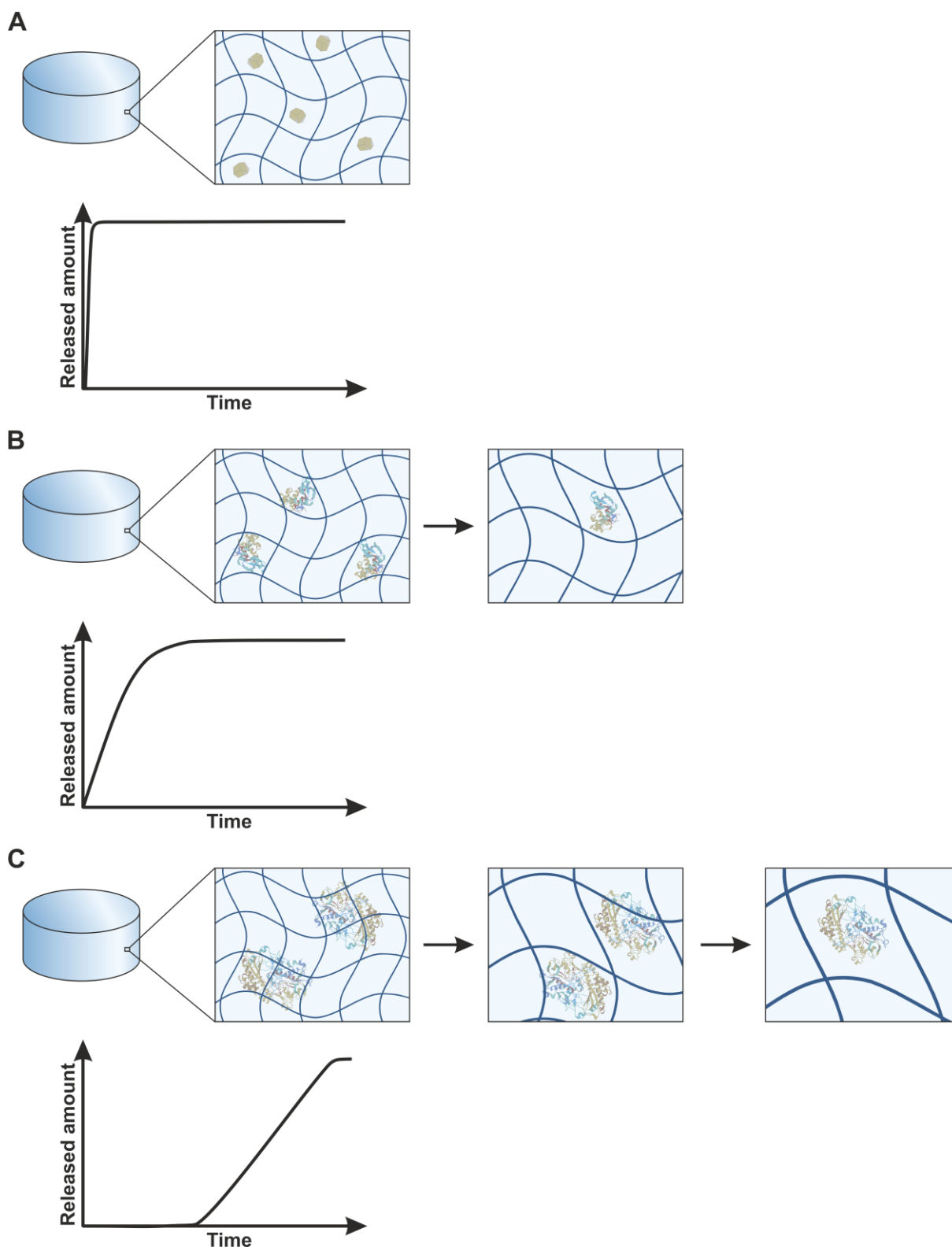


Figure 2: Release kinetics described by the ratio between hydrodynamic radius of the embedded cargo (r_H) and mesh size of the hydrogel (ξ). Rapid diffusion-controlled release for $2r_H \ll \xi$ (A), more sustained release for $2r_H = \xi$ (B), and delayed release for $2r_H > \xi$ (C). For C, complete release is achieved by mesh size increase due to swelling and degradation. Images from the RCSB PDB (www.rcsb.org) of PDB ID 6LZM [213] and 1CF3 [239] were created with Mol* viewer [214].

If a drug is encapsulated into a hydrogel network without covalent or physical attachment, the network mesh size and the hydrodynamic diameter of the drug determine how fast the cargo gets released

(Figure 2). The drug is only able to leave the network if its hydrodynamic diameter is smaller than the mesh size of the hydrogel. Therefore, embedding drugs with significantly smaller hydrodynamic diameters than the mesh size of the hydrogel leads to a very fast diffusion-controlled release. Usually, the release is maintained over hours to a day at most [223]. This is what most hydrogels are prepared for. Using drugs with a hydrodynamic diameter in the range of the mesh size, the release gets more sustained. To achieve delayed release, the hydrodynamic diameter of the cargo has to be larger than the mesh size. In this case, the molecules are entrapped in the network, and diffusion out of the matrix is only enabled by mesh size increase through hydrogel swelling or degradation [65]. This release behavior is degradation- or swelling-controlled.

For a sustained release over an extended time, the mesh size distribution gets more important. Due to the inhomogeneities caused by the polymerization process, the hydrogel network consists of a variety of differently sized meshes, whereas the mesh size is given as an average value [42,225]. If the average mesh size is smaller than the hydrodynamic diameter of the drug, the drug can only pass larger meshes. During this period, a reduced release is observed. If the network does not expand, the release would gradually stop, and still remaining cargo would be entrapped in the hydrogel. To continue the controlled release, the meshes have to enlarge. This can be achieved by the incorporation of cleavable groups in the hydrogel backbone, as described in section 4. By the degradation time of these functional groups, the release time can be controlled. Slowly degrading groups can prolong the release. For example, we developed hydrogels with slowly hydrolytically cleavable ester groups [65]. Using a polymer concentration of 15% (w/v) led to hydrogels being stable for more than 500 days. The average mesh size was found to be approximately 4.1 nm. When embedding glucose oxidase with a hydrodynamic diameter of 8.6 nm [228], a sustained release over more than 250 days was achieved.

This method is ideal for large drugs such as therapeutic proteins. For smaller molecules, a different approach is required because hydrogel mesh size can only be reduced to a limited extent [223]. For example, covalent tethering of the cargo to the hydrogel network represents one way to control the release of smaller molecules from the hydrogel. In this way, complete initial release via diffusion is prevented and the drug is only released when the linkage between drug and tether is cleaved. The mechanisms causing cleavage of the linker are similar to those that lead to hydrogel degradation (e.g., hydrolysis, oxidation, enzymes) as described in section 4. Hammer et al. showed that lysozyme can be released over a time of 28 days despite having a hydrodynamic diameter of 3.8 nm that is significantly smaller than the average mesh size of the used 5% (w/v) four-armed PEG-hydrogels that was found to be in the range of 16.3 to 21.2 nm for comparable hydrogels [52,99,240]. Due to covalent binding of lysozyme to the hydrogel backbone, a reduced initial release was obtained [52]. The use of differently stable carbamates as biodegradable linkages between lysozyme and the hydrogel backbone allowed the tuning of the release time from 4 to 28 days. The possibility of tailoring the time of release that can also be seen for other linkages [57,58] is advantageous, as it can be adjusted for various needs of the respective application. However, one obstacle of tethering molecules to the hydrogel backbone is

that the conjugation may decrease the bioactivity of fragile drugs such as proteins and peptides [211]. Additionally, released fractions of the tethers or drug hydrogel conjugates can lead to unwanted immunogenic responses.

To circumvent this, tethering to the hydrogel backbone can also be achieved by exploiting physical interactions such as electrostatics or hydrophobicity. In this case, the drug is non-covalently linked to the hydrogel backbone and enabled to be released when the interactions are reduced by hydrogel erosion or inwardly diffusing water. For this, hydrogel backbones that contain drug affine functionalities are synthesized. Huynh and Wylie modified agarose with desthiobiotin to extend the release of a streptavidin-bevacizumab conjugate from agarose-desthiobiotin hydrogels [222]. The underlying mechanism was the streptavidin-desthiobiotin complexation that led to an extended release of bevacizumab over 100 days. As a further advantage, the release kinetics of the antibody could be tuned by altering the biotin concentration.

Besides the use of drug affine functionalities in the hydrogel backbone, additional unconnected macromolecules can be embedded into the hydrogel that exhibit affinity to the respective drug. Thereby, these macromolecules are larger than the mesh size of the hydrogel and are retained in the network. The polyanion heparin is one such macromolecule that was successfully used to tune the release of cationic growth factors [90,241]. In this way, the amount released of the vascular endothelial growth factor from hyaluronic acid-based hydrogels was reduced from 30 to 21% for hydrogels containing 0.03% heparin and to 19% for 3% heparin compared to hydrogels without heparin after 42 days [90].

A release of antibodies over 100 days is also possible by using self-assembling peptides as hydrogel scaffolds as shown by Koutsopoulos and Zhang [242]. Thereby, embedding of the human immunoglobulin G (IgG) was carried out via self-assembling in the presence of an electrolyte solution. Due to the affinity between protein and peptide, IgG could be released over an extended time of more than 100 days.

Based on the similar principle, Wang et al. developed an injectable PEG-based hydrogel for the affinity-controlled release of neurotrophin-3 [89]. The incorporation of peptides into the hydrogel resulted in a threefold slower release than unmodified PEG-hydrogels. The release kinetics could be changed by the ratio of peptides to proteins in the hydrogel. By using three different peptides, the authors additionally showed how the affinity to the respective peptide influenced the protein release.

However, one limitation of using physical affinity for tuning the release kinetics is the limited broad applicability. For affinity-controlled release, the matching affine group has to be found that seems not possible for every drug.

Another way to delay the release is to increase the drug size. This can be done via encapsulation of the drug into a carrier material such as particles. Subsequently, these particles are embedded into hydrogels. Due to an adjustable size, the particles release can be tailored based on the aforementioned principle of hydrogel mesh size. As the last step, degradation of the released particles leads to the liberation of the drug. For the preparation of different particle sizes, various methods have been used, thus far. PLGA

microspheres containing dexamethasone were prepared using a solvent evaporation method [243]. Embedding into PVA-based hydrogels resulted in a release over 120 days with different release kinetics depending on the microsphere size.

Peng et al. incorporated biodegradable poly(3-hydroxybutyrate-co-3-hydroxyhexanoate) (PHBHHx) nanoparticles into chitosan-based hydrogels for the long-term release of insulin [244]. Compared to the release of free insulin that lasted 15 days, the PHBHHx nanoparticles significantly prolonged the release, as only approximately 20% of the protein was released after 30 days.

While the use of mediated carrier systems makes the extended controlled release of small molecules possible, loading capacity gets impacted for larger drugs such as proteins. Here, the additional embedding of material decreases the already limited loading capacity of common hydrogels [28].

This limited loading capacity represents a common obstacle for a variety of hydrogels. For example, hydrogels prepared for the release of small hydrophobic molecules generally show low loading capacity due to the poor water solubility of these drugs. A way to increase the number of hydrophobic drugs in hydrogels was described by Ci et al. [245]. They used *in situ* crystallization of 10-hydroxycamptothecin that was triggered after shifting the pH value and occurred after gelation. In this manner, an increased amount of drug could be loaded and released over 30 days.

Regarding the delivery of therapeutic proteins, the application becomes more challenging. Here, the presence of higher molecular weight proteins causes more imperfections in the network during cross-linking. Thereby, the cross-linking density decreases with more present proteins, which in turn accelerates the release kinetics [246]. Thus, typical loading capacities of conventional hydrogels for sustained release are in a range of 0.01 to 1.0 mg/ml (i.e., approximately 0.001 to 0.1% (w/w)) [247]. Since the tolerable injection volume of subcutaneous injections is below 2 ml [248,249], this low loading capacity is especially a challenge for the maintenance of a sufficient plasma concentration of antibodies over a therapeutic time of months to years.

To overcome this limitation, the addition of clay nanoparticles in alginate-based hydrogels resulted in an increased loading capacity of 8 mg/ml (i.e., approximately 0.8% (w/w)) [247]. The authors suggested that the large negative surface of the nanoparticles adsorbed the positively charged insulin-like growth factor-1 mimetic protein conjugated with a linear PEG chain, which caused the assemblance into microparticles. Additional to the higher loading capacity, the release kinetics were slowed and extended by this increased protein amount. While this approach seems promising, a loading capacity of hydrogels should be ideally in the order of 10% (w/w) [28].

To achieve such high loading, our anhydrous preparation of PEG-based hydrogels can be used [37]. Due to the absence of water, more proteins can be embedded without detrimentally impacting the cross-linking density. Loading capacities of 5, 10, and 15% (w/w) did not impact the release kinetics and led to similar releases over 100 days. Furthermore, even higher loading capacities seem possible in this way.

8 General considerations and obstacles

In the last section, general considerations considering hydrogel preparation will be subject of the discussion. One important aspect of a successful biomedical hydrogel application is cytocompatibility. The more toxic, the more unlikely a hydrogel will be considered for *in vivo* use. Toxicity can occur for different steps of a hydrogel preparation. If toxic educts are used during the synthesis, the purification steps have to guarantee no remaining educts in the final product. Further, the right choice of the polymer backbone is crucial. For example, natural polymers can evoke immunogenic reactions [12]. Therefore, switching to synthetic polymers that can be designed to the respective requirements is often advantageous. Also, the right cross-linking reaction has to be considered. Functional groups such as maleimide, acrylate, or aldehyde that show toxicity for example via cross-reactivity to the tissue or via changing the pH should be avoided if the benefit of using them does not outweigh the disadvantages [126,212]. Likewise, catalysts can cause severe damage to biomolecules at the operating site [118]. The copper ions used for the CuAAC reaction cause harm to proteins, nucleic acid, polysaccharides, and lipids even at low concentrations either by themselves or as a result of the formation of reactive oxygen species [119]. Therefore, the CuAAC should be exchanged by a copper-free alternative. Moreover, the creation of non-toxic products and side-products is a vital characteristic of cross-linking reactions. Here, reactions generating potential toxic side-products such as NCL or oxidizing environment harmful to cells such as the SPOQC should be used with careful consideration [64,167].

Another aspect that affects the usability of hydrogels are the syntheses of the respective hydrogel precursors. Materials that are easy to synthesize and store are superior to polymers, which are laborious and cumbersome to produce. In this way, money can be saved, which is a crucial factor for development. For example, the syntheses of the cyclooctynes for the SPAAC reaction and the *trans*-cyclooctene for the iEDDA reaction involve multiple difficult synthesis steps, which makes the syntheses and the produced polymer very expensive [54,177,250]. This in turn is disadvantageous for scale-up syntheses [59]. As a further example, the tetrazine groups of the iEDDA reaction require expensive nitrile compounds as educts. Furthermore, the yields of tetrazine synthesis are quite low, especially for additionally substituted tetrazines [61,65]. Additionally, water-sensitive functional groups also pose an obstacle, as they require water-free handling and storage. Otherwise, hydrolysis would reduce the number of reactive groups adversely impacting the reproducibility of the hydrogel preparation.

The last point to be mentioned regarding hydrogel preparation is sterilization. Since hydrogels are used in the human organism, sterilization or aseptic preparation are mandatory. Otherwise, contaminated material could lead to major health concerns. Different sterilization methods are known for already formed hydrogels but as hydrogels are aqueous materials with well-defined architecture, care has to be taken to ensure that the properties of the three-dimensional network are maintained as much as possible. A case-by-case consideration is required for each hydrogel and bioactive substance contained in the hydrogel. Each hydrogel responds differently to the respective sterilization method. Changes due

to sterilization may include reduction of swelling, accelerated release kinetics, decrease in surface roughness, and increase in free-radical concentrations [251]. Sterilization methods used for hydrogels include steam heat, ionizing irradiation, gases, and liquids [252].

Another approach is sterilization prior to hydrogel formation, which concerns *in situ* forming hydrogels. To avoid any damage on the hydrogel precursors and their functional groups, handling with care is required as well. For example, polymers such as poly[N-(2-hydroxypropyl)methacrylamide] and PVP show lower sensitivity to ionizing radiation than PEG and poly(2-ethyl-2-oxazoline) [253]. A less aggressive sterilization method is sterile filtration through a filter membrane with a maximum pore size of 0.22 μm . However, highly concentrated solutions lead to an increase in viscosity and, thus, complicate filtration. Furthermore, dissolution of these hydrogel precursors in a suitable sterilizing liquid such as ethanol is also possible. After sufficient time, the solvent has to be removed. However, until administration, work has to be carried out under sterile conditions.

9 Conclusion

Due to their complex three-dimensionality, chemically cross-linked hydrogels are a versatile material for biomedical applications such as tissue engineering, drug delivery, and personal hygiene. However, to increase the prospects of successful hydrogel development, a wide range of criteria has to be weighed. For example, hydrogels with tunable mechanical properties and stability are beneficial in the field of tissue engineering. In contrast, when used as a depot system for active pharmaceutical ingredients, factors such as release kinetics or off-target interaction should be taken into account in the selection of the respective hydrogel formulation. Biodegradation, gelation rate, and stability of the functional groups are further features that are crucial for the handling and the performance of hydrogels. In addition, it is also important to take a closer look at aspects that are often neglected such as toxicity, synthesis, and sterilization.

References

- [1] M.O. Haque, M.I.H. Mondal, Cellulose-Based Hydrogel for Personal Hygiene Applications, in: M.I.H. Mondal (Ed.), Cellulose-Based Superabsorbent Hydrogels, Springer International Publishing, Cham, 2018, pp. 1–21.
- [2] C.-H. Lin, Y.-H. Yeh, W.-C. Lin, M.-C. Yang, Novel silicone hydrogel based on PDMS and PEGMA for contact lens application, *Colloids Surf., B* 123 (2014) 986–994.
- [3] M.L. Pita-López, G. Fletes-Vargas, H. Espinosa-Andrews, R. Rodríguez-Rodríguez, Physically cross-linked chitosan-based hydrogels for tissue engineering applications: A state-of-the-art review, *Eur. Polym. J.* 145 (2021) 110176.
- [4] S. Cascone, G. Lamberti, Hydrogel-based commercial products for biomedical applications: A review, *Int. J. Pharm. (Amsterdam, Neth.)* 573 (2020) 118803.
- [5] H. Zhao, K. Xu, P. Zhu, C. Wang, Q. Chi, Smart hydrogels with high tunability of stiffness as a biomimetic cell carrier, *Cell Biol. Int.* 43 (2019) 84–97.
- [6] K. Nešović, V. Mišković-Stanković, A comprehensive review of the polymer-based hydrogels with electrochemically synthesized silver nanoparticles for wound dressing applications, *Polym. Eng. Sci.* 60 (2020) 1393–1419.
- [7] J. Bae, J. Park, S. Kim, H. Cho, H.J. Kim, S. Park, D.-S. Shin, Tailored hydrogels for biosensor applications, *J. Ind. Eng. Chem. (Amsterdam, Neth.)* 89 (2020) 1–12.
- [8] C.K. Song, M.-K. Kim, J. Lee, E. Davaa, R. Baskaran, S.-G. Yang, Dopa-Empowered Schiff Base Forming Alginate Hydrogel Glue for Rapid Hemostatic Control, *Macromol. Res.* 27 (2019) 119–125.
- [9] E.M. Ahmed, Hydrogel: Preparation, characterization, and applications: A review, *J. Adv. Res.* 6 (2015) 105–121.
- [10] R. Fang, W. He, H. Xue, W. Chen, Synthesis and characterization of a high-capacity cationic hydrogel adsorbent and its application in the removal of Acid Black 1 from aqueous solution, *React. Funct. Polym.* 102 (2016) 1–10.
- [11] X.J. Loh, *In-Situ Gelling Polymers*, Springer Singapore, Singapore, 2015.
- [12] S. Kirchhof, A.M. Goepferich, F.P. Brandl, Hydrogels in ophthalmic applications, *Eur. J. Pharm. Biopharm.* 95 (2015) 227–238.
- [13] P. Ray, M. Maity, H. Barik, G.S. Sahoo, M.S. Hasnain, M.N. Hoda, A.K. Nayak, Alginate-based hydrogels for drug delivery applications, in: *Alginates in Drug Delivery*, Elsevier, 2020, pp. 41–70.
- [14] D.E. Ciolacu, R. Nicu, F. Ciolacu, Cellulose-Based Hydrogels as Sustained Drug-Delivery Systems, *Materials* 13 (2020).
- [15] J. Yang, M. Shen, Y. Luo, T. Wu, X. Chen, Y. Wang, J. Xie, Advanced applications of chitosan-based hydrogels: From biosensors to intelligent food packaging system, *Trends Food Sci. Technol.* 110 (2021) 822–832.

-
- [16] I.S. Bayer, Hyaluronic Acid and Controlled Release: A Review, *Molecules* 25 (2020).
- [17] T. Vermonden, R. Censi, W.E. Hennink, Hydrogels for protein delivery, *Chem. Rev.* (Washington, DC, U. S.) 112 (2012) 2853–2888.
- [18] Y. Mao, M. Pan, H. Yang, X. Lin, L. Yang, Injectable hydrogel wound dressing based on strontium ion cross-linked starch, *Front. Mater. Sci.* 14 (2020) 232–241.
- [19] C. Gutierrez Cisneros, V. Bloemen, A. Mignon, Synthetic, Natural, and Semisynthetic Polymer Carriers for Controlled Nitric Oxide Release in Dermal Applications: A Review, *Polymers* (Basel, Switz.) 13 (2021).
- [20] M. Graf, C.E. Ziegler, M. Gregoritz, A.M. Goepferich, Hydrogel microspheres evading alveolar macrophages for sustained pulmonary protein delivery, *Int. J. Pharm.* (Amsterdam, Neth.) 566 (2019) 652–661.
- [21] C. Mazzuca, L. Severini, F. Domenici, Y. Toumia, F. Mazzotta, L. Micheli, M. Titubante, B. Di Napoli, G. Paradossi, A. Palleschi, Polyvinyl alcohol based hydrogels as new tunable materials for application in the cultural heritage field, *Colloids Surf., B* 188 (2020) 110777.
- [22] O. Timaeva, I. Pashkin, S. Mulakov, G. Kuzmicheva, P. Konarev, R. Terekhova, N. Sadvovskaya, O. Czakkel, S. Prevost, Synthesis and physico-chemical properties of poly(N-vinyl pyrrolidone)-based hydrogels with titania nanoparticles, *J. Mater. Sci.* 55 (2020) 3005–3021.
- [23] M.T. Frassica, S.K. Jones, J. Suriboot, A.S. Arabiyat, E.M. Ramirez, R.A. Culibrk, M.S. Hahn, M.A. Grunlan, Enhanced Osteogenic Potential of Phosphonated-Siloxane Hydrogel Scaffolds, *Biomacromolecules* 21 (2020) 5189–5199.
- [24] A. Ahsan, W.-X. Tian, M.A. Farooq, D.H. Khan, An overview of hydrogels and their role in transdermal drug delivery, *Int. J. Polym. Mater. Polym. Biomater.* 70 (2021) 574–584.
- [25] R. Parhi, Cross-Linked Hydrogel for Pharmaceutical Applications: A Review, *Adv. Pharm. Bull.* 7 (2017) 515–530.
- [26] M.W. Tibbitt, K.S. Anseth, Hydrogels as extracellular matrix mimics for 3D cell culture, *Biotechnol. Bioeng.* 103 (2009) 655–663.
- [27] A.Z. Unal, J.L. West, Synthetic ECM: Bioactive Synthetic Hydrogels for 3D Tissue Engineering, *Bioconjugate Chem.* 31 (2020) 2253–2271.
- [28] L.M. Ickenstein, P. Garidel, Hydrogel formulations for biologicals: current spotlight from a commercial perspective, *Ther. Delivery* 9 (2018) 221–230.
- [29] T.R. Hoare, D.S. Kohane, Hydrogels in drug delivery: Progress and challenges, *Polymer* 49 (2008) 1993–2007.
- [30] J.L. Dávila, M.A. d'Ávila, Laponite as a rheology modifier of alginate solutions: Physical gelation and aging evolution, *Carbohydr. Polym.* 157 (2017) 1–8.

- [31] H.H. Winter, F. Chambon, Analysis of Linear Viscoelasticity of a Crosslinking Polymer at the Gel Point, *J. Rheol.* (Melville, NY, U. S.) 30 (1986) 367–382.
- [32] A.M. Kloxin, C.J. Kloxin, C.N. Bowman, K.S. Anseth, Mechanical properties of cellularly responsive hydrogels and their experimental determination, *Adv. Mater.* 22 (2010) 3484–3494.
- [33] M. Fan, Y. Ma, Z. Zhang, J. Mao, H. Tan, X. Hu, Biodegradable hyaluronic acid hydrogels to control release of dexamethasone through aqueous Diels-Alder chemistry for adipose tissue engineering, *Mater. Sci. Eng., C* 56 (2015) 311–317.
- [34] S. Kirchhof, F.P. Brandl, N. Hammer, A.M. Goepferich, Investigation of the Diels–Alder reaction as a cross-linking mechanism for degradable poly(ethylene glycol) based hydrogels, *J. Mater. Chem. B* 1 (2013) 4855.
- [35] S. Kirchhof, M. Gregoritz, V. Messmann, N. Hammer, A.M. Goepferich, F.P. Brandl, Diels-Alder hydrogels with enhanced stability: First step toward controlled release of bevacizumab, *Eur. J. Pharm. Biopharm.* 96 (2015) 217–225.
- [36] H.-L. Wei, Z. Yang, L.-M. Zheng, Y.-M. Shen, Thermosensitive hydrogels synthesized by fast Diels–Alder reaction in water, *Polymer* 50 (2009) 2836–2840.
- [37] C.E. Ziegler, M. Graf, S. Beck, A.M. Goepferich, A novel anhydrous preparation of PEG hydrogels enables high drug loading with biologics for controlled release applications, *Eur. Polym. J.* 147 (2021) 110286.
- [38] M. Gregoritz, V. Messmann, A.M. Goepferich, F.P. Brandl, Design of hydrogels for delayed antibody release utilizing hydrophobic association and Diels–Alder chemistry in tandem, *J. Mater. Chem. B* 4 (2016) 3398–3408.
- [39] S. Kirchhof, A. Strasser, H.-J. Wittmann, V. Messmann, N. Hammer, A.M. Goepferich, F.P. Brandl, New insights into the cross-linking and degradation mechanism of Diels–Alder hydrogels, *J. Mater. Chem. B* 3 (2015) 449–457.
- [40] M. Gregoritz, V. Messmann, K. Abstiens, F.P. Brandl, A.M. Goepferich, Controlled Antibody Release from Degradable Thermoresponsive Hydrogels Cross-Linked by Diels-Alder Chemistry, *Biomacromolecules* 18 (2017) 2410–2418.
- [41] C.M. Nimmo, S.C. Owen, M.S. Shoichet, Diels-Alder Click cross-linked hyaluronic acid hydrogels for tissue engineering, *Biomacromolecules* 12 (2011) 824–830.
- [42] S. Kirchhof, M. Abrami, V. Messmann, N. Hammer, A.M. Goepferich, M. Grassi, F.P. Brandl, Diels-Alder Hydrogels for Controlled Antibody Release: Correlation between Mesh Size and Release Rate, *Mol. Pharmaceutics* 12 (2015) 3358–3368.
- [43] S. Dimida, C. Demitri, V.M. de Benedictis, F. Scalera, F. Gervaso, A. Sannino, Genipin-cross-linked chitosan-based hydrogels: Reaction kinetics and structure-related characteristics, *J. Appl. Polym. Sci.* 132 (2015) n/a-n/a.
- [44] F. Song, L.-M. Zhang, C. Yang, Li Yan, Genipin-crosslinked casein hydrogels for controlled drug delivery, *Int. J. Pharm.* (Amsterdam, Neth.) 373 (2009) 41–47.

- [45] S. Maiz-Fernández, O. Guaresti, L. Pérez-Álvarez, L. Ruiz-Rubio, N. Gabilondo, J.L. Vilas-Vilela, S. Lanceros-Mendez, β -Glycerol phosphate/genipin chitosan hydrogels: A comparative study of their properties and diclofenac delivery, *Carbohydr. Polym.* 248 (2020) 116811.
- [46] M. Clark, P. Kiser, In situ crosslinked hydrogels formed using Cu(I)-free Huisgen cycloaddition reaction, *Polym. Int.* 58 (2009) 1190–1195.
- [47] D.A. Ossipov, J. Hilborn, Poly(vinyl alcohol)-Based Hydrogels Formed by “Click Chemistry”, *Macromolecules* (Washington, DC, U. S.) 39 (2006) 1709–1718.
- [48] V. Crescenzi, L. Cornelio, C. Di Meo, S. Nardecchia, R. Lamanna, Novel hydrogels via click chemistry: synthesis and potential biomedical applications, *Biomacromolecules* 8 (2007) 1844–1850.
- [49] N.-T. Huynh, Y.-S. Jeon, D. Kim, J.-H. Kim, Preparation and swelling properties of “click” hydrogel from polyaspartamide derivatives using tri-arm PEG and PEG-co-poly(amino urethane) azides as crosslinking agents, *Polymer* 54 (2013) 1341–1349.
- [50] S.Q. Liu, P.L.R. Ee, C.Y. Ke, J.L. Hedrick, Y.Y. Yang, Biodegradable poly(ethylene glycol)-peptide hydrogels with well-defined structure and properties for cell delivery, *Biomaterials* 30 (2009) 1453–1461.
- [51] A. Koschella, M. Hartlieb, T. Heinze, A “click-chemistry” approach to cellulose-based hydrogels, *Carbohydr. Polym.* 86 (2011) 154–161.
- [52] N. Hammer, F.P. Brandl, S. Kirchof, A.M. Goepferich, Cleavable carbamate linkers for controlled protein delivery from hydrogels, *J. Controlled Release* 183 (2014) 67–76.
- [53] C.A. DeForest, K.S. Anseth, Cytocompatible click-based hydrogels with dynamically tunable properties through orthogonal photoconjugation and photocleavage reactions, *Nat. Chem.* 3 (2011) 925–931.
- [54] S.M. Hodgson, E. Bakaic, S.A. Stewart, T. Hoare, A. Adronov, Properties of Poly(ethylene glycol) Hydrogels Cross-Linked via Strain-Promoted Alkyne-Azide Cycloaddition (SPAAC), *Biomacromolecules* 17 (2016) 1093–1100.
- [55] P.J. LeValley, R. Neelarapu, B.P. Sutherland, S. Dasgupta, C.J. Kloxin, A.M. Kloxin, Photolabile Linkers: Exploiting Labile Bond Chemistry to Control Mode and Rate of Hydrogel Degradation and Protein Release, *J. Am. Chem. Soc.* 142 (2020) 4671–4679.
- [56] J. Xu, E. Feng, J. Song, Bioorthogonally cross-linked hydrogel network with precisely controlled disintegration time over a broad range, *J. Am. Chem. Soc.* 136 (2014) 4105–4108.
- [57] G.W. Ashley, J. Henise, R. Reid, D.V. Santi, Hydrogel drug delivery system with predictable and tunable drug release and degradation rates, *Proc. Natl. Acad. Sci. U. S. A.* 110 (2013) 2318–2323.
- [58] E.L. Schneider, J. Henise, R. Reid, G.W. Ashley, D.V. Santi, Hydrogel Drug Delivery System Using Self-Cleaving Covalent Linkers for Once-a-Week Administration of Exenatide, *Bioconjugate Chem.* 27 (2016) 1210–1215.

- [59] V.X. Truong, K. Zhou, G.P. Simon, J.S. Forsythe, Nitrile Oxide-Norbornene Cycloaddition as a Bioorthogonal Crosslinking Reaction for the Preparation of Hydrogels, *Macromol. Rapid Commun.* 36 (2015) 1729–1734.
- [60] V.X. Truong, M.L. Hun, F. Li, A.P. Chidgey, J.S. Forsythe, In situ-forming click-crosslinked gelatin based hydrogels for 3D culture of thymic epithelial cells, *Biomater. Sci.* 4 (2016) 1123–1131.
- [61] D.L. Alge, M.A. Azagarsamy, D.F. Donohue, K.S. Anseth, Synthetically tractable click hydrogels for three-dimensional cell culture formed using tetrazine-norbornene chemistry, *Biomacromolecules* 14 (2013) 949–953.
- [62] Z. Zhang, C. He, X. Chen, Injectable Click Polypeptide Hydrogels via Tetrazine-Norbornene Chemistry for Localized Cisplatin Release, *Polymers (Basel, Switz.)* 12 (2020).
- [63] Y. Zhang, H. Chen, T. Zhang, Y. Zan, T. Ni, M. Liu, R. Pei, Fast-forming BMSC-encapsulating hydrogels through bioorthogonal reaction for osteogenic differentiation, *Biomater. Sci.* 6 (2018) 2578–2581.
- [64] H. Zhan, H. de Jong, D.W.P.M. Löwik, Comparison of Bioorthogonally Cross-Linked Hydrogels for in Situ Cell Encapsulation, *ACS Appl. Bio Mater.* 2 (2019) 2862–2871.
- [65] C.E. Ziegler, M. Graf, M. Nagaoka, H. Lehr, A.M. Goepferich, In Situ Forming iEDDA Hydrogels with Tunable Gelation Time Release High-Molecular Weight Proteins in a Controlled Manner over an Extended Time, *Biomacromolecules* (2021).
- [66] H. Tan, C.R. Chu, K.A. Payne, K.G. Marra, Injectable in situ forming biodegradable chitosan-hyaluronic acid based hydrogels for cartilage tissue engineering, *Biomaterials* 30 (2009) 2499–2506.
- [67] H. Tan, J.P. Rubin, K.G. Marra, Injectable in situ forming biodegradable chitosan-hyaluronic acid based hydrogels for adipose tissue regeneration, *Organogenesis* 6 (2010) 173–180.
- [68] X. Ding, G. Li, C. Xiao, X. Chen, Enhancing the Stability of Hydrogels by Doubling the Schiff Base Linkages, *Macromol. Chem. Phys.* 220 (2019) 1800484.
- [69] F.-Y. Hsieh, L. Tao, Y. Wei, S.-H. Hsu, A novel biodegradable self-healing hydrogel to induce blood capillary formation, *NPG Asia Mater.* 9 (2017) e363-e363.
- [70] X. Wu, C. He, Y. Wu, X. Chen, Synergistic therapeutic effects of Schiff's base cross-linked injectable hydrogels for local co-delivery of metformin and 5-fluorouracil in a mouse colon carcinoma model, *Biomaterials* 75 (2016) 148–162.
- [71] U.G.T.M. Sampath, Y.C. Ching, C.H. Chuah, R. Singh, P.-C. Lin, Preparation and characterization of nanocellulose reinforced semi-interpenetrating polymer network of chitosan hydrogel, *Cellulose (Dordrecht, Neth.)* 24 (2017) 2215–2228.
- [72] J. Boekhoven, J.M. Poolman, C. Maity, F. Li, L. van der Mee, C.B. Minkenberg, E. Mendes, J.H. van Esch, R. Eelkema, Catalytic control over supramolecular gel formation, *Nat. Chem.* 5 (2013) 433–437.

- [73] T. Kageyama, T. Osaki, J. Enomoto, D. Myasnikova, T. Nittami, T. Hozumi, T. Ito, J. Fukuda, In Situ Cross-Linkable Gelatin-CMC Hydrogels Designed for Rapid Engineering of Perfusable Vasculatures, *ACS Biomater. Sci. Eng.* 2 (2016) 1059–1066.
- [74] J. Karvinen, T.O. Ihalainen, M.T. Calejo, I. Jönkkäri, M. Kellomäki, Characterization of the microstructure of hydrazone crosslinked polysaccharide-based hydrogels through rheological and diffusion studies, *Mater. Sci. Eng., C* 94 (2019) 1056–1066.
- [75] G.N. Grover, R.L. Braden, K.L. Christman, Oxime cross-linked injectable hydrogels for catheter delivery, *Adv. Mater.* 25 (2013) 2937–2942.
- [76] F. Lin, J. Yu, W. Tang, J. Zheng, A. Defante, K. Guo, C. Wesdemiotis, M.L. Becker, Peptide-functionalized oxime hydrogels with tunable mechanical properties and gelation behavior, *Biomacromolecules* 14 (2013) 3749–3758.
- [77] D.L. Elbert, A.B. Pratt, M.P. Lutolf, S. Halstenberg, J.A. Hubbell, Protein delivery from materials formed by self-selective conjugate addition reactions, *J. Controlled Release* 76 (2001) 11–25.
- [78] J. Wang, H. He, R.C. Cooper, H. Yang, In Situ-Forming Polyamidoamine Dendrimer Hydrogels with Tunable Properties Prepared via Aza-Michael Addition Reaction, *ACS Appl. Mater. Interfaces* 9 (2017) 10494–10503.
- [79] O. Guaresti, S. Basasoro, K. González, A. Eceiza, N. Gabilondo, In situ cross-linked chitosan hydrogels via Michael addition reaction based on water-soluble thiol-maleimide precursors, *Eur. Polym. J.* 119 (2019) 376–384.
- [80] X. Bi, A. Liang, Y. Tan, P. Maturavongsadit, A. Higginbotham, T. Gado, A. Gramling, H. Bahn, Q. Wang, Thiol-ene crosslinking polyamidoamine dendrimer-hyaluronic acid hydrogel system for biomedical applications, *J. Biomater. Sci., Polym. Ed.* 27 (2016) 743–757.
- [81] N.J. Darling, Y.-S. Hung, S. Sharma, T. Segura, Controlling the kinetics of thiol-maleimide Michael-type addition gelation kinetics for the generation of homogenous poly(ethylene glycol) hydrogels, *Biomaterials* 101 (2016) 199–206.
- [82] S.T. Lust, D. Hoogland, M.D.A. Norman, C. Kerins, J. Omar, G.M. Jowett, T.T.L. Yu, Z. Yan, J.Z. Xu, D. Marciano, R.M.P. Da Silva, C.A. Dreiss, P. Lamata, R.J. Shipley, E. Gentleman, Selectively Cross-Linked Tetra-PEG Hydrogels Provide Control over Mechanical Strength with Minimal Impact on Diffusivity, *ACS Biomater. Sci. Eng.* (2021).
- [83] A.D. Baldwin, K.L. Kiick, Reversible maleimide-thiol adducts yield glutathione-sensitive poly(ethylene glycol)-heparin hydrogels, *Polym. Chem.* 4 (2013) 133–143.
- [84] K.C. Koehler, K.S. Anseth, C.N. Bowman, Diels-Alder mediated controlled release from a poly(ethylene glycol) based hydrogel, *Biomacromolecules* 14 (2013) 538–547.
- [85] M.P. Lutolf, F.E. Weber, H.G. Schmoekel, J.C. Schense, T. Kohler, R. Müller, J.A. Hubbell, Repair of bone defects using synthetic mimetics of collagenous extracellular matrices, *Nat. Biotechnol.* 21 (2003) 513–518.

- [86] S.P. Zustiak, J.B. Leach, Hydrolytically degradable poly(ethylene glycol) hydrogel scaffolds with tunable degradation and mechanical properties, *Biomacromolecules* 11 (2010) 1348–1357.
- [87] C. Hiemstra, Z. Zhong, M.J. van Steenbergen, W.E. Hennink, J. Feijen, Release of model proteins and basic fibroblast growth factor from in situ forming degradable dextran hydrogels, *J. Controlled Release* 122 (2007) 71–78.
- [88] P. van de Wetering, A.T. Metters, R.G. Schoenmakers, J.A. Hubbell, Poly(ethylene glycol) hydrogels formed by conjugate addition with controllable swelling, degradation, and release of pharmaceutically active proteins, *J. Controlled Release* 102 (2005) 619–627.
- [89] J. Wang, R. Youngblood, L. Cassinotti, M. Skoumal, G. Corfas, L. Shea, An injectable PEG hydrogel controlling neurotrophin-3 release by affinity peptides, *J. Controlled Release* 330 (2021) 575–586.
- [90] D.B. Pike, S. Cai, K.R. Pomraning, M.A. Firpo, R.J. Fisher, X.Z. Shu, G.D. Prestwich, R.A. Peattie, Heparin-regulated release of growth factors in vitro and angiogenic response in vivo to implanted hyaluronan hydrogels containing VEGF and bFGF, *Biomaterials* 27 (2006) 5242–5251.
- [91] Z. Fan, P. Cheng, M. Liu, D. Li, G. Liu, Y. Zhao, Z. Ding, F. Chen, B. Wang, X. Tan, Z. Wang, J. Han, Poly(glutamic acid) hydrogels crosslinked via native chemical ligation, *New J. Chem.* 41 (2017) 8656–8662.
- [92] I. Strehin, D. Gourevitch, Y. Zhang, E. Heber-Katz, P.B. Messersmith, Hydrogels Formed by Oxo-ester Mediated Native Chemical Ligation, *Biomater. Sci.* 1 (2013) 603–613.
- [93] J. Su, B.-H. Hu, W.L. Lowe, D.B. Kaufman, P.B. Messersmith, Anti-inflammatory peptide-functionalized hydrogels for insulin-secreting cell encapsulation, *Biomaterials* 31 (2010) 308–314.
- [94] L.J. Macdougall, V.X. Truong, A.P. Dove, Efficient In Situ Nucleophilic Thiol-yne Click Chemistry for the Synthesis of Strong Hydrogel Materials with Tunable Properties, *ACS Macro Lett.* 6 (2017) 93–97.
- [95] L. Gao, X. Li, Y. Wang, W. Zhu, Z. Shen, X. Li, Injectable thiol-epoxy “click” hydrogels, *J. Polym. Sci. Part A: Polym. Chem.* 54 (2016) 2651–2655.
- [96] S.S. Anumolu, A.R. Menjoge, M. Deshmukh, D. Gerecke, S. Stein, J. Laskin, P.J. Sinko, Doxycycline hydrogels with reversible disulfide crosslinks for dermal wound healing of mustard injuries, *Biomaterials* 32 (2011) 1204–1217.
- [97] S.-Y. Choh, D. Cross, C. Wang, Facile synthesis and characterization of disulfide-cross-linked hyaluronic acid hydrogels for protein delivery and cell encapsulation, *Biomacromolecules* 12 (2011) 1126–1136.
- [98] R.S. Navath, A.R. Menjoge, H. Dai, R. Romero, S. Kannan, R.M. Kannan, Injectable PAMAM dendrimer-PEG hydrogels for the treatment of genital infections: formulation and in vitro and in vivo evaluation, *Mol. Pharmaceutics* 8 (2011) 1209–1223.

- [99] F. Brandl, N. Hammer, T. Blunk, J. Tessmar, A. Goepferich, Biodegradable hydrogels for time-controlled release of tethered peptides or proteins, *Biomacromolecules* 11 (2010) 496–504.
- [100] F.P. Brandl, A.K. Seitz, J.K.V. Tessmar, T. Blunk, A.M. Göpferich, Enzymatically degradable poly(ethylene glycol) based hydrogels for adipose tissue engineering, *Biomaterials* 31 (2010) 3957–3966.
- [101] S.J. Buwalda, A. Bethry, S. Hunger, S. Kandoussi, J. Coudane, B. Nottelet, Ultrafast in situ forming poly(ethylene glycol)-poly(amido amine) hydrogels with tunable drug release properties via controllable degradation rates, *Eur. J. Pharm. Biopharm.* 139 (2019) 232–239.
- [102] R. Kelmansky, A. Shagan, B. Rozenblit, R. Omar, M. Lufton, B. Mizrahi, In Situ Dual Cross-Linking of Neat Biogel with Controlled Mechanical and Delivery Properties, *Mol. Pharmaceutics* 14 (2017) 3609–3616.
- [103] R. Kelmansky, B.J. McAlvin, A. Nyska, J.C. Dohlman, H.H. Chiang, M. Hashimoto, D.S. Kohane, B. Mizrahi, Strong tissue glue with tunable elasticity, *Acta Biomater.* 53 (2017) 93–99.
- [104] N. Shimony, A. Shagan, B.-H. Eylon, A. Nyska, A. Gross, B. Mizrahi, Liquid Copolymers as Biodegradable Surgical Sealant, *Adv. Healthcare Mater.* (2021) e2100803.
- [105] A.M. Jonker, A. Borrmann, E.R.H. van Eck, F.L. van Delft, D.W.P.M. Löwik, J.C.M. van Hest, A fast and activatable cross-linking strategy for hydrogel formation, *Adv. Mater.* 27 (2015) 1235–1240.
- [106] S.-H. Kim, S.-H. Lee, J.-E. Lee, S.J. Park, K. Kim, I.S. Kim, Y.-S. Lee, N.S. Hwang, B.-G. Kim, Tissue adhesive, rapid forming, and sprayable ECM hydrogel via recombinant tyrosinase crosslinking, *Biomaterials* 178 (2018) 401–412.
- [107] O. Hasturk, K.E. Jordan, J. Choi, D.L. Kaplan, Enzymatically crosslinked silk and silk-gelatin hydrogels with tunable gelation kinetics, mechanical properties and bioactivity for cell culture and encapsulation, *Biomaterials* 232 (2020) 119720.
- [108] B.Y. Kim, Y. Lee, J.Y. Son, K.M. Park, K.D. Park, Dual Enzyme-Triggered In Situ Crosslinkable Gelatin Hydrogels for Artificial Cellular Microenvironments, *Macromol. Biosci.* 16 (2016) 1570–1576.
- [109] A. Ranga, M.P. Lutolf, J. Hilborn, D.A. Ossipov, Hyaluronic Acid Hydrogels Formed in Situ by Transglutaminase-Catalyzed Reaction, *Biomacromolecules* 17 (2016) 1553–1560.
- [110] M.R. Arkenberg, C.-C. Lin, Orthogonal enzymatic reactions for rapid crosslinking and dynamic tuning of PEG-peptide hydrogels, *Biomater. Sci.* 5 (2017) 2231–2240.
- [111] K.A. Mosiewicz, K. Johnsson, M.P. Lutolf, Phosphopantetheinyl transferase-catalyzed formation of bioactive hydrogels for tissue engineering, *J. Am. Chem. Soc.* 132 (2010) 5972–5974.
- [112] L.S.M. Teixeira, J. Feijen, C.A. van Blitterswijk, P.J. Dijkstra, M. Karperien, Enzyme-catalyzed crosslinkable hydrogels: emerging strategies for tissue engineering, *Biomaterials* 33 (2012) 1281–1290.

- [113] V. Nele, J.P. Wojciechowski, J.P.K. Armstrong, M.M. Stevens, Tailoring Gelation Mechanisms for Advanced Hydrogel Applications, *Adv. Funct. Mater.* 30 (2020) 2002759.
- [114] F.-Y. Hsieh, T.-C. Tseng, S.-H. Hsu, Self-healing hydrogel for tissue repair in the central nervous system, *Neural Regener. Res.* 10 (2015) 1922–1923.
- [115] M. Gregoritz, K. Abstiens, M. Graf, A.M. Goepferich, Fabrication of antibody-loaded microgels using microfluidics and thiol-ene photoclick chemistry, *Eur. J. Pharm. Biopharm.* 127 (2018) 194–203.
- [116] V.V. Rostovtsev, L.G. Green, V.V. Fokin, K.B. Sharpless, A Stepwise Huisgen Cycloaddition Process: Copper(I)-Catalyzed Regioselective “Ligation” of Azides and Terminal Alkynes, *Angew. Chem., Int. Ed. Engl.* 41 (2002) 2596–2599.
- [117] C.W. Tornøe, C. Christensen, M. Meldal, Peptidotriazoles on solid phase: 1,2,3-triazoles by regiospecific copper(i)-catalyzed 1,3-dipolar cycloadditions of terminal alkynes to azides, *J. Org. Chem.* 67 (2002) 3057–3064.
- [118] G.J. Brewer, Risks of copper and iron toxicity during aging in humans, *Chem. Res. Toxicol.* 23 (2010) 319–326.
- [119] Y. Jiang, J. Chen, C. Deng, E.J. Suuronen, Z. Zhong, Click hydrogels, microgels and nanogels: emerging platforms for drug delivery and tissue engineering, *Biomaterials* 35 (2014) 4969–4985.
- [120] N.J. Agard, J.A. Prescher, C.R. Bertozzi, A strain-promoted 3 + 2 azide-alkyne cycloaddition for covalent modification of biomolecules in living systems, *J. Am. Chem. Soc.* 126 (2004) 15046–15047.
- [121] J. Escorihuela, A.T.M. Marcelis, H. Zuilhof, Metal-Free Click Chemistry Reactions on Surfaces, *Adv. Mater. Interfaces* 2 (2015) 1500135.
- [122] Z. Xu, K.M. Bratlie, Click Chemistry and Material Selection for in Situ Fabrication of Hydrogels in Tissue Engineering Applications, *ACS Biomater. Sci. Eng.* 4 (2018) 2276–2291.
- [123] K. Gutmiedl, C.T. Wirges, V. Ehmke, T. Carell, Copper-free “click” modification of DNA via nitrile oxide-norbornene 1,3-dipolar cycloaddition, *Org. Lett.* 11 (2009) 2405–2408.
- [124] M. Gregoritz, F.P. Brandl, The Diels–Alder reaction: A powerful tool for the design of drug delivery systems and biomaterials, *Eur. J. Pharm. Biopharm.* 97 (2015) 438–453.
- [125] A.-C. Knall, C. Slugovc, Inverse electron demand Diels–Alder (IEDDA)-initiated conjugation: a (high) potential click chemistry scheme, *Chem. Soc. Rev.* 42 (2013) 5131–5142.
- [126] X. Bi, A. Liang, In Situ-Forming Cross-linking Hydrogel Systems: Chemistry and Biomedical Applications, in: S.B. Majee (Ed.), *Emerging Concepts in Analysis and Applications of Hydrogels*, InTech, 2016.
- [127] Q.V. Nguyen, D.P. Huynh, J.H. Park, D.S. Lee, Injectable polymeric hydrogels for the delivery of therapeutic agents: A review, *Eur. Polym. J.* 72 (2015) 602–619.

- [128] F. Cellesi, N. Tirelli, J.A. Hubbell, Materials for cell encapsulation via a new tandem approach combining reverse thermal gelation and covalent crosslinking, *Macromol. Chem. Phys.* 203 (2002) 1466–1472.
- [129] V.X. Truong, M.P. Ablett, S.M. Richardson, J.A. Hoyland, A.P. Dove, Simultaneous orthogonal dual-click approach to tough, in-situ-forming hydrogels for cell encapsulation, *J. Am. Chem. Soc.* 137 (2015) 1618–1622.
- [130] V. Delplace, P.E.B. Nickerson, A. Ortin-Martinez, A.E.G. Baker, V.A. Wallace, M.S. Shoichet, Nonswelling, Ultralow Content Inverse Electron-Demand Diels–Alder Hyaluronan Hydrogels with Tunable Gelation Time: Synthesis and In Vitro Evaluation, *Adv. Funct. Mater.* 30 (2020) 1903978.
- [131] A. Famili, K. Rajagopal, Bio-Orthogonal Cross-Linking Chemistry Enables In Situ Protein Encapsulation and Provides Sustained Release from Hyaluronic Acid Based Hydrogels, *Mol. Pharmaceutics* 14 (2017) 1961–1968.
- [132] L.J. Smith, S.M. Taimoory, R.Y. Tam, A.E.G. Baker, N. Bintah Mohammad, J.F. Trant, M.S. Shoichet, Diels-Alder Click-Cross-Linked Hydrogels with Increased Reactivity Enable 3D Cell Encapsulation, *Biomacromolecules* 19 (2018) 926–935.
- [133] J. Geittner, R. Huisgen, R. Sustmann, Kinetics of 1,3-dipolar cycloaddition reactions of diazomethane; A correlation with homo-lumo energies, *Tetrahedron Lett.* 18 (1977) 881–884.
- [134] J.C. Jewett, C.R. Bertozzi, Cu-free click cycloaddition reactions in chemical biology, *Chem. Soc. Rev.* 39 (2010) 1272–1279.
- [135] Y. Liang, J.L. Mackey, S.A. Lopez, F. Liu, K.N. Houk, Control and design of mutual orthogonality in bioorthogonal cycloadditions, *J. Am. Chem. Soc.* 134 (2012) 17904–17907.
- [136] F. Lee, J.E. Chung, M. Kurisawa, An injectable enzymatically crosslinked hyaluronic acid-hydrogel system with independent tuning of mechanical strength and gelation rate, *Soft Matter* 4 (2008) 880–887.
- [137] M.A. Haq, Y. Su, D. Wang, Mechanical properties of PNIPAM based hydrogels: A review, *Mater. Sci. Eng., C* 70 (2017) 842–855.
- [138] M.L. Oyen, Mechanical characterisation of hydrogel materials, *Int. Mater. Rev.* 59 (2014) 44–59.
- [139] F. Brandl, F. Sommer, A. Goepferich, Rational design of hydrogels for tissue engineering: impact of physical factors on cell behavior, *Biomaterials* 28 (2007) 134–146.
- [140] A. M. Grillet, N. B. Wyatt, L. M. Gloe, B., L. M., Polymer Gel Rheology and Adhesion, in: *Rheology* (2012), pp. 59–80.
- [141] H.A. Barnes, J.F. Hutton, K. Walters, An introduction to rheology, Elsevier; Distributors for the U.S. and Canada Elsevier Science Pub. Co, Amsterdam, New York, 1989.
- [142] K.S. Anseth, C.N. Bowman, L. Brannon-Peppas, Mechanical properties of hydrogels and their experimental determination, *Biomaterials* 17 (1996) 1647–1657.

- [143] L.A. Shah, R. Javed, A. Khan, I. Bibi, N.S. Khattak, S. Alam, One-Pot Synthesis and Rheological Study of Cationic Poly (3-acrylamidopropyltrimethyl ammoniumchloride) P(APTMACl) Polymer Hydrogels, *Z. Phys. Chem. (Muenchen, Ger.)* 233 (2019) 1145–1159.
- [144] N. Kong, Q. Peng, H. Li, Rationally Designed Dynamic Protein Hydrogels with Reversibly Tunable Mechanical Properties, *Adv. Funct. Mater.* 24 (2014) 7310–7317.
- [145] A.G. Savelyev, K.N. Bardakova, E.V. Khaydukov, A.N. Generalova, V.K. Popov, B.N. Chichkov, V.A. Semchishen, Flavin mononucleotide photoinitiated cross-linking of hydrogels: Polymer concentration threshold of strengthening, *J. Photochem. Photobiol., A* 341 (2017) 108–114.
- [146] M.B. Browning, T. Wilems, M. Hahn, E. Cosgriff-Hernandez, Compositional control of poly(ethylene glycol) hydrogel modulus independent of mesh size, *J. Biomed. Mater. Res., Part A* 98 (2011) 268–273.
- [147] K. Vats, G. Marsh, K. Harding, I. Zampetakis, R.E. Waugh, D.S.W. Benoit, Nanoscale physicochemical properties of chain- and step-growth polymerized PEG hydrogels affect cell-material interactions, *J. Biomed. Mater. Res., Part A* 105 (2017) 1112–1122.
- [148] M.G. Ondeck, A.J. Engler, Mechanical Characterization of a Dynamic and Tunable Methacrylated Hyaluronic Acid Hydrogel, *J. Biomech. Eng.* 138 (2016) 21003.
- [149] D. Lu, M. Zhu, J. Jin, B.R. Saunders, Triply-responsive OEG-based microgels and hydrogels: regulation of swelling ratio, volume phase transition temperatures and mechanical properties, *Polym. Chem.* (2021).
- [150] J.W. Seo, S.R. Shin, M.-Y. Lee, J.M. Cha, K.H. Min, S.C. Lee, S.Y. Shin, H. Bae, Injectable hydrogel derived from chitosan with tunable mechanical properties via hybrid-crosslinking system, *Carbohydr. Polym.* 251 (2021) 117036.
- [151] M. Dolmat, V. Kozlovskaya, D. Crokek, E. Kharlampieva, Free-Standing Thin Hydrogels: Effects of Composition and pH-Dependent Hydration on Mechanical Properties, *ACS Appl. Polym. Mater.* (2021).
- [152] J.A. Burdick, W.L. Murphy, Moving from static to dynamic complexity in hydrogel design, *Nat. Commun.* 3 (2012) 1269.
- [153] J.V. Alemán, A.V. Chadwick, J. He, M. Hess, K. Horie, R.G. Jones, P. Kratochvíl, I. Meisel, I. Mita, G. Moad, S. Penczek, R.F.T. Stepto, Definitions of terms relating to the structure and processing of sols, gels, networks, and inorganic-organic hybrid materials (IUPAC Recommendations 2007), *Pure Appl. Chem.* 79 (2007) 1801–1829.
- [154] Y.-S. Jung, W. Park, H. Park, D.-K. Lee, K. Na, Thermo-sensitive injectable hydrogel based on the physical mixing of hyaluronic acid and Pluronic F-127 for sustained NSAID delivery, *Carbohydr. Polym.* 156 (2017) 403–408.
- [155] K. Haraguchi, T. Takehisa, Nanocomposite Hydrogels: A Unique Organic–Inorganic Network Structure with Extraordinary Mechanical, Optical, and Swelling/De-swelling Properties, *Adv. Mater.* 14 (2002) 1120.

- [156] J.K. Carrow, A.K. Gaharwar, Bioinspired Polymeric Nanocomposites for Regenerative Medicine, *Macromol. Chem. Phys.* 216 (2015) 248–264.
- [157] S. Faghihi, M. Gheysour, A. Karimi, R. Salarian, Fabrication and mechanical characterization of graphene oxide-reinforced poly (acrylic acid)/gelatin composite hydrogels, *J. Appl. Phys.* (Melville, NY, U. S.) 115 (2014) 83513.
- [158] A.T. Metters, C.N. Bowman, K.S. Anseth, A Statistical Kinetic Model for the Bulk Degradation of PLA- b -PEG- b -PLA Hydrogel Networks, *J. Phys. Chem. B* 104 (2000) 7043–7049.
- [159] X. Zhang, S. Malhotra, M. Molina, R. Haag, Micro- and nanogels with labile crosslinks - from synthesis to biomedical applications, *Chem. Soc. Rev.* 44 (2015) 1948–1973.
- [160] G. Zhang, Q. Zhao, L. Yang, W. Zou, X. Xi, T. Xie, Exploring Dynamic Equilibrium of Diels–Alder Reaction for Solid State Plasticity in Remoldable Shape Memory Polymer Network, *ACS Macro Lett.* 5 (2016) 805–808.
- [161] M.D. Konieczynska, M.W. Grinstaff, On-Demand Dissolution of Chemically Cross-Linked Hydrogels, *Acc. Chem. Res.* 50 (2017) 151–160.
- [162] C. Mo, Li Xiang, Y. Chen, Advances in Injectable and Self-healing Polysaccharide Hydrogel Based on the Schiff Base Reaction, *Macromol. Rapid Commun.* 42 (2021) e2100025.
- [163] Li Liu, J.-P. Yang, X.-J. Ju, R. Xie, Y.-M. Liu, W. Wang, J.-J. Zhang, C.H. Niu, L.-Y. Chu, Monodisperse core-shell chitosan microcapsules for pH-responsive burst release of hydrophobic drugs, *Soft Matter* 7 (2011) 4821.
- [164] C.C. Deng, W.L. Brooks, K.A. Abboud, B.S. Sumerlin, Boronic Acid-Based Hydrogels Undergo Self-Healing at Neutral and Acidic pH, *ACS Macro Lett.* 4 (2015) 220–224.
- [165] M.E. Smithmyer, C.C. Deng, S.E. Cassel, P.J. LeValley, B.S. Sumerlin, A.M. Kloxin, Self-healing boronic acid-based hydrogels for 3D co-cultures, *ACS Macro Lett.* 7 (2018) 1105–1110.
- [166] W. Shi, B. Hass, M.A. Kuss, H. Zhang, S. Ryu, D. Zhang, T. Li, Y.-L. Li, B. Duan, Fabrication of versatile dynamic hyaluronic acid-based hydrogels, *Carbohydr. Polym.* 233 (2020) 115803.
- [167] J. Su, Thiol-Mediated Chemoselective Strategies for In Situ Formation of Hydrogels, *Gels* 4 (2018).
- [168] A.D. Baldwin, K.L. Kiick, Tunable degradation of maleimide-thiol adducts in reducing environments, *Bioconjugate Chem.* 22 (2011) 1946–1953.
- [169] J. Hansen, N. Mørk, H. Bundgaard, Phenyl carbamates of amino acids as prodrug forms for protecting phenols against first-pass metabolism, *Int. J. Pharm. (Amsterdam, Neth.)* 81 (1992) 253–261.
- [170] A.F. Hegarty, L.N. Frost, Elimination–addition mechanism for the hydrolysis of carbamates. Trapping of an isocyanate intermediate by an o-amino-group, *J. Chem. Soc., Perkin Trans. 2* (1972-1999) (1973) 1719–1728.

- [171] N. McCann, D. Phan, D. Fernandes, M. Maeder, A systematic investigation of carbamate stability constants by ¹H NMR, *Int. J. Greenhouse Gas Control* 5 (2011) 396–400.
- [172] S. Oldenhof, S. Mytnyk, A. Arranja, M. de Puit, J.H. van Esch, Imaging-assisted hydrogel formation for single cell isolation, *Sci. Rep.* 10 (2020) 6595.
- [173] W. Kang, B. Bi, R. Zhuo, X. Jiang, Photocrosslinked methacrylated carboxymethyl chitin hydrogels with tunable degradation and mechanical behavior, *Carbohydr. Polym.* 160 (2017) 18–25.
- [174] H.W. Ng, Y. Zhang, R. Naffa, S. Prabakar, Monitoring the Degradation of Collagen Hydrogels by Collagenase *Clostridium histolyticum*, *Gels* 6 (2020).
- [175] C. Liu, Z. Zhang, X. Liu, X. Ni, J. Li, Gelatin-based hydrogels with β -cyclodextrin as a dual functional component for enhanced drug loading and controlled release, *RSC Adv.* 3 (2013) 25041.
- [176] S. Pan, X. Yin, Y.-F. He, Y. Xiong, R.-M. Wang, Influence of Preparation Conditions on the Properties of Keratin-Based Polymer Hydrogel, *Arabian J. Sci. Eng.* 40 (2015) 2853–2859.
- [177] S.J. Buwalda, T. Vermonden, W.E. Hennink, Hydrogels for Therapeutic Delivery: Current Developments and Future Directions, *Biomacromolecules* 18 (2017) 316–330.
- [178] P. Scrimin, P. Tecilla, U. Tonellato, Leaving group effect in the cleavage of picolinate esters catalyzed by hydroxy-functionalized metallomicelles, *J. Org. Chem.* 59 (1994) 18–24.
- [179] D. Stefanidis, W.P. Jencks, General base catalysis of ester hydrolysis, *J. Am. Chem. Soc.* 115 (1993) 6045–6050.
- [180] V. Nummert, M. Piirsalu, V. Mäemets, I. Koppel, Kinetic Study of Hydrolysis of Benzoates. Part XXV. Ortho Substituent Effect in Alkaline Hydrolysis of Phenyl Esters of Substituted Benzoic Acids in Water, *Collect. Czech. Chem. Commun.* 71 (2006) 107–128.
- [181] N.G. Ricapito, J. Mares, D. Petralia, D. Putnam, Insight into the Unexpectedly Rapid Degradation of Dihydroxyacetone-Based Hydrogels, *Macromol. Chem. Phys.* 217 (2016) 1917–1925.
- [182] K. Bowden, Intramolecular catalysis: carbonyl groups in ester hydrolysis, *Chem. Soc. Rev.* 24 (1995) 431.
- [183] W.N.E. van Dijk-Wolthuis, J.A.M. Hoogeboom, M.J. van Steenberg, S.K.Y. Tsang, W.E. Hennink, Degradation and Release Behavior of Dextran-Based Hydrogels, *Macromolecules (Washington, DC, U. S.)* 30 (1997) 4639–4645.
- [184] C. Yang, A. Lee, S. Gao, S. Liu, J.L. Hedrick, Y.Y. Yang, Hydrogels with prolonged release of therapeutic antibody: Block junction chemistry modification of 'ABA' copolymers provides superior anticancer efficacy, *J. Controlled Release* 293 (2019) 193–200.
- [185] B.C. Ilochonwu, A. Urtti, W.E. Hennink, T. Vermonden, Intravitreal hydrogels for sustained release of therapeutic proteins, *J. Controlled Release* 326 (2020) 419–441.

- [186] J. Wang, S. Yang, K. Zhang, Multi-arm PEG-maleimide conjugation intermediate characterization and hydrolysis study by a selective HPLC method, *J. Pharm. Biomed. Anal.* 164 (2019) 452–459.
- [187] R.I. Nathani, V. Chudasama, C.P. Ryan, P.R. Moody, R.E. Morgan, R.J. Fitzmaurice, M.E.B. Smith, J.R. Baker, S. Caddick, Reversible protein affinity-labelling using bromomaleimide-based reagents, *Org. Biomol. Chem.* 11 (2013) 2408–2411.
- [188] S. Matsui, H. Aida, Hydrolysis of some N-alkylmaleimides, *J. Chem. Soc., Perkin Trans. 2* (1972-1999) (1978) 1277.
- [189] S. Zalipsky, Alkyl succinimidyl carbonates undergo Lossen rearrangement in basic buffers, *Chem. Commun. (Cambridge, U. K.)* (1998) 69–70.
- [190] J.C. Oxley, J.L. Smith, J. Zhang, Decomposition Pathways of Some 3,6-Substituted s - Tetrazines, *J. Phys. Chem. A* 104 (2000) 6764–6777.
- [191] M.R. Karver, R. Weissleder, S.A. Hilderbrand, Synthesis and evaluation of a series of 1,2,4,5-tetrazines for bioorthogonal conjugation, *Bioconjugate Chem.* 22 (2011) 2263–2270.
- [192] P.W. Groundwater, M. Nyerges, I. Fejes, D.E. Hibbs, D. Bendell, R.J. Anderson, A. McKillop, T. Sharif, W. Zhang, Preparation and reactivity of some stable nitrile oxides and nitrones, *ARKIVOC (Gainesville, FL, U. S.)* 2000 (2000) 684–697.
- [193] K. Bast, M. Christl, R. Huisgen, W. Mack, 1,3-Dipolare Cycloadditionen, 68. Additionen der Nitriloxide an CN-Mehrfachbindungen, *Chem. Ber.* 105 (1972) 2825–2840.
- [194] A. Borrmann, O. Fatunsin, J. Dommerholt, A.M. Jonker, D.W.P.M. Löwik, J.C.M. van Hest, F.L. van Delft, Strain-promoted oxidation-controlled cyclooctyne-1,2-quinone cycloaddition (SPOCQ) for fast and activatable protein conjugation, *Bioconjugate Chem.* 26 (2015) 257–261.
- [195] D.P. Tabor, R. Gómez-Bombarelli, L. Tong, R.G. Gordon, M.J. Aziz, A. Aspuru-Guzik, Mapping the frontiers of quinone stability in aqueous media: implications for organic aqueous redox flow batteries, *J. Mater. Chem. A* 7 (2019) 12833–12841.
- [196] R. Stevens, L. Stevens, N.C. Price, The stabilities of various thiol compounds used in protein purifications, *Biochem. Educ.* 11 (1983) 70.
- [197] J.-B. Béquignat, N. Ty, A. Rondon, L. Taiariol, F. Degoul, D. Canitrot, M. Quintana, I. Navarro-Teulon, E. Miot-Noirault, C. Boucheix, J.-M. Chezal, E. Moreau, Optimization of IEDDA bioorthogonal system: Efficient process to improve trans-cyclooctene/tetrazine interaction, *Eur. J. Med. Chem.* 203 (2020) 112574.
- [198] F. Thalhammer, U. Wallfahrer, J. Sauer, Reaktivität einfacher offenkettiger und cyclischer dienophile bei Diels-Alder-reaktionen mit inversem elektronenbedarf, *Tetrahedron Lett.* 31 (1990) 6851–6854.
- [199] M.T. Taylor, M.L. Blackman, O. Dmitrenko, J.M. Fox, Design and synthesis of highly reactive dienophiles for the tetrazine-trans-cyclooctene ligation, *J. Am. Chem. Soc.* 133 (2011) 9646–9649.

- [200] R. Rossin, S.M. van den Bosch, W. ten Hoeve, M. Carvelli, R.M. Versteegen, J. Lub, M.S. Robillard, Highly reactive trans-cyclooctene tags with improved stability for Diels-Alder chemistry in living systems, *Bioconjugate Chem.* 24 (2013) 1210–1217.
- [201] Arthur C. Cope/Beverly A. Pawson, Molecular Asymmetry of Olefins. IV. Kinetics of Racemization of (+ or -)-trans-Cyclooctene¹.
- [202] Yoshihisa Inoue/Tomokazu Kobata/Tadao Hakushi, Reinvestigation of triplet-sensitized cis-trans photoisomerization of cyclooctene. Alkene-concentration and sensitizer-ET dependence of photostationary trans/cis ratio.
- [203] A. Darko, S. Wallace, O. Dmitrenko, M.M. Machovina, R.A. Mehl, J.W. Chin, J.M. Fox, Conformationally Strained trans-Cyclooctene with Improved Stability and Excellent Reactivity in Tetrazine Ligation, *Chem. Sci.* 5 (2014) 3770–3776.
- [204] C. Wang, H. Zhang, T. Zhang, X. Zou, H. Wang, J.E. Rosenberger, R. Vannam, W.S. Trout, J.B. Grimm, L.D. Lavis, C. Thorpe, X. Jia, Z. Li, J.M. Fox, Enabling In Vivo Photocatalytic Activation of Rapid Bioorthogonal Chemistry by Repurposing Silicon-Rhodamine Fluorophores as Cytocompatible Far-Red Photocatalysts, *J. Am. Chem. Soc.* 143 (2021) 10793–10803.
- [205] A.T. Blomquist, L.H. Liu, Many-membered Carbon Rings. VII. Cyclooctyne, *J. Am. Chem. Soc.* 75 (1953) 2153–2154.
- [206] L.K. Montgomery, L.E. Applegate, Quantitative evidence concerning the relative stabilities of cycloalkynes and arynes, *J. Am. Chem. Soc.* 89 (1967) 5305–5307.
- [207] E.M. Sletten, H. Nakamura, J.C. Jewett, C.R. Bertozzi, Difluorobenzocyclooctyne: synthesis, reactivity, and stabilization by beta-cyclodextrin, *J. Am. Chem. Soc.* 132 (2010) 11799–11805.
- [208] G. de Almeida, E.M. Sletten, H. Nakamura, K.K. Palaniappan, C.R. Bertozzi, Thiacycloalkynes for Copper-Free Click Chemistry, *Angew. Chem.* 124 (2012) 2493–2497.
- [209] R. Chadwick, S. van Gyzen, S. Liogier, A. Adronov, Scalable Synthesis of Strained Cyclooctyne Derivatives, *Synthesis* 46 (2014) 669–677.
- [210] M. Gregoritzka, A.M. Goepferich, F.P. Brandl, Polyanions effectively prevent protein conjugation and activity loss during hydrogel cross-linking, *J. Controlled Release* 238 (2016) 92–102.
- [211] C.-C. Lin, K.S. Anseth, PEG hydrogels for the controlled release of biomolecules in regenerative medicine, *Pharm. Res.* 26 (2009) 631–643.
- [212] N. Hammer, F.P. Brandl, S. Kirchhof, V. Messmann, A.M. Goepferich, Protein compatibility of selected cross-linking reactions for hydrogels, *Macromol. Biosci.* 15 (2015) 405–413.
- [213] J.A. Bell, K.P. Wilson, X.J. Zhang, H.R. Faber, H. Nicholson, B.W. Matthews, Comparison of the crystal structure of bacteriophage T4 lysozyme at low, medium, and high ionic strengths, *Proteins: Struct., Funct., Genet.* 10 (1991) 10–21.

- [214] D. Sehnal, S. Bittrich, M. Deshpande, R. Svobodová, K. Berka, V. Bazgier, S. Velankar, S.K. Burley, J. Koča, A.S. Rose, Mol* Viewer: modern web app for 3D visualization and analysis of large biomolecular structures, *Nucleic Acids Res.* 49 (2021) W431–W437.
- [215] T. Kämpchen, W. Massa, W. Overheu, R. Schmidt, G. Seitz, Zur Kenntnis von Reaktionen des 1,2,4,5-Tetrazin-3,6-dicarbonsäure-dimethylesters mit Nucleophilen, *Chem. Ber.* 115 (1982) 683–694.
- [216] H. Zhao, J.H. Waite, Linking adhesive and structural proteins in the attachment plaque of *Mytilus californianus*, *J. Biol. Chem.* 281 (2006) 26150–26158.
- [217] F. de Sarlo, A. Guarna, Behaviour of nitrile oxides towards nucleophiles. Part II. Substituent effect on the rate of dimerisation of aromatic nitrile oxides to 3,6-diaryl-1,4,2,5-dioxadiazines, *J. Chem. Soc., Perkin Trans. 2* (1972–1999) (1976) 626.
- [218] M. Friedman, J.F. Cavins, J.S. Wall, Relative Nucleophilic Reactivities of Amino Groups and Mercaptide Ions in Addition Reactions with α,β -Unsaturated Compounds 1,2, *J. Am. Chem. Soc.* 87 (1965) 3672–3682.
- [219] A.S. Yang, B. Honig, On the pH dependence of protein stability, *J. Mol. Biol.* 231 (1993) 459–474.
- [220] R. Censi, T. Vermonden, M.J. van Steenberg, H. Deschout, K. Braeckmans, S.C. de Smedt, C.F. van Nostrum, P. Di Martino, W.E. Hennink, Photopolymerized thermosensitive hydrogels for tailorable diffusion-controlled protein delivery, *J. Controlled Release* 140 (2009) 230–236.
- [221] M. Stanković, H.W. Frijlink, W.L.J. Hinrichs, Polymeric formulations for drug release prepared by hot melt extrusion: application and characterization, *Drug Discovery Today* 20 (2015) 812–823.
- [222] V. Huynh, R.G. Wylie, Competitive Affinity Release for Long-Term Delivery of Antibodies from Hydrogels, *Angew. Chem., Int. Ed. Engl.* 57 (2018) 3406–3410.
- [223] J. Li, D.J. Mooney, Designing hydrogels for controlled drug delivery, *Nat. Rev. Mater.* 1 (2016).
- [224] F. Brandl, F. Kastner, R.M. Gschwind, T. Blunk, J. Tessmar, A. Göpferich, Hydrogel-based drug delivery systems: comparison of drug diffusivity and release kinetics, *J. Controlled Release* 142 (2010) 221–228.
- [225] M.S. Rehmann, K.M. Skeens, P.M. Kharkar, E.M. Ford, E. Maverakis, K.H. Lee, A.M. Kloxin, Tuning and Predicting Mesh Size and Protein Release from Step Growth Hydrogels, *Biomacromolecules* 18 (2017) 3131–3142.
- [226] M.P. Di Cagno, F. Clarelli, J. Våbenø, C. Lesley, S.D. Rahman, J. Cauzzo, E. Franceschinis, N. Realdon, P.C. Stein, Experimental Determination of Drug Diffusion Coefficients in Unstirred Aqueous Environments by Temporally Resolved Concentration Measurements, *Mol. Pharmaceutics* 15 (2018) 1488–1494.

- [227] S.K. Li, M.R. Liddell, H. Wen, Effective electrophoretic mobilities and charges of anti-VEGF proteins determined by capillary zone electrophoresis, *J. Pharm. Biomed. Anal.* 55 (2011) 603–607.
- [228] S. Nakamura, S. Hayashi, K. Koga, Effect of periodate oxidation on the structure and properties of glucose oxidase, *Biochim. Biophys. Acta* 445 (1976) 294–308.
- [229] J. Danielsson, J. Jarvet, P. Damberg, A. Gräslund, Translational diffusion measured by PFG-NMR on full length and fragments of the Alzheimer A β (1-40) peptide. Determination of hydrodynamic radii of random coil peptides of varying length, *Magn. Reson. Chem.* 40 (2002) S89-S97.
- [230] S.G. SCHULTZ, A.K. SOLOMON, Determination of the effective hydrodynamic radii of small molecules by viscometry, *J. Gen. Physiol.* 44 (1961) 1189–1199.
- [231] P. Akbarzadehlaleh, M. Mirzaei, M. Mashahdi-keshtiban, H.R. Heidari, The Effect of Length and Structure of Attached Polyethylene Glycol Chain on Hydrodynamic Radius, and Separation of PEGylated Human Serum Albumin by Chromatography, *Adv. Pharm. Bull.* (2020).
- [232] B. Amsden, Solute Diffusion within Hydrogels. Mechanisms and Models, *Macromolecules* (Washington, DC, U. S.) 31 (1998) 8382–8395.
- [233] S.R. Lustig, N.A. Peppas, Solute diffusion in swollen membranes. IX. Scaling laws for solute diffusion in gels, *J. Appl. Polym. Sci.* 36 (1988) 735–747.
- [234] D.J. Waters, K. Engberg, R. Parke-Houben, L. Hartmann, C.N. Ta, M.F. Toney, C.W. Frank, Morphology of Photopolymerized End-linked Poly(ethylene glycol) Hydrogels by Small Angle X-ray Scattering, *Macromolecules* (Washington, DC, U. S.) 43 (2010) 6861–6870.
- [235] M. Iza, S. Woerly, C. Danumah, S. Kaliaguine, M. Bousmina, Determination of pore size distribution for mesoporous materials and polymeric gels by means of DSC measurements: thermoporometry, *Polymer* 41 (2000) 5885–5893.
- [236] P.J. Flory, Principles of polymer chemistry, 10th edn ed., Cornell Univ. Press, Ithaca, N. Y., Ithaca, N. Y., 1953.
- [237] J.C. Bray, E.W. Merrill, Poly(vinyl alcohol) hydrogels. Formation by electron beam irradiation of aqueous solutions and subsequent crystallization, *J. Appl. Polym. Sci.* 17 (1973) 3779–3794.
- [238] T. Canal, N.A. Peppas, Correlation between mesh size and equilibrium degree of swelling of polymeric networks, *J. Biomed. Mater. Res.* 23 (1989) 1183–1193.
- [239] G. Wohlfahrt, S. Witt, J. Hendle, D. Schomburg, H.M. Kalisz, H.-J. Hecht, 1.8 and 1.9Å resolution structures of the -Penicillium amagasakiense and Aspergillus niger glucose oxidases as a basis for modelling substrate complexes, *Acta Crystallogr., Sect. D: Struct. Biol.*
- [240] J.J. Grigsby, H.W. Blanch, J.M. Prausnitz, Diffusivities of Lysozyme in Aqueous MgCl₂ Solutions from Dynamic Light-Scattering Data: Effect of Protein and Salt Concentrations, *J. Phys. Chem. B* 104 (2000) 3645–3650.

- [241] K.W. Lee, J.J. Yoon, J.H. Lee, S.Y. Kim, H.J. Jung, S.J. Kim, J.W. Joh, H.H. Lee, D.S. Lee, S.K. Lee, Sustained release of vascular endothelial growth factor from calcium-induced alginate hydrogels reinforced by heparin and chitosan, *Transplant. Proc.* 36 (2004) 2464–2465.
- [242] S. Koutsopoulos, S. Zhang, Two-layered injectable self-assembling peptide scaffold hydrogels for long-term sustained release of human antibodies, *J. Controlled Release* 160 (2012) 451–458.
- [243] U. Bhardwaj, R. Sura, F. Papadimitrakopoulos, D.J. Burgess, PLGA/PVA hydrogel composites for long-term inflammation control following s.c. implantation, *Int. J. Pharm. (Amsterdam, Neth.)* 384 (2010) 78–86.
- [244] Q. Peng, X. Sun, T. Gong, C.-Y. Wu, T. Zhang, J. Tan, Z.-R. Zhang, Injectable and biodegradable thermosensitive hydrogels loaded with PHBHHx nanoparticles for the sustained and controlled release of insulin, *Acta Biomater.* 9 (2013) 5063–5069.
- [245] T. Ci, Y. Shen, S. Cui, R. Liu, L. Yu, J. Ding, Achieving High Drug Loading and Sustained Release of Hydrophobic Drugs in Hydrogels through In Situ Crystallization, *Macromol. Biosci.* 17 (2017).
- [246] M.B. Mellott, K. Searcy, M.V. Pishko, Release of protein from highly cross-linked hydrogels of poly(ethylene glycol) diacrylate fabricated by UV polymerization, *Biomaterials* 22 (2001) 929–941.
- [247] J. Li, E. Weber, S. Guth-Gundel, M. Schuleit, A. Kuttler, C. Halleux, N. Accart, A. Doelemeyer, A. Basler, B. Tigani, K. Wuersch, M. Fornaro, M. Kneissel, A. Stafford, B.R. Freedman, D.J. Mooney, Tough Composite Hydrogels with High Loading and Local Release of Biological Drugs, *Adv. Healthcare Mater.* 7 (2018) e1701393.
- [248] S.J. Shire, Z. Shahrokh, J. Liu, Challenges in the development of high protein concentration formulations, *J. Pharm. Sci.* 93 (2004) 1390–1402.
- [249] G.I. Frost, Recombinant human hyaluronidase (rHuPH20): an enabling platform for subcutaneous drug and fluid administration, *Expert Opin. Drug Delivery* 4 (2007) 427–440.
- [250] E.M.F. Billaud, E. Shahbazali, M. Ahamed, F. Cleeren, T. Noël, M. Koole, A. Verbruggen, V. Hessel, G. Bormans, Micro-flow photosynthesis of new dienophiles for inverse-electron-demand Diels-Alder reactions. Potential applications for pretargeted in vivo PET imaging, *Chem. Sci.* 8 (2017) 1251–1258.
- [251] D. Kanjickal, S. Lopina, M.M. Evancho-Chapman, S. Schmidt, D. Donovan, Effects of sterilization on poly(ethylene glycol) hydrogels, *J. Biomed. Mater. Res., Part A* 87 (2008) 608–617.
- [252] R. Galante, T.J.A. Pinto, R. Colaço, A.P. Serro, Sterilization of hydrogels for biomedical applications: A review, *J. Biomed. Mater. Res., Part B* 106 (2018) 2472–2492.
- [253] O. Sedlacek, J. Kucka, B.D. Monnery, M. Slouf, M. Vetrik, R. Hoogenboom, M. Hruby, The effect of ionizing radiation on biocompatible polymers: From sterilization to radiolysis and hydrogel formation, *Polym. Degrad. Stab.* 137 (2017) 1–10.

Chapter 2

Goals of the thesis

Besides applications such as tissue engineering, wound dressing, and contact lenses hydrogels serve as powerful platform for the preparation of drug delivery systems to treat various diseases [1,2]. Especially, *in situ* forming hydrogels being used as drug depots are advantageous since they can be administered simply via injection [3]. Thereby, more benefit of hydrogels is achieved with the ability to release the cargo continuously over a long timescale avoiding booster injections and increasing therapeutic success. In this regard, there are many approaches among hydrogel cargo combinations for a multitude of diseases. A very attractive opportunity is the delivery of biopharmaceuticals. In recent years, a great deal of effort has been invested in the research and development of this class, which includes a broad spectrum of pharmaceutical drugs originating from biological sources [4]. Due to their suitable size, therapeutic proteins in particular show great potential for the controlled release from the three-dimensional structure of hydrogels. These proteins are used for the treatment of various diseases such as age-related macular degeneration, cancer, rheumatoid arthritis, or psoriasis [5–8]. Conventionally, they are injected intravenously at a specific interval to maintain therapeutic levels. For example, the human epidermal growth factor receptor 2 monoclonal antibody trastuzumab is administered once every three weeks over a time of a year for the treatment of early-stage breast cancer [9]. However, the systemic administration of high doses of these proteins might cause side effects such as cardiac dysfunction or immune reactions [10]. Here, the use of hydrogels as drug depots is of great benefit in the delivery of therapeutic proteins since high antibody doses can be avoided while maintaining the therapeutic level over a long timescale, leading to reduced side effects.

While a high quantity of literature reveals the effort that was devoted to this field, there are still limitations complicating the successful usage of hydrogels for protein delivery as described in **Chapter 1**. Even though water compared to alternative solvents such as NMP or DMSO is beneficial regarding compatibility and creating a microenvironment for biopharmaceuticals similar to tissues [11], many of these obstacles originate from its use. For example, the presence of water can impact the stability of the hydrogel precursor and the protein and can facilitate off-target reactions between functional groups of the polymer moieties and the cargo [12,13]. Furthermore, polymeric systems with a high amount of water often show reduced mechanical properties and low drug loading capacity [14]. Thereby, an obvious exchange of water to an organic solvent would only shift the issue. Therefore, the goal of the thesis was to develop anhydrous *in situ* forming hydrogels for the controlled release of proteins over an extended time. In this way, the benefits of hydrogels as protein delivery systems were maintained while avoiding the water-related drawbacks of conventional hydrogel preparation.

To enable solvent-free cross-linking, the mobility of the macromonomers has to be ensured by another way for competitive groups to find and react with each other. In the first approach, furan- and maleimide-functionalized eight-armed poly(ethylene glycol) (PEG), which were used for the preparation of conventional hydrogels so far, were investigated for solvent-free polymerization via Diels-Alder (DA) reaction and the ability of embedding proteins. This was to be achieved by working above the melting point of these precursors. In this way, hydrolysis-prone maleimide groups should be protected and off-

target reactions between proteins and polymer moieties prevented. In addition, due to the absence of solvent, more space should be provided for the cargo, leading to an increased loading capacity without the release kinetics being impacted by the loading level (**Chapter 3**).

The DA reaction between furan and maleimide offers many benefits (e.g., no toxic side-products, reversible cross-linking, no requirement of catalysts). However, the slow reaction kinetics does not allow the DA reaction for the preparation of *in situ* forming hydrogels. To solve this, the fast-proceeding inverse electron demand Diels-Alder (iEDDA) reaction between norbornene and tetrazine could be used as cross-linking reaction. As additional advantage, this reaction exhibits bioorthogonality resulting in reduced off-target reactions with proteins in aqueous solution. To assess the suitability of the iEDDA reaction as cross-linking reaction in combination with multi-armed PEG macromonomers for the preparation of protein delivery systems, eight-armed PEGs were modified with norbornene and tetrazine. The resulting conventional hydrogels were characterized regarding gelation time, off-target reaction, stability, and protein release (**Chapter 4**).

As mentioned above, the iEDDA reaction between norbornene and tetrazine shows a substantially higher reaction rate than the classical DA reaction without losing the same benefits. Only reversibility is no longer feasible due to the additional formation of nitrogen. To prepare biodegradable hydrogels, the incorporation of cleavable groups into the hydrogel precursors is necessary. To achieve this, different hydrolyzable groups were synthesized into the macromonomers, and the degradation time of the hydrogels was measured. Moreover, the impact of the cleavable groups on the gelation time, mechanical properties, and release was investigated (**Chapter 5**).

Finally, an administration of a water-free protein depot via simple injection would be superior to surgical implantation regarding patient compliance and personnel costs. In this way, complementarily modified macromonomers that are liquid below body temperature would lead to the formation of a protein delivery system after contact. However, eight-armed PEGs show melting points above 37 °C. Therefore, four-armed PEG macromonomers with a small molecular weight that are liquid even at low temperatures were functionalized with norbornene and tetrazine. The polymerization time, mechanical properties, and polymer structure were analyzed as a function of the chemical nature of the used functional groups. Moreover, biodegradation and protein release were evaluated (**Chapter 6**).

References

- [1] G. Orsborn, K. Dumbleton, Eye care professionals' perceptions of the benefits of daily disposable silicone hydrogel contact lenses, *Cont. Lens. Anterior Eye* 42 (2019) 373–379.
- [2] S. Jacob, A.B. Nair, J. Shah, N. Sreeharsha, S. Gupta, P. Shinu, Emerging Role of Hydrogels in Drug Delivery Systems, *Tissue Engineering and Wound Management, Pharmaceutics* 13 (2021).
- [3] G.R. Shin, H.E. Kim, J.H. Kim, S. Choi, M.S. Kim, Advances in Injectable In Situ-Forming Hydrogels for Intratumoral Treatment, *Pharmaceutics* 13 (2021).
- [4] Y.-C. Chen, M.-K. Yeh, Introductory Chapter: Biopharmaceuticals, in: M.-K. Yeh, Y.-C. Chen (Eds.), *Biopharmaceuticals*, InTech, 2018.
- [5] H.A. Blair, Risankizumab: A Review in Moderate to Severe Plaque Psoriasis, *Drugs* 80 (2020) 1235–1245.
- [6] F. Ursini, C. Leporini, F. Bene, S. D'Angelo, D. Mauro, E. Russo, G. de Sarro, I. Olivieri, C. Pitzalis, M. Lewis, R.D. Grembiale, Anti-TNF-alpha agents and endothelial function in rheumatoid arthritis: a systematic review and meta-analysis, *Sci. Rep.* 7 (2017) 5346.
- [7] A.J. Genuino, U. Chaikledkaew, D.O. The, T. Reungwetwattana, A. Thakkestian, Adjuvant trastuzumab regimen for HER2-positive early-stage breast cancer: a systematic review and meta-analysis, *Expert Rev. Clin. Pharmacol.* 12 (2019) 815–824.
- [8] S.R. Rufai, H. Almuhtaseb, R.M. Paul, B.L. Stuart, T. Kendrick, H. Lee, A.J. Lotery, A systematic review to assess the 'treat-and-extend' dosing regimen for neovascular age-related macular degeneration using ranibizumab, *Eye (London, U. K.)* 31 (2017) 1337–1344.
- [9] K. Xu, F. Lee, S. Gao, M.-H. Tan, M. Kurisawa, Hyaluronidase-incorporated hyaluronic acid-tyramine hydrogels for the sustained release of trastuzumab, *J. Controlled Release* 216 (2015) 47–55.
- [10] T.T. Hansel, H. Kropshofer, T. Singer, J.A. Mitchell, A.J.T. George, The safety and side effects of monoclonal antibodies, *Nat. Rev. Drug Discovery* 9 (2010) 325–338.
- [11] M.W. Tibbitt, K.S. Anseth, Hydrogels as extracellular matrix mimics for 3D cell culture, *Biotechnol. Bioeng.* 103 (2009) 655–663.
- [12] M. Gregoritzka, A.M. Goepferich, F.P. Brandl, Polyanions effectively prevent protein conjugation and activity loss during hydrogel cross-linking, *J. Controlled Release* 238 (2016) 92–102.
- [13] S. Kirchhof, A. Strasser, H.-J. Wittmann, V. Messmann, N. Hammer, A.M. Goepferich, F.P. Brandl, New insights into the cross-linking and degradation mechanism of Diels–Alder hydrogels, *J. Mater. Chem. B* 3 (2015) 449–457.
- [14] L.M. Ickenstein, P. Garidel, Hydrogel formulations for biologicals: current spotlight from a commercial perspective, *Ther. Delivery* 9 (2018) 221–230.

Chapter 3

A novel anhydrous preparation of PEG hydrogels enables high drug loading with biologics for controlled release applications

Published in *European Polymer Journal*

Abstract

Hydrogels are very attractive materials to embed biologics for controlled release over long timescales. However, aqueous preparations pose certain obstacles regarding protein integrity, stability of functional groups, and loading capacity. To overcome these obstacles, the Diels-Alder reaction of furyl- and maleimide-functionalized eight-armed poly(ethylene glycol) (PEG) was used for the polymer preparation in the melt. The water-free reaction was investigated for protein interactions, protein- and maleimide group stability, and protein loading capacity. The melt polymerization was found to be highly protective against protein PEGylation and maleimide hydrolysis. The polymer gels were evaluated as a potential release system for biologics, achieving controlled release of the model protein glucose oxidase over a time period of 100 days. Furthermore, the loading could be increased to 15% (w/w) without influencing the release kinetics. This work represents a promising-preparation method for degradable and water-free drug delivery systems that can be used to encapsulate biologics for controlled release.

1 Introduction

Although hydrogels are promising materials for releasing biologics over long periods of time [1], aqueous processing is challenging for some systems. First, commonly used cross-linking reactions like Michael-type addition, Diels-Alder (DA) reaction, or radical polymerization tend to allow for side reactions with the embedded proteins [2]. Nucleophilic amino acid residues such as cysteine and lysine are particularly affected [3]. These side reactions can result in loss of bioactivity, delayed or incomplete protein release, and increased risk of an immune response [4,5]. To prevent uncontrolled cross-linking, Gregoritz et al. [6] used polyanions to “shield” the embedded proteins. However, only positively charged proteins can be protected by this strategy. Van de Wetering et al. [7] showed that precipitation of proteins such as human growth hormone by zinc ions or linear poly(ethylene glycol) (PEG) protects the protein from reaction with gel precursors during gelation. Nonetheless, protein aggregation and denaturation are not completely prevented during precipitation. Moreover, additional excipients are required for both the shielding and precipitation of proteins, which could negatively impact the already limited loading capacity. Furthermore, the presence of water is pivotal to the question of protein stability. Many of them are prone to chemical degradation in water [8,9] and should only be dissolved right before application to avoid unnecessary water contact. In addition to protein activity loss, functional groups of the polymer precursors such as maleimides and tetrazines tend to undergo hydrolytic degradation in water. While tetrazine groups degrade under both acidic and basic conditions [10,11], maleimide groups are especially prone to hydrolysis in basic solutions via OH⁻-catalyzed ring opening [12]. Because the degradation products are unreactive and result in poorly cross-linked systems, materials containing these functional groups require fast processing after dissolution in water. A final concern is the poor loading capacity of conventional hydrogels that severely limits their applicability [13,14]. A desired loading of around 10% (w/w) often results in a less cross-linked system that leads to fast and uncontrolled drug release.

All of these drawbacks of conventional hydrogel preparation could be overcome by embedding proteins in the solid state. For this, the polymeric material needs to be processed in the absence of water at a temperature above its melting point. Embedding proteins in solid state, e.g., via hot-melt extrusion, has been carried out successfully with well-known polymers, such as poly(lactic-co-glycolic acid) (PLGA) [15]. But the high temperatures required to produce long-term release implants can induce protein denaturation [16]. Combining extrusion with melt polymerization via high temperature DA reaction between furan and maleimide-modified macromers has already been performed in material engineering for the synthesis of self-healing polymers [17–19]. However, the applied temperatures were above 80 °C, which could, as mentioned before, harm the integrity of temperature-sensitive proteins. Therefore, to date, no protein depot system has been developed via cross-linking by DA reaction in the melt at temperatures suitable for proteins.

The aim of this study was to establish protein-loaded polymer hydrogels via melt polymerization. For this purpose, a blend of furyl- and maleimide-functionalized multi-armed PEGs were prepared. After melting at protein-compatible temperatures, furan and maleimide groups undergo DA reaction and form a three-dimensional network. The melt polymerization was followed by rheology to determine polymerization time and the gel point. The stability of the functional groups was investigated, and possible interactions with the model protein lysozyme were explored. Afterwards, swelling and degradation studies were performed, and cytotoxicity was assessed. Finally, the polymers were loaded with different amounts of the model drugs lysozyme and glucose oxidase (GOx), and the *in vitro* release was analyzed.

2 Materials and methods

2.1 Materials

Deuterated chloroform, *N,N'*-dicyclohexylcarbodiimide, diisopropyl azodicarboxylate, 3-(2-furyl)propanoic acid, Eagle's minimum essential medium (EMEM), fetal calf serum (FCS), GOx (Type X-S, from *Aspergillus niger*), hydrazine monohydrate, *N*-hydroxysuccinimide, lysozyme (from chicken egg white), anhydrous methanol, *N*-methoxycarbonylmaleimide, *Micrococcus lysodeikticus*, protein LoBind Eppendorf tubes, QuantiPro™ BCA Assay Kit, sodium bicarbonate, and anhydrous tetrahydrofuran were purchased from Sigma-Aldrich (Taufkirchen, Germany). Eight-armed PEGs with molecular masses of 10 kDa (8armPEG10k), 20 kDa (8armPEG20k), and 40 kDa (8armPEG40k) were received from JenKem Technology (Allen, TX, USA) and functionalized with furyl (e.g., 8armPEG10k-furan) and maleimide groups (e.g., 8armPEKG10k-maleimide) as previously described [20]. Phthalimide and anhydrous sodium sulfate were received from Acros Organics (Geel, Belgium). Cyclohexane and dichloromethane were purchased from Fisher Chemical (Loughborough, UK). Diethyl ether (technical grade) was obtained from Jäcklechemie (Nuremberg, Germany). Ammonium persulfate, barium chloride dihydrate, 1,4-dioxane, glacial acetic acid, glycine, hydrochloric acid, di-potassium hydrogen phosphate trihydrate, sodium azide, sodium dihydrogen phosphate monohydrate, sodium hydroxide, and triphenylphosphine were received from Merck KGaA (Darmstadt, Germany). Iodine solution and tetramethylethylenediamine were purchased from Carl Roth GmbH & Co. KG (Karlsruhe, Germany). Acrylamide/bis-acrylamide (37.5:1) solution, bromophenol blue sodium salt, and Coomassie brilliant blue G-250 were obtained from Serva Electrophoresis GmbH (Heidelberg, Germany). Glycerol, 3-(4,5-dimethylthiazol-2-yl)-2,5-diphenyltetrazolium bromide (MTT), and sodium dodecyl sulfate (SDS) were purchased from PanReac AppliChem (Darmstadt, Germany). 2-Amino-2-hydroxymethylpropane-1,3-diol was received from Affymetrix (Santa Clara CA, USA). Ethanol was purchased from Labochem International (Heidelberg, Germany). Gibco Dulbecco's phosphate-buffered saline was received from Life Technologies (Darmstadt, Germany). Mouse fibroblast cells were a kind gift from

the group of Prof. Armin Buschauer (University of Regensburg). Purified water was freshly prepared using a Milli-Q water purification system from Millipore (Schwalbach, Germany).

2.2 Production of polymer precursor blends

For production of 8armPEG-furan and -maleimide blends, precursors with similar molecular weight were used. For example, equal amounts of 8armPEG10k-furan and 8armPEG10k-maleimide were added to cyclohexane. Subsequently, the suspension was minced and mixed using an Ultra-Turrax homogenizer adjusted with a Thyristor Regler (all Ika, Janke & Kunkel, Staufen, Germany) to yield small and uniform particles. The solvent was evaporated by vacuum drying to obtain a polymer precursor blend.

2.3 Differential Scanning Calorimetry (DSC)

To study the melting points of the different blends, DSC measurements were carried out using a DSC 2920 (TA Instruments, Eschborn, Germany). Each blend was weighed and sealed into an aluminum pan (SieberAnalytik G. Sieber, Meiningen, Austria). An empty pan was used as a reference. Throughout the experiment, nitrogen gas with a flow rate of 65 cc/min was used to purge the cell. Blends were heated from 0 °C to 100 °C with a heating rate of 10 °C/min. To evaluate the raw data, TA Universal Analysis 2000 software was used.

2.4 Rheological characterization

Oscillatory shear experiments were performed on a Malvern Kinexus Lab+ rheometer (Malvern, Kassel, Germany) using an 8 mm parallel plate geometry with a gap size of 500 μm at a constant frequency of 1.0 Hz. After casting 30 mg of a precursor blend onto the lower plate of the rheometer, vacuum was applied using a vacuum chamber (Figure 1) to avoid air bubbles that could cause falsely high measurements of the stiffness of the system [21]. To ensure fast and complete melting, temperatures approximately 4 °C above the respective melting point were used, i.e., 45 °C for 8armPEG-macromonomers with a molecular weight of 10 kDa, 52 °C for 20 kDa, and 58 °C for 40 kDa. As soon as the blend was melted, vacuum was stopped, the vacuum chamber was removed, and the experiment was started immediately. Storage modulus (G'), loss modulus (G''), complex shear modulus (G^*), and phase angle (δ) were measured as a function of time. The gel point, which is the cross-over point of G' and G'' , was determined for all polymers.

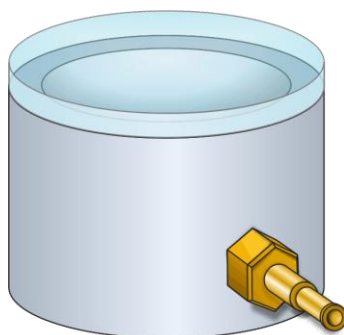


Figure 1: Vacuum chamber for bubble free melting of the polymer precursor blends.

2.5 Preparation of melt polymers

Polymers were prepared by heating the dry powder blends in a Vacuum Compression Molding (VCM) tool (MeltPrep GmbH, Graz, Austria) equipped with a low-pressure lid for 16 h. Each blend was allowed to melt approximately 4 °C above its specific melting point as explained in section 2.4. To avoid air bubbles, vacuum (50 mbar) and a slight compression force were applied. After completion of the polymerization, the VCM tool was cooled (0.05 °C/min) to room temperature.

2.6 General characterization

To determine the cross-linking mechanism, FTIR-spectra of 8armPEG10k-furan, 8armPEG10k-maleimide, and an 8armPEG10k melt polymer were recorded using an Agilent Cary 630 FTIR (Agilent Technologies, Santa Clara, USA).

The polymerization was monitored by UV-VIS spectroscopy. A blend of 8armPEG10k-furan and 8armPEG10k-maleimide were cast on an LVis plate (BMG Labtech, Ortenberg, Germany). The blend was heated at 45 °C, and UV-VIS spectra were recorded at predetermined time points on a microplate reader (BMG Labtech, Ortenberg, Germany).

The structure of 8armPEG10k melt polymers was imaged after polymerization, after incubation for 1 day in water, and after incubation for around 100 days in water with scanning electron microscopy (SEM). Before imaging, the incubated polymers were freeze-dried.

2.7 Stability of functional groups

To investigate a possible decrease in the number of functional groups after melt preparation, absorbance of both precursors was recorded and compared to conventional hydrogel preparation. For melt preparation, both 8armPEG10k-furan and 8armPEG10k-maleimide were separately processed according to section 2.2 and 2.5. To mimic conventional hydrogel preparation, 10 mg of each precursor were separately dissolved in 1 ml of 50 mM phosphate buffer (pH 7.4) and stored at 37 °C for 16 h. After the different treatments, 10 mg/ml solutions in 50 mM phosphate buffer (pH 7.4) were used to

measure the absorbance of furan at 260 nm and maleimide at 299 nm using a microplate reader (BMG Labtech, Ortenberg, Germany). A 10 mg/ml solution of the non-functionalized 8armPEG10k served as blank. Each precursor was referenced to the respective fresh precursor solution.

2.8 Influence of preparation on proteins

The influence of the melt polymerization on proteins was examined by processing lysozyme with each precursor. Therefore, blends with 10% (w/w) lysozyme, equivalent to a 5% loaded melt polymer, and either 8armPEG10k-furan or 8armPEG10k-maleimide were produced as described in section 2.2. The blends were then stored under vacuum for 16 h at 58 °C. After cooling, PEG macromolecules were removed from lysozyme by dissolving and washing in anhydrous methanol. Lysozyme was subsequently dried. The activity of lysozyme was measured as described by Shugar [22] with modifications according to Gregoritz et al. [6]. To visualize possible PEGylation, SDS-PAGE was used following methods described in the literature [2]. Results were compared to the effects of conventional hydrogel preparation on lysozyme. For this preparation, 7.5% (w/v) solutions of one hydrogel precursor and 10% (w/w) lysozyme treated with methanol were dissolved, imitating a hydrogel with a polymer concentration of 15% (w/v) and a loading of 5% (w/w). These solutions were stored at 37 °C for 16 h in 50 mM phosphate buffer (pH 7.4). Both methods were referenced to lysozyme treated with methanol.

2.9 Swelling and degradation studies

For swelling and degradation studies, melt polymers from each precursor blend (approximately 20 mg each) were prepared as described in section 2.5. The melt polymers were then transferred to a protein LoBind Eppendorf tube and incubated in 5 ml of a 50 mM phosphate buffer (pH 7.4) with 0.02% sodium azide at 37 °C in a shaking water bath. Swelling and degradation was studied as previously described [23].

2.10 Cytotoxicity

Cytotoxicity of the melt polymers was assessed according to ISO 10993-5:2009 (Biological evaluation of medical devices, part 5: Tests for *in vitro* cytotoxicity) by using extracts as previously described [24]. In brief, approximately 20 mg of melt polymers were produced from 10, 20, or 40 kDa macromonomers. Extracts were prepared by incubating the melt polymers in 2 ml of EMEM supplemented with 10% FCS for 24 h at 37 °C. 10,000 mouse fibroblast L-929 cells were seeded per well in 96-well microtiter plates. The cells were cultivated overnight. 100 µl of extract was added to each well. 0.1% SDS was used as negative control and pure medium was used as positive control. Six replicates of each sample were produced. The medium was removed after 24 h of incubation. 200 µl of a 1.5 mM MTT solution was

added to each well, removed after 6 h of incubation, and replaced with PBS containing 10% SDS. Samples were incubated for 16 h at room temperature. Subsequently, the absorbance at 570 and 690 nm was measured using a FluoStar Omega microplate reader. To calculate cell viability, the difference in absorbance at 570 and 690 nm was calculated. The results were normalized to the positive control.

2.11 Release studies and analytics

Polymer precursor blends containing 5% (w/w) lyophilized powder of GOx or lysozyme were produced using precursors with a molecular weight of 10 kDa as described in section 2.2. For example, to prepare a precursor blend containing 5% (w/w) GOx, 95 mg 8armPEG10k-furan, 95 mg 8armPEG10k-maleimide, and 10 mg GOx were added to cyclohexane, mixed, and vacuum dried. Melt polymers loaded with 5% (w/w) protein were produced from around 20 mg of this blend as described in section 2.5. For comparison, DA hydrogels loaded with 5% (w/v) lysozyme with a polymer concentration of 10% (w/v) were prepared from the same precursors. All polymers and hydrogels were transferred to protein LoBind Eppendorf tubes and incubated in 5 ml of 50 mM phosphate buffer (pH 7.4) with 0.02% sodium azide. The release experiments were performed in a shaking water bath at 37 °C. At regular time points, 300 µl samples were withdrawn and replaced with fresh buffer. The withdrawn samples were stored at 2–8 °C until further analysis. The lysozyme concentration was determined using a FluoStar Omega fluorescence microplate reader (BMG Labtech, Ortenberg, Germany). The GOx concentration was quantified with a BCA assay. To investigate the loading capacity, melt polymers with a loading of 10 and 15% (w/w) glucose oxidase were produced, and release experiments were performed as mentioned before.

To determine the impact of the preparation method on proteins, the enzymes were analyzed after release. For lysozyme released from melt polymers and conventional DA hydrogels, activity after 13 and 30 days was determined. The activity was compared to that of a fresh enzyme solution with the same concentration.

Samples of GOx taken after one day of incubation were investigated using size-exclusion chromatography (SEC). GOx incubated for one day with 8armPEG10k-maleimide served as positive control. The experiment was carried out using an Agilent 1260 Infinity II HPLC system (Agilent Technologies, Waldbronn, Germany) equipped with a fluorescence detector on a Tosoh G3000SWXL column (Tosoh Bioscience, Griesheim, Germany) at 30 °C. 20 µl samples were injected, and the analysis was performed at a flow rate of 0.45 ml/min for 40 min. The mobile phase was a 50 mM phosphate buffer (pH 7.4). For detection, an excitation wavelength of 278 nm and an emission wavelength of 340 nm were used.

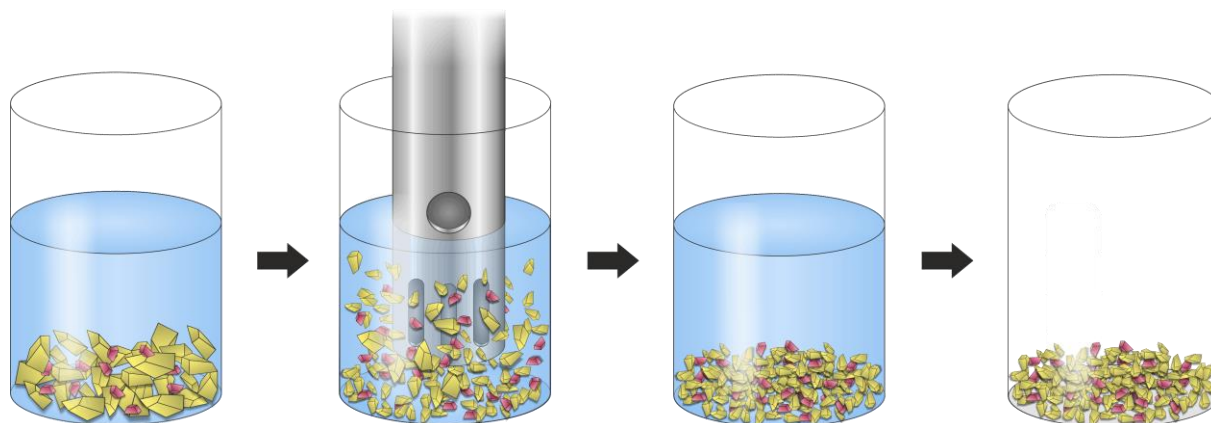
2.12 Statistical analysis

All experiments were performed in triplicate, and the results are shown as mean \pm standard deviation. Statistical significance was assessed using one-way ANOVA. Post hoc analysis was determined by Tukey's test (GraphPad Prism 6.0, GraphPad Software Inc., La Jolla, CA, USA).

3 Results and discussion

3.1 Polymer preparation and mechanical characterization

Blends of 8armPEG-furan and 8armPEG-maleimide were produced for water-free polymer preparation to ensure homogeneous cross-linking of the macromonomers after melting. An Ultra-Turrax was used to mince and mix the PEG particles suspended in cyclohexane (Scheme 1). Cyclohexane was chosen because the insolubility of PEG in cyclohexane prevents the precursors from reacting prematurely. Additionally, this organic solvent stabilizes the active conformation of certain enzymes, e.g., α -amylase [25], which may protect them during the mincing and mixing process.



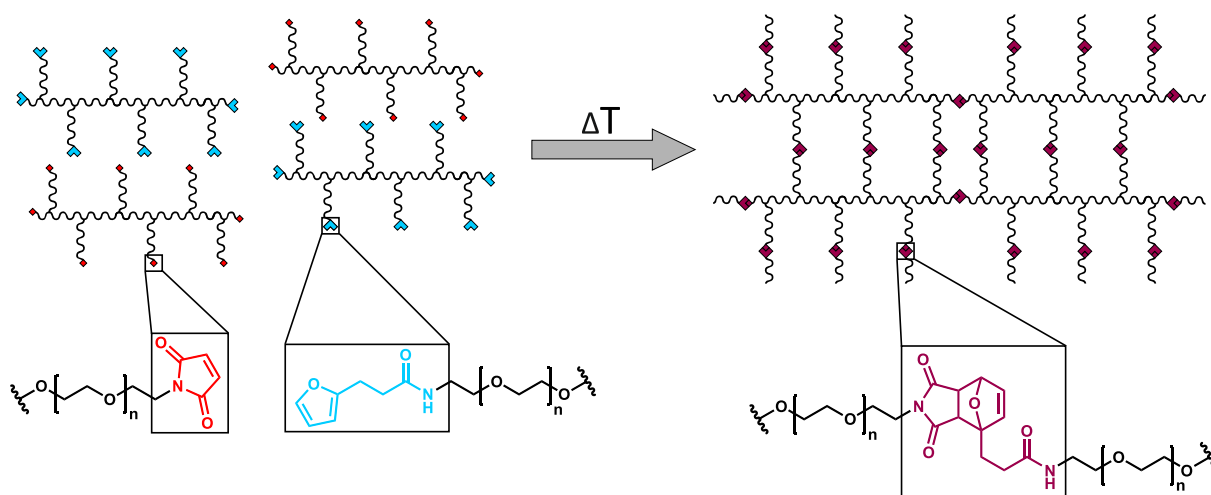
Scheme 1: Preparation of the protein-containing precursor blend. First, cyclohexane was added to a blend of furyl- and maleimide-functionalized 8armPEG (yellow particles) and protein (red particles), and the insoluble powder was mixed by an Ultra-Turrax. Subsequently, the blend was vacuum dried to yield a homogeneous powder blend.

DSC measurements (Table 1) revealed that the melting point of the 8armPEG10k blend is below 41 °C - a considerably lower processing temperature than that used to make traditional PLGA implants for the long-term release of proteins [26,27]. Blends of larger macromolecules containing longer PEG chains had higher melting points because of their higher molecular weight. The low melting points of 8armPEGs were exploited to avoid thermal denaturation of the embedded proteins.

Table 1: Melting point of 8armPEG precursor blends consisting of macromonomers with different molecular weights.

Molecular weight [kDa]	Melting point [°C]
10	40.7 ± 0.4
20	47.8 ± 0.2
40	53.9 ± 0.0

The DA reaction was confirmed as cross-linking reaction by FTIR and UV-VIS spectroscopy (Figure S1 and S2). After melting, sufficient molecular mobility of the macromonomers is ensured so that furan and maleimide groups can find each other and start cross-linking (Scheme 2). However, the DA reaction is known to progress slowly at low temperatures in solution and in the molten state [28,29]. Therefore, we investigated the polymerization time of each melt polymer using oscillatory shear experiments. For the polymer prepared from the 8armPEG10k precursors, the slope of the complex shear modulus after 960 min was negligible compared to the increase at the beginning (Figure 2A). Hence, 960 min was considered as the completion time for the polymerization.

**Scheme 2:** Cross-linking of 8armPEG-furan and 8armPEG-maleimide via DA reaction in molten state. The precursor blend is heated above its melting point. The polymerization is initiated directly after melting.

The gel point served to compare the polymerization of polymers with different molecular weights (Figure 2B). Polymers made of larger macromonomers took longer to reach their gel point (47.4 ± 1.1 min for 8armPEG10k, 54.7 ± 1.7 min for 8armPEG20k, and 74.3 ± 3.5 min for 8armPEG40k) because their higher viscosity after melting leads to diminished mobility: 21.7 ± 5.7 Pa·s for 8armPEG40k and 13.0 ± 1.3 Pa·s for 8armPEG20k compared to 5.6 ± 2.3 Pa·s for 8armPEG10k (Figure S3). In addition, the number of molecules per mass unit is reduced for larger molecules. Because polymer samples of equal mass were used for rheological characterization, the number of molecules decreased for 8armPEG20k to a half and for 8armPEG40k to a quarter compared to 8armPEG10k. This reduces the number of reactive groups present, therefore decreasing the likelihood of every functional group finding its corresponding counterpart and forming an active chain [20].

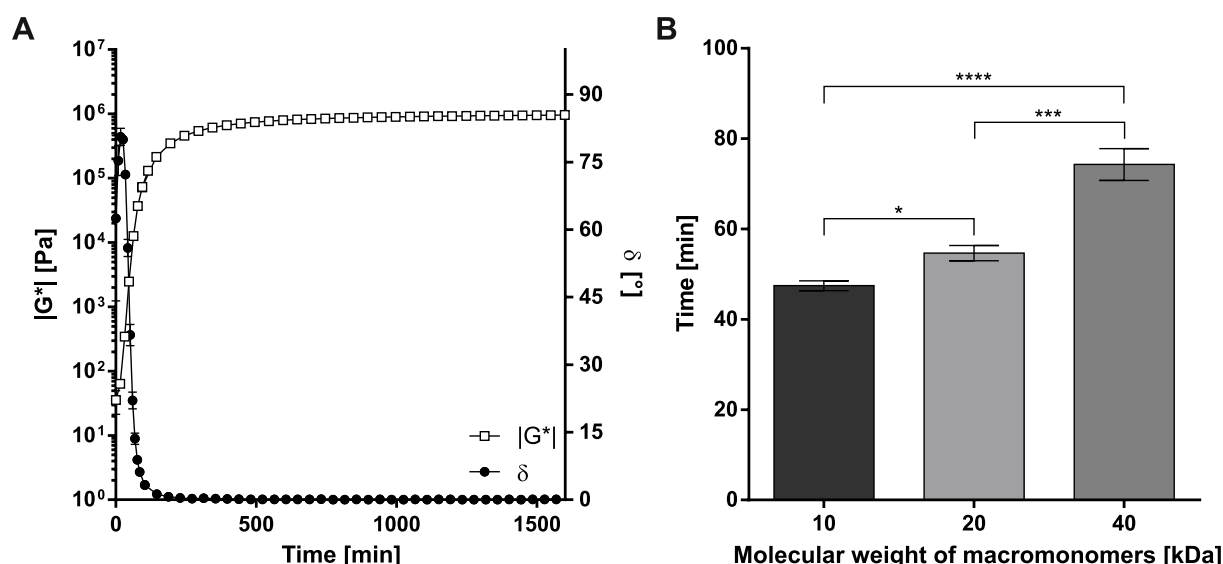


Figure 2: Melt polymerization of 8armPEG10k-furan and 8armPEG10k-maleimide followed by oscillatory rheology (A). Complex shear modulus ($|G^*|$) and phase angle (δ) were recorded as a function of time. All oscillatory measurements were performed about 4 °C above respective melting points with a frequency of 1.0 Hz using an 8 mm parallel plate geometry with a gap size of 0.5 mm. Gel points (i.e., the cross-over points of G' and G'') of melt polymers prepared from macromonomers with a molecular weight of 10, 20, and 40 kDa (B). Levels of statistical significance are indicated as * $p \leq 0.05$, *** $p \leq 0.001$ and **** $p \leq 0.0001$.

Consequently, all polymers were allowed to polymerize for 16 h, which we considered an adequate time to account for the different mobility in each blend. To ensure reproducibility, the VCM tool was chosen as reaction vessel. Polymerization was performed approximately 4 °C above the blend's melting point to compensate for the temperature gradient in the VCM tool and to ensure fast and complete melting. After 16 h, the melt polymers were cooled at a rate of 0.05 °C/min to prevent stress that could lead to cracks in the matrix.

3.2 Functional groups' stability and protein interactions

Many cross-linkers used for hydrogel preparation (e.g., tetrazine, maleimide, and carbonate groups) are known to hydrolyze in water to form inactive products [30–32]. Melt polymerization is an attractive water-free preparation method that is able to run in the absence of any solvent. In this way, the functional groups are protected from hydrolysis. To confirm this assumption, the effects of melt polymerization and conventional hydrogel preparation on functional group stability were investigated by UV spectroscopy (Figure 3). A decrease of the maleimide content to $14.8 \pm 0.4\%$ was found for conventional hydrogel preparation due to hydrolysis [33,34]. In contrast, melt polymerization did not change the number of maleimide groups ($103.2 \pm 1.5\%$). As expected, no chemical degradation was observed for the furan groups with either preparation method ($103.5 \pm 5.4\%$ after conventional preparation and $106.7 \pm 0.7\%$ after melt polymerization). Therefore, more functional groups are available for cross-linking in the molten state, leading to a more homogeneous and stable system.

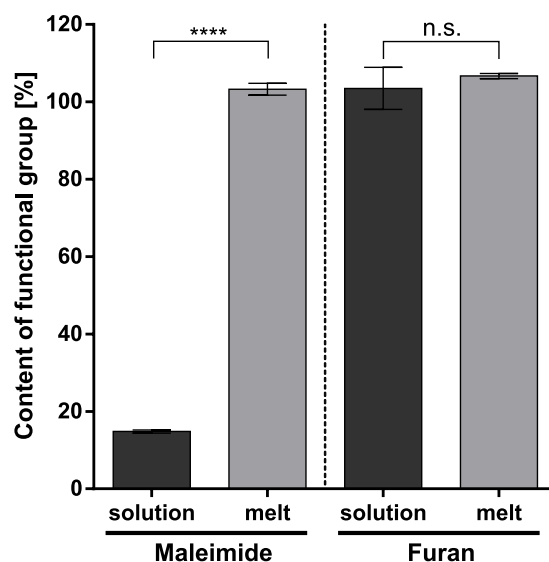


Figure 3: Content of maleimide and furan groups on the respective functionalized 8armPEG10k macromonomers after storage in phosphate buffer (pH 7.4) for 16 h (solution) and in molten state at 58 °C for 16 h (melt) referenced to fresh precursor solutions, respectively. Level of statistical significance is indicated as **** $p \leq 0.0001$.

In addition to hydrolysis, maleimide groups are also prone to reacting with nucleophilic amino acid residues on proteins, which can tether the protein to the hydrogel matrix and lead to denaturation. Therefore, activity and PEGylation of the model protein lysozyme were investigated for melt polymerization and conventional hydrogel preparation. First, the activity of lysozyme was examined (Figure 4A). Methanol-treated lysozyme was used as reference, and had an activity of 28092 ± 1120 U/mg. No significant difference was found when lysozyme was processed with 8armPEG10k-furan by either the conventional hydrogel preparation (27180 ± 585 U/mg) or the melt polymerization (28604 ± 934 U/mg). After incubation with 8armPEG10k-maleimide in buffer representing conventional hydrogel preparation, the lysozyme had no detectable activity. To determine the reason for this complete inactivation, SDS-PAGE was performed (Figure 4B). No band of lysozyme could be found, indicating the absence of free enzyme. In contrast, mixing and heating the lysozyme with molten 8armPEG10k-maleimide did not cause a significant decrease in its activity (26802 ± 768 U/min) or increase in PEGylation. Processing lysozyme with 8armPEG10k-furan did not lead to PEGylation with either preparation method. Only incubation of the enzyme with maleimide groups in buffer resulted in PEGylation, which can be explained by Michael-type addition of nucleophilic amino acid residues of the enzyme with maleimide groups [2]. Summarized, melt polymerization protects functional groups from hydrolysis and prevents proteins from off-target interactions during matrix formation.

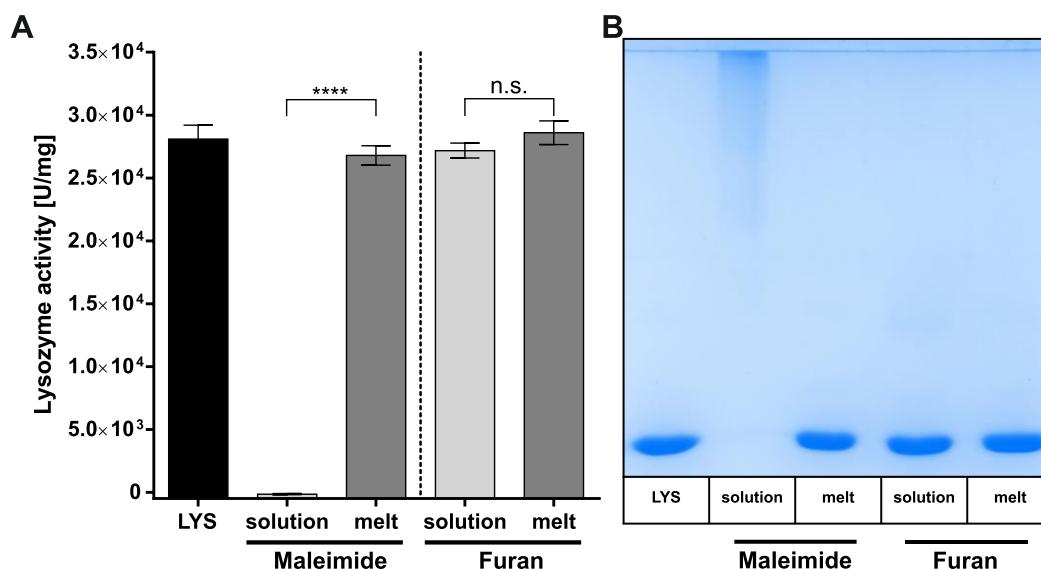


Figure 4: Lysozyme activity determined before (LYS) and after storage either with 8armPEG10k-maleimide (Maleimide) or 8armPEG10k-furan (Furan) in phosphate buffer (pH 7.4) for 16 h (solution) or in the melt of one precursor at 58 °C for 16 h (melt) (A). SDS-PAGE of lysozyme before (LYS) and after storage either with 8armPEG10k-maleimide (Maleimide) or 8armPEG10k-furan (Furan) in phosphate buffer (pH 7.4) for 16 h (solution) or in the melt of one precursor at 58 °C for 16 h (melt) (B). Level of statistical significance is indicated as **** $p \leq 0.0001$.

3.3 Swelling studies

Swelling and degradation behavior are pivotal considerations for designing drug delivery systems. Adequate stability of the system is important to guarantee controlled release of therapeutic proteins over a long timescale. On the other hand, biodegradation is necessary to avoid having residual matrix material left at the end of treatment. To examine the swelling and degradation behavior, the polymers were incubated in phosphate buffer (pH 7.4) at 37 °C, and the relative mass increase was measured (Figure 5). Additionally, the change of the structure was followed by SEM imaging (Figure S4).

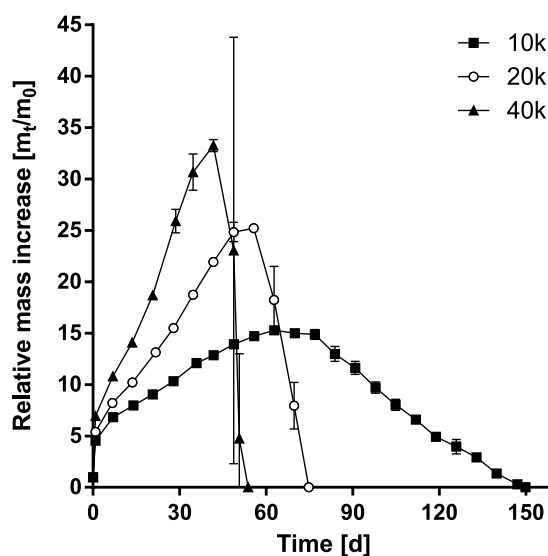


Figure 5: Swelling and degradation of melt polymers made from precursors with different molecular weights in phosphate buffer (pH 7.4) at 37 °C.

After reaching a maximum, the masses of all polymers started to decrease, and the polymers were fully degraded after 54 days (8armPEG40k), 75 days (8armPEG20k), and 150 days (8armPEG10k). This can be explained by the water uptake of the polymers and the reversibility of the DA reaction resulting in free macromonomers that are removed from the polymer matrix by diffusion [35]. Polymers prepared with smaller macromonomers were more stable. This result is in accordance with the observation of Kirchhof et al. [20] for hydrogels prepared from the same PEG derivatives. More elastically active chains are present in polymers made of smaller macromonomers that have to be broken via retro-DA reaction, resulting in higher stability of the polymer.

3.4 Release of lysozyme and GOx

When polymers are used as a carrier system for proteins in an aqueous environment, swelling of the polymers to hydrogels poses a threat to the proteins as they are dissolved in the incoming water and subjected to interactions with any remaining unreacted maleimide groups. To investigate such possible off-target interactions, the chemical integrity of released protein was assessed. For comparison, conventional DA hydrogels were prepared with a polymer concentration of 10% (w/v) of 10 kDa precursors. Melt polymers and DA hydrogels were loaded with 5% (w/w) lysozyme. Lysozyme was chosen because it has a small hydrodynamic radius of approximately 1.9 nm [36]. It has already been shown that lysozyme is rapidly and completely released from DA hydrogels prepared with 10% (w/v) of 10 kDa precursors when it is prevented from off-target interactions. In contrast, without protection, lysozyme was released degradation-controlled due to covalent binding to the hydrogel network [6]. Therefore, the same result was expected for the melt polymers. The release experiments were performed in 50 mM phosphate buffer (pH 7.4) with 0.02% sodium azide at 37 °C. The shape of the release curve shows that lysozyme was released from the melt polymer only by diffusion (Figure 6A). Additionally, the high burst release of 84% after 1 day and the complete release after 10 days implies that no covalent binding to the polymer network occurred. In contrast, 44% of lysozyme was released from the conventional hydrogel after 1 day, and it was completely released after 30 days when the hydrogel was degraded. These findings suggest that there was no covalent binding of the protein when embedded via melt polymerization. To confirm this assumption, the activity of the enzyme after 13 and 30 days was measured for both methods (Figure 6B). The activity of the enzyme released from conventional hydrogels decreased to $85.9 \pm 3.2\%$ after 13 days and $40.0 \pm 2.7\%$ after 30 days, suggesting that the enzyme was PEGylated. However, when released from the melt-polymerized matrix, the lysozyme did not have a significant decrease in activity after 13 days ($97.6 \pm 1.6\%$) or 30 days ($97.7 \pm 1.4\%$). This demonstrates that there was no interaction between lysozyme and cross-linker in the melt polymerization method.

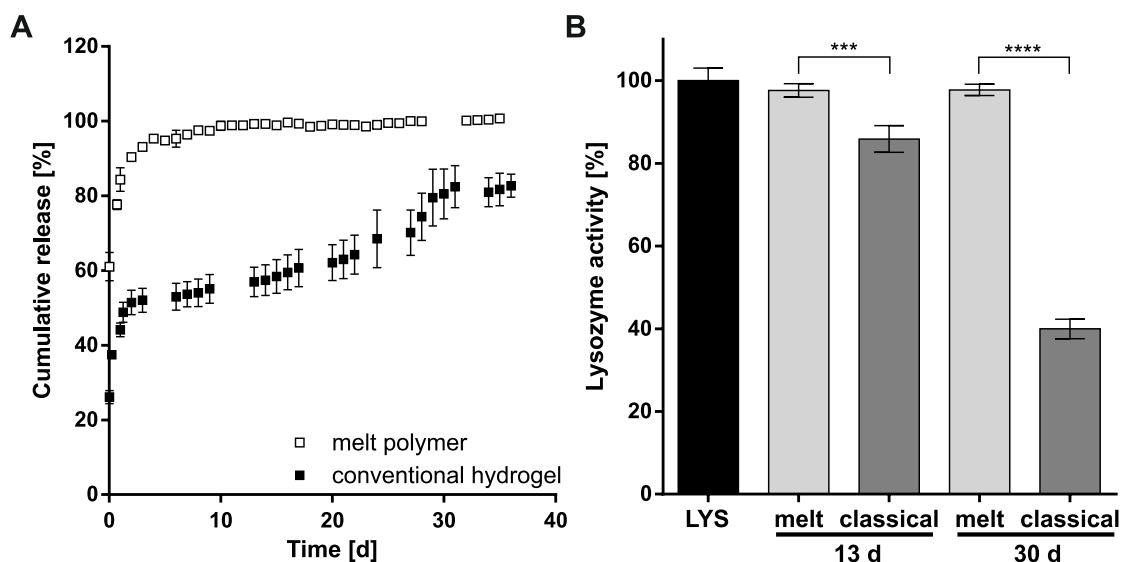


Figure 6: Release of lysozyme from 8armPEG10k melt polymers and 8armPEG10k-hydrogels (A). Lysozyme activity after release from melt polymers and hydrogels after 13 and 30 days (B). Activities were referenced to the activity of a fresh lysozyme solution (LYS). Levels of statistical significance are indicated as *** $p \leq 0.001$ and **** $p \leq 0.0001$.

In summary, the results of release and activity measurements show that melt polymerization avoids PEGylation not only during cross-linking but also during incubation in water, making the melt polymer a promising matrix material for preventing off-target interactions of proteins to be released.

The next experiment was to assess the ability of the polymers as drug delivery systems for a controlled release over time. This was investigated with GOx, which has a molecular weight of 160 kDa [37] and is, therefore, a good surrogate for common therapeutic proteins with similar molecular weights such as bevacizumab or trastuzumab [38,39]. GOx was embedded in a polymer made of the 8armPEG10k precursors. This polymer was selected because it has the lowest melt temperature, the highest stability, and, presumably, the smallest mesh sizes. Moreover, this polymer did not show considerable cytotoxicity in the MTT assay (Figure S5). The release experiments were performed in phosphate buffer (pH 7.4) at 37 °C.

For polymer loaded with 5% (w/w) lyophilized GOx powder, an initial release of approximately 10% was found after 1 day (Figure 7A). This burst release can be attributed to free protein adsorbed to the surface of the implant that immediately dissolved in the buffer. Around 30% of GOx was slowly released over 38 days followed by a faster release. After 100 days, the protein was completely released. The biphasic behavior can be explained by the distribution and the development of mesh sizes and the diffusion path that the protein has to pass. Initially, both wide and narrow mesh sizes are present, but proteins are only released via meshes wider than the hydrodynamic diameter. Small meshes lead to protein retention. Larger proteins are only released if the network mesh size increases. After 40 days, the majority of the meshes expanded sufficiently, allowing a considerable amount of the protein to be released, which is additionally amplified by the decreasing diffusion path of the protein as polymer degradation occurs.

The released protein was analyzed by SEC-HPLC to confirm its integrity and investigate the impact of the melt preparation on high molecular proteins (Figure S6). Samples from day one of incubation were examined to assess the influence of preparation and avoid unspecific protein degradation. Fresh GOx and 8armPEG10k-maleimide-incubated GOx served as positive and negative control, respectively. Both the released GOx and the fresh GOx solution showed one peak at a retention time of 16 min, indicating that only intact GOx was present. Incubation of the enzyme with 8armPEG10k-maleimide resulted in a size increase due to PEGylation. Thus, the structure of GOx did not change after melt polymerization and release. Neither PEGylation nor fragmentation occurred during the melt embedding, which makes the melt polymerization via DA reaction a successful approach to maintain the integrity of embedded proteins.

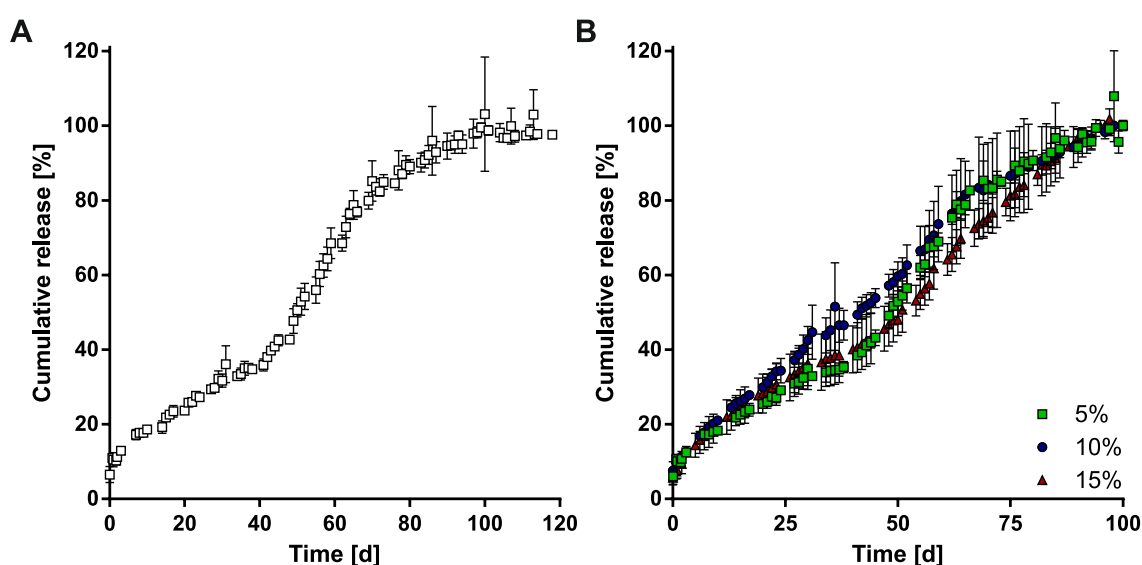


Figure 7: Release of 5% (w/w) GOx from 8armPEG10k melt polymers (A). Release of 5, 10, and 15% (w/w) GOx from 8armPEG10k melt polymers (B).

Finally, the loading capacity was determined (Figure 7B). For this purpose, melt polymers loaded with 10 and 15% (w/w) GOx were prepared, and the *in vitro* release was compared to a 5% (w/w) GOx polymer. Interestingly, the difference was minimal, and the release curves of all polymers were similar. The protein was released completely after 100 days for all loading quantities. These results are very promising, especially when considering that the loading capacity of conventional hydrogels is very low with only a few percent of protein that can be accommodated. High drug loading could influence the release kinetics [40]. Therefore, the volume of the hydrogel has to be increased if a higher drug dose with the same release behavior is desired. On the contrary, our polymerization method can be used to increase the drug dose without increasing the volume of the drug system. This is particularly important for use in patients because smaller implants lead to greater compliance.

4 Conclusion

DA hydrogel manufacturing via melt polymerization represents a highly promising method to prepare drug delivery systems for controlled protein release. Due to the water-free preparation, maleimide groups are protected from degradation, which results in a higher cross-linking density compared to conventional DA hydrogels obtained by polymerization in water. Additionally, solid state embedding of proteins prevents interactions with functional groups of the polymer and maintains the *in vitro* activity and integrity. The controlled release of up to 15% (w/w) GOx over 100 days showed that these polymers can be used as highly loaded drug delivery systems for high molecular weight proteins.

References

- [1] T. Vermonden, R. Censi, W.E. Hennink, Hydrogels for protein delivery, *Chem. Rev.* (Washington, DC, U. S.) 112 (2012) 2853–2888.
- [2] N. Hammer, F.P. Brandl, S. Kirchhof, V. Messmann, A.M. Goepferich, Protein compatibility of selected cross-linking reactions for hydrogels, *Macromol. Biosci.* 15 (2015) 405–413.
- [3] Y. Marsac, J. Cramer, D. Olschewski, K. Alexandrov, C.F.W. Becker, Site-specific attachment of polyethylene glycol-like oligomers to proteins and peptides, *Bioconjugate Chem.* 17 (2006) 1492–1498.
- [4] C.-C. Lin, K.S. Anseth, PEG hydrogels for the controlled release of biomolecules in regenerative medicine, *Pharm. Res.* 26 (2009) 631–643.
- [5] C. Hiemstra, Z. Zhong, M.J. van Steenbergen, W.E. Hennink, J. Feijen, Release of model proteins and basic fibroblast growth factor from in situ forming degradable dextran hydrogels, *J. Controlled Release* 122 (2007) 71–78.
- [6] M. Gregoritz, A.M. Goepferich, F.P. Brandl, Polyanions effectively prevent protein conjugation and activity loss during hydrogel cross-linking, *J. Controlled Release* 238 (2016) 92–102.
- [7] P. van de Wetering, A.T. Metters, R.G. Schoenmakers, J.A. Hubbell, Poly(ethylene glycol) hydrogels formed by conjugate addition with controllable swelling, degradation, and release of pharmaceutically active proteins, *J. Controlled Release* 102 (2005) 619–627.
- [8] M.C. Lai, E.M. Topp, Solid-state chemical stability of proteins and peptides, *J. Pharm. Sci.* (Philadelphia, PA, U. S.) 88 (1999) 489–500.
- [9] Y.-F. Maa, S. Prestrelski, Biopharmaceutical Powders Particle Formation and Formulation Considerations, *Curr. Pharm. Biotechnol.* 1 (2000) 283–302.
- [10] M.R. Karver, R. Weissleder, S.A. Hilderbrand, Synthesis and evaluation of a series of 1,2,4,5-tetrazines for bioorthogonal conjugation, *Bioconjugate Chem.* 22 (2011) 2263–2270.
- [11] J.C. Oxley, J.L. Smith, J. Zhang, Decomposition Pathways of Some 3,6-Substituted s - Tetrazines, *J. Phys. Chem. A* 104 (2000) 6764–6777.
- [12] S. Kirchhof, A. Strasser, H.-J. Wittmann, V. Messmann, N. Hammer, A.M. Goepferich, F.P. Brandl, New insights into the cross-linking and degradation mechanism of Diels–Alder hydrogels, *J. Mater. Chem. B* 3 (2015) 449–457.
- [13] L.M. Ickenstein, P. Garidel, Hydrogel formulations for biologicals: current spotlight from a commercial perspective, *Ther. Delivery* 9 (2018) 221–230.
- [14] J.-F.R. dos Santos, J.-J. Torres-Labandeira, N. Matthijs, T. Coenye, A. Concheiro, C. Alvarez-Lorenzo, Functionalization of acrylic hydrogels with alpha-, beta- or gamma-cyclodextrin modulates protein adsorption and antifungal delivery, *Acta Biomater.* 6 (2010) 3919–3926.

- [15] M. Stanković, H.W. Frijlink, W.L.J. Hinrichs, Polymeric formulations for drug release prepared by hot melt extrusion: application and characterization, *Drug Discovery Today* 20 (2015) 812–823.
- [16] H.K. Makadia, S.J. Siegel, Poly Lactic-co-Glycolic Acid (PLGA) as Biodegradable Controlled Drug Delivery Carrier, *Polymers (Basel, Switz.)* 3 (2011) 1377–1397.
- [17] T. Defize, R. Riva, J.-M. Thomassin, C. Jérôme, M. Alexandre, Thermo-Reversible Reactions for the Preparation of Smart Materials: Recyclable Covalently-Crosslinked Shape Memory Polymers, *Macromol. Symp.* 309-310 (2011) 154–161.
- [18] J.-M. Raquez, S. Vanderstappen, F. Meyer, P. Verge, M. Alexandre, J.-M. Thomassin, C. Jérôme, P. Dubois, Design of cross-linked semicrystalline poly(ϵ -caprolactone)-based networks with one-way and two-way shape-memory properties through Diels-Alder reactions, *Chem. - Eur. J.* 17 (2011) 10135–10143.
- [19] D.H. Turkenburg, H.R. Fischer, Diels-Alder based, thermo-reversible cross-linked epoxies for use in self-healing composites, *Polymer* 79 (2015) 187–194.
- [20] S. Kirchhof, F.P. Brandl, N. Hammer, A.M. Goepferich, Investigation of the Diels–Alder reaction as a cross-linking mechanism for degradable poly(ethylene glycol) based hydrogels, *J. Mater. Chem. B* 1 (2013) 4855.
- [21] L. Ducloué, O. Pitois, J. Goyon, X. Chateau, G. Ovarlez, Rheological behaviour of suspensions of bubbles in yield stress fluids, *J. Non-Newtonian Fluid Mech.* 215 (2015) 31–39.
- [22] D. Shugar, The measurement of lysozyme activity and the ultra-violet inactivation of lysozyme, *Biochim. Biophys. Acta* 8 (1952) 302–309.
- [23] F. Brandl, N. Hammer, T. Blunk, J. Tessmar, A. Goepferich, Biodegradable hydrogels for time-controlled release of tethered peptides or proteins, *Biomacromolecules* 11 (2010) 496–504.
- [24] M. Gregoritz, V. Messmann, K. Abstiens, F.P. Brandl, A.M. Goepferich, Controlled Antibody Release from Degradable Thermoresponsive Hydrogels Cross-Linked by Diels-Alder Chemistry, *Biomacromolecules* 18 (2017) 2410–2418.
- [25] M. Shafiei, A.-A. Ziaee, M.A. Amoozegar, Purification and characterization of a halophilic α -amylase with increased activity in the presence of organic solvents from the moderately halophilic *Nesterenkonia* sp. strain F, *Extremophiles* 16 (2012) 627–635.
- [26] Z. Ghalanbor, M. Körber, R. Bodmeier, Improved lysozyme stability and release properties of poly(lactide-co-glycolide) implants prepared by hot-melt extrusion, *Pharm. Res.* 27 (2010) 371–379.
- [27] A. Cossé, C. König, A. Lamprecht, K.G. Wagner, Hot Melt Extrusion for Sustained Protein Release: Matrix Erosion and In Vitro Release of PLGA-Based Implants, *AAPS PharmSciTech* 18 (2017) 15–26.

- [28] M. Gregoritz, V. Messmann, A.M. Goepferich, F.P. Brandl, Design of hydrogels for delayed antibody release utilizing hydrophobic association and Diels–Alder chemistry in tandem, *J. Mater. Chem. B* 4 (2016) 3398–3408.
- [29] Z. Stirn, A. Rucigaj, M. Krajnc, Characterization and kinetic study of Diels-Alder reaction: Detailed study on N-phenylmaleimide and furan based benzoxazine with potential self-healing application, *eXPRESS Polym. Lett.* 10 (2016) 537–547.
- [30] M. Pagel, R. Meier, K. Braun, M. Wiessler, A.G. Beck-Sickinger, On-resin Diels-Alder reaction with inverse electron demand: an efficient ligation method for complex peptides with a varying spacer to optimize cell adhesion, *Org. Biomol. Chem.* 14 (2016) 4809–4816.
- [31] J. Wang, S. Yang, K. Zhang, Multi-arm PEG-maleimide conjugation intermediate characterization and hydrolysis study by a selective HPLC method, *J. Pharm. Biomed. Anal.* 164 (2019) 452–459.
- [32] S. Zalipsky, Alkyl succinimidyl carbonates undergo Lossen rearrangement in basic buffers, *Chem. Commun. (Cambridge, U. K.)* (1998) 69–70.
- [33] S. Matsui, H. Aida, Hydrolysis of some N-alkylmaleimides, *J. Chem. Soc., Perkin Trans. 2* (1972-1999) (1978) 1277.
- [34] S. Kirchhof, M. Gregoritz, V. Messmann, N. Hammer, A.M. Goepferich, F.P. Brandl, Diels-Alder hydrogels with enhanced stability: First step toward controlled release of bevacizumab, *Eur. J. Pharm. Biopharm.* 96 (2015) 217–225.
- [35] K.C. Koehler, K.S. Anseth, C.N. Bowman, Diels-Alder mediated controlled release from a poly(ethylene glycol) based hydrogel, *Biomacromolecules* 14 (2013) 538–547.
- [36] J.J. Grigsby, H.W. Blanch, J.M. Prausnitz, Diffusivities of Lysozyme in Aqueous MgCl₂ Solutions from Dynamic Light-Scattering Data: Effect of Protein and Salt Concentrations, *J. Phys. Chem. B* 104 (2000) 3645–3650.
- [37] H. Tsuge, O. Natsuaki, K. Ohashi, Purification, properties, and molecular features of glucose oxidase from *Aspergillus niger*, *J. Biochem.* 78 (1975) 835–843.
- [38] S.K. Li, M.R. Liddell, H. Wen, Effective electrophoretic mobilities and charges of anti-VEGF proteins determined by capillary zone electrophoresis, *J. Pharm. Biomed. Anal.* 55 (2011) 603–607.
- [39] M.D. Pegram, G. Konecny, D.J. Slamon, The molecular and cellular biology of HER2/neu gene amplification/overexpression and the clinical development of herceptin (trastuzumab) therapy for breast cancer, *Cancer Treat. Res.* 103 (2000) 57–75.
- [40] P.I. Lee, C.-J. Kim, Probing the mechanisms of drug release from hydrogels, *J. Controlled Release* 16 (1991) 229–236.

Chapter 3 – Supporting information

A novel anhydrous preparation of PEG hydrogels enables high drug loading with biologics for controlled release applications

1 Mechanism of melt polymerization

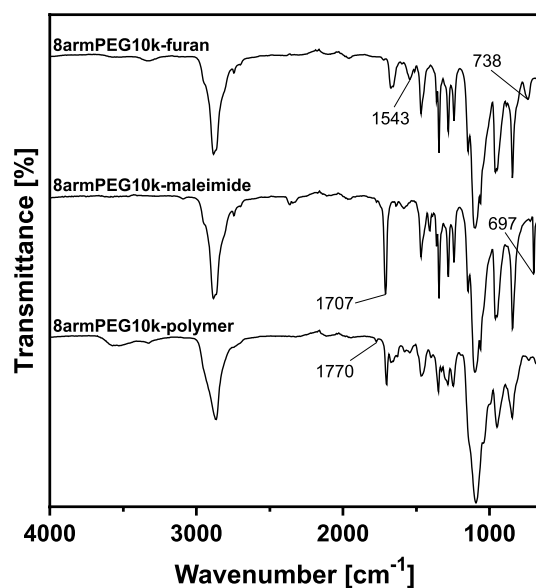


Figure S1: FTIR spectra of 8armPEG10k-furan, 8armPEG10k-maleimide, and the melt polymer prepared from both precursors. The decrease of absorption characteristic for furan (1543 and 738 cm⁻¹) and maleimide (1707 and 697 cm⁻¹) indicated the occurrence of the DA reaction. Additionally, adduct band at 1770 cm⁻¹ confirmed the formation of the DA adduct.

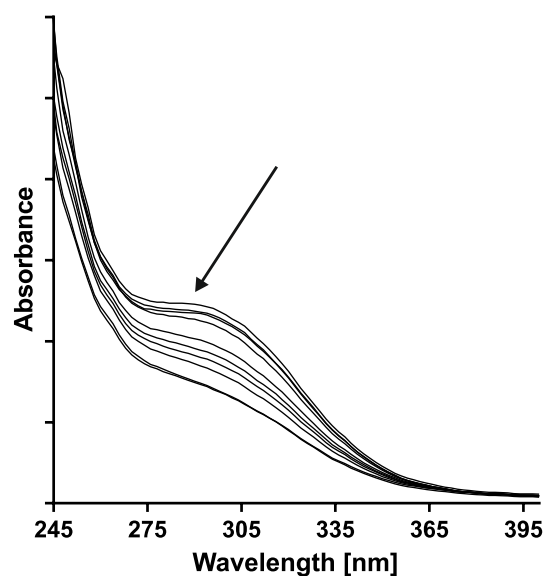


Figure S2: UV-VIS absorption spectra following the melt polymerization. The peak at 299 nm characteristic for unreacted maleimide decreases due to the formation of the DA adduct and the corresponding conjugation loss.

2 Shear viscosity

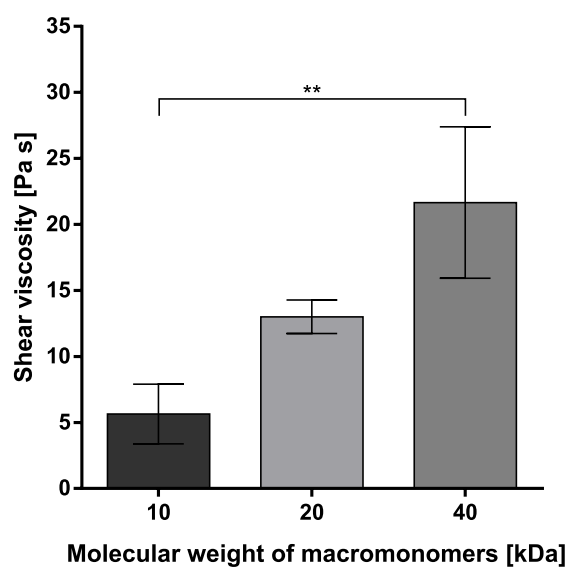


Figure S3: Shear viscosity of precursor blends after complete melting depending on molecular weight. Level of statistical significance is indicated as $**p \leq 0.01$.

3 SEM

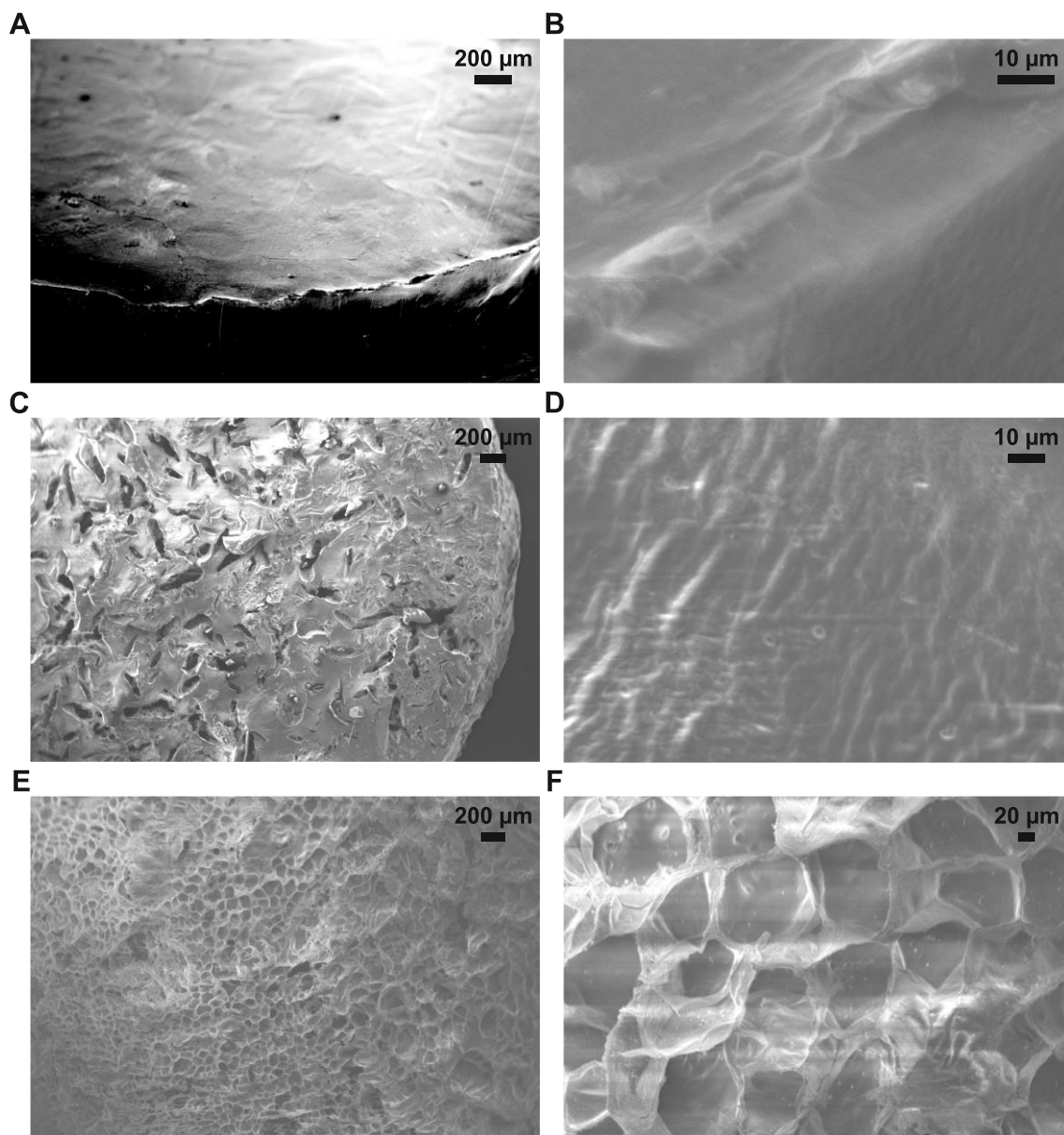


Figure S4: SEM images of 8armPEG10k-polymers after melt polymerization (A and B), after swelling 1 day (C and D), and after swelling around 100 days (E and F). Images B-D were taken after freeze-drying of the swollen polymers.

4 Cytotoxicity

Although PEG is FDA approved [1] and its derivatives are commonly used excipients in the pharmaceutical field, these polymers had to be analyzed regarding possible toxic effects on cells. Unreacted macromonomers and potential side products of the precursor synthesis might have cytotoxic effects. To assess cytotoxicity, an MTT assay was carried out in accordance with ISO 10993-5:2009. To avoid additional stress for the cells due to contact between cells and polymers, extracts were produced by incubating all polymers in 10% FCS EMEM for 24 h. Subsequently, the extracts were administered to the cells, and the cytotoxicity was assessed using pure medium as positive control and

medium containing 0.1% (w/v) SDS as negative control. The relative cell viability was $78.3 \pm 5.6\%$ for polymers prepared from precursors with a molecular weight of 10 kDa, $77.5 \pm 4.0\%$ for 20 kDa, and $65.7 \pm 2.7\%$ for 40 kDa. Polymers prepared from the smaller precursors showed similar cell viability and passed the 70% threshold value stated in ISO 10993. Only the polymers consisting of 8armPEG40k did not pass the threshold. A decrease in cell viability after exposure to the extracts can be explained by the acidic degradation product of maleimide groups. Maleamic acid can decrease the pH of the medium. Additionally, after the polymerization process, unreacted functional groups are still present in the polymer. Maleimide groups in particular have toxic potential to the cells due to their electrophilic nature. For further investigation, *in vivo* experiments are necessary to examine the biocompatibility of the DA melt polymers.

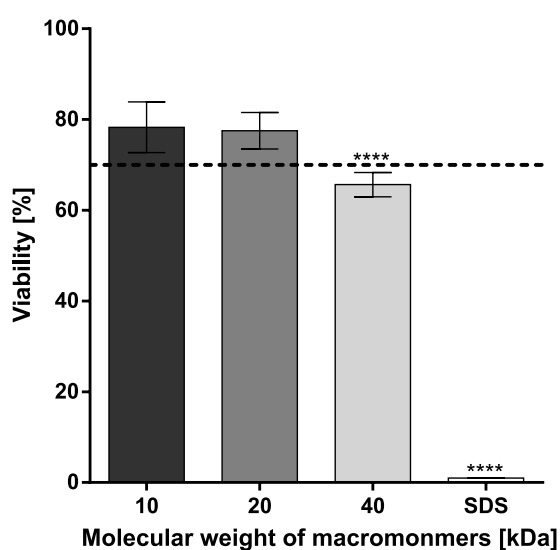


Figure S5: Viability of L-929 cells after incubation with extracts from melt polymers. Medium containing 0.1% (w/v) SDS was used as negative control. 70% cell viability (dotted line) indicates the threshold for cytocompatibility. Levels of statistical significance are indicated as **** $p \leq 0.0001$.

5 HPLC-SEC of GOx

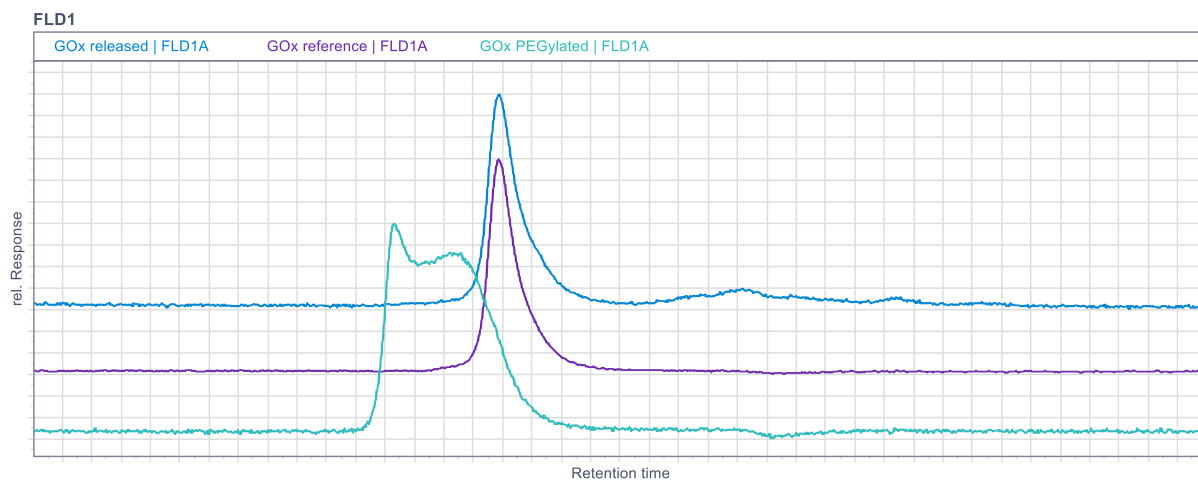


Figure S6: Size exclusion chromatogram of the released GOx (blue) compared to fresh GOx (purple) and with 8armPEG10k-maleimide-incubated GOx (turquoise). The experiment proved the integrity of the released enzyme.

Reference

- [1] Q. Huang, D. Li, A. Kang, W. An, B. Fan, X. Ma, G. Ma, Z. Su, T. Hu, PEG as a spacer arm markedly increases the immunogenicity of meningococcal group Y polysaccharide conjugate vaccine, *J. Controlled Release* 172 (2013) 382–389.

Chapter 4

In situ forming iEDDA hydrogels with tunable gelation time release high molecular weight proteins in a controlled manner over an extended time

Published in *Biomacromolecules*

Abstract

Off-target interactions between reactive hydrogel moieties and drug cargo as well as slow reaction kinetics and the absence of controlled protein release over an extended period of time are major drawbacks for chemically cross-linked hydrogels for biomedical applications. In this study, the inverse electron demand Diels-Alder (iEDDA) reaction between norbornene- and tetrazine-functionalized eight-armed poly(ethylene glycol) (PEG) macromonomers was used to overcome these obstacles. Oscillatory shear experiments revealed that the gel point of a 15% (w/v) eight-armed PEG-hydrogel with a molecular weight of 10 kDa was less than 15 s, suggesting the potential for fast *in situ* gelation. However, the high-speed reaction kinetics result in a risk of premature gel formation that complicates the injection process. Therefore, we investigated the effect of polymer concentration, temperature, and chemical structure on the gelation time. The cross-linking reaction was further characterized regarding bioorthogonality. Only 11% of the model protein lysozyme was found to be PEGylated by the iEDDA reaction, whereas 53% interacted with the classical Diels-Alder reaction. After determination of the mesh size, fluorescein isothiocyanate-dextran was used to examine the release behavior of the hydrogels. When glucose oxidase was embedded into 15% (w/v) hydrogels, a controlled release over more than 250 days was achieved. Overall, the PEG-based hydrogels cross-linked via the fast iEDDA reaction represent a promising material for the long-term administration of biologics.

1 Introduction

Since the first report of a hydrogel for biological use by Wichterle and Lím [1], hydrogels have reached a position of great prominence in biomedical research, especially in the field of drug delivery [2]. They are particularly useful for the development of minimally invasive injectable protein delivery systems if they fulfill certain requirements. First, the chosen cross-linking reaction has to be fast enough to ensure instant gelation after injection. To this end, the Diels-Alder (DA) reaction, oxime click chemistry, or classical Cu(I)-free Huisgen cycloaddition have been suggested [3–5]. Due to their relatively long gelation times, they are not suitable for *in situ* gelation under physiological conditions. In addition, reactions fast enough for *in situ* gelation often require toxic catalysts or additional initiators. For example, the copper catalyst involved in the copper-catalyzed azide-alkyne cycloaddition is toxic to healthy tissue even at low concentrations [6]. Furthermore, free-radical polymerization and thiol-ene click chemistry can lead to possible toxic side reactions with proteins or tissues [7,8].

On the other hand, the high reaction rate is at odds with the requirement that the gelation time is precisely controlled in order to facilitate injection handling and to avoid premature viscosity increase which would result in the clogging of syringe needles. Bi et al. demonstrated how to influence the reaction kinetics of the Michael-type addition by changing the electron density of alkenyl structures [9]. However, alkenyl groups represent a target for unwanted side reactions with nucleophilic residues of proteins such as amine and thiol groups [10]. As a different approach, the gelation time of the strain-promoted oxidation-controlled cyclo-octyne-1,2-quinone cycloaddition is adjustable by the concentration of mushroom tyrosinase [11]. Even if the use of toxic substances can be avoided, the addition of enzymes could have a negative effect on the already limited loading capacity of common hydrogels [12].

A final demand is that the cross-linker must be selective for its counterpart to avoid off-target reactions with the protein cargo as well as proteins in the tissue of the injection site. Hence, reactions that are susceptible to amine structures or nucleophiles like Schiff-base reactions, genipin coupling, β -aminoacrylate formation, and *o*-phthalaldehyde condensation pose too great a risk of interacting with proteins or body tissues [13–15].

To overcome these obstacles, the use of inverse electron demand Diels-Alder (iEDDA) reaction represents a promising approach for the preparation of *in situ* forming protein delivery systems. The electron-rich norbornene and the electron-poor tetrazine interact efficiently and rapidly in bioorthogonal and catalyst-free reaction that generates only negligible amounts of nitrogen gas but no toxic side products [16–18]. These attractive characteristics have made iEDDA chemistry very appealing for biological applications like synthesizing hydrogels for cell encapsulation [19,20] and protein delivery [21,22]. While the release of therapeutic proteins over long periods of time from months to years could be advantageous for the therapy of diseases like cancer, rheumatoid arthritis, or age-related macular degeneration [23–25], no hydrogels based on iEDDA cross-linking via norbornene and tetrazine groups have been developed for long-term protein release thus far. Commonly used approaches for long-term

release rely on the inclusion of drug-loaded micro- or nanoparticles into hydrogels [26,27], leading to a further decrease of the already limited drug loading capacity of hydrogels [12]. Yet another way to prolong the release from hydrogels is to exploit the affinity of the drug for groups incorporated into the hydrogel backbone such as heparin [28], biotin derivatives [29], or peptides [30] which is, however, of limited broad applicability. Tuning the characteristics of a hydrogel itself is a more appealing alternative. A wide range of drugs could be released in a controlled way based on their size relative to the hydrogel mesh size and without the need for additional excipients. For this, the use of the iEDDA reaction is advantageous because its bioorthogonality reduces side reactions with proteins that makes it ideal for protein delivery [21]. Moreover, iEDDA reaction is irreversible [19] but in combination with hydrolytically cleavable groups such as ester groups the degradation time of the hydrogels can be controlled and hydrogels with tailored stability for long-term release applications can be developed. In this study, poly(ethylene glycol) (PEG) based iEDDA hydrogels with tunable reaction kinetics were prepared for the release of high molecular weight proteins over months to years. To prepare hydrogel precursors, eight-armed PEGs were modified with either tetrazine or norbornene functional groups. The hydrogel formation was monitored via oscillatory shear experiments. We investigated the effects of the number of functional groups, temperature, and functional group modification on reaction kinetics. Additionally, hydrogel stiffness and Young's modulus of compression (compressive modulus) were determined depending on the polymer concentration and the molecular weight of the used macromonomers. The bioorthogonality of the iEDDA reaction was examined and compared to the classical DA reaction. Afterwards, cytotoxicity was assessed. To further characterize the hydrogels, mesh sizes were calculated and swelling and degradation studies were performed. To explore the feasibility of the controlled release of large molecules from the material, fluorescein isothiocyanate-dextran (FITC-dextran) with a molecular weight of 150 kDa was embedded and released from hydrogels of different concentrations. Finally, the model protein glucose oxidase (GOx) was loaded into the hydrogels and the release was analyzed.

2 Materials and methods

2.1 Materials

Anhydrous acetonitrile, deuterated chloroform (CDCl_3), anhydrous dichloromethane (DCM), *N,N'*-dicyclohexylcarbodiimide (DCC), diisopropyl azodicarboxylate (DIAD), anhydrous *N,N*-dimethylformamide (DMF), FITC-dextran with a molecular mass of 150 kDa, furan, 3-(2-furyl)propanoic acid, Eagle's minimum essential medium (EMEM), absolute ethanol, anhydrous ethyl acetate, fetal calf serum (FCS), glacial acetic acid, GOx (Type X-S, from *Aspergillus niger*), hexane, hydrazine monohydrate, *N*-hydroxysuccinimide (NHS), lysozyme (from chicken egg white), maleimide, *N*-methoxycarbonylmaleimide, *Micrococcus lysodeikticus*, methoxy PEG with a molecular weight of 5 kDa (mPEG5k), *exo*-5-norbornenecarboxylic acid, Pierce™ Unstained Protein MW Marker,

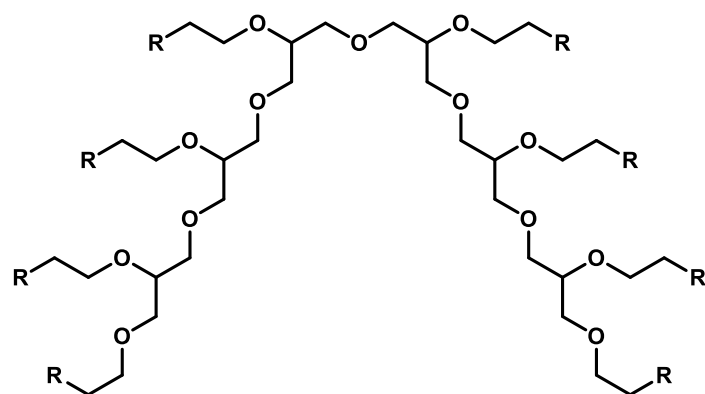
protein LoBind Eppendorf tubes, QuantiPro™ BCA Assay Kit, sodium bicarbonate, sulfur, and anhydrous tetrahydrofuran were purchased from Sigma-Aldrich (Taufkirchen, Germany). Eight-armed PEGs (8armPEG) with molecular masses of 10 kDa (8armPEG10k), 20 kDa (8armPEG20k), and 40 kDa (8armPEG40k) were received from JenKem Technology (Allen, TX, USA). 4-dimethylaminopyridine (DMAP), phthalimide, and anhydrous sodium sulfate were received from Acros Organics (Geel, Belgium). DCM p.a. was purchased from Fisher Chemical (Loughborough, UK). Diethyl ether (technical grade) was obtained from Jäcklechemie (Nuremberg, Germany). Ammonium persulfate, barium chloride dihydrate, 1,4-dioxane, glycine, hydrochloric acid, di-potassium hydrogen phosphate trihydrate, pyridine, silica gel 60 (0.063–0.200 mm), sodium azide, sodium chloride, sodium dihydrogen phosphate monohydrate, sodium hydroxide, sodium nitrite, and triphenylphosphine were received from Merck KGaA (Darmstadt, Germany). 3-(4-Cyanophenyl)-propionic acid was obtained from abcr GmbH (Karlsruhe, Germany). Iodine solution and tetramethylethylenediamine were purchased from Carl Roth GmbH & Co. KG (Karlsruhe, Germany). Acrylamide/bis-acrylamide (37.5:1) solution, bromophenol blue sodium salt, and coomassie brilliant blue G-250 were obtained from Serva Electrophoresis GmbH (Heidelberg, Germany). Glycerol, 3-(4,5-dimethylthiazol-2-yl)-2,5-diphenyltetrazolium bromide (MTT) and sodium dodecyl sulfate (SDS) were purchased from PanReac AppliChem (Darmstadt, Germany). 2-Amino-2-hydroxymethyl-propane-1,3-diol (TRIS) was received from Affymetrix (Santa Clara CA, USA). Ethanol was purchased from Labochem international (Heidelberg, Germany). Gibco Dulbecco's phosphate-buffered saline was received from Life Technologies (Darmstadt, Germany). Mouse fibroblast cells were a kind gift from the group of Prof. Armin Buschauer (University of Regensburg). Purified water was freshly prepared using a Milli-Q water purification system from Millipore (Schwalbach, Germany).

2.2 ¹H and ¹³C NMR Spectroscopy

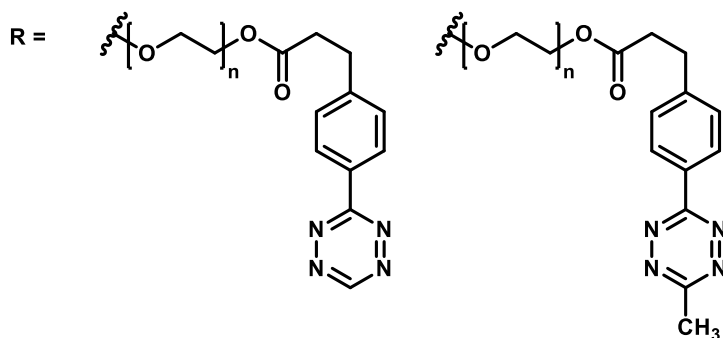
¹H and ¹³C NMR spectra were recorded in CDCl₃ using a Bruker Avance III 400 spectrometer (Bruker BioSpin GmbH, Rheinstetten, Germany). The end-group conversions of 8armPEGs were calculated by comparing the integral of the proton peak of the respective functional group to the integrated PEG backbone proton peak at δ3.75–3.40 ppm.

2.3 Synthesis of 3-(4-(1,2,4,5-tetrazin-3-yl)phenyl)propanoic acid

3-(4-(1,2,4,5-Tetrazin-3-yl)phenyl)propanoic acid was synthesized similarly to previously published protocols [31]. 3-(4-Cyanophenyl)propionic acid was used instead of 4-cyanophenylacetic acid. The yield was 58%.

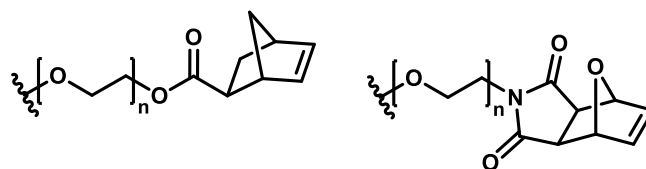


hexaglycerol core of 8armPEG



8armPEG-Tz

8armPEG-methyl-Tz



8armPEG-Nb

8armPEG-ETPI

Scheme 1: Chemical structures of differently functionalized 8armPEGs. The hydrogel precursors had molecular weights of 10 kDa, 20 kDa, or 40 kDa. 8armPEG-ETPI was obtained in *endo* and *exo* form. For simplification, 8armPEG-ETPI is only shown in *exo* position.

2.4 Synthesis of tetrazine-functionalized 8armPEGs (Scheme 1)

To synthesize tetrazine-functionalized 8armPEGs with a molecular weight of 10 kDa (8armPEG10k-Tz), 20 kDa (8armPEG20k-Tz), and 40 kDa (8armPEG40k-Tz), the procedure was adapted from a previously published protocol for the esterification of multiarmed PEGs [32]. In brief, 3-(4-(1,2,4,5-tetrazin-3-yl)phenyl)propanoic acid (4.3-fold of PEG-OH groups) and DCC (2.2-fold of PEG-OH groups) were dissolved in a mixture of anhydrous DCM and anhydrous DMF and stirred for 30 min at 0 °C. Afterwards, the precipitate was filtered. The filtrate was combined with a solution of 8armPEG-OH in anhydrous DCM with pyridine (4.3-fold of PEG-OH groups) and DMAP (0.4-fold of PEG-OH groups). After the solution was stirred overnight in an ice bath, it was washed with 5% sodium

bicarbonate solution twice and brine once, dried over sodium sulfate, and then filtered and concentrated via rotary evaporator. Then, the product was precipitated by dropwise addition of cold diethyl ether. For purification, the crystallization step was repeated. The precipitate was collected by filtration and dried under vacuum. The yield was 81% for 8armPEG10k-Tz, 90% for 8armPEG20k-Tz, and 87% for 8armPEG40k-Tz. The degree of end-group conversion was 81% for 8armPEG10k-Tz, 78% for 8armPEG20k-Tz, and 77% for 8armPEG40k-Tz, as determined by ^1H NMR spectroscopy.

2.5 Synthesis of 3-(4-(6-methyl-1,2,4,5-tetrazin-3-yl)phenyl)propanoic acid

3-(4-(6-Methyl-1,2,4,5-tetrazin-3-yl)phenyl)propanoic acid was synthesized as described for 3-(4-(1,2,4,5-tetrazin-3-yl)phenyl)propanoic acid with the following modifications. One equivalent of 3-(4-cyanophenyl)-propionic acid, one equivalent of anhydrous acetonitrile, and two equivalents of sulfur were combined in a microwave reaction tube. 17 equivalents of ethanol were added to obtain a suspension upon mixing. Afterwards, hydrazine monohydrate (eight-fold to nitrile group) was added, and the vessel was sealed. The mixture was heated to 50 °C for 24 h. The next day, DCM and a sodium nitrite solution (10-fold to nitrile group) were added. Subsequently, an excess of acetic acid (60-fold to nitrile group) was added slowly during which the solution turned bright red in color. The product was extracted with DCM. The organic phase was dried over anhydrous sodium sulfate, filtered, and concentrated under reduced pressure. The residue was purified using silica gel chromatography to yield 6% product. For a synthesis of methylphenyl substituted tetrazine with a higher yield, the reader is referred to the work by Zhan et al. [33].

2.6 Synthesis of methyl-tetrazine-functionalized 8armPEG10k (8armPEG10k-methyl-Tz) (Scheme 1)

For the esterification of 8armPEG10k with methyl-substituted tetrazine, the protocol of section 2.4 was slightly varied. 3-(4-(6-Methyl-1,2,4,5-tetrazin-3-yl)phenyl)propanoic acid was used instead of 3-(4-(1,2,4,5-tetrazin-3-yl)phenyl)propanoic acid. The yield was 86%, and the degree of end-group conversion was 76%, as determined by ^1H NMR spectroscopy.

2.7 Synthesis of norbornene-functionalized 8armPEGs (Scheme 1)

Norbornene esterified 8armPEGs with a molecular weight of 10 kDa (8armPEG10k-Nb), 20 kDa (8armPEG20k-Nb), and 40 kDa (8armPEG40k-Nb) were synthesized as previously described [34].

2.8 Synthesis of 3,6-epoxy-1,2,3,6-tetrahydrophthalimide-substituted 8armPEG10k (8armPEG10k-ETPI) (Scheme 1)

3,6-Epoxy-1,2,3,6-tetrahydrophthalimide (ETPI) and 8armPEG10k-ETPI were synthesized as previously described for 4armPEG10k-ETPI [35]. The yield was 69%, and the degree of end-group conversion was 81%, as determined by ^1H NMR spectroscopy.

2.9 Functionalization of mPEG5k

mPEG5k-furan and mPEG5k-maleimide were synthesized as previously described [10]. The esterification of mPEG5k with norbornene and tetrazine groups was achieved according to the protocol of 8armPEG-Nb and 8armPEG-Tz, respectively. The yield was 68 and 41%, and the degree of end-group conversion was 97 and 98%, as determined by ^1H NMR spectroscopy for mPEG5k-norbornene and mPEG5k-tetrazine, respectively.

2.10 iEDDA hydrogel preparation

For iEDDA hydrogel preparation, macromonomers with similar molecular weight were used. Equal molar amounts of 8armPEG-Nb and 8armPEG-Tz were separately dissolved in water. After combining both solutions, 200 μl were transferred into cylindrical glass molds (7 mm inner diameter) and allowed to gel for 1 h at 37 $^\circ\text{C}$, leading to hydrogels with an overall polymer concentration of 5, 10, and 15% (w/v). For example, 14.5 mg of 8armPEG10k-Nb and 15.5 mg of 8armPEG10k-Tz were dissolved in 100 μl water, respectively. The gelation started immediately after mixing both solutions leading to a 15% (w/v) 8armPEG10k-hydrogel.

2.11 iEDDA hydrogel characterization

Rheological experiments were carried out on a Malvern Kinexus Lab+ rheometer (Malvern, Kassel, Germany) with a 25 mm parallel plate geometry, an oscillation frequency of 1.0 Hz, and a strain of 1%. After casting 270 μl of the combined precursor solutions, the upper plate was lowered to a gap size of 500 μm , and the experiment was started. Storage modulus (G'), loss modulus (G''), and complex shear modulus (G^*) were measured over time. The cross-over point of G' and G'' was regarded as the gel point. The absolute value of the complex shear modulus ($|G^*|$) was determined after 30 min when polymerization was considered complete. To reduce water evaporation, a solvent trap was used.

The average mesh sizes (ξ) of the hydrogels were determined using the equilibrium swelling theory [36,37]. In brief, hydrogels were prepared as described in section 2.10. The matrices were weighed in air and hexane before and after swelling in Milli-Q water for 1 day at 37 $^\circ\text{C}$. The gel volumes after cross-linking (V_{gc}) and after swelling (V_{gs}) were calculated based on Archimedes' principle of buoyancy.

Afterwards, the hydrogels were freeze-dried to determine the dry polymer volume (V_p). The density of PEG was taken as 1.12 g/ml [35]. The polymer fraction of the hydrogel after cross-linking ($v_{2c} = V_p/V_{gc}$) and the polymer fraction in swollen state ($v_{2s} = V_p/V_{gs}$) were calculated. A modified Flory-Rehner equation (1) was used to calculate the number of moles of elastically active chains in the hydrogel network (v_e) [38–40]:

$$v_e = -\frac{V_p}{V_1 v_{2c}} \cdot \frac{[\ln(1 - v_{2s}) + v_{2s} + \chi_1 v_{2s}^2]}{\left[\left(\frac{v_{2s}}{v_{2c}} \right)^{\frac{1}{3}} - \frac{2}{f} \left(\frac{v_{2s}}{v_{2c}} \right) \right]} \quad (1)$$

V_1 is the molar volume of solvent (18 ml/mol) [41], χ_1 is the Flory-Huggins interaction parameter of PEG in water (0.426) [42], and f is the branching factor of the macromonomers (eight for 8armPEG). ξ was obtained by [43]:

$$\xi = v_{2s}^{-\frac{1}{3}} l \left(\frac{2m_p}{v_e M_r} \right)^{\frac{1}{2}} C_n^{\frac{1}{2}} \quad (2)$$

In equation (2), l is the average bond length along the PEG backbone (0.146 nm) [44], m_p is the total mass of polymer in the hydrogel, M_r is the molecular mass of the PEG repeating unit (44 g/mol), and C_n is the Flory characteristic ratio (four for PEG) [44].

The compressive modulus was determined according to a modified version in the literature [45]. Hydrogels with a volume of 200 μ l were prepared as described in section 2.10. For 8armPEG10k-hydrogels, polymer concentrations of 5, 10, and 15% (w/v) were used. 8armPEG20k- and 8armPEG40k-hydrogels consisted of 5% (w/v) polymer. First, hydrogel diameter and height were determined using a caliper. Hydrogel cylinders were cast on the lower plate of an Instron 5542 materials testing machine (Norwood, MA, USA). Subsequently, the samples were compressed uniaxially at a speed of 1 mm/min. Compressive force (N) and compressive strain (%) were recorded as a function of time. The linear part of the curve between 10 and 20% compression was used to calculate the compressive modulus.

2.12 Cytotoxicity

Cytotoxicity of the hydrogels was assessed according to ISO 10993-5:2009 (Biological evaluation of medical devices, part 5: Tests for *in vitro* cytotoxicity) by using extracts as previously described [46]. In brief, 10,000 mouse fibroblast L-929 cells per well were seeded in a 96-well microtiter plate and cultivated overnight. 15 % (w/v) 8armPEG10k-, 8armPEG20k-, and 8armPEG40k-hydrogels with a

volume of 200 μ l were prepared as described in section 2.10. The hydrogels were incubated in 2 ml of EMEM supplemented with 10% FCS for 24 h at 37 °C. The extracts were prepared by separating the supernatants from the hydrogels. 100 μ l extract was added to each well. 0.1% SDS served as the negative control, whereas pure medium was used as the positive control. For each sample, at least six replicates were prepared. After 24 h of incubation at 37 °C, the medium was removed and replaced with 200 μ l of a 1.5 mM MTT solution. The MTT solution was removed after 6 h of incubation at 37 °C. PBS containing 10% SDS was added, and the samples were incubated for 16 h at room temperature. The absorbance at 570 and 690 nm was measured using a FluoStar Omega microplate reader (BMG Labtech, Ortenberg, Germany). The difference in absorbance at 570 and 690 nm relative to the positive control was used to calculate cell viability. The viability was normalized to the positive control. 70% cell viability indicates the threshold for cytocompatibility [46–48].

2.13 Protein interaction with DA cross-linking reactions

The influence of classical DA reaction and iEDDA reaction on proteins was investigated according to a modified protocol [10]. Lysozyme was incubated with different functionalized mPEG5k derivatives in 50 mM phosphate buffer (pH 7.4) at 37 °C in a shaking water bath for 1 day. To simulate the DA reaction, 0.5 mg of lysozyme was dissolved with 9.15 mg of mPEG5k-furan and 9.15 mg of mPEG5k-maleimide. iEDDA reaction was mimicked by incubating 0.5 mg of lysozyme with 9.15 mg of mPEG5k-norbornene and 9.15 mg of mPEG5k-tetrazine. After incubation, PEGylation of lysozyme was examined by SDS-PAGE as previously described [49]. In brief, polyacrylamide gels of 14% cross-linking were prepared. Lanes were loaded with 5 μ g protein. A constant voltage of 120 V and a decreasing current of 68 mA were applied. The gels were stained with Coomassie Brilliant Blue G-250. The ChemiDoc™ MP gel imaging system was used for imaging. The relative abundance was calculated by the band intensity via Image Lab™ (all Bio-Rad Laboratories GmbH, Munich, Germany). PEG was visualized by iodine staining as described by Natarajan et al. [50].

The activity of the enzyme was measured by following a modified version of the method described by Shugar [10,51]. In brief, lysozyme solutions were diluted with 70 mM phosphate buffer (pH 6.2) to a concentration of 0.01 mg/ml. To 100 μ l of the diluted lysozyme solutions, 2.5 ml of a micrococcus lysodeikticus suspension (0.015%) in the same buffer was added. The change in optical density was measured for 6 min at 25 °C using a Kotron UVIKON 941 spectrophotometer (Kotron Instruments S.p.A., Milan, Italy). The slope of the absorbance was used for the calculation of lysozyme activity.

2.14 Swelling and degradation studies

Swelling and degradation studies were performed similarly to those previously described [37]. Hydrogels with a volume of 200 μ l were prepared as described in section 2.10. After weighing, the

hydrogels were transferred to protein LoBind Eppendorf tubes and incubated in 5 ml of a 50 mM phosphate buffer (pH 7.4) containing 0.02% sodium azide at 37 °C in a shaking water bath. The gels were separated from the buffer and weighed at various intervals. Afterwards, the hydrogels were incubated in 5 ml fresh buffer solution. The degradation was considered complete when no remaining material could be detected.

2.15 Release of FITC-dextran and GOx

iEDDA hydrogels made of precursors with a molecular weight of 10 kDa were chosen to assess the release kinetics of protein drug surrogates. The polymer concentrations of 5, 10, and 15% (w/v) were investigated. For the release of FITC-dextran, 200 μ l hydrogels containing 2 mg of FITC-dextran were prepared. For the release of GOx, the hydrogels contained 0.4 mg of GOx. For example, to prepare a hydrogel with 15% polymer concentration containing FITC-dextran, 14.5 mg of 8armPEG10k-Nb were dissolved in 100 μ l of a solution with a FITC-dextran concentration of 20 mg/ml. To this mixture, 100 μ l of a solution containing 15.5 mg of 8armPEG10k-Tz was added. After mixing, the hydrogel was formed after 1 h at 37 °C. The hydrogels were transferred into 5 ml LoBind Eppendorf tubes and incubated in 5 ml of 50 mM phosphate buffer (pH 7.4) with 0.02% sodium azide. The release experiments were carried out in a shaking water bath at 37 °C. At regular time points, samples were withdrawn and replaced with fresh buffer. Only 300 μ l were removed to keep possible mechanical stress as low as possible. Additionally, over a long-term release, we expected concentrations in the medium to be very low and wanted to avoid falling below the detection limit. The amount of FITC-dextran was determined via fluorescence using a fluorescence microplate reader (BMG, Labtech, Ortenberg, Germany) [35]. GOx was quantified with a BCA assay.

2.16 Statistical analysis

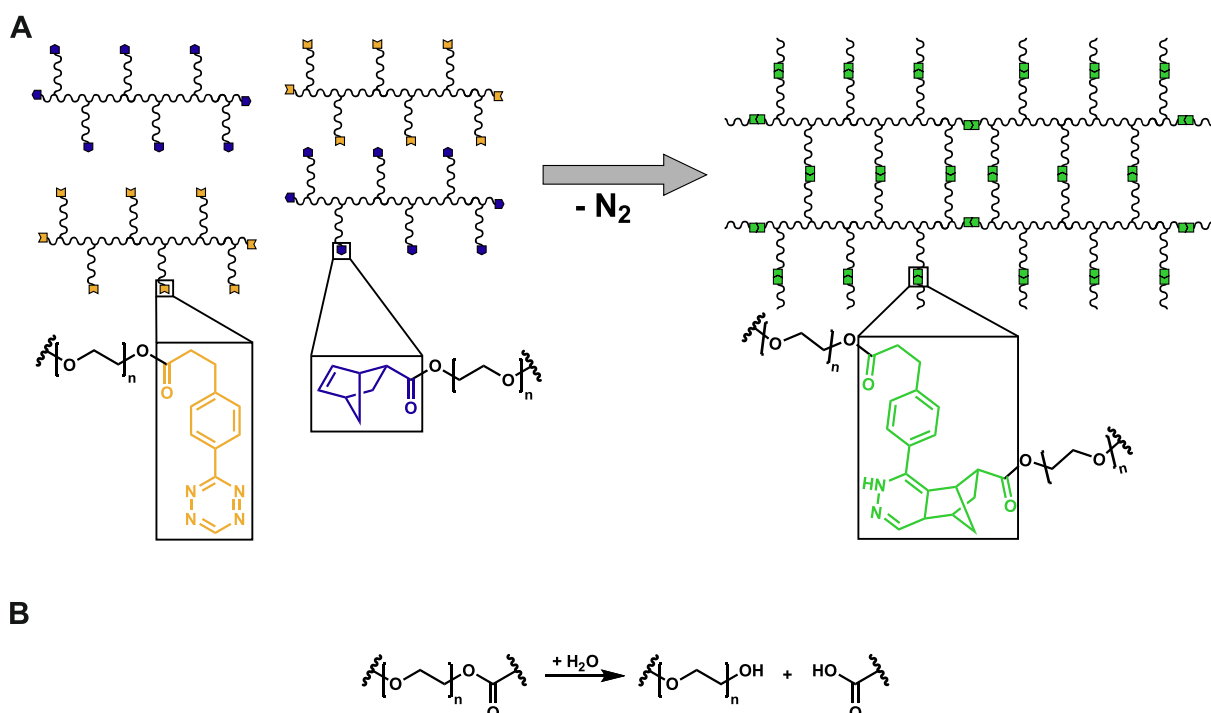
All experiments were performed with at least three samples, and the results are shown as mean \pm standard deviation. Statistical significance was assessed using one-way ANOVA. Post hoc analysis was determined by Tukey's test (GraphPad Prism 6.0, GraphPad Software Inc., La Jolla, CA, USA).

3 Results and discussion

3.1 Synthesis of norbornene- and tetrazine-functionalized PEG derivatives

3-(4-(1,2,4,5-Tetrazin-3-yl)phenyl)propanoic acid was successfully synthesized using the method reported by Qu et al. [31]. Yields of 58% were achieved. Furthermore, the replacement of DCM by acetonitrile as a second nitrile compound led to methyl-substituted tetrazines. 8armPEGs were functionalized with 3-(4-(1,2,4,5-tetrazin-3-yl)phenyl)propanoic acid via DCC chemistry according to

previously published protocols for esterification of PEG derivatives with norbornene groups [32,34]. With this method, end-group conversions were obtained in a range of 76–81%, which is satisfactory for cross-linking. The combination of the tetrazine synthesis and the PEG esterification represents a cost-effective and easy way for the production of functionalized polymers in the range of 10 g or higher. Since tetrazine synthesis and subsequent functionalization of polymers used for hydrogel preparation have so far usually been accomplished in the milligram range [52], this method represents a more efficient approach.



Scheme 2: Hydrogel formation via iEDDA reaction of 8armPEG-tetrazine and 8armPEG-norbornene in water (A). For simplification, only one isoform of the iEDDA adduct is shown. Degradation of the hydrogel due to ester hydrolysis (B).

3.2 Rheological characterization and tuning of the reaction rate

A fast reaction rate is a key requirement for the use of covalently cross-linked hydrogels as *in situ* forming depot systems. Directly after injection into the organism, the liquid should start to gel and create a three-dimensional network (Scheme 2A) that embeds proteins rapidly to avoid loss by diffusion into the surrounding tissue. The gel point of the iEDDA hydrogels was investigated by oscillatory shear experiments. This point indicates the transition from a liquid-like to a solid-like behavior and is a critical design factor for *in situ* forming hydrogels. Figure 1 shows a representative rheogram of a 15% (w/v) 8armPEG10k-hydrogel. Immediately after the start of the experiment, a very fast increase of G' can be observed, which reaches a plateau after approximately 300 s. The gel point was found to be at 14.7 ± 1.5 s (Figure 2A), which shows the ability of rapid *in situ* gelation.

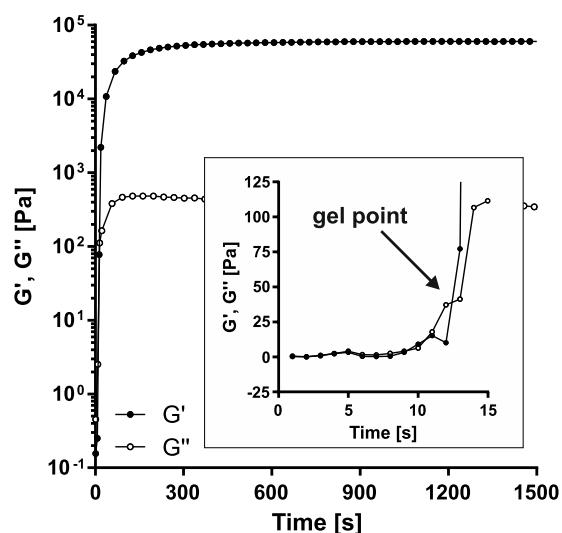


Figure 1: Rheogram of a 15% (w/v) 8armPEG10k-hydrogel with an inset showing the gel point. Storage (G') and loss modulus (G'') were measured as a function of time. A 25 mm parallel plate geometry with a gap size of 500 μm at an oscillation frequency of 1.0 Hz was used.

While this fast reaction rate is necessary to form *in situ* depots, it also poses some challenges. In general, hydrogels should not be subjected to shear forces once they have reached the gel point so as to maintain an intact network. Additionally, gelation that occurs too quickly could lead to clogging of the injection needle resulting in incomplete administration [53]. These characteristics of hydrogels make handling more difficult because the injection procedure after combining the precursor solutions must be very quick. To overcome this limitation, various parameters were changed, and the adjustability of this system towards longer gelation times was investigated. The first method to increase the gelation time was to decrease the number of functional groups. This could be achieved by reducing the polymer concentration of the functionalized 8armPEG10k derivatives (Figure 2A) or by increasing the molecular weight of the 8armPEG macromonomers (Figure 2B). For the first case, a polymer concentration of 10% (w/v) resulted in an insignificant decrease of the gelation time to 21.1 ± 1.2 s. In contrast, a reduction of the concentration from 15 to 5% (w/v) led to a significantly longer gelation time of 30.9 ± 8.1 s. For all further rheological experiments, a polymer concentration of 5% (w/v) was used. In this way, differences were more apparent due to the lower number of functional groups. Another option to decrease the number of functional groups was to use larger macromonomers. By only changing the molecular weight of the macromonomers, but not the concentration or the branching factor, the number of functional groups was halved for 8armPEG20k and quartered for 8armPEG40k. A gelation time of 81.8 ± 9.2 s was found for the 8armPEG20k-hydrogel and 123.7 ± 7.6 s for the 8armPEG40k-hydrogel. As expected, larger macromonomers prolonged the gelation time significantly. This is in accordance with the results found for DA hydrogels prepared with similar macromonomers [35,54]. Due to the reduced number of functional groups, the likelihood that two different functional groups find each other and react to form an elastically active chain is decreased. Furthermore, 8armPEGs with higher molecular weight consist of larger PEG chains, which are bulkier and more difficult to access than smaller ones.

For completeness, the influence of various molar ratios of the functional groups on the gelation time was investigated (Figure S1). No significant difference could be found for tetrazine norbornene ratios of 1:2 and 2:1. A further increase in ratio was not investigated, since the risk of remaining unreacted tetrazine groups interacting with thiol groups of proteins increases for biomedical applications [55]. On the other hand, an increased amount of norbornene led to poor hydrogel formation. Poor to no gelation due to changing the ratio of the used hydrogel precursors has already been described in the literature [56].

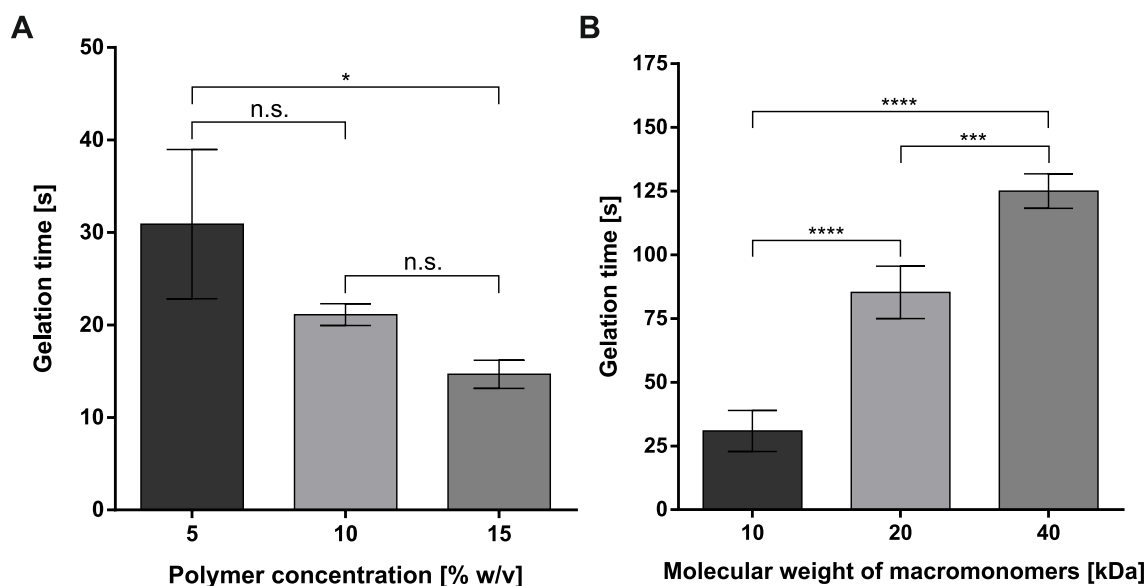


Figure 2: Gelation times of iEDDA hydrogels prepared with 8armPEG10k derivatives with polymer concentrations of 5, 10, and 15% (w/v) (A) and gelation times of 5% (w/v) iEDDA hydrogels prepared with 8armPEG derivatives with molecular weights of 10, 20, and 40 kDa (B). All experiments were performed at 37 °C. Levels of statistical significance are indicated as * $p \leq 0.05$, *** $p \leq 0.001$, and **** $p \leq 0.0001$.

Temperature is another parameter that can be altered to influence the reaction rate. Since it has been shown that the gelation time of iEDDA cross-linked hydrogels can be increased by reducing the temperature [21], a decrease of the gelation temperature should also slow down the reaction rate of the 8armPEG system. Therefore, gelation at lower temperatures was investigated and compared to gelation at body temperature, which is 37 °C (Figure 3). A decrease in temperature from 37 to 20 °C led to a significant increase in the gelation time from 30.9 ± 8.1 to 60.3 ± 0.6 s. A further reduction of the temperature resulted in a higher difference. The gelation time determined at 10 °C was 212.7 ± 5.1 s, significantly longer than at 37 °C. These findings show that at 20 °C both precursor solutions can be mixed and handled. The time would suffice for injection without the risk of clogging the syringe. After injection, the reaction rate of the injected solution would increase due to the heat transfer from the surrounding tissue towards the gel and would favor the formation of a monolithic depot [57].

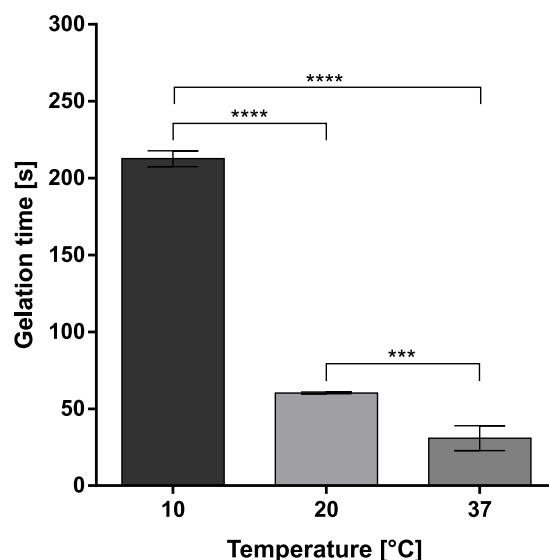


Figure 3: Gelation time of 5% (w/v) iEDDA hydrogels prepared from 8armPEG10k derivatives at 10, 20, and 37 °C. Levels of statistical significance are indicated as *** $p \leq 0.001$ and **** $p \leq 0.0001$.

A final parameter for tuning the reaction rate is the change of the chemical nature of the cross-linkers (Figure 4). The principle of the iEDDA reaction is based on the reaction of an electron-poor diene (tetrazine) and an electron-rich dienophile (norbornene) [58]. Our approach was to change the electron density of the groups either by attaching functional groups or atom exchange. For electron-poor tetrazine groups, it is known that groups substituted on tetrazine have a tremendous impact on the reaction rate [59]. If the substituent is an electron donor, the electron density increases and the kinetics of the iEDDA reaction will be slowed down. Additionally, steric hindrance due to substitution also adversely affects the reaction rate [59,60]. Hence, tetrazine groups were modified with electron-donating methyl-substituents (Scheme 1). The methyl-substituent decelerated the gel point 10-fold (301.3 ± 7.6 s), indicating a significant increase in the gelation time. In contrast, norbornene represents an electron-rich dienophile. Therefore, the exchange of a carbon atom by a more electron negative oxygen should lead to a lower electron density and a reduced reactivity that ultimately results in a slower reaction rate. To obtain respective norbornene derivatives, 8armPEGs were functionalized with the adduct of the classical DA reaction between furan and maleimide (Scheme 1). Similar to the iEDDA hydrogel cross-linked with the methyl-substituted tetrazine, 8armPEG10k-ETPI slowed the gelation time significantly to 297.5 ± 63.3 s.

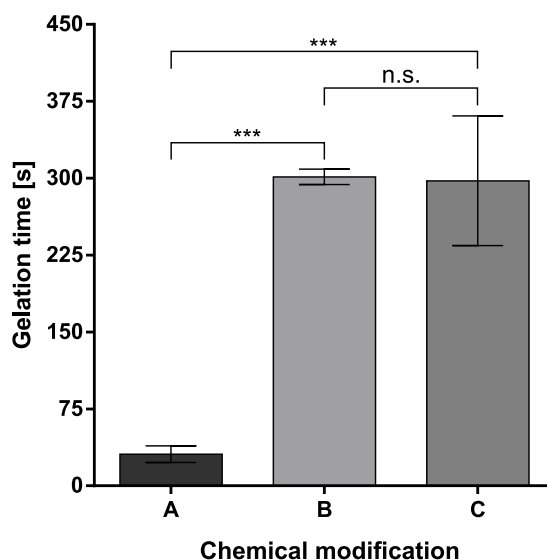


Figure 4: Gelation time of 5% (w/v) iEDDA hydrogels at 37 °C. Hydrogels consisting of 8armPEG10k-Nb and 8armPEG10k-Tz (A) were compared to hydrogels prepared from 8armPEG10k-Nb and 8armPEG10k-methyl-Tz (B) and hydrogels prepared from 8armPEG10k-ETPI and 8armPEG10k-Tz (C). Levels of statistical significance are indicated as *** $p \leq 0.001$.

After determination of the gelation time, stiffness described by the absolute value of the complex shear modulus ($|G^*|$) and the compressive modulus were measured as a function of polymer concentration and molecular weight of the precursors (Figure 5). Raising the polymer concentration from 5 to 15% (w/v) (Figure 5A) increased $|G^*|$ significantly from 1.8 ± 0.1 to 55.7 ± 4.1 kPa. This can be explained by the physical entanglements and the number of elastically active chains formed during cross-linking [61]. For 15% (w/v) hydrogels, the highest number of cross-links and entanglements are created, resulting in the significantly highest stiffness. In contrast, the number of possible elastically active chains formed during cross-linking was reduced for 10% (w/v) polymer concentration, decreasing the overall stiffness of the system. A concentration of 5% (w/v) further reduced the number of elastically active chains and led to the significantly lowest $|G^*|$ for the 8armPEG10k-hydrogels. Besides $|G^*|$, the compressive modulus also depends on the number of elastically active chains. The compressive modulus significantly increased from 7.9 ± 0.3 to 135.1 ± 21.9 kPa by increasing the polymer concentration from 5 to 15% (w/v) (Figure 5B). Using macromonomers with a higher molecular weight, $|G^*|$ and the compressive modulus should decrease due to the lower number of possible cross-links. However, increasing the molecular weight of the precursors used for 5% (w/v) 8armPEG-hydrogels, we found significantly higher $|G^*|$ (Figure 5C) and compressive modulus values (Figure 5D) for hydrogels prepared from higher molecular weight macromonomers. This paradoxical outcome can be explained by the gelation time and nitrogen formation. Because 8armPEG10k-hydrogels showed the fastest gelation, the network formed very rapidly, leading to a less homogeneously cross-linked system with an increased number of defects. Additionally, for the 8armPEG10k-hydrogels, more nitrogen bubbles were created at the same polymer concentration, contributing to further irregularities in the hydrogel network. Together, these defects further reduce the cross-linking density and lead to a lower mechanical strength

of the respective hydrogels [62]. In contrast, the significantly longer gelation time and the reduced nitrogen production of the 8armPEG40k-hydrogels resulted in a more uniform cross-linked system with the highest $|G^*|$ and compressive modulus values.

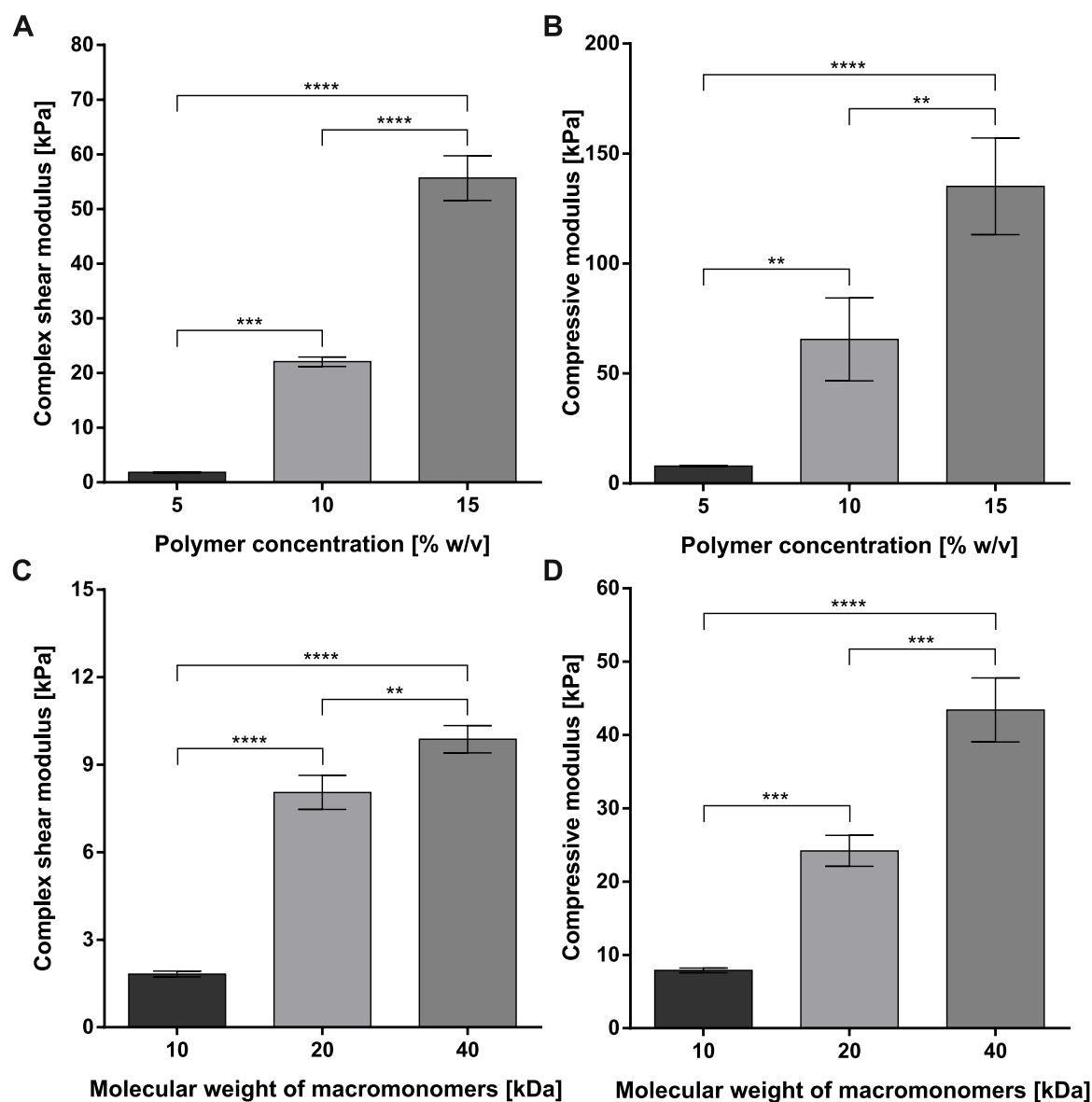


Figure 5: Absolute values of the complex shear modulus ($|G^*|$) of 8armPEG10k-hydrogels with polymer concentrations of 5, 10, and 15% (w/v) (A). The compressive modulus of 8armPEG10k-hydrogels with polymer concentrations of 5, 10, and 15% (w/v) (B). $|G^*|$ of 5% (w/v) 8armPEG-hydrogels prepared with macromonomers with a molecular weight of 10, 20, and 40 kDa (C). Compressive modulus of 5% (w/v) 8armPEG-hydrogels prepared with macromonomers with a molecular weight of 10, 20, and 40 kDa (D). Levels of statistical significance are indicated as ** $p \leq 0.01$, *** $p \leq 0.001$, and **** $p \leq 0.0001$.

3.3 Protein interaction during DA reactions

Bioorthogonal reactions are achieved by using functional groups with high selectivity to their reactive counterpart under physiological conditions [63]. Thus, minimal side reactions occur, and interactions with biomolecules in the reaction surroundings are avoided as much as possible. The iEDDA reaction between norbornene and tetrazine groups is one such bioorthogonal reaction, making it an ideal

candidate for protein delivery [64]. Inadvertently tethering proteins to the matrix could cause a delayed or even incomplete release that complicates drug administration [65]. Also, interactions with the hydrogel components could cause structural damage to the protein that could make it immunogenic [66]. To investigate potential interactions with proteins, we incubated the model protein lysozyme with norbornene- and tetrazine-functionalized mPEG5k to imitate the iEDDA gelation process and then evaluated the extent of PEGylation and the activity of the lysozyme. These results were compared to lysozyme incubated with furan- and maleimide-functionalized mPEG5k, representing classical DA gelation. The mPEG5k derivatives were used rather than 8armPEGs because cross-linking conditions could be simulated without gel formation that would hinder the analysis of reaction products [10]. First, the activity of the enzyme was analyzed (Figure 6). Native lysozyme had an activity of 37338 ± 565 U/mg, but after incubation with the DA reaction monomers, it significantly decreased to 24709 ± 1963 U/mg. In contrast, the incubation with the iEDDA monomers led to a slight, but not significant, activity increase (39857 ± 261 U/mg). The activity changes can be explained by possible PEGylation of the enzyme [67–69]. For the DA reaction, the presence of maleimide-functionalized mPEG5k resulted in a PEGylation of lysozyme lysine residues via Michael-type addition. PEGylation occurs in particular for the lysine residues Lys33 and Lys97 [10]. Thereby, activity decrease can be attributed to PEGylation of Lys97 that is located in a region necessary for substrate interaction.

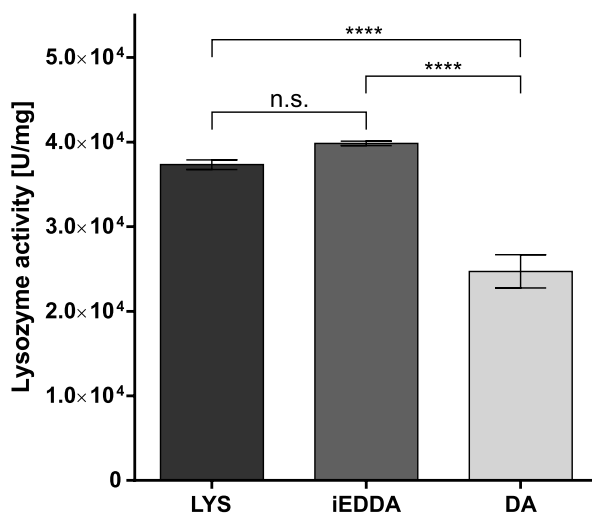


Figure 6: Lysozyme activity after incubation with different cross-linking reactions. The activity was determined for native lysozyme prior to incubation (LYS), after cross-linking via iEDDA reaction with norbornene- and tetrazine-functionalized mPEG5k (iEDDA), and after cross-linking via DA reaction with furan- and maleimide-functionalized mPEG5k (DA). Levels of statistical significance are indicated as **** $p \leq 0.0001$.

Next, SDS-PAGE was used to visualize the PEGylation state of the enzyme after incubation with the iEDDA and DA reaction monomers (Figure 7A). Protein PEGylation was confirmed by iodine staining (Figure S2). Native lysozyme resulted in one band, indicating no molecular modifications. For the iEDDA reaction, an additional band, which means PEGylation with one PEG chain, was found. The amount of free enzyme was $88.7 \pm 0.8\%$. In contrast, only $46.9 \pm 2.0\%$ unmodified lysozyme was found for the classical DA reaction. $42.3 \pm 1.1\%$ of the enzyme was PEGylated once and $10.8 \pm 1.4\%$ twice.

The reason for the high amount of PEGylated protein is the Michael-type addition of nucleophile amino acid residues of lysozyme with maleimide groups as explained above [70]. Therefore, the iEDDA reaction resulted in a significantly higher amount of unmodified, active protein. To determine which functional group interacted with lysozyme, the enzyme was incubated only with mPEG5k-norbornene or mPEG5k-tetrazine (Figure 7B). An additional band was found for lysozyme after incubation with mPEG5k-tetrazine, whereas no PEGylation could be seen after incubation with mPEG5k-norbornene. $24.8 \pm 0.8\%$ of lysozyme was PEGylated by mPEG5k-Tz, which indicates a possible cross-reaction with thiols due to the electrophilic nature of tetrazine [55]. For hydrogel formation, the iEDDA reaction of tetrazine with norbornene takes place preferentially, which protects the protein and causes only a small amount of PEGylation. This significantly lower interaction with proteins makes the iEDDA reaction a more promising candidate for protein delivery than the classical DA reaction.

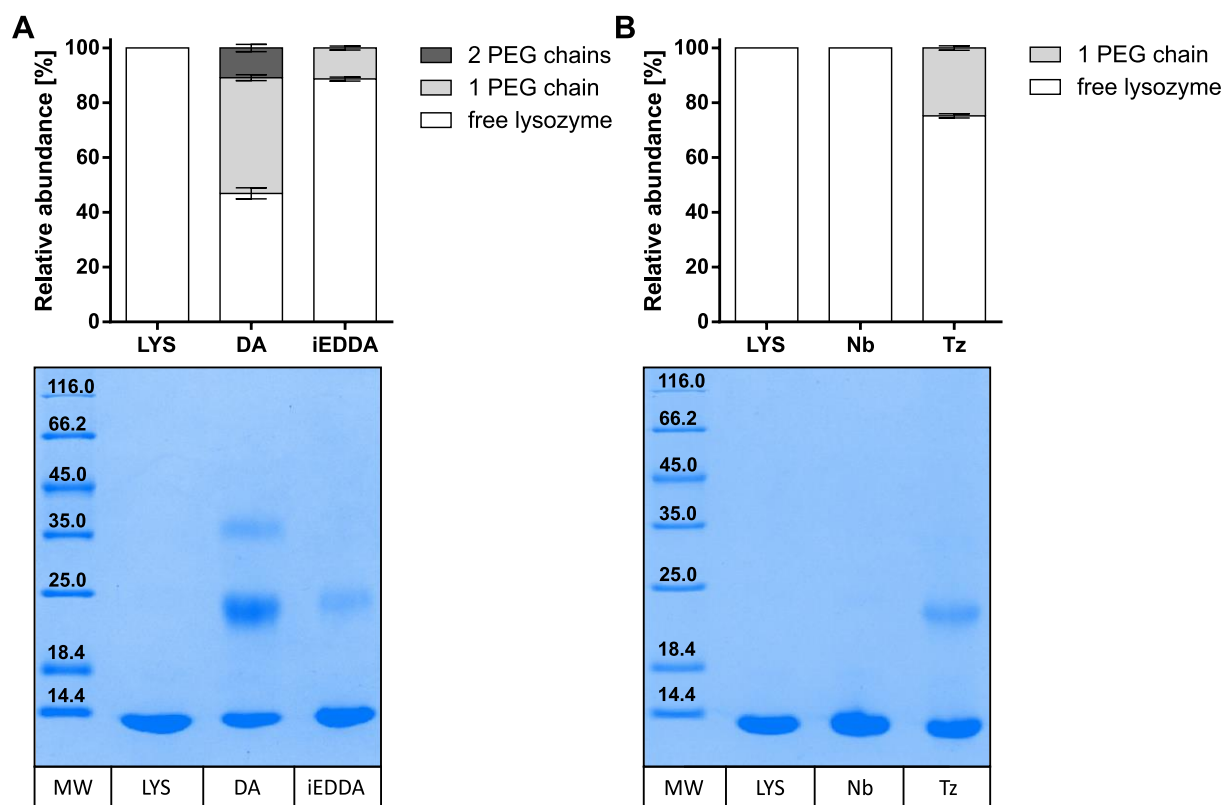


Figure 7: SDS-PAGE of lysozyme after incubation in 50 mM phosphate buffer (pH 7.4) at 37 °C with furan- and maleimide-functionalized mPEG5k (DA) and with norbornene- and tetrazine-functionalized mPEG5k (iEDDA) (A). SDS-PAGE of lysozyme after incubation in 50 mM phosphate buffer (pH 7.4) at 37 °C with norbornene (Nb)- and tetrazine (Tz)-functionalized mPEG5k, respectively (B). All gels were stained with Coomassie brilliant blue. Lysozyme incubated in 50 mM phosphate buffer (pH 7.4) at 37 °C (LYS) and a protein molecular weight marker (MW) were used as the references for both gels. Molecular weight is presented in kDa.

3.4 Swelling and degradation studies

For use as long-term drug delivery systems, hydrogels should show high stability during administration. To examine the influence of polymer concentration and molecular weight on stability and degradation of the iEDDA hydrogels, swelling and degradation studies were performed. Hydrogels that did not show

cytotoxicity (Figure S3) were investigated. The hydrogels were incubated in phosphate buffer (pH 7.4) at 37 °C, and the change of mass was determined at specific time points (Figure 8).

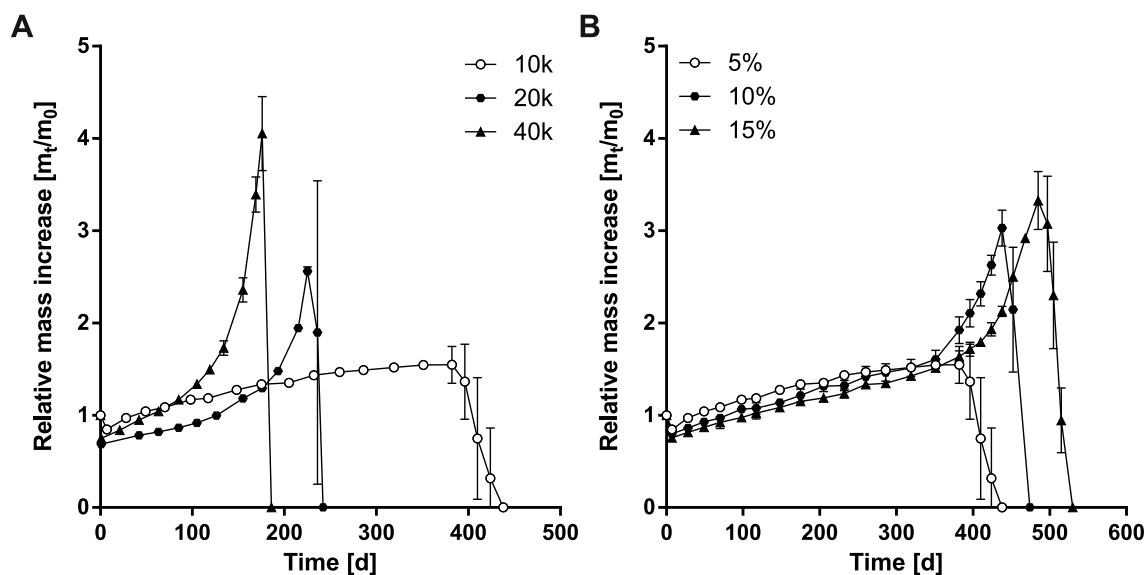


Figure 8: Swelling and degradation of iEDDA hydrogels in 50 mM phosphate buffer (pH 7.4) at 37 °C. 5% (w/v) iEDDA hydrogels prepared with 8armPEG precursors with a molecular weight of 10, 20, and 40 kDa (A). 8armPEG10k-hydrogels prepared from polymer concentrations of 5, 10, and 15% (w/v) (B).

Initially, the relative mass of all hydrogels decreased due to syneresis, which occurs alongside solvent expulsion and network collapse of the hydrogel network after incubation in buffer as previously described for other PEG-based hydrogels [71]. Afterwards, the mass started to increase continuously. For hydrogels with the same polymer concentration of 5% (w/v), swelling behavior depended on the molecular weight of the macromonomers used for the hydrogel preparation (Figure 8A). The higher the molecular weight, the faster the mass increase and the degradation. After reaching a maximum, 8armPEG10k-hydrogels degraded after 438 days, 8armPEG20k-hydrogels after 242 days, and 8armPEG40k-hydrogels after 186 days. Complete dissolution occurs due to hydrolysis of ester bonds (Scheme 2B). Enhanced stability was achieved not only by using smaller macromonomers but also by increasing the polymer concentration (Figure 8B). Both changes result in an increased number of ester groups that take longer to dissolve. Increasing the polymer concentration of an 8armPEG10k-hydrogel from 5 to 10% (w/v) prolonged the dissolution time to 473 days. The use of an even higher concentration of 15% (w/v) led to very high stability. In this case, the hydrogels were dissolved after 530 days. This high stability makes these hydrogels candidates for use as long-term release systems. Interestingly, 5% (w/v) 8armPEG10k-hydrogels showed the lowest degree of swelling of all hydrogel compositions. This can be explained by the lower stability compared to 10 and 15% (w/v) hydrogels. Approximately at 380 days, the 10 and 15% (w/v) 8armPEG10k-hydrogels reached a critical degree of degradation with sufficient free end groups to accelerate hydrogel swelling without significant material erosion. However, at this point too many ester groups were already hydrolytically cleaved in the 5% (w/v) 8armPEG10k-hydrogels preventing the hydrogel from any further swelling but rather entering into a process of erosion. Moreover, compared to hydrogels prepared from larger macromonomers, 8armPEG10k precursors

resulted in hydrogels with smaller chain length between the cross-links. As previously described, the degree of swelling decreases with reduced PEG chain length for hydrogels of equal polymer concentration [72].

3.5 Release of FITC-dextran and GOx

In the previous sections, the applicability of the iEDDA reaction as cross-linking reaction for an 8armPEG-based system was confirmed considering reaction kinetics, cross-reactivity, and stability. In the last experiment, the release kinetics were analyzed, as they are the most crucial attribute of a protein delivery system. In many cases, uniform release over the therapy timeframe is desired. Besides hydrogel swelling, polymer degradation, and drug diffusivity, drug release depends on the hydrogel mesh size and the hydrodynamic diameter of the embedded protein [73–75]. If the mesh size is smaller than the hydrodynamic diameter of the protein, the drug will be retained in the matrix [76]. Only after the network swells will the drug be released. To investigate the release kinetics of the iEDDA hydrogels, the model substance FITC-dextran with a molecular weight of 150 kDa was embedded in 8armPEG10k-hydrogels with different polymer concentrations. The release kinetics were analyzed (Figure 9) with regard to the respective average mesh sizes, which were determined as previously described [35]. The hydrodynamic diameter of 150 kDa FITC-dextran is approximately 18 nm, as described in the literature [77]. Therefore, hydrogels with smaller mesh sizes should be selected to guarantee controlled release. Polymer concentrations of 5% (w/v) (10.3 ± 0.4 nm), 10% (w/v) (5.6 ± 0.2 nm), and 15% (w/v) (4.1 ± 0.2 nm) resulted in average mesh sizes smaller than the hydrodynamic diameter of FITC-dextran (Table S1). Hence, all hydrogels should be suitable as delivery systems for this type of FITC-dextran. However, after a high burst release of 89% (5% hydrogel) and 58% (10% hydrogel), FITC-dextran was completely released by day 4 and day 19 for the 5 and 10% (w/v) hydrogels, respectively (Figure 9A and B). Only 15% (w/v) hydrogels were able to release FITC-dextran over a long time (Figure 9C). The initial FITC-dextran release of around 17% was followed by a faster release. After 19 days, 33% of FITC-dextran was released continuously over 239 days. The release experiment was stopped after approximately 75% of FITC-dextran had been released from the hydrogels.

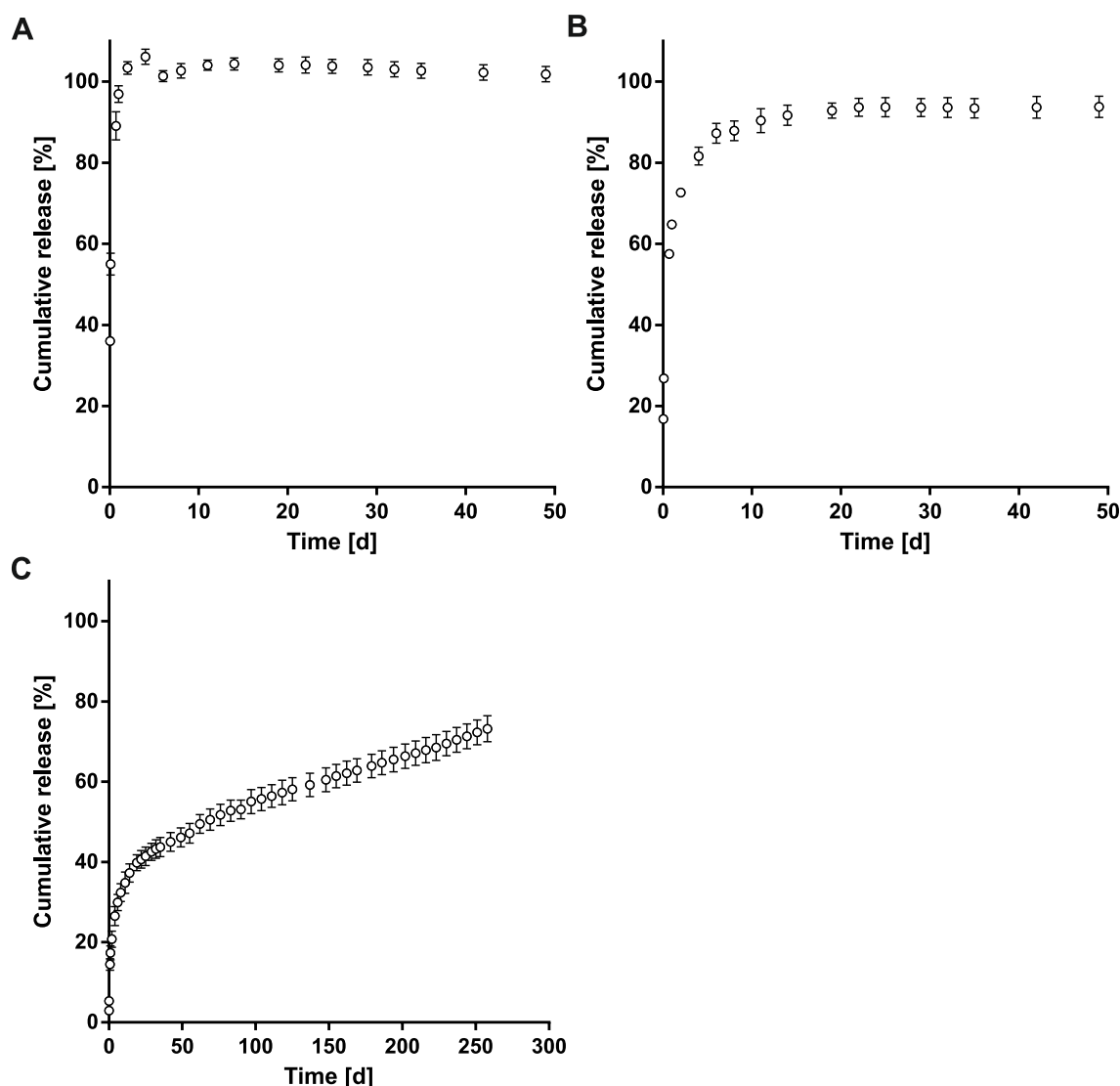


Figure 9: Release of 150 kDa FITC-dextran from 8armPEG10k-hydrogels in 50 mM phosphate buffer (pH 7.4) at 37 °C. Hydrogels were prepared with polymer concentrations of 5% (w/v) (A), 10% (w/v) (B), and 15% (w/v) (C).

There are different reasons for the fast release from 5 and 10% (w/v) hydrogels and why the equilibrium swelling theory for mesh size determination seems not to fit the results. First of all, the values of mesh sizes determined by swelling studies are only reference points. While they represent the average mesh size, the release depends on the mesh size distribution. By using low field NMR, Kirchhof et al. found that the most abundant mesh size of a comparable 10% (w/v) 8armPEG10k-hydrogel, cross-linked via DA reaction, was nearly twice as big as the value of the average mesh size [78]. However, although similar mesh size values of 5.8 ± 0.1 nm were found for 10% (w/v) 8armPEG10k-hydrogels cross-linked via DA reaction compared to our 10% (w/v) 8armPEG10k-hydrogels cross-linked via iEDDA reaction, DA hydrogels were able to release FITC-dextran in a more controlled manner [78]. The most notable difference between these systems is the presence of bubbles created by the nitrogen gas, which is generated during the polymerization. They could have a larger impact on the actual mesh size than expressed by the calculation. Moreover, FITC-dextran is polydisperse [79]. Thus, smaller chains can

release quickly while leaving larger ones behind. These larger chains in turn are able to migrate in a wormlike manner via “reptation” out of the hydrogel networks [80]. Finally, the mesh sizes were determined for pure hydrogels. The presence of an additional high molecular weight substance influences the cross-linking density that can result in larger mesh sizes and a faster release. This can be observed when comparing the release kinetics of different amounts of FITC-dextran from 10% (w/v) 8armPEG10k-hydrogels. Our hydrogels were loaded with 1% (w/v) FITC-dextran. In contrast, comparable DA hydrogels that controlled release over 30 days contained only 0.1% (w/v) FITC-dextran [78]. Therefore, the functional groups of the DA hydrogels were less hindered during cross-linking and able to form a denser network. To achieve an extended controlled release, the polymer concentration was further increased to 15% (w/v), resulting in a higher cross-linking density. In this way, the influence of the discussed aspects is reduced, and FITC-dextran is released over a very long time of more than 250 days in a controlled way.

It is known that drug release from hydrogels does not necessarily correlate exclusively with mesh sizes. According to Rehmann et al. mesh sizes serve as an indicator but are not the only parameter that determines drug release from hydrogels [73]. Therefore, concrete release experiments remain pivotal to assess the potential of a hydrogel to control the release of a drug.

With the release of FITC-dextran, we wanted to investigate if these hydrogels can be used for controlled release applications. Since several commonly used therapeutic proteins such as monoclonal antibodies have a smaller hydrodynamic diameter, we decided to proceed with a protein of similar size [77,81]. Therefore, GOx with a hydrodynamic diameter of 8.6 nm was chosen as a model protein for the release experiments (Figure 10) [82]. Based on the result for the release of FITC-dextran, only hydrogels consisting of 15% (w/v) polymer were considered for the GOx release experiments. Lower polymer concentrations were unsuited to retain the larger dextran with time (Figure 9A and B) and would have accelerated the release of the smaller GOx even further. After 1 day, a slight burst release of around 7% was observed due to initial network contraction. Subsequently, 30% was released faster over 62 days due to the swelling of the network that facilitates diffusion of the enzyme out of the matrix. After this phase, the release slowed. During this period, the network might retain the protein in the inner layer. At approximately 80 days, a drop can be seen. Considering the cumulative nature of this release study, we did not expect a decrease in the release. However, due to the low amount of GOx released over this long timescale, small errors such as drawing too small of a quantity have high impact on the release curve. The release was increased only after 225 days, as hydrolysis of the ester bonds enlarged the meshes allowing the protein to escape the gel. After 265 days, the experiment was ended, and 75% of GOx had been released by this point.

This auspicious release behavior could be used for the administration of biologics, for which it is important to maintain therapeutic levels over a long time. Examples of potential applications are the treatment of early-stage breast cancer or age-related macular degeneration. Here, the antibodies trastuzumab or bevacizumab are administered repeatedly over a year that can lead to injection-related

complications in the patient [25,83]. Additionally, trained personnel are required, representing a burden to the health system in the case of repetitive administration [83]. This could be overcome by using a controlled release system such as ours. A single injection creates a depot from which biologics are released, and frequent injections can be avoided, leading to higher compliance for the patients and reduced personnel costs.

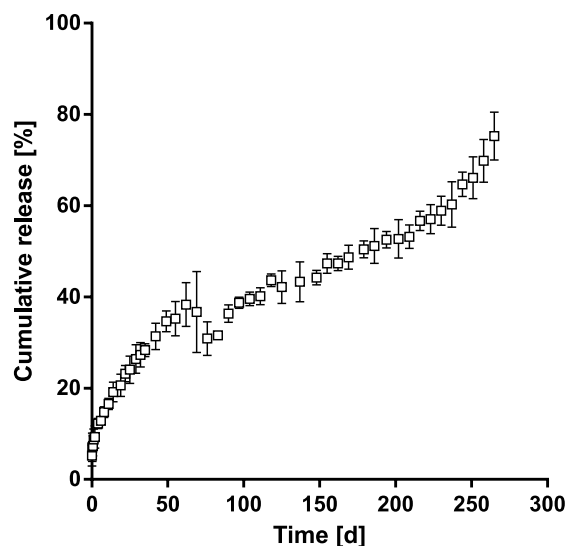


Figure 10: Release of GOx from 15% (w/v) 8armPEG10k-hydrogels in 50 mM phosphate buffer (pH 7.4) at 37 °C.

Nevertheless, the long release time of our 15% (w/v) hydrogel may represent an obstacle for some therapeutic proteins regarding activity. However, hydrogels can provide a protective environment against protein degradation. Huynh and Wylie, for example, showed that bevacizumab released after 100 days from an agarose-based hydrogel retained VEGF binding properties [29]. Therefore, further research is required for the application as an *in vivo* depot system.

4 Conclusion

The controlled release of GOx over more than 250 days makes the iEDDA reaction between norbornene and tetrazine groups attached to multiarmed PEGs highly promising for the preparation of *in situ* gelling long-term protein delivery systems. Biodegradation of these hydrogels could be obtained by esterification of the PEG macromonomers. Additionally, reduction of protein cross-linker interactions due to the bioorthogonal nature of the iEDDA reaction enabled 89% of the protein to remain active and non-PEGylated. Furthermore, the ability to influence the high reaction rate by changes in cross-linker concentration, temperature, and chemical structure represents a promising approach, especially for use in the field of medical applications.

References

- [1] O. Wichterle, D. Lím, Hydrophilic Gels for Biological Use, *Nature* (London, U. K.) 185 (1960) 117–118.
- [2] E. Caló, V.V. Khutoryanskiy, Biomedical applications of hydrogels: A review of patents and commercial products, *Eur. Polym. J.* 65 (2015) 252–267.
- [3] S. Kirchhof, M. Gregoritz, V. Messmann, N. Hammer, A.M. Goepferich, F.P. Brandl, Diels-Alder hydrogels with enhanced stability: First step toward controlled release of bevacizumab, *Eur. J. Pharm. Biopharm.* 96 (2015) 217–225.
- [4] G.N. Grover, R.L. Braden, K.L. Christman, Oxime cross-linked injectable hydrogels for catheter delivery, *Adv. Mater.* 25 (2013) 2937–2942.
- [5] M. Clark, P. Kiser, In situ crosslinked hydrogels formed using Cu(I)-free Huisgen cycloaddition reaction, *Polym. Int.* 58 (2009) 1190–1195.
- [6] J. Collins, Z. Xiao, M. Müllner, L.A. Connal, The emergence of oxime click chemistry and its utility in polymer science, *Polym. Chem.* 7 (2016) 3812–3826.
- [7] M.U. Minhas, M. Ahmad, L. Ali, M. Sohail, Synthesis of chemically cross-linked polyvinyl alcohol-co-poly (methacrylic acid) hydrogels by copolymerization; a potential graft-polymeric carrier for oral delivery of 5-fluorouracil, *Daru, J. Fac. Pharm., Tehran Univ. Med. Sci.* 21 (2013) 44.
- [8] M. Graf, C.E. Ziegler, M. Gregoritz, A.M. Goepferich, Hydrogel microspheres evading alveolar macrophages for sustained pulmonary protein delivery, *Int. J. Pharm. (Amsterdam, Neth.)* 566 (2019) 652–661.
- [9] X. Bi, A. Liang, Y. Tan, P. Maturavongsadit, A. Higginbotham, T. Gado, A. Gramling, H. Bahn, Q. Wang, Thiol-ene crosslinking polyamidoamine dendrimer-hyaluronic acid hydrogel system for biomedical applications, *J. Biomater. Sci., Polym. Ed.* 27 (2016) 743–757.
- [10] M. Gregoritz, A.M. Goepferich, F.P. Brandl, Polyanions effectively prevent protein conjugation and activity loss during hydrogel cross-linking, *J. Controlled Release* 238 (2016) 92–102.

- [11] A.M. Jonker, A. Borrmann, E.R.H. van Eck, F.L. van Delft, D.W.P.M. Löwik, J.C.M. van Hest, A fast and activatable cross-linking strategy for hydrogel formation, *Adv. Mater.* 27 (2015) 1235–1240.
- [12] L.M. Ickenstein, P. Garidel, Hydrogel formulations for biologicals: current spotlight from a commercial perspective, *Ther. Delivery* 9 (2018) 221–230.
- [13] X. Bi, A. Liang, In Situ-Forming Cross-linking Hydrogel Systems: Chemistry and Biomedical Applications, in: S.B. Majee (Ed.), *Emerging Concepts in Analysis and Applications of Hydrogels*, InTech, 2016.
- [14] O.S. Fenton, J.L. Andresen, M. Paolini, R. Langer, β -Aminoacrylate Synthetic Hydrogels: Easily Accessible and Operationally Simple Biomaterials Networks, *Angew. Chem., Int. Ed. Engl.* 57 (2018) 16026–16029.
- [15] Z. Zhang, C. He, Y. Rong, H. Ren, T. Wang, Z. Zou, X. Chen, A fast and versatile cross-linking strategy via o-phthalaldehyde condensation for mechanically strengthened and functional hydrogels, *Natl. Sci. Rev.* 8 (2021).
- [16] H.-S. Han, N.K. Devaraj, J. Lee, S.A. Hilderbrand, R. Weissleder, M.G. Bawendi, Development of a bioorthogonal and highly efficient conjugation method for quantum dots using tetrazine-norbornene cycloaddition, *J. Am. Chem. Soc.* 132 (2010) 7838–7839.
- [17] A.-C. Knall, M. Hollauf, C. Slugovc, Kinetic studies of inverse electron demand Diels-Alder reactions (iEDDA) of norbornenes and 3,6-dipyridin-2-yl-1,2,4,5-tetrazine, *Tetrahedron Lett.* 55 (2014) 4763–4766.
- [18] K. Lang, L. Davis, J. Torres-Kolbus, C. Chou, A. Deiters, J.W. Chin, Genetically encoded norbornene directs site-specific cellular protein labelling via a rapid bioorthogonal reaction, *Nat. Chem.* 4 (2012) 298–304.
- [19] D.L. Alge, M.A. Azagarsamy, D.F. Donohue, K.S. Anseth, Synthetically tractable click hydrogels for three-dimensional cell culture formed using tetrazine-norbornene chemistry, *Biomacromolecules* 14 (2013) 949–953.
- [20] R.M. Desai, S.T. Koshy, S.A. Hilderbrand, D.J. Mooney, N.S. Joshi, Versatile click alginate hydrogels crosslinked via tetrazine-norbornene chemistry, *Biomaterials* 50 (2015) 30–37.

- [21] A. Famili, K. Rajagopal, Bio-Orthogonal Cross-Linking Chemistry Enables In Situ Protein Encapsulation and Provides Sustained Release from Hyaluronic Acid Based Hydrogels, *Mol. Pharmaceutics* 14 (2017) 1961–1968.
- [22] V. Delplace, A.J. Pickering, M.H. Hettiaratchi, S. Zhao, T. Kivijärvi, M.S. Shoichet, Inverse Electron-Demand Diels-Alder Methylcellulose Hydrogels Enable the Co-delivery of Chondroitinase ABC and Neural Progenitor Cells, *Biomacromolecules* 21 (2020) 2421–2431.
- [23] S. Yoon, Y.-S. Kim, H. Shim, J. Chung, Current perspectives on therapeutic antibodies, *Biotechnol. Bioprocess Eng.* 15 (2010) 709–715.
- [24] S. Koutsopoulos, S. Zhang, Two-layered injectable self-assembling peptide scaffold hydrogels for long-term sustained release of human antibodies, *J. Controlled Release* 160 (2012) 451–458.
- [25] D.F. Martin, M.G. Maguire, G. Ying, J.E. Grunwald, S.L. Fine, G.J. Jaffe, Ranibizumab and bevacizumab for neovascular age-related macular degeneration, *N. Engl. J. Med.* 364 (2011) 1897–1908.
- [26] U. Bhardwaj, R. Sura, F. Papadimitrakopoulos, D.J. Burgess, PLGA/PVA hydrogel composites for long-term inflammation control following s.c. implantation, *Int. J. Pharm. (Amsterdam, Neth.)* 384 (2010) 78–86.
- [27] Q. Peng, X. Sun, T. Gong, C.-Y. Wu, T. Zhang, J. Tan, Z.-R. Zhang, Injectable and biodegradable thermosensitive hydrogels loaded with PHBHHx nanoparticles for the sustained and controlled release of insulin, *Acta Biomater.* 9 (2013) 5063–5069.
- [28] K.W. Lee, J.J. Yoon, J.H. Lee, S.Y. Kim, H.J. Jung, S.J. Kim, J.W. Joh, H.H. Lee, D.S. Lee, S.K. Lee, Sustained release of vascular endothelial growth factor from calcium-induced alginate hydrogels reinforced by heparin and chitosan, *Transplant. Proc.* 36 (2004) 2464–2465.
- [29] V. Huynh, R.G. Wylie, Competitive Affinity Release for Long-Term Delivery of Antibodies from Hydrogels, *Angew. Chem., Int. Ed. Engl.* 57 (2018) 3406–3410.
- [30] K. Vulic, M.S. Shoichet, Tunable growth factor delivery from injectable hydrogels for tissue engineering, *J. Am. Chem. Soc.* 134 (2012) 882–885.

- [31] Y. Qu, F.-X. Sauvage, G. Clavier, F. Miomandre, P. Audebert, Metal-Free Synthetic Approach to 3-Monosubstituted Unsymmetrical 1,2,4,5-Tetrazines Useful for Bioorthogonal Reactions, *Angew. Chem., Int. Ed. Engl.* 57 (2018) 12057–12061.
- [32] B.D. Fairbanks, M.P. Schwartz, A.E. Halevi, C.R. Nuttelman, C.N. Bowman, K.S. Anseth, A Versatile Synthetic Extracellular Matrix Mimic via Thiol-Norbornene Photopolymerization, *Adv. Mater.* 21 (2009) 5005–5010.
- [33] H. Zhan, H. de Jong, D.W.P.M. Löwik, Comparison of Bioorthogonally Cross-Linked Hydrogels for in Situ Cell Encapsulation, *ACS Appl. Bio Mater.* 2 (2019) 2862–2871.
- [34] M. Gregoritza, K. Abstiens, M. Graf, A.M. Goepferich, Fabrication of antibody-loaded microgels using microfluidics and thiol-ene photoclick chemistry, *Eur. J. Pharm. Biopharm.* 127 (2018) 194–203.
- [35] S. Kirchhof, F.P. Brandl, N. Hammer, A.M. Goepferich, Investigation of the Diels–Alder reaction as a cross-linking mechanism for degradable poly(ethylene glycol) based hydrogels, *J. Mater. Chem. B* 1 (2013) 4855.
- [36] N. Peppas, Hydrogels in pharmaceutical formulations, *Eur. J. Pharm. Biopharm.* 50 (2000) 27–46.
- [37] F. Brandl, N. Hammer, T. Blunk, J. Tessmar, A. Goepferich, Biodegradable hydrogels for time-controlled release of tethered peptides or proteins, *Biomacromolecules* 11 (2010) 496–504.
- [38] P.J. Flory, Principles of polymer chemistry, 10th edn ed., Cornell Univ. Press, Ithaca, N. Y., Ithaca, N. Y., 1953.
- [39] J.C. Bray, E.W. Merrill, Poly(vinyl alcohol) hydrogels. Formation by electron beam irradiation of aqueous solutions and subsequent crystallization, *J. Appl. Polym. Sci.* 17 (1973) 3779–3794.
- [40] D.L. Elbert, A.B. Pratt, M.P. Lutolf, S. Halstenberg, J.A. Hubbell, Protein delivery from materials formed by self-selective conjugate addition reactions, *J. Controlled Release* 76 (2001) 11–25.
- [41] N.A. Peppas, E.W. Merrill, Crosslinked poly(vinyl alcohol) hydrogels as swollen elastic networks, *J. Appl. Polym. Sci.* 21 (1977) 1763–1770.

- [42] E.W. Merrill, K.A. Dennison, C. SUNG, Partitioning and diffusion of solutes in hydrogels of poly(ethylene oxide), *Biomaterials* 14 (1993) 1117–1126.
- [43] T. Canal, N.A. Peppas, Correlation between mesh size and equilibrium degree of swelling of polymeric networks, *J. Biomed. Mater. Res.* 23 (1989) 1183–1193.
- [44] G.P. Raeber, M.P. Lutolf, J.A. Hubbell, Molecularly engineered PEG hydrogels: a novel model system for proteolytically mediated cell migration, *Biophys. J.* 89 (2005) 1374–1388.
- [45] M. Gregoritz, V. Messmann, A.M. Goepferich, F.P. Brandl, Design of hydrogels for delayed antibody release utilizing hydrophobic association and Diels–Alder chemistry in tandem, *J. Mater. Chem. B* 4 (2016) 3398–3408.
- [46] M. Gregoritz, V. Messmann, K. Abstiens, F.P. Brandl, A.M. Goepferich, Controlled Antibody Release from Degradable Thermoresponsive Hydrogels Cross-Linked by Diels–Alder Chemistry, *Biomacromolecules* 18 (2017) 2410–2418.
- [47] O. Jung, R. Smeets, P. Hartjen, R. Schnettler, F. Feyerabend, M. Klein, N. Wegner, F. Walther, D. Stangier, A. Henningsen, C. Rendenbach, M. Heiland, M. Barbeck, A. Kopp, Improved In Vitro Test Procedure for Full Assessment of the Cytocompatibility of Degradable Magnesium Based on ISO 10993-5/-12, *Int. J. Mol. Sci.* 20 (2019) 255.
- [48] B. Zvarova, F.E. Uhl, J.J. Uriarte, Z.D. Borg, A.L. Coffey, N.R. Bonenfant, D.J. Weiss, D.E. Wagner, Residual Detergent Detection Method for Nondestructive Cytocompatibility Evaluation of Decellularized Whole Lung Scaffolds, *Tissue Eng., Part C* 22 (2016) 418–428.
- [49] N. Hammer, F.P. Brandl, S. Kirchhof, V. Messmann, A.M. Goepferich, Protein compatibility of selected cross-linking reactions for hydrogels, *Macromol. Biosci.* 15 (2015) 405–413.
- [50] A. Natarajan, C.-Y. Xiong, H. Albrecht, G.L. DeNardo, S.J. DeNardo, Characterization of site-specific ScFv PEGylation for tumor-targeting pharmaceuticals, *Bioconjugate Chem.* 16 (2005) 113–121.
- [51] D. Shugar, The measurement of lysozyme activity and the ultra-violet inactivation of lysozyme, *Biochim. Biophys. Acta* 8 (1952) 302–309.
- [52] A.-C. Knall, C. Slugovc, Inverse electron demand Diels–Alder (IEDDA)-initiated conjugation: a (high) potential click chemistry scheme, *Chem. Soc. Rev.* 42 (2013) 5131–5142.
- [53] F.-Y. Hsieh, T.-C. Tseng, S.-H. Hsu, Self-healing hydrogel for tissue repair in the central nervous system, *Neural Regener. Res.* 10 (2015) 1922–1923.

- [54] C.E. Ziegler, M. Graf, S. Beck, A.M. Goepferich, A novel anhydrous preparation of PEG hydrogels enables high drug loading with biologics for controlled release applications, *Eur. Polym. J.* 147 (2021) 110286.
- [55] R.J. Blizzard, D.R. Backus, W. Brown, C.G. Bazewicz, Y. Li, R.A. Mehl, Ideal Bioorthogonal Reactions Using A Site-Specifically Encoded Tetrazine Amino Acid, *J. Am. Chem. Soc.* 137 (2015) 10044–10047.
- [56] C.C. Ahrens, M.E. Welch, L.G. Griffith, P.T. Hammond, Uncharged Helical Modular Polypeptide Hydrogels for Cellular Scaffolds, *Biomacromolecules* 16 (2015) 3774–3783.
- [57] D. Schweizer, I. Vostiar, A. Heier, T. Serno, K. Schoenhammer, M. Jahn, S. Jones, A. Piequet, C. Beerli, H. Gram, A. Goepferich, Pharmacokinetics, biocompatibility and bioavailability of a controlled release monoclonal antibody formulation, *J. Controlled Release* 172 (2013) 975–982.
- [58] M. Pagel, Inverse electron demand Diels-Alder (IEDDA) reactions in peptide chemistry, *J. Pept. Sci.* 25 (2019) e3141.
- [59] M.R. Karver, R. Weissleder, S.A. Hilderbrand, Synthesis and evaluation of a series of 1,2,4,5-tetrazines for bioorthogonal conjugation, *Bioconjugate Chem.* 22 (2011) 2263–2270.
- [60] Y. Liang, J.L. Mackey, S.A. Lopez, F. Liu, K.N. Houk, Control and design of mutual orthogonality in bioorthogonal cycloadditions, *J. Am. Chem. Soc.* 134 (2012) 17904–17907.
- [61] M.P. Lutolf, J.A. Hubbell, Synthesis and physicochemical characterization of end-linked poly(ethylene glycol)-co-peptide hydrogels formed by Michael-type addition, *Biomacromolecules* 4 (2003) 713–722.
- [62] A. Metters, J. Hubbell, Network formation and degradation behavior of hydrogels formed by Michael-type addition reactions, *Biomacromolecules* 6 (2005) 290–301.
- [63] E.M. Sletten, C.R. Bertozzi, Bioorthogonal chemistry: fishing for selectivity in a sea of functionality, *Angew. Chem., Int. Ed. Engl.* 48 (2009) 6974–6998.
- [64] M. Zheng, L. Zheng, P. Zhang, J. Li, Y. Zhang, Development of bioorthogonal reactions and their applications in bioconjugation, *Molecules* 20 (2015) 3190–3205.
- [65] C.-C. Lin, A.T. Metters, Enhanced protein delivery from photopolymerized hydrogels using a pseudospecific metal chelating ligand, *Pharm. Res.* 23 (2006) 614–622.

- [66] C.-C. Lin, A.T. Metters, Hydrogels in controlled release formulations: network design and mathematical modeling, *Adv. Drug Delivery Rev.* 58 (2006) 1379–1408.
- [67] R. Federico, A. Cona, P. Caliceti, F.M. Veronese, Histaminase PEGylation: preparation and characterization of a new bioconjugate for therapeutic application, *J. Controlled Release* 115 (2006) 168–174.
- [68] H.F. Gaertner, A.J. Puigserver, Increased activity and stability of poly(ethylene glycol)-modified trypsin, *Enzyme Microb. Technol.* 14 (1992) 150–155.
- [69] H.F. Gaertner, R.E. Offord, Site-specific attachment of functionalized poly(ethylene glycol) to the amino terminus of proteins, *Bioconjugate Chem.* 7 (1996) 38–44.
- [70] T.M. Pabst, J.J. Buckley, N. Ramasubramanian, A.K. Hunter, Comparison of strong anion-exchangers for the purification of a PEGylated protein, *J. Chromatogr. A* 1147 (2007) 172–182.
- [71] T.M. O'Shea, A.A. Aimetti, E. Kim, V. Yesilyurt, R. Langer, Synthesis and characterization of a library of in-situ curing, nonswelling ethoxylated polyol thiol-ene hydrogels for tailorable macromolecule delivery, *Adv. Mater.* 27 (2015) 65–72.
- [72] K. Olofsson, M. Malkoch, A. Hult, Soft hydrogels from tetra-functional PEGs using UV-induced thiol–ene coupling chemistry: a structure-to-property study, *RSC Adv.* 4 (2014) 30118.
- [73] M.S. Rehmann, K.M. Skeens, P.M. Kharkar, E.M. Ford, E. Maverakis, K.H. Lee, A.M. Kloxin, Tuning and Predicting Mesh Size and Protein Release from Step Growth Hydrogels, *Biomacromolecules* 18 (2017) 3131–3142.
- [74] F. Brandl, F. Kastner, R.M. Gschwind, T. Blunk, J. Tessmar, A. Göpferich, Hydrogel-based drug delivery systems: comparison of drug diffusivity and release kinetics, *J. Controlled Release* 142 (2010) 221–228.
- [75] J. Li, D.J. Mooney, Designing hydrogels for controlled drug delivery, *Nat. Rev. Mater.* 1 (2016).
- [76] F. Brandl, M. Henke, S. Rothschenk, R. Gschwind, M. Breunig, T. Blunk, J. Tessmar, A. Göpferich, Poly(Ethylene Glycol) Based Hydrogels for Intraocular Applications, *Adv. Eng. Mater.* 9 (2007) 1141–1149.

- [77] H. Wen, J. Hao, S.K. Li, Characterization of human sclera barrier properties for transscleral delivery of bevacizumab and ranibizumab, *J. Pharm. Sci.* 102 (2013) 892–903.
- [78] S. Kirchhof, M. Abrami, V. Messmann, N. Hammer, A.M. Goepferich, M. Grassi, F.P. Brandl, Diels-Alder Hydrogels for Controlled Antibody Release: Correlation between Mesh Size and Release Rate, *Mol. Pharmaceutics* 12 (2015) 3358–3368.
- [79] B.T. Henry, M.S. Cheema, S.S. Davis, Gel permeation chromatography used to determine the stability of FITC-Dextran in human saliva and porcine small intestinal mucus, *Int. J. Pharm.* (Amsterdam, Neth.) 73 (1991) 81–88.
- [80] P.G. de Gennes, Reptation of a Polymer Chain in the Presence of Fixed Obstacles, *J. Chem. Phys.* 55 (1971) 572–579.
- [81] S.K. Li, M.R. Liddell, H. Wen, Effective electrophoretic mobilities and charges of anti-VEGF proteins determined by capillary zone electrophoresis, *J. Pharm. Biomed. Anal.* 55 (2011) 603–607.
- [82] S. Nakamura, S. Hayashi, K. Koga, Effect of periodate oxidation on the structure and properties of glucose oxidase, *Biochim. Biophys. Acta* 445 (1976) 294–308.
- [83] K. Xu, F. Lee, S. Gao, M.-H. Tan, M. Kurisawa, Hyaluronidase-incorporated hyaluronic acid-tyramine hydrogels for the sustained release of trastuzumab, *J. Controlled Release* 216 (2015) 47–55.

Chapter 4 – Supporting information

**In situ forming iEDDA hydrogels with tunable gelation time
release high molecular weight proteins in a controlled manner
over an extended time**

1 Rheology

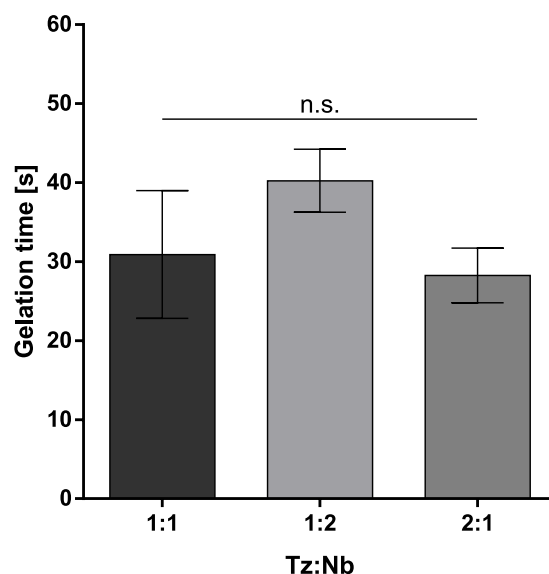


Figure S1: Gelation time of 5% (w/v) 8armPEG10k-hydrogels at three different tetrazine and norbornene ratios (Tz:Nb).

2 SDS-PAGE

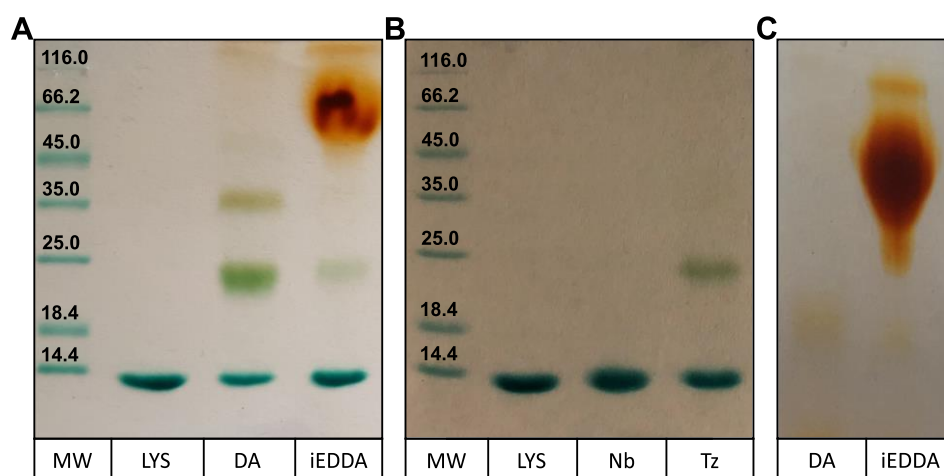


Figure S2: SDS-PAGE of lysozyme after incubation in 50 mM phosphate buffer (pH 7.4) at 37 °C with furan- and maleimide-functionalized mPEG5k (DA) and with norbornene- and tetrazine-functionalized mPEG5k (iEDDA) (A). SDS-PAGE of lysozyme after incubation in 50 mM phosphate buffer (pH 7.4) at 37 °C with norbornene (Nb)- and tetrazine (Tz)-functionalized mPEG5k (B). SDS-PAGE of furan- and maleimide-functionalized mPEG5k (DA) and norbornene- and tetrazine-functionalized mPEG5k (iEDDA) after incubation in 50 mM phosphate buffer (pH 7.4) at 37 °C, indicating migration of PEG for the iEDDA lane. All gels were stained with barium iodide. Lysozyme incubated in 50 mM phosphate buffer (pH 7.4) at 37 °C (LYS) and a protein molecular weight marker (MW) were used as the references for gels A and B. Molecular weight is presented in kDa.

3 Cytotoxicity

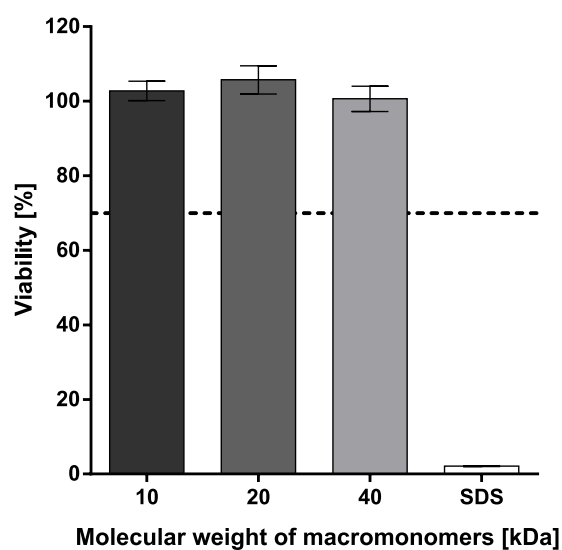


Figure S3: Viability of L-929 cells after incubation with extracts from 15% (w/v) 200 μ l 8armPEG-iEDDA hydrogels that were made with precursors with molecular weights of 10, 20, and 40 kDa. Extracts were prepared by incubation of hydrogels in 2 ml of EMEM supplemented with 10% FCS for 24 h at 37 $^{\circ}$ C. 0.1% (w/v) SDS in cell medium served as the negative control. Cytotoxicity of the hydrogels was assessed with an MTT assay according to ISO 10993-5:2009 (Biological evaluation of medical devices, part 5: Tests for *in vitro* cytotoxicity). 70% cell viability (dotted line) indicates the threshold for cytocompatibility. All hydrogels showed no cytotoxicity due to cell viability values above 100%.

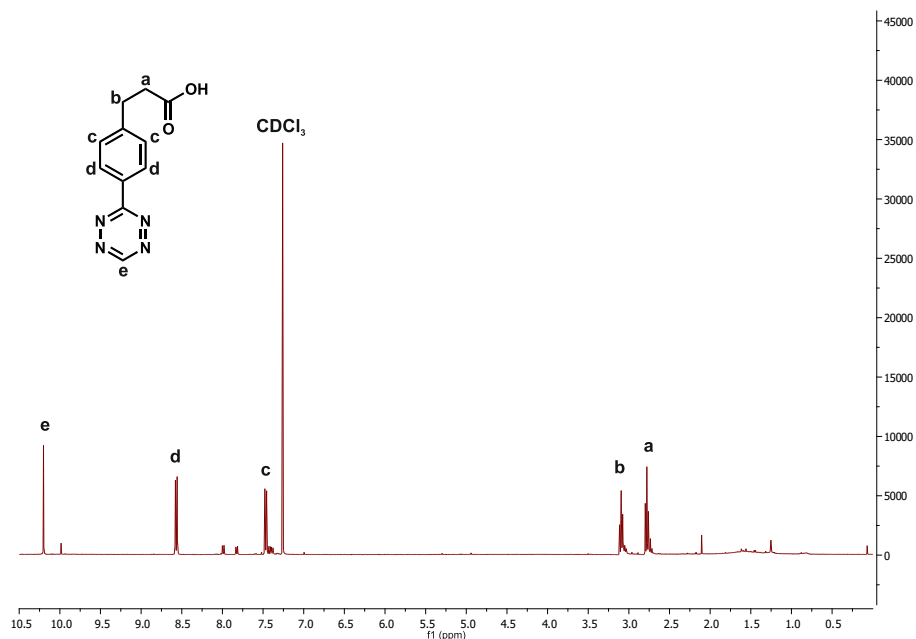
4 Mesh size

Table S1: Average mesh size (ξ) of 8armPEG10k-hydrogels prepared with polymer concentrations of 5, 10, and 15% (w/v).

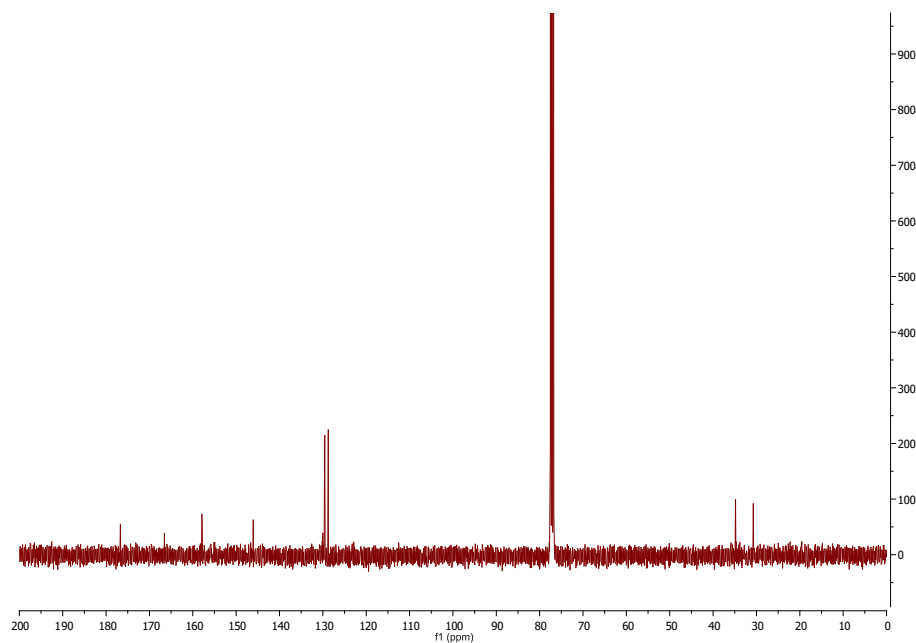
Precursor	Concentration (% (w/v))	ξ (nm)
8armPEG10k	5	10.3 \pm 0.4
	10	5.6 \pm 0.2
	15	4.1 \pm 0.2

5 Spectroscopic data

3-(4-(1,2,4,5-tetrazin-3-yl)phenyl)propanoic acid

**Figure S4:** ^1H NMR spectrum of 3-(4-(1,2,4,5-tetrazin-3-yl)phenyl)propanoic acid

^1H NMR (CDCl_3 , 400 MHz): δ (ppm) = 2.78 (t, 2H, $-\text{C}(\text{O})\text{CH}_2\text{CH}_2\text{Ar}$), 3.09 (t, 2H, $-\text{C}(\text{O})\text{CH}_2\text{CH}_2\text{Ar}$), 7.47 (d, 2H, Ar), 8.57 (d, 2H, Ar), 10.20 (s, 1H, $-\text{N}=\text{CH}-\text{N}=\text{}$).

**Figure S5:** ^{13}C NMR spectrum of 3-(4-(1,2,4,5-tetrazin-3-yl)phenyl)propanoic acid

^{13}C NMR (CDCl_3 , 100 MHz): δ (ppm) = 192.54, 176.68, 166.53, 157.89, 146.06, 130.01, 129.56, 128.75, 34.82, 30.73

LRMS (ESI) calculated for $\text{C}_{11}\text{H}_{11}\text{N}_4\text{O}_2^+$ (MH^+) 231.0882, found 231.0881

3-(4-(6-methyl-1,2,4,5-tetrazin-3-yl)phenyl)propanoic acid

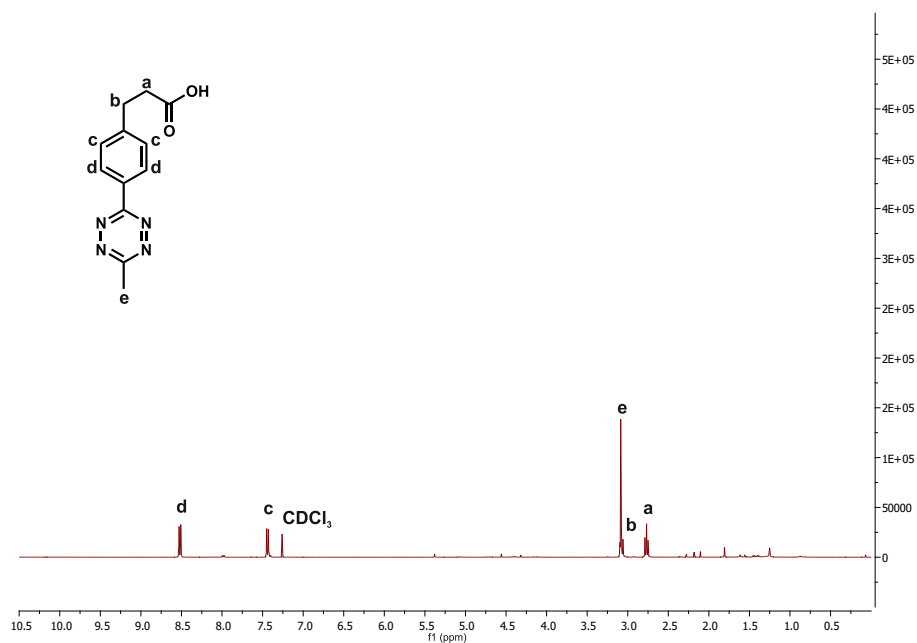


Figure S6: ^1H NMR spectrum of 3-(4-(6-methyl-1,2,4,5-tetrazin-3-yl)phenyl)propanoic acid

^1H NMR (CDCl_3 , 400 MHz): δ (ppm) = 2.77 (t, 2H, $-\text{C}(\text{O})\text{CH}_2\text{CH}_2\text{Ar}$), 3.08 (t, 2H, $-\text{C}(\text{O})\text{CH}_2\text{CH}_2\text{Ar}$), 3.09 (s, 3H, CH_3Ar), 7.44 (d, 2H, Ar), 8.52 (d, 2H, Ar).

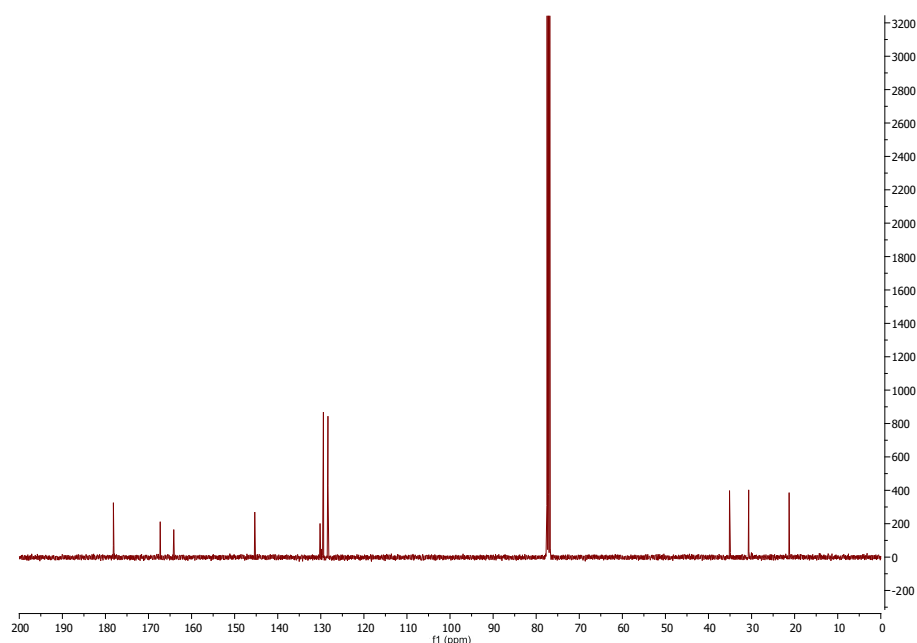


Figure S7: ^{13}C NMR spectrum of 3-(4-(6-methyl-1,2,4,5-tetrazin-3-yl)phenyl)propanoic acid

^{13}C NMR (CDCl_3 , 100 MHz): δ (ppm) = 178.16, 167.28, 164.13, 145.33, 130.17, 129.40, 128.34, 35.12, 30.67, 21.28

LRMS (ESI) calculated for $\text{C}_{12}\text{H}_{14}\text{N}_4\text{O}_2^+$ (MH^+) 245.1039, found 245.1034

8armPEG10k-Tz

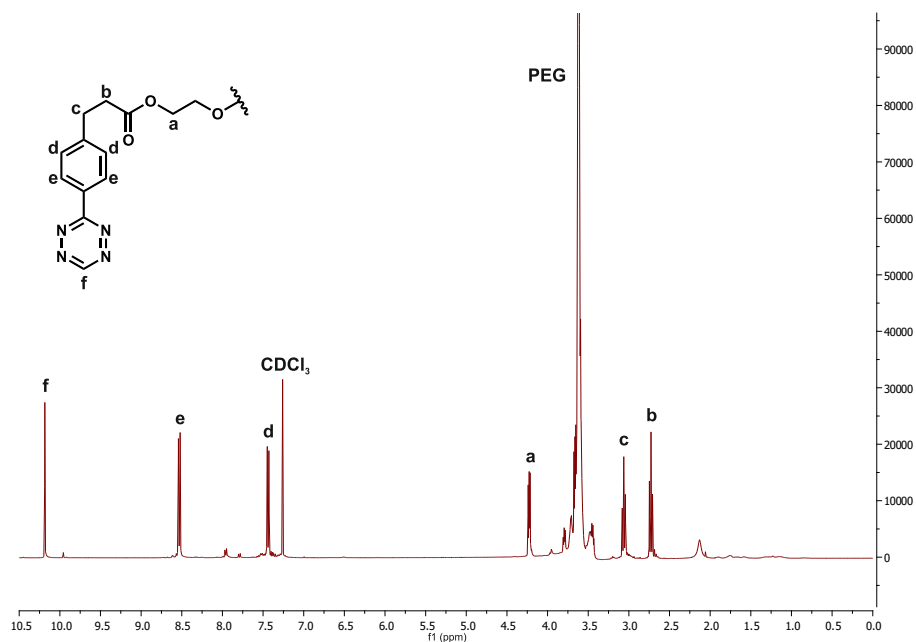


Figure S8: ^1H NMR spectrum of 8armPEG10k-Tz

^1H NMR (CDCl_3 , 400 MHz): δ (ppm) = 2.73 (t, 16H, $-\text{C}(\text{O})\text{CH}_2\text{CH}_2\text{Ar}$), 3.06 (t, 16H, $-\text{C}(\text{O})\text{CH}_2\text{CH}_2\text{Ar}$), 3.62 (s, $-\text{OCH}_2\text{CH}_2\text{O}-$), 4.23 (t, 16H, $-\text{OCH}_2\text{CH}_2\text{O}$), 7.44 (d, 16H, Ar), 8.53 (d, 16H, Ar), 10.18 (s, 8H, $-\text{N}=\text{CH}-\text{N}=\text{}$).

8armPEG20k-Tz

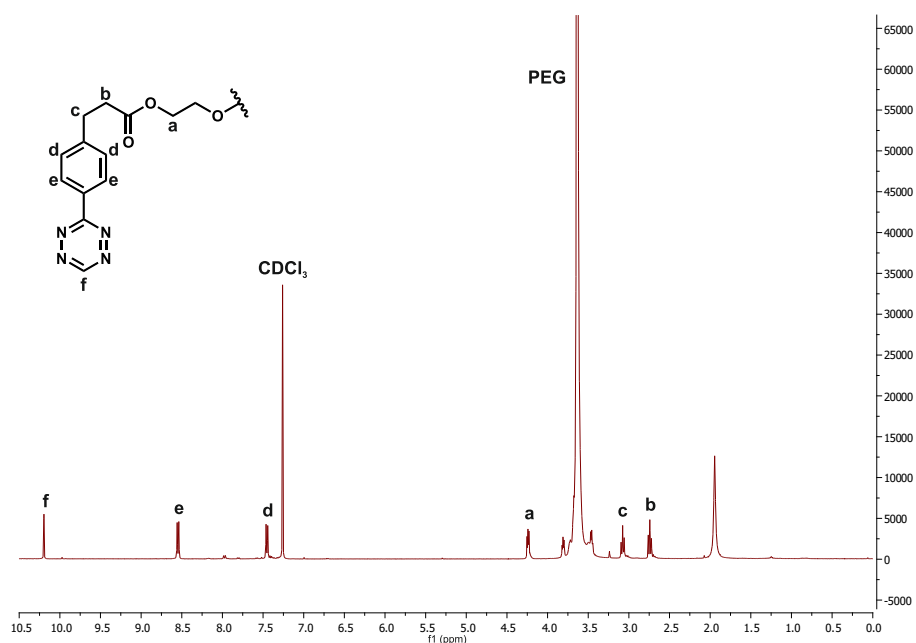
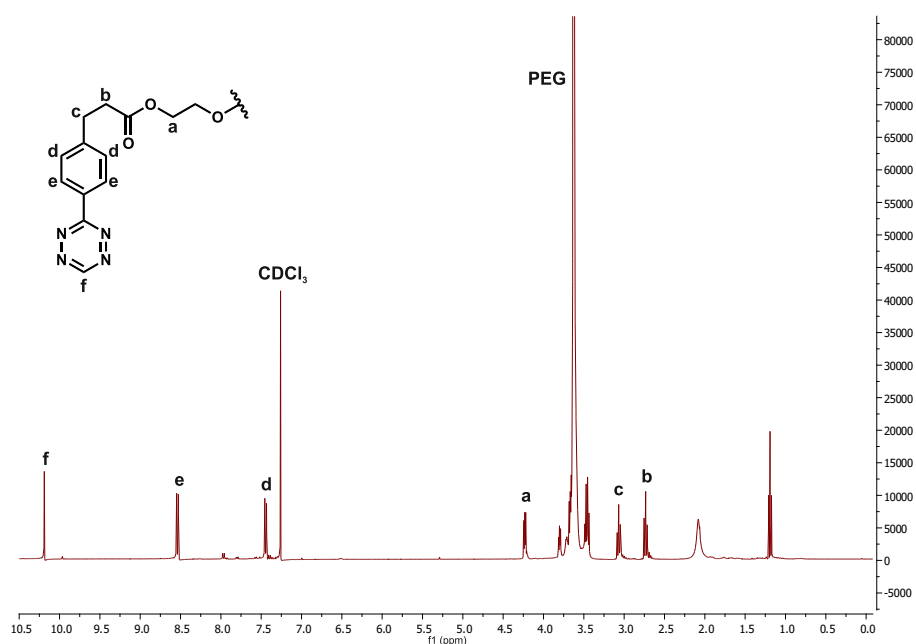
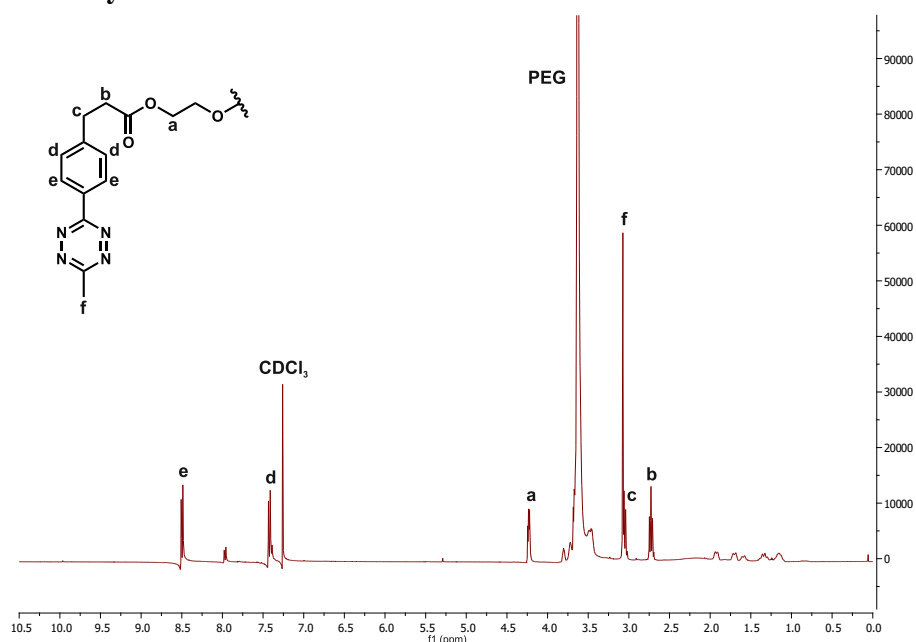


Figure S9: ^1H NMR spectrum of 8armPEG20k-Tz

^1H NMR (CDCl_3 , 400 MHz): δ (ppm) = 2.74 (t, 16H, $-\text{C}(\text{O})\text{CH}_2\text{CH}_2\text{Ar}$), 3.08 (t, 16H, $-\text{C}(\text{O})\text{CH}_2\text{CH}_2\text{Ar}$), 3.64 (s, $-\text{OCH}_2\text{CH}_2\text{O}-$), 4.24 (t, 16H, $-\text{OCH}_2\text{CH}_2\text{O}$), 7.45 (d, 16H, Ar), 8.55 (d, 16H, Ar), 10.20 (s, 8H, $-\text{N}=\text{CH}-\text{N}=\text{}$).

8armPEG40k-Tz**Figure S10:** ¹H NMR spectrum of 8armPEG40k-Tz

¹H NMR (CDCl₃, 400 MHz): δ (ppm) = 2.73 (t, 16H, $-\text{C}(\text{O})\text{CH}_2\text{CH}_2\text{Ar}$), 3.06 (t, 16H, $-\text{C}(\text{O})\text{CH}_2\text{CH}_2\text{Ar}$), 3.62 (s, $-\text{OCH}_2\text{CH}_2\text{O}-$), 4.23 (t, 16H, $-\text{OCH}_2\text{CH}_2\text{O}$), 7.44 (d, 16H, Ar), 8.53 (d, 16H, Ar), 10.18 (s, 8H, $-\text{N}=\text{CH}-\text{N}=\text{N}$).

8armPEG10k-methyl-Tz**Figure S11:** ¹H NMR spectrum of 8armPEG10k-methyl-Tz

¹H NMR (CDCl₃, 400 MHz): δ (ppm) = 2.73 (t, 16H, $-\text{C}(\text{O})\text{CH}_2\text{CH}_2\text{Ar}$), 3.06 (t, 16H, $-\text{C}(\text{O})\text{CH}_2\text{CH}_2\text{Ar}$), 3.07 (s, 24H, CH_3Ar), 3.63 (s, $-\text{OCH}_2\text{CH}_2\text{O}-$), 4.23 (t, 16H, $-\text{OCH}_2\text{CH}_2\text{O}$), 7.42 (d, 16H, Ar), 8.50 (d, 16H, Ar).

8armPEG10k-ETPI

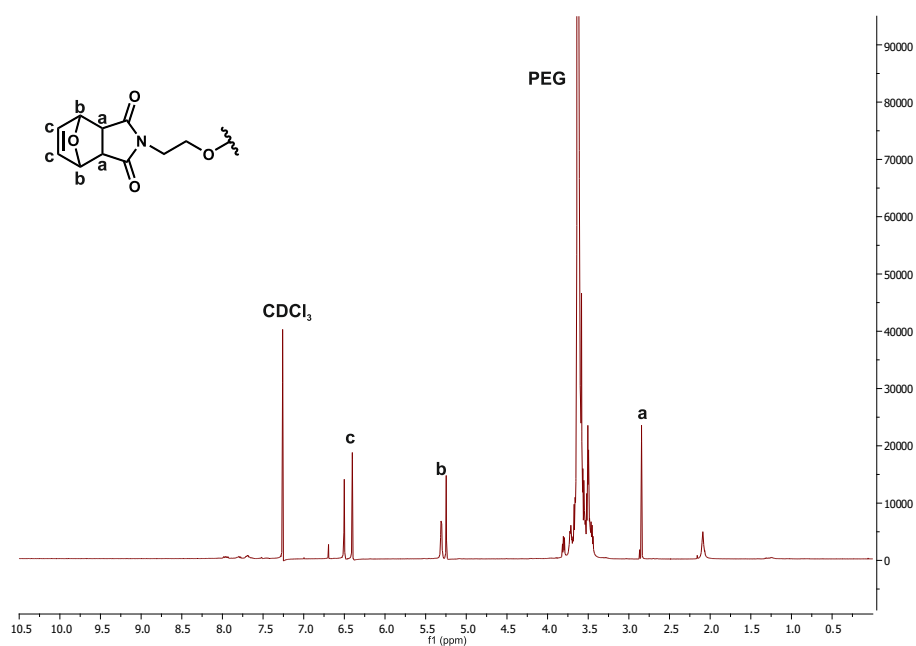


Figure S12: ^1H NMR spectrum of 8armPEG10k-ETPI

^1H NMR (CDCl_3 , 400 MHz): δ (ppm) = 2.84 (s, 16H, $-\text{C}(\text{O})\text{CHRCHRC}(\text{O})-$, *exo*), 3.63 (s, $-\text{OCH}_2\text{CH}_2\text{O}-$), 5.25 (s, 16H, $-\text{RCHOCHR}-$, *endo*), 5.30 (m, 16H, $-\text{RCHOCHR}-$, *exo*), 6.40 (s, 16H, $-\text{CH}=\text{CH}-$, *endo*), 6.50 (s, 16H, $-\text{CH}=\text{CH}-$, *exo*).

mPEG5k-Tz

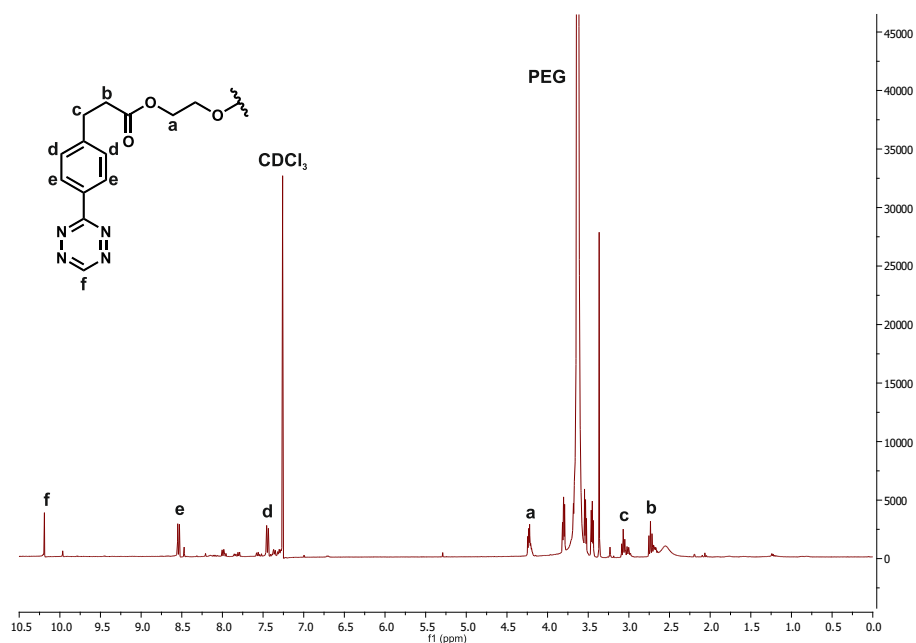


Figure S13: ^1H NMR spectrum of mPEG5k-Tz

^1H NMR (CDCl_3 , 400 MHz): δ (ppm) = 2.73 (t, 2H, $-\text{C}(\text{O})\text{CH}_2\text{CH}_2\text{Ar}$), 3.07 (t, 2H, $-\text{C}(\text{O})\text{CH}_2\text{CH}_2\text{Ar}$), 3.37 (s, 3 H, $\text{H}_3\text{CO}-$), 3.63 (s, $-\text{OCH}_2\text{CH}_2\text{O}-$), 4.22 (t, 2H, $-\text{CH}_2\text{CH}_2\text{COO}$), 7.45 (d, 2H, Ar), 8.54 (d, 2H, Ar), 10.19 (s, 1H, $-\text{N}=\text{CH}-\text{N}=\text{}$).

Chapter 5

Investigation of the impact of hydrolytically cleavable groups on the stability of PEG-based iEDDA hydrogels

To be submitted to a peer-reviewed journal

Abstract

Eight-armed poly(ethylene glycol) (PEG) hydrogels cross-linked via inverse electron demand Diels-Alder reaction between norbornene and tetrazine groups are promising materials for long-term protein delivery. While a controlled release over 265 days was achieved for 15% (w/v) hydrogels in our previous study, the material showed high stability over 500 days. In this study, hydrolyzable linkers were incorporated into the PEG-norbornene precursor structure to reduce the degradation time. To this end, 3,6-epoxy-1,2,3,6-tetrahydrophthalimide, carbamate, carbonate ester, and phenyl carbonate ester were introduced as degradable functional groups. Oscillatory shear experiments revealed that they did not affect the *in situ* gelation. All hydrogel types had gel points of less than 20 s even at a low polymer concentration of 5% (w/v). Hydrogels with varying polymer concentrations had similar mesh sizes, all of which fell in the range of 4 to 12 nm. All hydrogels passed the 70% threshold of cytotoxicity assessment according to ISO 10993-5:2009. The inclusion of phenyl carbonate ester accelerated degradation considerably, with complete dissolution of 15% (w/v) hydrogels after 302 days of incubation in 50 mM phosphate buffer (pH 7.4). Controlled release of 150 kDa fluorescein isothiocyanate-dextran over a period of at least 150 days was achieved with 15% (w/v) hydrogels.

1 Introduction

In situ forming hydrogels are of great importance in the field of protein drug delivery because they can be injected in a much less invasive procedure as compared to implantation, which decreases cost and improves patient compliance [1–3]. One way to achieve *in situ* gelation in delivery systems is the formation of covalent bonds between pre-functionalized hydrogel precursors by using chemical cross-linking [2]. To improve the material's potential for medical use, it is of utmost importance that these delivery systems do not have to be removed by explantation at the end of the therapy, but rather degrade into water-soluble products leading to polymer erosion and complete hydrogel dissolution. While degradation refers to the actual bond cleavage reaction, erosion designates the loss of mass from the polymer matrix [4]. For complete hydrogel erosion of covalently cross-linked hydrogels, there are two common degradation mechanisms. A simple approach is using cross-linking reactions of kinetically reversible nature [5]. These cross-links are cleaved by the removal of educts from the reaction equilibrium leading to degradation of the hydrogel network. For example, the degradation mechanism of hydrogels cross-linked via Diels-Alder (DA) reaction between furan and maleimide relies on the hydrolysis of maleimide groups to non-reactive maleamic acid [6,7]. However, the DA reaction is not ideal for *in situ* gelation due to its slow reaction kinetics [8–10]. Further examples of biodegradable materials are systems cross-linked via Schiff base reactions such as imines and their derivatives including hydrazones and oximes [11,12]. Unfortunately, the hydrogel formation via Schiff base reactions poses a high risk for off-target reactions with cargo or molecules at the injection site by reactive groups such as ketones and aldehydes [13,14]. This could additionally lead to structural damage to the embedded protein cargo or changes in the release kinetics [15]. Therefore, cross-linking reactions with higher reaction rate and selectivity are required.

A promising reaction is the inverse electron demand Diels-Alder (iEDDA) reaction between norbornene and tetrazine groups [16]. In addition to its fast reaction kinetics, the iEDDA reaction is bioorthogonal and highly efficient without using a catalyst or producing toxic byproducts [17–19]. The major drawback to the iEDDA reaction is that it is irreversible and, therefore, via iEDDA reaction cross-linked hydrogels require a different degradation pathway to make them degradable. Here, erosion can be achieved by incorporating hydrolytically, oxidatively, or enzymatically cleavable groups as predetermined breaking points into hydrogel precursors [5]. Polymers such as chitin, chitosan, dextran, and hyaluronic acid allow for enzymatic cleavage [20–23]. However, enzymatic degradation complicates the control and predictability of degradation because enzyme concentrations vary spatially within the tissue as well between individuals. When enzymes are added to the polymer matrix in an attempt to solve this problem, the loading capacity of the hydrogel is reduced, which is less than ideal [24].

To overcome this drawback, passively hydrolyzable functional groups need to be incorporated into the polymer backbone. Prominent examples are ester, amide, carbamate, and carbonate ester groups that degrade at different rates [25–28].

The goal of this study was to prepare poly(ethylene glycol) (PEG)-based hydrogels that degrade at different rates. For this purpose, 3,6-epoxy-1,2,3,6-tetrahydrophthalimide (ETPI), carbamate, carbonate ester, and phenyl carbonate ester were introduced into the norbornene-functionalized eight-armed PEG-hydrogel precursor as hydrolytically cleavable groups. Hydrogel formation was based on an iEDDA reaction of norbornene- and tetrazine-functionalized macromonomers. The gelation was evaluated by rheology to determine gel point and stiffness. Additionally, Young's modulus of compression (compressive modulus) was measured. The degradation time of the hydrogels was investigated as well as cytotoxicity and the mesh size. Finally, the hydrogels were loaded with fluorescein isothiocyanate-dextran (FITC-dextran) with a molecular weight of 150 kDa to determine the *in vitro* release kinetics.

2 Materials and methods

2.1 Materials

4-Aminophenol, anhydrous acetonitrile, deuterated chloroform (CDCl_3), anhydrous dichloromethane (DCM), *N,N'*-dicyclohexylcarbodiimide, diisopropyl azodicarboxylate, anhydrous *N,N*-dimethylformamide (DMF), 2,2-dimethyl-2-silapentane-5-sulfonate sodium salt (DSS), deuterated dimethyl sulfoxide (DMSO), *N,N'*-disuccinimidyl carbonate (DSC), Eagle's minimum essential medium (EMEM), absolute ethanol, anhydrous ethyl acetate (EtOAc), fetal calf serum (FCS), FITC-dextran with a molecular mass of 150 kDa, 3-(2-furyl)propanoic acid, glacial acetic acid, hexane, hydrazine monohydrate, *N*-methoxycarbonylmaleimide, 5-norbornenecarboxylic acid (mixture of *endo* and *exo*), protein LoBind Eppendorf tubes, pyridine, QuantiPro™ BCA Assay Kit, sodium bicarbonate, sulfur, anhydrous tetrahydrofuran (THF), triethylamine (TEA), and triphosgene were acquired from Sigma-Aldrich (Taufkirchen, Germany). Eight-armed poly(ethylene glycol) with a molecular mass of 10 kDa (8armPEG10k) and methoxy poly(ethylene glycol) with a molecular weight of 5 kDa (mPEG5k) were purchased from JenKem Technology (Allen, TX, USA) and functionalized with amine, maleimide, and tetrazine groups as previously described [29–31]. 4-Dimethylaminopyridine (DMAP), phthalimide, and anhydrous sodium sulfate were received from Acros Organics (Geel, Belgium). Cyclohexane p.a. and DCM p.a. were obtained from Fisher Chemical (Loughborough, UK). Diethyl ether (technical grade) was purchased from Jäcklechemie (Nuremberg, Germany). *O*-(Benzotriazol-1-yl)-*N,N,N',N'*-tetramethyluronium-hexafluorophosphate (HBTU), citric acid monohydrate, hydrochloric acid, silica gel 60 (0.063–0.200 mm), sodium azide, sodium dihydrogen phosphate monohydrate, sodium hydroxide, sodium nitrite, thionyl chloride, and triphenylphosphine were purchased from Merck KGaA (Darmstadt, Germany). 5-Norbornene-2-methanol and 5-norbornene-2-methylamine were obtained from TCI Chemicals (Eschborn, Germany). 3-(4-Cyanophenyl)-propionic acid was obtained from abcr GmbH (Karlsruhe, Germany). Tetramethylethylenediamine was purchased from Carl Roth GmbH & Co. KG (Karlsruhe, Germany). 3-(4,5-Dimethylthiazol-2-yl)-2,5-diphenyltetrazolium bromide (MTT) and sodium dodecyl sulfate (SDS) were received from PanReac AppliChem (Darmstadt, Germany)

Ethanol was purchased from Labochem international (Heidelberg, Germany). Gibco Dulbecco's phosphate-buffered saline was acquired from Life Technologies (Darmstadt, Germany). Mouse fibroblast cells were a kind gift from the group of Prof. Armin Buschauer (University of Regensburg). Purified water was freshly prepared using a Milli-Q water purification system from Millipore (Schwalbach, Germany).

2.2 ^1H and ^{13}C NMR Spectroscopy

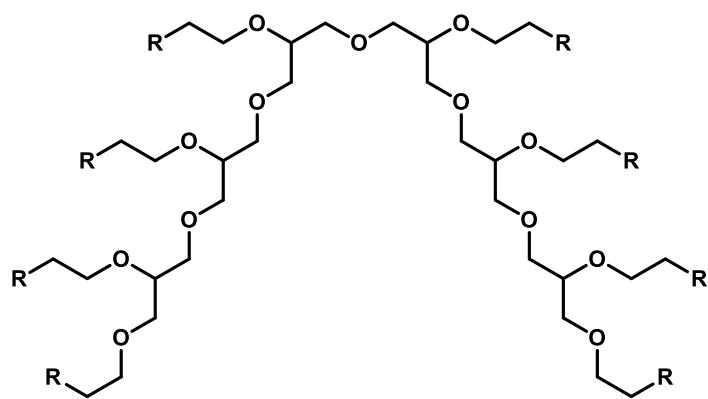
^1H and ^{13}C NMR spectra were recorded using a Bruker Avance III 400 spectrometer (Bruker BioSpin GmbH, Rheinstetten, Germany). To calculate end-group conversion, the integral of the alkene proton peak of norbornene groups was compared to the integral of the PEG backbone peak at δ 3.75–3.40 ppm.

2.3 Synthesis of *N*-((bicyclo[2.2.1]hept-5-en-2-yl)methyl)-3-(furan-2-yl)propanamide

3-(2-Furyl)-propanoic acid chloride was synthesized as previously described [32]. Amidation was performed using a modified version of the synthesis described in literature [33]. In brief, 3-(2-furyl)-propanoic acid chloride was dissolved in anhydrous THF (10 ml), and the solution was added to a stirred solution of 5-norbornene-2-methylamine and pyridine (1.1 eq) in anhydrous THF (15 ml) at 0 °C. Afterwards, the mixture was warmed to 20 °C, at which it was maintained overnight. It was then diluted with water (60 ml), extracted with EtOAc (3x30 ml) and dried over anhydrous sodium sulfate. The solution was concentrated by rotary evaporation. The crude product was purified by column chromatography. The yield was 70%.

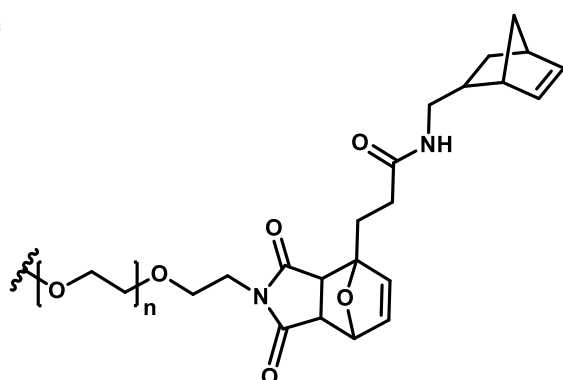
2.4 Synthesis of 8armPEG10k-ETPI-Nb (Scheme 1)

A mixture of 8armPEG10k-maleimide and *N*-((bicyclo[2.2.1]hept-5-en-2-yl)methyl)-3-(furan-2-yl)propanamide in anhydrous ethyl acetate (10 ml) was stirred for 3 days at room temperature. Afterwards, the product was precipitated in cold diethyl ether three times. The residue was dissolved in ethyl acetate and extracted with water four times. The aqueous layer was washed twice with diethyl ether and filtered. Subsequently, the product was extracted with DCM three times, and the organic phase was dried over sodium sulfate. The solvent was concentrated, and the product was precipitated several times with cold diethyl ether. Finally, the product was dried under vacuum. The yield was 98%, and the degree of end-group conversion was 64%, as determined by ^1H NMR spectroscopy.

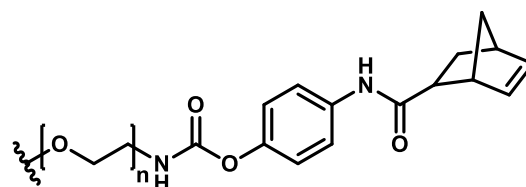


hexaglycerol core of 8armPEG10k

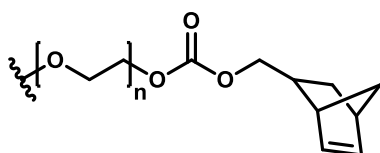
R =



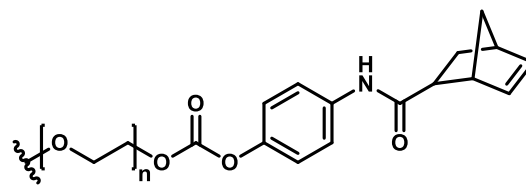
8armPEG10k-ETPI-Nb



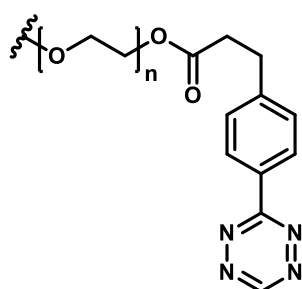
8armPEG10k-carbamate-Nb



8armPEG10k-carbonate-Nb



8armPEG10k-phenyl carbonate-Nb



8armPEG10k-Tz

Scheme 1: Chemical structures of 8armPEG10k-Tz and 8armPEG10k-Nb precursors with ETPI, carbamate, carbonate ester, and phenyl carbonate ester linkers. For simplification, only one isoform of the norbornene position is shown.

2.5 Synthesis of *N*-(4-hydroxyphenyl)bicyclo[2.2.1]hept-5-ene-2-carboxamide

5-Norbornene-2-carboxylic acid, 4-aminophenol, and TEA were dissolved in anhydrous DMF. HBTU was dissolved in anhydrous DMF. Both solutions were combined and stirred for 2 h at room temperature under argon atmosphere. Subsequently, the solvent was evaporated. The residue was dissolved in ethyl acetate, washed with HCl solution (pH 3), brine and water, and dried over sodium sulfate. After evaporation of the solvent, the product was further purified by column chromatography. The yield was 96%.

2.6 Synthesis of 4-(bicyclo[2.2.1]hept-5-ene-2-carboxamido)phenyl (2,5-dioxopyrrolidin-1-yl) carbonate

N-(4-Hydroxyphenyl)bicyclo[2.2.1]hept-5-ene-2-carboxamide was dissolved in anhydrous acetonitrile, and pyridine and DSC were added. The solution was stirred for 18 h at room temperature. Afterwards, the solvent was concentrated, DCM was added, and the formed solid was filtered off. The solvent was completely evaporated, and the residue was taken up in ethyl acetate to give a suspension. The organic phase was washed with 5% citric acid twice and brine once and dried over sodium sulfate. The solvent was evaporated and, finally, vacuum dried. The yield was 80%.

2.7 Synthesis of 8armPEG10k-carbamate-Nb (Scheme 1)

8armPEG10k-NH₂ and 4-(bicyclo[2.2.1]hept-5-ene-2-carboxamido)phenyl (2,5-dioxopyrrolidin-1-yl) carbonate were dissolved separately in anhydrous acetonitrile. The two solutions were combined, and TEA was added. The solution was stirred for 18 h under argon atmosphere. Afterwards, the precipitate was filtered off and the solvent was evaporated. The residue was taken up in DCM and the suspension was centrifuged several times to separate the precipitate. Subsequently, the product was crystallized with diethyl ether. The crystallization step was repeated several times. The product was finally vacuum dried. The yield was 71% and the degree of end-group conversion was 83%, as determined by ¹H NMR spectroscopy.

2.8 Synthesis 8armPEG10k-carbonate-Nb (Scheme 1)

5-Norbornene-2-methanol, triphosgene, and TEA were dissolved in anhydrous DCM at 0 °C and stirred for 3 h. A solution of 8armPEG10k and DMAP in anhydrous DCM was added, and the combined solution was warmed up to room temperature. The solution was stirred 2 days. Then, the solvent was evaporated, and the residue was dissolved in anhydrous THF. Subsequently, the suspension was centrifuged, and the precipitate was removed. This step was repeated. Afterwards, the product was

precipitated with cold cyclohexane several times and dried under vacuum. The yield was 55% and the degree of end-group conversion was 79%, as determined by ^1H NMR spectroscopy.

2.9 Synthesis of 8armPEG10k-phenyl carbonate-Nb (Scheme 1)

N-(4-Hydroxyphenyl)bicyclo[2.2.1]hept-5-ene-2-carboxamide, triphosgene, and TEA were dissolved in anhydrous DCM at 0 °C and stirred for 3 h. A solution of 8armPEG10k and DMAP in anhydrous DCM was added and the combined solution was warmed up to room temperature. The solution was stirred for 2 days. Then, the solvent was evaporated. The residue was taken up in anhydrous THF. Subsequently, the suspension was centrifuged, and the precipitate was removed. This step was repeated. Afterwards, the product was precipitated with cold cyclohexane several times and dried under vacuum. The yield was 98% and the degree of end-group conversion was 71%, as determined by ^1H NMR spectroscopy.

2.10 Hydrogel preparation and characterization

For hydrogel preparation, equal molar amounts of norbornene- and tetrazine-functionalized 8armPEG10k-precursors (Scheme 1) were dissolved separately in water. After combining both solutions, 200 μl were transferred into cylindrical glass molds. The solution was allowed to gel for 1 h at 37 °C. The overall polymer concentrations were 5, 10, and 15% (w/v).

2.11 Hydrogel characterization

Oscillatory shear experiments were performed on a Malvern Kinexus Lab+ rheometer (Malvern, Kassel, Germany) at 37 °C with 25 mm parallel plate geometry, gap size of 500 μm , constant oscillation frequency of 1.0 Hz, and a strain of 1%. Storage (G'), loss modulus (G''), and complex shear modulus (G^*) were recorded over time. The cross over point of G' and G'' was regarded as the gel point. The absolute values of the complex shear modulus ($|G^*|$) were determined after 30 min when polymerization was considered complete. Water evaporation was reduced by using a solvent trap. Only hydrogels with a polymer concentration of 5% (w/v) were analyzed because higher concentrations resulted in faster gelation, which complicated handling.

The determination of the average mesh size (ξ) was carried out according to the equilibrium swelling theory [28,34]. The gel volumes after cross-linking (V_{gc}) and after swelling (V_{gs}) were determined using Archimedes' principle of buoyancy. With the PEG density taken as 1.12 g/ml [30], the dry polymer volume (V_p) was obtained after freeze-drying the hydrogels. Subsequently, the polymer fraction of the hydrogel after cross-linking ($v_{2c} = V_p/V_{gc}$) and in swollen state ($v_{2s} = V_p/V_{gs}$) were calculated. The number of moles of elastically active chains in the hydrogel network (ν_e) was calculated by means of a modified version of the Flory-Rehner equation [35–37]:

$$v_e = -\frac{V_p}{V_1 v_{2c}} \cdot \frac{[\ln(1 - v_{2s}) + v_{2s} + \chi_1 v_{2s}^2]}{\left[\left(\frac{v_{2s}}{v_{2c}}\right)^{\frac{1}{3}} - \frac{2}{f} \left(\frac{v_{2s}}{v_{2c}}\right) \right]} \quad (1)$$

Parameters required for equation (1) are the molar volume of solvent, V_1 , (18 ml/mol for water) [38], the Flory-Huggins interaction parameter of PEG in water, χ_1 , (0.426) [39], and the branching factor of the macromonomers, f , (eight for 8armPEG). The average network mesh size (ξ) was calculated as suggested by Canal and Peppas [40]:

$$\xi = v_{2s}^{-\frac{1}{3}} l \left(\frac{2m_p}{v_e M_r} \right)^{\frac{1}{2}} C_n^{\frac{1}{2}} \quad (2)$$

In equation (2), l is the average bond length along the PEG backbone (0.146 nm) [41], m_p is the total mass of polymer in the hydrogel, M_r is the molecular mass of the PEG repeating unit (44 g/mol), and C_n is the Flory characteristic ratio (four for PEG) [41].

The compressive modulus was determined according to the literature [31]. In brief, 5% (w/v) 8armPEG10k-hydrogels with a volume of 200 μ l were prepared for all linkers as described in section 2.10. The diameter and height of the hydrogels were measured. After casting the hydrogel cylinders on the lower plate of an Instron 5542 materials testing machine (Norwood, MA, USA), the samples were compressed uniaxially at a speed of 1 mm/min. Compressive force (N) and compressive strain (%) were monitored over time. The compressive modulus was calculated by using the linear part of the curve between 10 and 20% compression.

2.12 Cytotoxicity

To assess cytotoxicity according to ISO 10993-5:2009 (Biological evaluation of medical devices, part 5: Tests for *in vitro* cytotoxicity), extracts were prepared and analyzed via MTT assay as previously described [42]. In brief, 200 μ l 15% (w/v) 8armPEG10k-hydrogels were prepared for all linkers as described in section 2.10. These hydrogels were incubated in 2 ml of EMEM supplemented with 10% FCS for 24 h at 37 °C. Afterwards, extracts were prepared by separating the supernatant from the hydrogels. Meanwhile, mouse fibroblast L-929 cells were seeded in a 96-well microtiter plate at a density of 10,000 cells per well and cultivated overnight. 100 μ l extract was added to each well. 0.1% SDS was used as negative control and pure medium served as positive control. At least six replicates were prepared for each type of hydrogel. After 24 h of incubation at 37 °C, the medium was replaced with 200 μ l of a 1.5 mM MTT solution. After 6 h of further incubation at 37 °C, the MTT solution was

replaced with PBS containing 10% SDS, and the samples were incubated for 16 h at room temperature. Finally, the absorbance at 570 and 690 nm was measured using a FluoStar Omega microplate reader (BMG Labtech, Ortenberg, Germany). Cell viability was calculated by the difference in absorbance. The viability was normalized to the positive control. For best evidence, hydrogel formulations with the highest polymer concentration of 15% (w/v) were investigated. By using extracts, contact between hydrogels and cells was prevented, which could lead to a negative impact on the cells due to abrasion.

2.13 Swelling and degradation studies

Swelling and degradation studies were performed according to literature [28]. For all linkers, 8armPEG10k-hydrogels with polymer concentrations of 5, 10, and 15% (w/v) were prepared as described in section 2.10. The hydrogels were weighed after cross-linking and transferred to LoBind Eppendorf tubes. 5 ml of a 50 mM phosphate buffer (pH 7.4) with 0.02% sodium azide was added and the hydrogels were incubated at 37 °C in a shaking water bath. At predetermined time points, the hydrogels were weighed and incubated in 5 ml of fresh buffer solution. Complete dissolution was achieved when no remaining material could be detected.

2.14 Release of FITC-dextran

To assess the influence of the biodegradable linkers on the release kinetics, FITC-dextran was used as model substance. 2 mg of 150 kDa FITC-dextran was embedded in 200 µl hydrogels with a polymer concentration of 15% (w/v). To prepare a hydrogel containing FITC-dextran, the respective norbornene-functionalized precursor was dissolved in 100 µl of a solution with a FITC-dextran concentration of 20 mg/ml. To this mixture, 100 µl of a solution containing equal molar amounts of 8armPEG10k-Tz were added. Gelation was carried out for 1 h at 37 °C. The hydrogels were transferred into 5 ml LoBind Eppendorf tubes and incubated in 5 ml of 50 mM phosphate buffer (pH 7.4). The release experiments were performed in a shaking water bath at 37 °C. At regular time points, samples were withdrawn and replaced with fresh buffer. The samples were stored at 2–8 °C for further analysis. A FluoStar Omega fluorescence microplate reader (BMG Labtech, Ortenberg, Germany) was used to quantify the FITC-dextran concentration.

2.15 Statistical analysis

All experiments were performed in triplicate, and the results are shown as mean ± standard deviation. Statistical significance was assessed using one-way ANOVA. Post hoc analysis was determined by Tukey's test (GraphPad Prism 6.0, GraphPad Software Inc., La Jolla, CA, USA).

3 Results and discussion

3.1 Synthesis of PEG-Nb-derivatives with different biodegradable linkers

To introduce various cleavable groups as predetermined degradation points into hydrogels, different polymer functionalization mechanisms were used. For all the linkers synthesized for this work, end-group conversions ranging from 64–83% were achieved, which is satisfactory for cross-linking and comparable to other multiarmed PEG modifications [30,43]. The new biodegradable groups were synthesized into the PEG-norbornene precursor rather than the more reactive tetrazine groups to prevent hydrolysis and possible side reactions. Tetrazine-functionalized precursors were synthesized by esterification as previously published [31]. For the carbamate linker, a phenol was chosen as the leaving group. Carbamates consisting of phenols are chemically more labile than those made of aliphatic alcohols due to their lower pK_a values [44,45]. Using aliphatic alcohols as the leaving group for carbamate linkers would even lead to higher stability than the corresponding ester [46]. Similar to the carbamate linker, a phenol group was used as the leaving group for the phenyl carbonate ester linker to accelerate degradation. Overall, the syntheses presented here are a straightforward and cost-effective method to produce norbornene-functionalized multiarmed PEGs with different cleavable groups.

3.2 Gelation time and mechanical properties

In situ forming systems are advantageous because they undergo gelation rapidly, thus avoiding material loss from the injection site. The gel formation rate can be characterized by the gel point, which is the time of the cross-over point of storage (G') and loss modulus (G''). This point is where the transition from liquid-like to solid-like behavior occurs [47]. The gelation for each hydrogel was followed by oscillatory shear experiments.

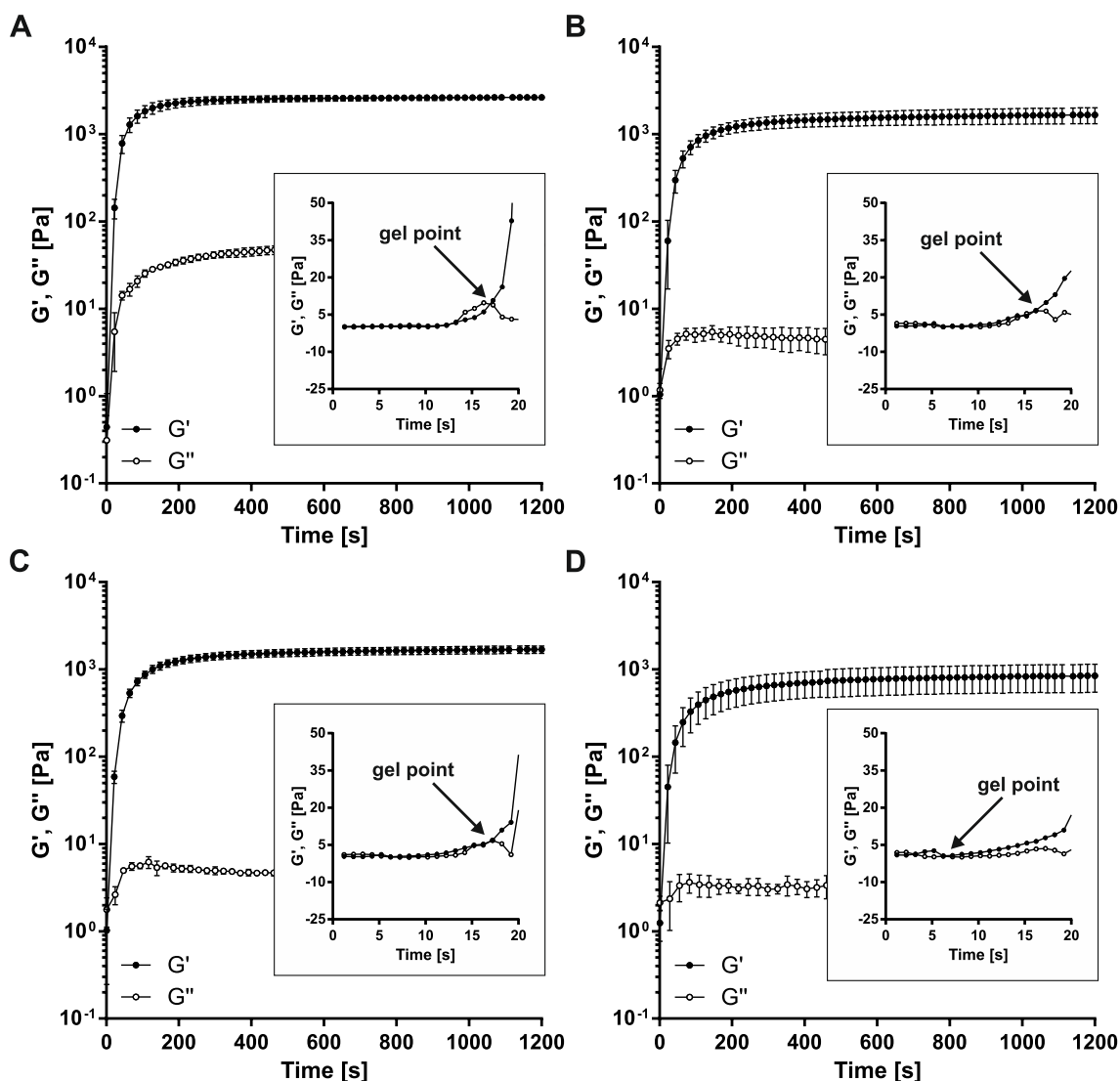


Figure 1: Rheograms of 5% (w/v) 8armPEG10k-hydrogels with ETPI linker (A), carbamate linker (B), carbonate ester linker (C), and phenyl carbonate ester linker (D) with insets showing the gel points of one representative hydrogel for each type. Storage (G') and loss modulus (G'') were determined over time at 37 °C. All experiments were carried out at an oscillation frequency of 1.0 Hz using a 25 mm parallel plate geometry and a gap size of 500 μm .

Figure 1 shows the rheograms of 5% (w/v) hydrogels with different degradable linkers. A very fast increase of G' ending in a plateau can be seen for all hydrogels. Gel points (Figure 2) of 16.6 ± 0.6 s (ETPI linker), 9.9 ± 6.0 s (carbamate linker), 12.2 ± 8.7 s (carbonate ester linker), and 5.9 ± 3.8 s (phenyl carbonate ester linker) were found, indicating very rapid *in situ* gelation already for a low polymer concentration of 5% (w/v). Even though differences in the gelation time were not found to be significant for the ETPI linker, lower end-group conversion of the macromonomers could explain the increased gelation time for that linker.

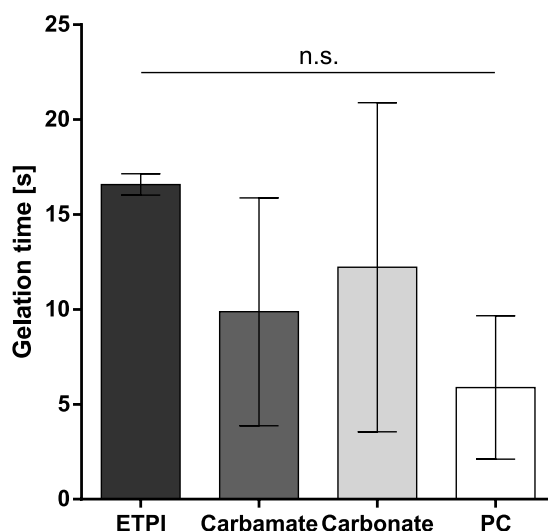


Figure 2: Gelation time of 5% (w/v) 8armPEG10k-hydrogels containing ETPI linker, carbamate linker, carbonate ester linker, and phenyl carbonate ester linker (PC) at 37 °C.

In addition to the gel point determination, rheology was used to measure the stiffness of the hydrogels after 30 min, when gelation was considered complete (Figure 4A). The absolute value of the complex shear modulus of hydrogels with the ETPI linker was found to be the significantly highest (2.7 ± 0.2 kPa). ETPI is the DA adduct between furan and maleimide. Since this DA adduct contains a norbornene derivative (7-oxanorbornene), it is possible that tetrazine reacts with the additional norbornene derivative as well as the unmodified norbornene groups. Previously, it was shown that tetrazine-functionalized 8armPEGs formed hydrogels with ETPI-functionalized 8armPEGs [31]. To check if tetrazine groups reacted with the incorporated ETPI linker, ^1H NMR spectroscopy was used. An aqueous mixture of 8armPEG10k-ETPI-norbornene and 8armPEG10k-tetrazine would make a highly cross-linked hydrogel, which could not have been investigated with classical ^1H NMR spectroscopy. Therefore, we used linear mPEG5k-tetrazine instead of 8armPEG10k-tetrazine so that the reaction products stayed in solution after polymerization and could be detected by ^1H NMR spectroscopy. To determine the prevalence of the side reaction between tetrazine groups and 7-oxanorbornene, norbornene groups were used in excess to tetrazine groups. First, spectra of 8armPEG10k-ETPI-norbornene and mPEG5k-tetrazine dissolved in D_2O with DSS as internal standard were recorded (Figure 3A and B). To maintain the same norbornene and DSS concentrations, solid mPEG5k-tetrazine was added to the NMR tube containing 8armPEG10k-ETPI-norbornene. After incubating at 37 °C for 1 h, the spectrum of the formed product was measured (Figure 3C). The disappearance of signal d indicated the complete consumption of tetrazine. The peaks at 6.63, 6.50, and 6.34 ppm represented the protons of the alkene bond in 7-oxanorbornene in the *exo* and *endo* positions (signal b). The protons at position c appeared as three peaks at 6.24 and 6.15 (*endo*) and 5.95 ppm (*exo*). Using the ratio of tetrazine to norbornene groups and integrating the peaks of the functional groups related to the internal standard, it was possible to calculate the percentage of groups that had reacted. Besides the decrease of the proton peak for the alkene bond at position c, the peaks of the protons at

positions a and b decreased, indicating a side reaction of tetrazine with the ETPI linker. 82.5% of the unmodified norbornene and 17.5% of the 7-oxanorbornene were found to react with tetrazine groups.

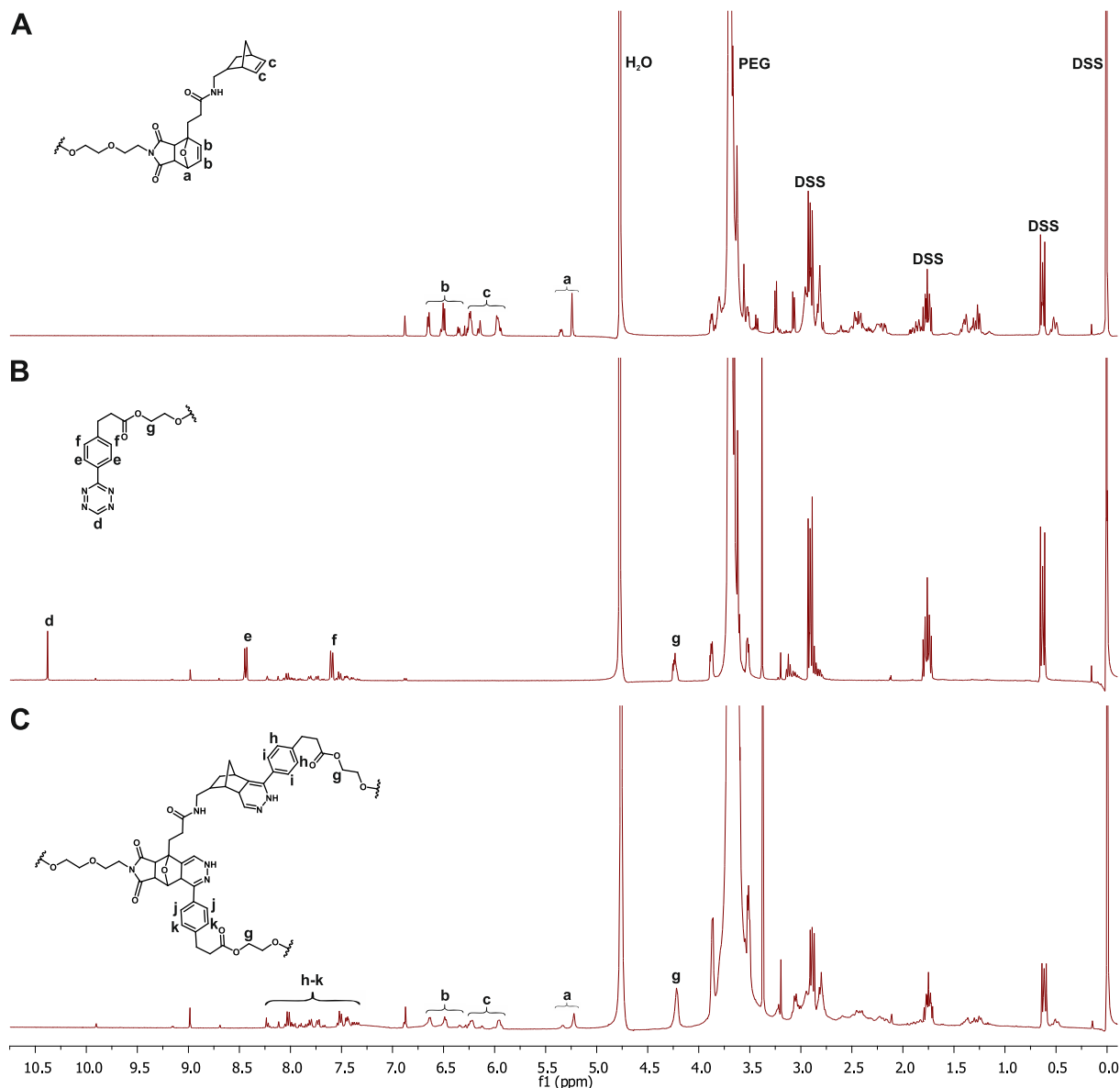


Figure 3: ¹H NMR spectra of 8armPEG10k-ETPI-Nb (A), mPEG5k-Tz (B), and the product between 8armPEG10k-ETPI-Nb and mPEG5k-Tz after reaction in D₂O at 37 °C for 1 h (C). All spectra were recorded in D₂O with DSS as internal standard.

These findings suggested that there are twice as many norbornene derivative groups present compared to tetrazine groups. This increases the likelihood for a tetrazine group to find a cross-linking counterpart for hydrogel formation. Consequently, the number of elastically active chains increases, giving the product a higher stiffness compared to systems with equimolar amounts of tetrazine and norbornene. No significant difference in stiffness was obtained for hydrogels containing carbamate (1.7 ± 0.4 kPa) or carbonate ester (1.8 ± 0.2 kPa) as cleavable linkers (Figure 4A). The significantly lowest stiffness was found for the hydrogel with the phenyl carbonate ester linker (0.9 ± 0.3 kPa). This type of hydrogel is expected to degrade most quickly due to its high lability, which also has a negative impact on stiffness.

Similar behavior was found for the compressive modulus (Figure 4B), which is defined as the ratio of compressive stress to compressive strain. Hydrogels with the phenyl carbonate ester linker showed the significantly lowest values (1.4 ± 0.2 kPa). Besides higher stiffness, the ETPI linker also had a significantly higher compressive modulus (9.0 ± 0.4 kPa) because of the increased number of binding partners for tetrazine groups. Hydrogels containing the carbamate (5.0 ± 1.0 kPa) and carbonate ester linkers (4.7 ± 0.8 kPa) did not show any significant differences in compressive modulus.

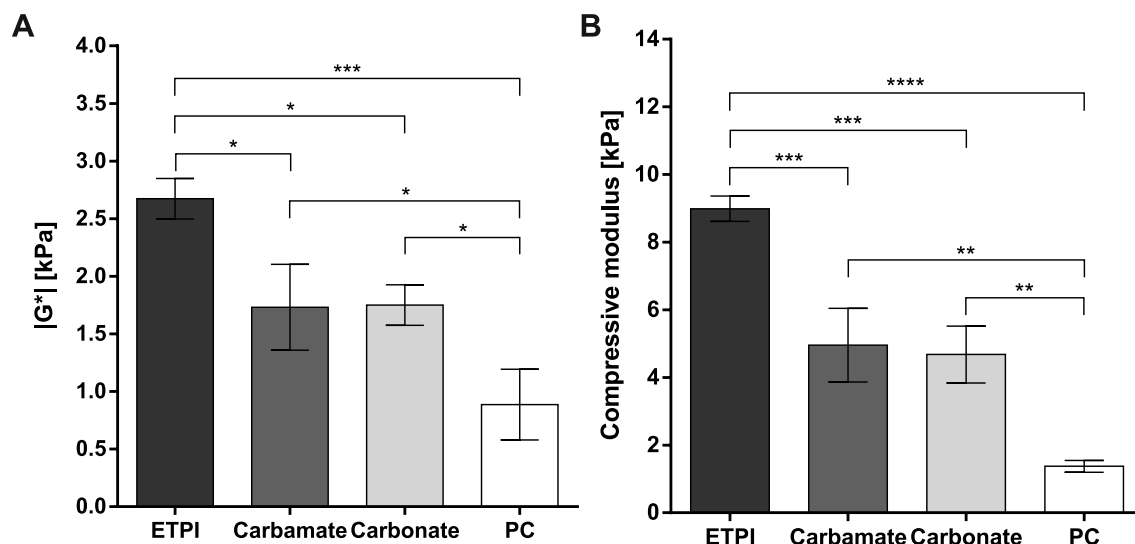


Figure 4: Stiffness represented by the absolute value of the complex shear modulus ($|G^*$) after 30 min of gelation time for 5% (w/v) 8armPEG10k-hydrogels containing ETPI linker, carbamate linker, carbonate ester linker, and phenyl carbonate ester linker (PC) (A). The compressive modulus of 5% (w/v) 8armPEG10k-hydrogels containing ETPI linker, carbamate linker, carbonate ester linker, and phenyl carbonate ester linker (PC) (B). Levels of statistical significance are indicated as * $p \leq 0.05$, ** $p \leq 0.001$, *** $p \leq 0.001$, and **** $p \leq 0.0001$.

3.3 Cytotoxicity

Carbonate ester and carbamate groups are targets for nucleophilic groups such as amines and alcohols. Contact with proteins can lead to interactions, including covalent bonds. Additionally, synthesis residues of educts such as phosgene and its derivatives can cause toxicity [48,49]. To exclude toxicity, cytocompatibility of all hydrogels consisting of different biodegradable linkers was assessed (Figure 5). For hydrogels with different biodegradable linkers, cell viabilities of $98.2 \pm 4.1\%$ (ETPI), $100.7 \pm 5.1\%$ (carbamate), $96.2 \pm 4.9\%$ (carbonate ester), and $89.1 \pm 4.2\%$ (phenyl carbonate ester) were found. Hydrogels containing the ETPI and carbamate linkers both had minimal impacts on viability. The higher stability imparted by the ETPI and carbamate linkers might have protected the cells from detrimental interactions and resulted in no toxicity. In contrast, carbonate ester and phenyl carbonate ester as biodegradable linker resulted in significant viability decreases. The reason for this becomes apparent upon examining the syntheses of 8armPEG10k-carbonate-Nb and 8armPEG10k-phenyl carbonate-Nb, which included phosgene and its derivatives. Possible educt residues after purification could explain the observed decreases in the cell number. Additionally, the phenyl carbonate ester linker is expected to degrade faster than the carbonate ester linker due to the incorporation of a phenyl elimination group.

Therefore, nucleophilic residues from the cells can preferentially attack the electrophilic structure. In summary, all hydrogels exceeded the 70% threshold value of ISO 10993 clearly. However, *in vivo* biocompatibility tests are necessary for a full evaluation of toxicity.

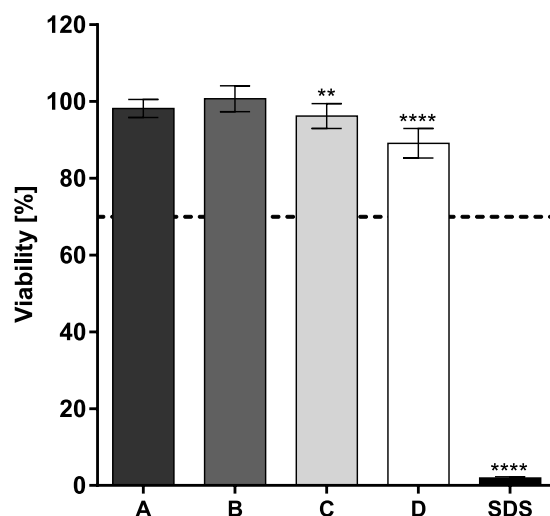
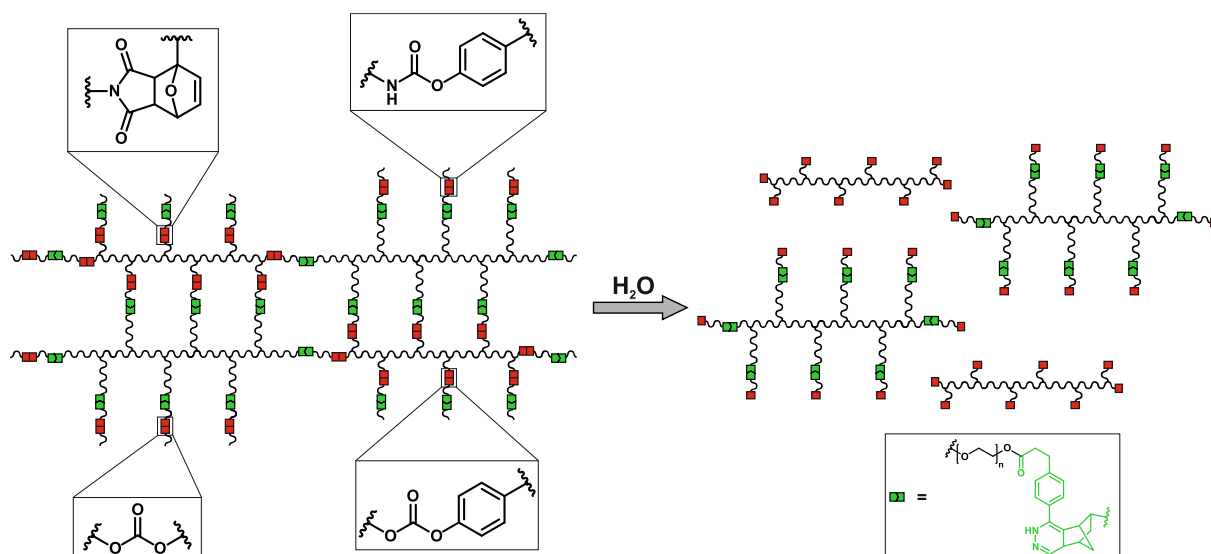


Figure 5: Viability of L-929 cells after incubation with extracts from 15% (w/v) 8armPEG-iEDDA hydrogels that contained ETPI (A), carbamate (B), carbonate ester (C), and phenyl carbonate ester (D) as biodegradable linkers. 0.1% (w/v) SDS in cell medium served as negative control. The dotted line at 70% cell viability indicates the threshold for cytocompatibility. All hydrogels passed this threshold showing no cytotoxicity. Statistical significance was assessed relative to the positive control, which was pure medium. Levels of statistical significance are indicated as ** $p \leq 0.01$ and **** $p \leq 0.0001$.

3.4 Swelling and degradation studies

The aim of this study was to investigate the influence of the different hydrolytically cleavable groups on the stability of 8armPEG10k-hydrogels. In contrast to former studies, the ester group of the PEG-norbornene precursor was replaced by a new cleavable linker, while the ester group of PEG-tetrazine was unchanged [31]. In this manner, we should be able to decrease the long degradation time of 8armPEG10k-hydrogels cross-linked via iEDDA reaction with two incorporated ester groups as designated breaking points (Scheme 2).

To examine the stability of these hydrogels, swelling studies were performed. All hydrogels were placed in 50 mM phosphate buffer (pH 7.4) at 37 °C, and the development of the relative mass was followed over time. The degradation time was defined as the time for complete dissolution of the hydrogels. For each linker, hydrogels were prepared with polymer concentrations of 5, 10, and 15% (w/v) to meet diverse application requirements (Figure S1). To better see the difference in mass change, Figure 6 shows the relative mass development of all hydrogels prepared with an overall polymer concentration of 5% (w/v).



Scheme 2: Degradation of 8armPEG10k-hydrogels due to the hydrolytically cleavage of different linkers.

For ETPI and carbonate ester, we observed swelling behavior similar to that of hydrogels containing two ester groups. After a decrease in the relative mass due to syneresis and network contraction, the hydrogels started to take up water, leading to slow bulk degradation with simultaneous mass increase [26,50]. For 400 days, no mass decrease was seen, and no faster degradation was obtained with either of these linkers. Carbamate groups also led to a volume contraction followed by a larger mass increase. However, the hydrogel mass started to decrease after reaching a maximum at 175 days due to linker cleavage and erosion. After 409 days, the hydrogel matrix still eroded, and no faster degradation could be detected. In contrast, no mass increase could be found for hydrogels containing the phenyl carbonate ester linker. For this linker, the hydrogel eroded from beginning to complete erosion after 153 days. The phenyl carbonate ester linker degraded faster than the carbonate ester linker because of resonance stabilization in the phenyl leaving group. This degradation results in a diffusion of the free macromonomers from the hydrogels to the surrounding solution and mass loss starting immediately after incubation with buffer. Interestingly, hydrogels containing the phenyl carbonate ester linker were the only hydrogel type that showed differences in swelling behavior for higher polymer concentrations (Figure S1D). After surface erosion over 109 days, the remaining matrix of the 10 and 15% (w/v) hydrogels started to gain mass. At this point for the 5% (w/v) hydrogels, most of the phenyl carbonate ester groups were already cleaved, preventing the hydrogel from swelling, and resulting in complete dissolution after 153 days. Only small differences in degradation time were detected for 10 and 15% (w/v) hydrogels. 15% (w/v) hydrogels completely dissolved after 309 days, whereas 10% (w/v) hydrogels were more stable and took 315 days to dissolve fully. We expected the more concentrated hydrogels to be more stable because 15% (w/v) hydrogels should have the largest number of elastically active chains and phenyl carbonate ester groups, which should take the longest to be completely degraded. This was already described for similar 8armPEG-hydrogels [51,52]. However, the 15% (w/v) hydrogels had the fastest gelation times, which caused them to have more irregularities compared to the

10% (w/v) hydrogels. Therefore, the 10% (w/v) hydrogels had more time to form a more homogeneous network during gelation, causing them to have similar stability to the 15% (w/v) hydrogels.

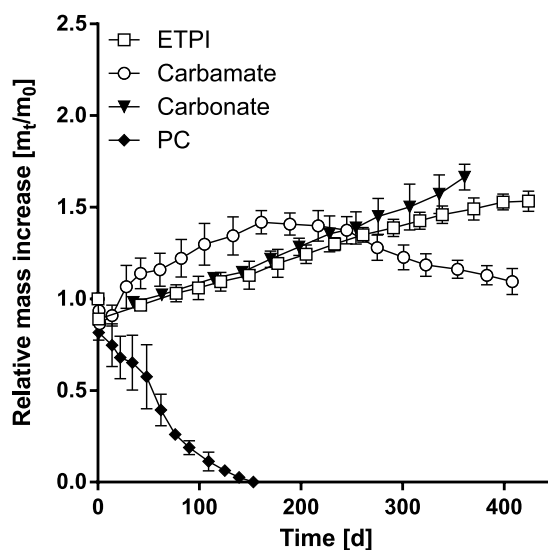
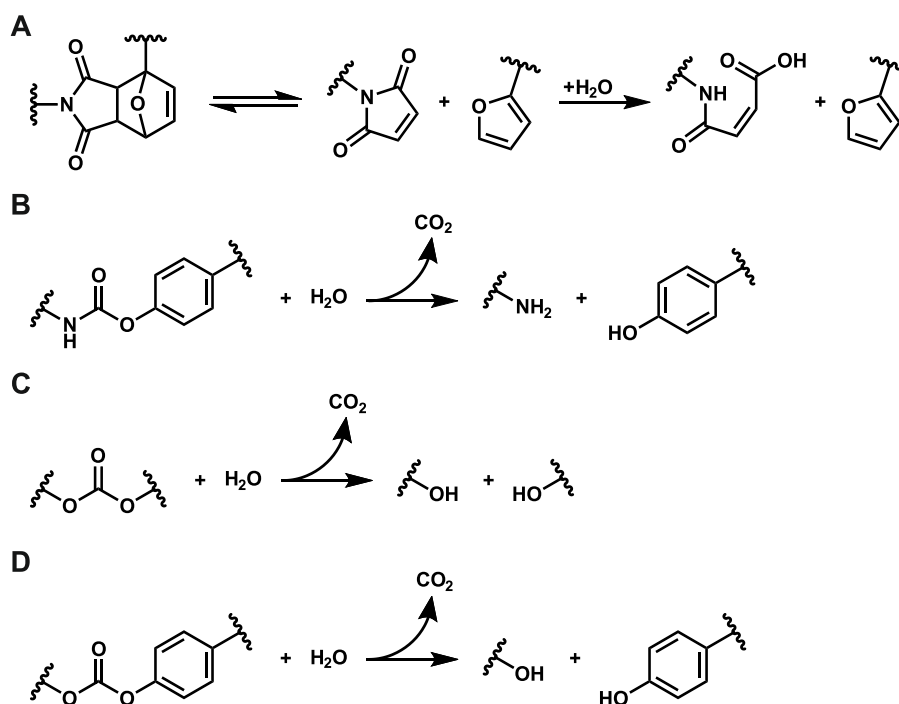


Figure 6: Swelling and degradation of 5% (w/v) 8armPEG10k-hydrogels containing ETPI, carbamate, carbonate ester, and phenyl carbonate ester (PC) as hydrolytically cleavable groups in 50 mM phosphate buffer (pH 7.4) at 37 °C.

The degradation mechanism (Scheme 3) of carbamate and carbonate ester involves the nucleophilic attack of water and the formation of carbon dioxide [53,54]. In neutral milieu, a B_{AC}2 mechanism is advanced for the carbonate ester hydrolysis [55]. Thereby, carbonate ester groups can show higher stability than ester groups [53]. On the other hand, introducing a resonance-stabilized leaving group results in lower stability as seen for the phenyl carbonate ester linkers. Carbamates hydrolyze via an E1cB elimination reaction mechanism [56,57]. An unstable isocyanate intermediate is formed, which reacts with water to form an amine and carbon dioxide. Again, a resonance-stabilized leaving group increases the degradation rate. For the ETPI linker, the hydrolysis of free maleimide groups removes maleimides from the reaction equilibrium, enhancing the retro-Diels-Alder reaction and degradation of the hydrogel. Previously, we showed that 5% (w/v) 8armPEG40k-hydrogels cross-linked via DA reaction containing one ETPI group per cross-link dissolved after approximately 10 days, whereas 5% (w/v) 8armPEG40k-hydrogels containing two ester groups per cross-link were completely dissolved after about 60 days [52,58]. Therefore, we assumed a significant difference in degradation time. However, no faster degradation could be found. The reason for this is that ETPI linkers are a target for tetrazine groups reacting as described above (Figure 3C). These additional cross-links are not subject to hydrolysis, making the system more stable. Hence, the ETPI linker is not a suitable hydrolyzable functional group for degradable hydrogel synthesis cross-linked via iEDDA reaction. However, for cross-linking reactions such as Schiff base formation or condensation reactions with no reactivity towards norbornene functionalities, the ETPI linker could be used.

In summary, only the incorporation of the phenyl carbonate ester linker into the 8armPEG10-Nb precursor led to faster degradation compared to our former hydrogels with two ester groups, which dissolved after 438 days.



Scheme 3: Degradation mechanism of ETPI (A), carbamate (B), carbonate ester (C), and phenyl carbonate ester linker (D) in water.

3.5 Mesh size and FITC-dextran release

After thoroughly characterizing the hydrogels synthesized with different biodegradable linkers, FITC-dextran release from the hydrogels was examined. First, the mesh sizes of hydrogels made with different polymer concentrations were determined. In addition to degradation behavior and drug diffusivity, the mesh size of a hydrogel is a pivotal factor in drug release kinetics [59–61]. It is necessary to choose a hydrogel with a mesh size in the range of the hydrodynamic diameter of the drug for controlled release over time without delay. The mesh sizes were compared to 8armPEG10k-hydrogels cross-linked via iEDDA reaction with two cleavable ester groups. Since for this hydrogel type, a controlled release of FITC-dextran over a time of more than 250 days could be achieved [31], the mesh sizes of the hydrogels with the new degradable linkers should be in the same range.

Table 1 shows the average mesh sizes of all hydrogels at three different polymer concentrations. For all four biodegradable linkers, mesh sizes comparable to our previously published values of iEDDA-hydrogels were found [31]. For the successful release of FITC-dextran from 8armPEG10-hydrogels, a polymer concentration of 15% (w/v) with an average mesh size of 4.1 ± 0.2 nm was used. Therefore, the same polymer concentration was chosen for the release experiments with the biodegradable linkers, with mesh size values of 4.4 ± 0.6 nm (ETPI), 4.6 ± 0.1 nm (carbamate), 4.2 ± 0.0 nm (carbonate ester),

and 4.9 ± 0.5 nm (phenyl carbonate ester). Differences in the mesh sizes of the various 15% (w/v) 8armPEG10k-hydrogels were not significant.

Table 1: Average mesh size of 8armPEG10k-hydrogels consisting of different biodegradable linkers. All hydrogel types were prepared with polymer concentrations of 5, 10, and 15% (w/v).

Linker	Concentration (% (w/v))	ξ (nm)
ETPI	5	11.4 ± 0.6
	10	6.2 ± 0.4
	15	4.4 ± 0.6
Carbamate	5	11.9 ± 1.0
	10	6.8 ± 0.4
	15	4.6 ± 0.1
Carbonate ester	5	10.6 ± 0.3
	10	5.8 ± 0.1
	15	4.2 ± 0.0
Phenyl carbonate ester	5	10.2 ± 1.2
	10	7.4 ± 0.3
	15	4.9 ± 0.5

The release of 150 kDa FITC-dextran from all hydrogel types with a polymer concentration of 15% (w/v) was examined to investigate the influence of the linker on the release kinetics. FITC-dextran was chosen as a model substance because of its high stability in phosphate buffer [62]. Figure 7 shows the release kinetics of FITC-dextran from the various hydrogels. For all hydrogels, controlled release over 150 days can be seen. The initial release varied from about 20% for the ETPI and carbonate ester linkers to approximately 13% for the carbamate and phenyl carbonate ester linkers. After the initial release, the model substance was released in a fast manner over 20 days for the ETPI and carbonate ester linkers. Subsequently, FITC-dextran was released continuously until the experiment was stopped. Thereby, FITC-dextran was released faster from hydrogels containing the ETPI linker.

Carbamate or phenyl carbonate ester linkers led to a slower initial release of the model substance followed by continuous release over the respective time frame. Subsequently, hydrogels with the phenyl carbonate ester linker released the FITC-dextran more quickly because of their lower stability, which resulted in faster mesh size increases and less hindered diffusion from the network. Interestingly, the amount released over the first 90 days was lower for the carbamate and phenyl carbonate ester linkers compared to the ETPI and carbonate ester linkers. Hydrogels with carbamate and phenyl carbonate ester share different swelling kinetics compared to the other hydrogels. Differences in swelling behavior most likely affect the release kinetics because of their influence on the network density.

In a recent study, we showed that it is possible to prepare a controlled release system based on 8armPEGk-precursors cross-linked via the iEDDA reaction between norbornene and tetrazine groups [31]. The model substance FITC-dextran with a molecular weight of 150 kDa was released over an extended time of 265 days. In contrast to other long-term release approaches that rely on the inclusion of additional substances such as micro- and nanoparticles [63,64] or incorporation of drug affine groups into the hydrogel backbone [65–67] the high stability and slow swelling behavior of the hydrogel itself were exploited. This is advantageous as no additional excipients are required, and arbitrary therapeutic proteins can be embedded in the hydrogel network without concern for their affinity. However, an overly long release time can cause challenges regarding protein stability, such as denaturation and activity loss. To shorten the release time, four different degradable groups were incorporated in the hydrogel backbone. Only the phenyl carbonate ester linker was found to degrade faster than the ester groups in our previous study.

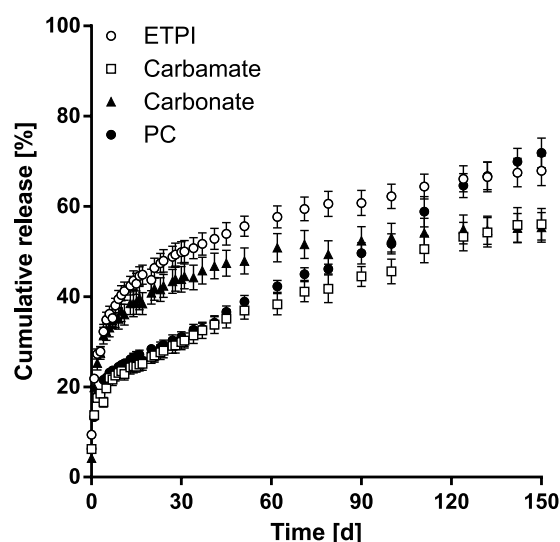


Figure 7: Release of FITC-dextran with a molecular weight of 150 kDa from 15% (w/v) 8armPEG10k-hydrogels containing ETPI linker, carbamate linker, carbonate ester linker, and phenyl carbonate ester linker (PC). The release experiments were carried out in 50 mM phosphate buffer (pH 7.4) at 37 °C.

The release experiments showed that the hydrogels with different hydrolyzable linkers were able to release a model substance with hydrodynamic diameter similar to common antibodies in a controlled manner over an extended time. These systems could be used to create drug depots for biologics like bevacizumab, ranibizumab, and trastuzumab to treat diseases such as early-stage breast cancer or age-related macular degeneration over long treatment periods while avoiding frequent injections and leading to higher patient compliance [68,69].

4 Conclusion

The introduction of different hydrolyzable groups as predetermined breaking points into multi-armed PEG-hydrogels led to a tunable degradation time. While hydrogels consisting of carbonate ester linkers

prepared from alcohols did not show faster degradation than the previously published hydrogels with ester groups, changing the leaving group from an alcohol to a phenol decreased the stability and accelerated hydrogel degradation. Furthermore, all of the biodegradable linkers we tested still formed hydrogels with rapid *in situ* gelation processes and consistent mesh sizes. Additionally, carbamate groups caused a change in swelling behavior. All hydrogels achieved controlled release of FITC-dextran for more than 150 days regardless of the type of hydrolyzable linker. The hydrogel syntheses presented here are promising methods for the creation of materials tailored to many diverse biomedical applications.

References

- [1] K.H. Bae, L.-S. Wang, M. Kurisawa, Injectable biodegradable hydrogels: progress and challenges, *J. Mater. Chem. B* 1 (2013) 5371–5388.
- [2] D.J. Overstreet, D. Dutta, S.E. Stabenfeldt, B.L. Vernon, Injectable hydrogels, *J. Polym. Sci., Part B: Polym. Phys.* 50 (2012) 881–903.
- [3] J.D. Kretlow, L. Klouda, A.G. Mikos, Injectable matrices and scaffolds for drug delivery in tissue engineering, *Adv. Drug Delivery Rev.* 59 (2007) 263–273.
- [4] A.T. Metters, C.N. Bowman, K.S. Anseth, A Statistical Kinetic Model for the Bulk Degradation of PLA- b -PEG- b -PLA Hydrogel Networks, *J. Phys. Chem. B* 104 (2000) 7043–7049.
- [5] X. Zhang, S. Malhotra, M. Molina, R. Haag, Micro- and nanogels with labile crosslinks - from synthesis to biomedical applications, *Chem. Soc. Rev.* 44 (2015) 1948–1973.
- [6] S. Kirchhof, A. Strasser, H.-J. Wittmann, V. Messmann, N. Hammer, A.M. Goepferich, F.P. Brandl, New insights into the cross-linking and degradation mechanism of Diels–Alder hydrogels, *J. Mater. Chem. B* 3 (2015) 449–457.
- [7] C.M. Madl, S.C. Heilshorn, Rapid Diels-Alder Cross-linking of Cell Encapsulating Hydrogels, *Chem. Mater.* 31 (2019) 8035–8043.
- [8] H. Tan, J.P. Rubin, K.G. Marra, Direct synthesis of biodegradable polysaccharide derivative hydrogels through aqueous Diels-Alder chemistry, *Macromol. Rapid Commun.* 32 (2011) 905–911.
- [9] I. Altinbasak, R. Sanyal, A. Sanyal, Best of both worlds: Diels–Alder chemistry towards fabrication of redox-responsive degradable hydrogels for protein release, *RSC Adv.* 6 (2016) 74757–74764.
- [10] C.E. Ziegler, M. Graf, S. Beck, A.M. Goepferich, A novel anhydrous preparation of PEG hydrogels enables high drug loading with biologics for controlled release applications, *Eur. Polym. J.* 147 (2021) 110286.
- [11] Z. Zhang, C. He, X. Chen, Hydrogels based on pH-responsive reversible carbon–nitrogen double-bond linkages for biomedical applications, *Mater. Chem. Front.* 2 (2018) 1765–1778.

- [12] J. Kalia, R.T. Raines, Hydrolytic stability of hydrazones and oximes, *Angew. Chem., Int. Ed. Engl.* 47 (2008) 7523–7526.
- [13] H. Jiang, S. Qin, H. Dong, Q. Lei, X. Su, R. Zhuo, Z. Zhong, An injectable and fast-degradable poly(ethylene glycol) hydrogel fabricated via bioorthogonal strain-promoted azide-alkyne cycloaddition click chemistry, *Soft Matter* 11 (2015) 6029–6036.
- [14] Q.V. Nguyen, D.P. Huynh, J.H. Park, D.S. Lee, Injectable polymeric hydrogels for the delivery of therapeutic agents: A review, *Eur. Polym. J.* 72 (2015) 602–619.
- [15] C.-C. Lin, A.T. Metters, Enhanced protein delivery from photopolymerized hydrogels using a pseudospecific metal chelating ligand, *Pharm. Res.* 23 (2006) 614–622.
- [16] Y. Liu, M. Liu, Y. Zhang, Y. Cao, R. Pei, Fabrication of injectable hydrogels via bio-orthogonal chemistry for tissue engineering, *New J. Chem.* 44 (2020) 11420–11432.
- [17] S.T. Koshy, R.M. Desai, P. Joly, J. Li, R.K. Bagrodia, S.A. Lewin, N.S. Joshi, D.J. Mooney, Click-Crosslinked Injectable Gelatin Hydrogels, *Adv. Healthcare Mater.* 5 (2016) 541–547.
- [18] D.S.B. Anugrah, M.P. Patil, X. Li, C.M.Q. Le, K. Ramesh, G.-D. Kim, K. Hyun, K.T. Lim, Click-cross-linked, doxorubicin-loaded hydrogels based on poly(styrene-alt-maleic anhydride), *eXPRESS Polym. Lett.* 14 (2020) 248–260.
- [19] A.-C. Knall, C. Slugovc, Inverse electron demand Diels-Alder (iEDDA)-initiated conjugation: a (high) potential click chemistry scheme, *Chem. Soc. Rev.* 42 (2013) 5131–5142.
- [20] W. Kang, B. Bi, R. Zhuo, X. Jiang, Photocrosslinked methacrylated carboxymethyl chitin hydrogels with tunable degradation and mechanical behavior, *Carbohydr. Polym.* 160 (2017) 18–25.
- [21] Y. Hong, H. Song, Y. Gong, Z. Mao, C. Gao, J. Shen, Covalently crosslinked chitosan hydrogel: properties of in vitro degradation and chondrocyte encapsulation, *Acta Biomater.* 3 (2007) 23–31.
- [22] W. Hennink, O. Franssen, W. van Dijk-Wolthuis, H. Talsma, Dextran hydrogels for the controlled release of proteins, *J. Controlled Release* 48 (1997) 107–114.
- [23] E.J. Oh, S.-W. Kang, B.-S. Kim, G. Jiang, I.H. Cho, S.K. Hahn, Control of the molecular degradation of hyaluronic acid hydrogels for tissue augmentation, *J. Biomed. Mater. Res., Part A* 86 (2008) 685–693.

- [24] S.J. Buwalda, T. Vermonden, W.E. Hennink, Hydrogels for Therapeutic Delivery: Current Developments and Future Directions, *Biomacromolecules* 18 (2017) 316–330.
- [25] M. Graf, C.E. Ziegler, M. Gregoritz, A.M. Goepferich, Hydrogel microspheres evading alveolar macrophages for sustained pulmonary protein delivery, *Int. J. Pharm. (Amsterdam, Neth.)* 566 (2019) 652–661.
- [26] P.J. LeValley, R. Neelarapu, B.P. Sutherland, S. Dasgupta, C.J. Kloxin, A.M. Kloxin, Photolabile Linkers: Exploiting Labile Bond Chemistry to Control Mode and Rate of Hydrogel Degradation and Protein Release, *J. Am. Chem. Soc.* 142 (2020) 4671–4679.
- [27] W.N.E. van Dijk-Wolthuis, J.A.M. Hoogeboom, M.J. van Steenberg, S.K.Y. Tsang, W.E. Hennink, Degradation and Release Behavior of Dextran-Based Hydrogels, *Macromolecules (Washington, DC, U. S.)* 30 (1997) 4639–4645.
- [28] F. Brandl, N. Hammer, T. Blunk, J. Tessmar, A. Goepferich, Biodegradable hydrogels for time-controlled release of tethered peptides or proteins, *Biomacromolecules* 11 (2010) 496–504.
- [29] F. Brandl, M. Henke, S. Rothschenk, R. Gschwind, M. Breunig, T. Blunk, J. Tessmar, A. Göpferich, Poly(Ethylene Glycol) Based Hydrogels for Intraocular Applications, *Adv. Eng. Mater.* 9 (2007) 1141–1149.
- [30] S. Kirchhof, F.P. Brandl, N. Hammer, A.M. Goepferich, Investigation of the Diels–Alder reaction as a cross-linking mechanism for degradable poly(ethylene glycol) based hydrogels, *J. Mater. Chem. B* 1 (2013) 4855.
- [31] C.E. Ziegler, M. Graf, M. Nagaoka, H. Lehr, A.M. Goepferich, In Situ Forming iEDDA Hydrogels with Tunable Gelation Time Release High-Molecular Weight Proteins in a Controlled Manner over an Extended Time, *Biomacromolecules* (2021).
- [32] O.A. Mukhina, D.M. Kuznetsov, T.M. Cowger, A.G. Kutateladze, Amino Azaxylylenes Photogenerated from o-Amido Imines: Photoassisted Access to Complex Spiro-Poly-Heterocycles, *Angew. Chem., Int. Ed. Engl.* 54 (2015) 11516–11520.
- [33] O.A. Mukhina, N.N.B. Kumar, T.M. Arisco, R.A. Valiulin, G.A. Metzger, A.G. Kutateladze, Rapid photoassisted access to N,O,S-polyheterocycles with benzoazocine and hydroquinoline cores: intramolecular cycloadditions of photogenerated azaxylylenes, *Angew. Chem., Int. Ed. Engl.* 50 (2011) 9423–9428.

- [34] N. Peppas, Hydrogels in pharmaceutical formulations, *Eur. J. Pharm. Biopharm.* 50 (2000) 27–46.
- [35] P.J. Flory, Principles of polymer chemistry, 10th edn ed., Cornell Univ. Press, Ithaca, N. Y., Ithaca, N. Y., 1953.
- [36] J.C. Bray, E.W. Merrill, Poly(vinyl alcohol) hydrogels. Formation by electron beam irradiation of aqueous solutions and subsequent crystallization, *J. Appl. Polym. Sci.* 17 (1973) 3779–3794.
- [37] D.L. Elbert, A.B. Pratt, M.P. Lutolf, S. Halstenberg, J.A. Hubbell, Protein delivery from materials formed by self-selective conjugate addition reactions, *J. Controlled Release* 76 (2001) 11–25.
- [38] N.A. Peppas, E.W. Merrill, Crosslinked poly(vinyl alcohol) hydrogels as swollen elastic networks, *J. Appl. Polym. Sci.* 21 (1977) 1763–1770.
- [39] E. MERRILL, K. DENNISON, C. SUNG, Partitioning and diffusion of solutes in hydrogels of poly(ethylene oxide), *Biomaterials* 14 (1993) 1117–1126.
- [40] T. Canal, N.A. Peppas, Correlation between mesh size and equilibrium degree of swelling of polymeric networks, *J. Biomed. Mater. Res.* 23 (1989) 1183–1193.
- [41] G.P. Raeber, M.P. Lutolf, J.A. Hubbell, Molecularly engineered PEG hydrogels: a novel model system for proteolytically mediated cell migration, *Biophys. J.* 89 (2005) 1374–1388.
- [42] M. Gregoritz, V. Messmann, K. Abstiens, F.P. Brandl, A.M. Goepferich, Controlled Antibody Release from Degradable Thermoresponsive Hydrogels Cross-Linked by Diels-Alder Chemistry, *Biomacromolecules* 18 (2017) 2410–2418.
- [43] F. van de Manakker, M. van der Pot, T. Vermonden, C.F. van Nostrum, W.E. Hennink, Self-Assembling Hydrogels Based on β -Cyclodextrin/Cholesterol Inclusion Complexes, *Macromolecules* (Washington, DC, U. S.) 41 (2008) 1766–1773.
- [44] N. Hammer, F.P. Brandl, S. Kirchhof, A.M. Goepferich, Cleavable carbamate linkers for controlled protein delivery from hydrogels, *J. Controlled Release* 183 (2014) 67–76.
- [45] A.K. Ghosh, M. Brindisi, Organic carbamates in drug design and medicinal chemistry, *J. Med. Chem.* 58 (2015) 2895–2940.

- [46] D. Aydin, M. Arslan, A. Sanyal, R. Sanyal, Hooked on Cryogels: A Carbamate Linker Based Depot for Slow Drug Release, *Bioconjugate Chem.* 28 (2017) 1443–1451.
- [47] J.L. Dávila, M.A. d'Ávila, Laponite as a rheology modifier of alginate solutions: Physical gelation and aging evolution, *Carbohydr. Polym.* 157 (2017) 1–8.
- [48] W.F. Diller, Pathogenesis of phosgene poisoning, *Toxicol. Ind. Health* 1 (1985) 7–15.
- [49] M.A. Mehlman, Health Effects and Toxicity of Phosgene Scientific Review, *Def. Sci. J.* 37 (1987) 269–279.
- [50] T.M. O'Shea, A.A. Aimetti, E. Kim, V. Yesilyurt, R. Langer, Synthesis and characterization of a library of in-situ curing, nonswelling ethoxylated polyol thiol-ene hydrogels for tailorable macromolecule delivery, *Adv. Mater.* 27 (2015) 65–72.
- [51] S. Kirchhof, M. Gregoritz, V. Messmann, N. Hammer, A.M. Goepferich, F.P. Brandl, Diels-Alder hydrogels with enhanced stability: First step toward controlled release of bevacizumab, *Eur. J. Pharm. Biopharm.* 96 (2015) 217–225.
- [52] M. Gregoritz, V. Messmann, A.M. Goepferich, F.P. Brandl, Design of hydrogels for delayed antibody release utilizing hydrophobic association and Diels–Alder chemistry in tandem, *J. Mater. Chem. B* 4 (2016) 3398–3408.
- [53] A.-C. Albertsson, M. Eklund, Influence of molecular structure on the degradation mechanism of degradable polymers: In vitro degradation of poly(trimethylene carbonate), poly(trimethylene carbonate-co-caprolactone), and poly(adipic anhydride), *J. Appl. Polym. Sci.* 57 (1995) 87–103.
- [54] I. Lee, C.K. Kim, B.C. Lee, Theoretical studies on the acid hydrolysis of methyl carbamate, *J. Comput. Chem.* 8 (1987) 794–800.
- [55] C.M. Comisar, S.E. Hunter, A. Walton, P.E. Savage, Effect of pH on Ether, Ester, and Carbonate Hydrolysis in High-Temperature Water, *Ind. Eng. Chem. Res.* 47 (2008) 577–584.
- [56] A.F. Hegarty, L.N. Frost, Elimination–addition mechanism for the hydrolysis of carbamates. Trapping of an isocyanate intermediate by an o-amino-group, *J. Chem. Soc., Perkin Trans. 2* (1972-1999) (1973) 1719–1728.
- [57] J. Hansen, N. Mørk, H. Bundgaard, Phenyl carbamates of amino acids as prodrug forms for protecting phenols against first-pass metabolism, *Int. J. Pharm. (Amsterdam, Neth.)* 81 (1992) 253–261.

- [58] M. Gregoritz, K. Abstiens, M. Graf, A.M. Goepferich, Fabrication of antibody-loaded microgels using microfluidics and thiol-ene photoclick chemistry, *Eur. J. Pharm. Biopharm.* 127 (2018) 194–203.
- [59] X. Tong, S. Lee, L. Bararpour, F. Yang, Long-Term Controlled Protein Release from Poly(Ethylene Glycol) Hydrogels by Modulating Mesh Size and Degradation, *Macromol. Biosci.* 15 (2015) 1679–1686.
- [60] F. Brandl, F. Kastner, R.M. Gschwind, T. Blunk, J. Tessmar, A. Göpferich, Hydrogel-based drug delivery systems: comparison of drug diffusivity and release kinetics, *J. Controlled Release* 142 (2010) 221–228.
- [61] J. Li, D.J. Mooney, Designing hydrogels for controlled drug delivery, *Nat. Rev. Mater.* 1 (2016).
- [62] P. Kurtzhals, C. Larsen, M. Johansen, High-performance size-exclusion chromatographic procedure for the determination of fluoresceinyl isothiocyanate dextrans of various molecular masses in biological media, *J. Chromatogr., Biomed. Appl.* 491 (1989) 117–127.
- [63] U. Bhardwaj, R. Sura, F. Papadimitrakopoulos, D.J. Burgess, PLGA/PVA hydrogel composites for long-term inflammation control following s.c. implantation, *Int. J. Pharm. (Amsterdam, Neth.)* 384 (2010) 78–86.
- [64] Q. Peng, X. Sun, T. Gong, C.-Y. Wu, T. Zhang, J. Tan, Z.-R. Zhang, Injectable and biodegradable thermosensitive hydrogels loaded with PHBHHx nanoparticles for the sustained and controlled release of insulin, *Acta Biomater.* 9 (2013) 5063–5069.
- [65] V. Huynh, R.G. Wylie, Competitive Affinity Release for Long-Term Delivery of Antibodies from Hydrogels, *Angew. Chem., Int. Ed. Engl.* 57 (2018) 3406–3410.
- [66] K.W. Lee, J.J. Yoon, J.H. Lee, S.Y. Kim, H.J. Jung, S.J. Kim, J.W. Joh, H.H. Lee, D.S. Lee, S.K. Lee, Sustained release of vascular endothelial growth factor from calcium-induced alginate hydrogels reinforced by heparin and chitosan, *Transplant. Proc.* 36 (2004) 2464–2465.
- [67] K. Vulic, M.S. Shoichet, Tunable growth factor delivery from injectable hydrogels for tissue engineering, *J. Am. Chem. Soc.* 134 (2012) 882–885.

- [68] K. Xu, F. Lee, S. Gao, M.-H. Tan, M. Kurisawa, Hyaluronidase-incorporated hyaluronic acid-tyramine hydrogels for the sustained release of trastuzumab, *J. Controlled Release* 216 (2015) 47–55.
- [69] D.F. Martin, M.G. Maguire, G. Ying, J.E. Grunwald, S.L. Fine, G.J. Jaffe, Ranibizumab and bevacizumab for neovascular age-related macular degeneration, *N. Engl. J. Med.* 364 (2011) 1897–1908.

Chapter 5 – Supporting information

Investigation of the impact of hydrolytically cleavable groups on the stability of PEG-based iEDDA hydrogels

1 Swelling and degradation studies

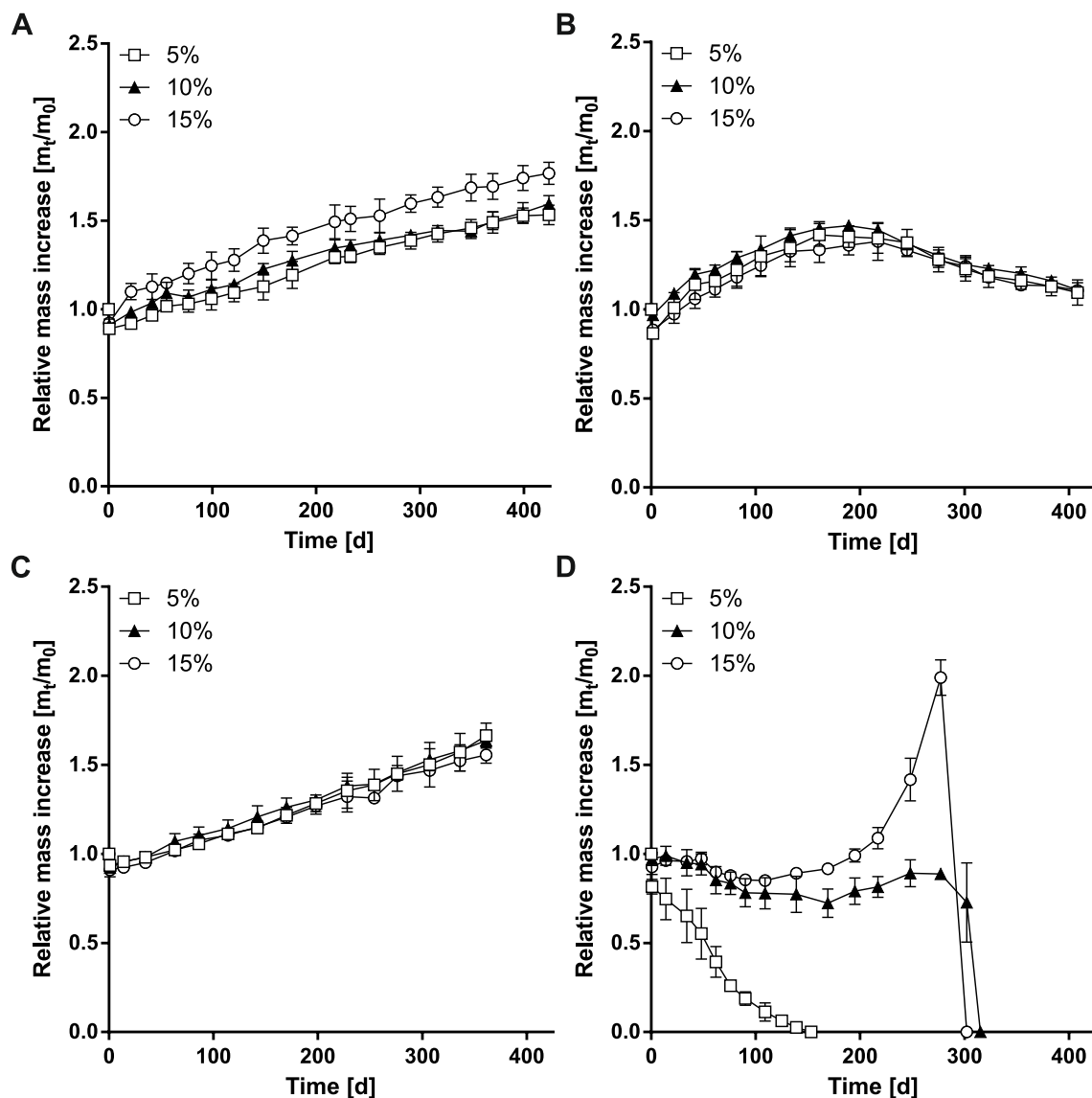
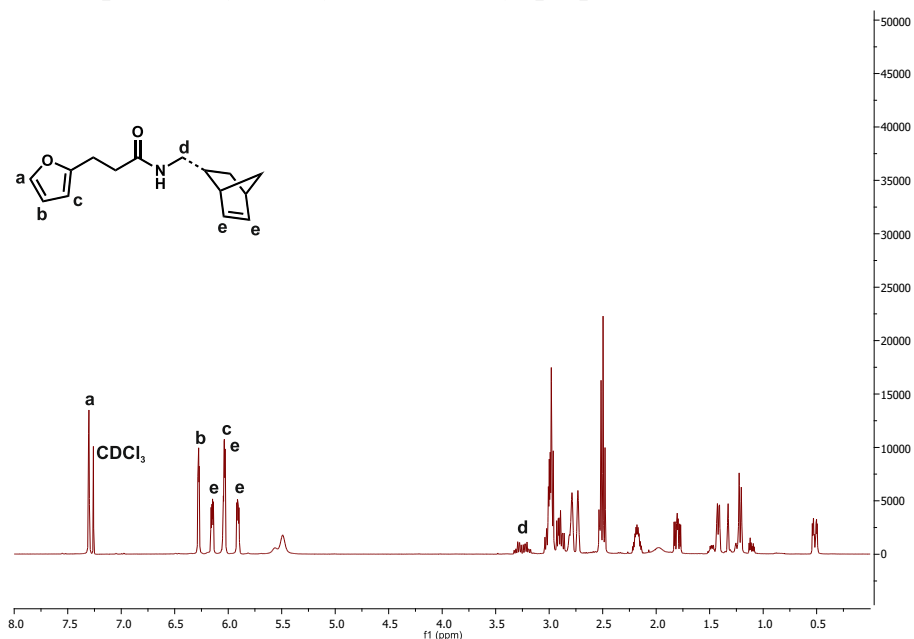
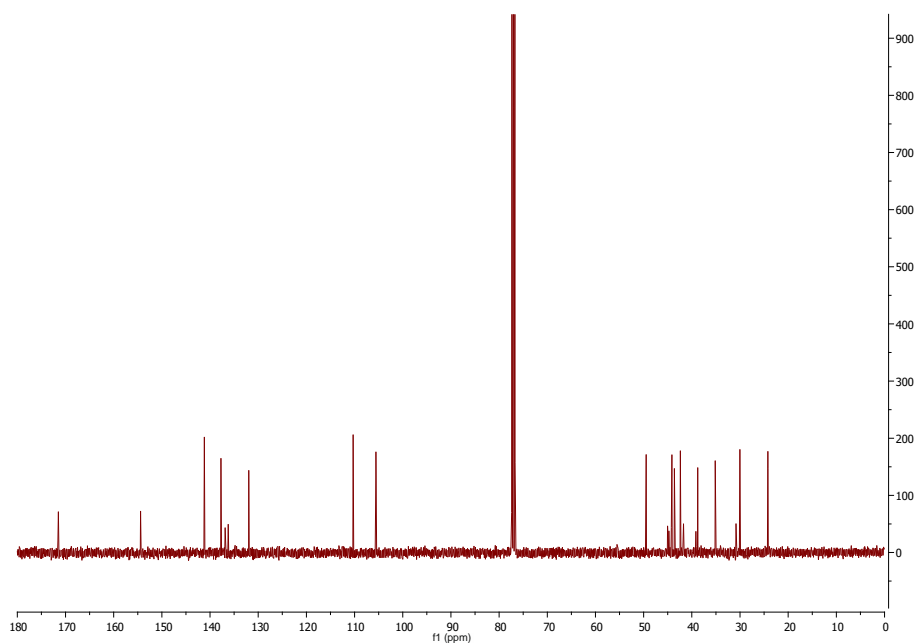


Figure S1: Swelling and degradation of 5, 10, and 15% (w/v) 8armPEG10k-hydrogels containing ETPI linker (A), carbamate linker (B), carbonate linker (C), and phenyl carbonate linker (D) in 50 mM phosphate buffer (pH 7.4) at 37 °C.

2 Spectroscopic data

N-((bicyclo[2.2.1]hept-5-en-2-yl)methyl)-3-(furan-2-yl)propenamide**Figure S2:** ^1H NMR spectrum of *N*-((bicyclo[2.2.1]hept-5-en-2-yl)methyl)-3-(furan-2-yl)propenamide

^1H NMR (CDCl_3 , 400 MHz): δ (ppm) = 3.23 (m, 2H, $-\text{HNCH}_2\text{CHR}_2-$), 5.91–6.15 (m, 2H, $-\text{HC}=\text{CH}-$, *endo* and *exo*), 6.04 (m, 1H, Ar), 6.28 (m, 1H, Ar), 7.30 (m, 1H, Ar).

**Figure S3:** ^{13}C NMR spectrum of *N*-((bicyclo[2.2.1]hept-5-en-2-yl)methyl)-3-(furan-2-yl)propenamide

^{13}C NMR (CDCl_3 , 100 MHz): δ (ppm) = 24.34, 30.15, 35.27, 38.91, 42.50, 43.75, 44.27, 49.61, 105.71, 110.44, 132.09, 137.86, 141.31, 154.55, 171.61

8armPEG10k-ETPI-Nb

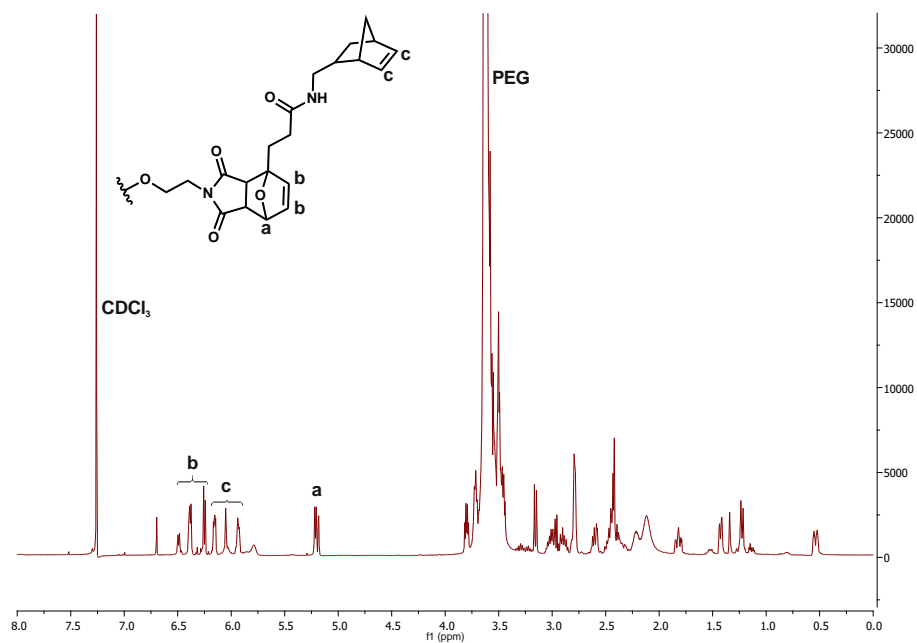
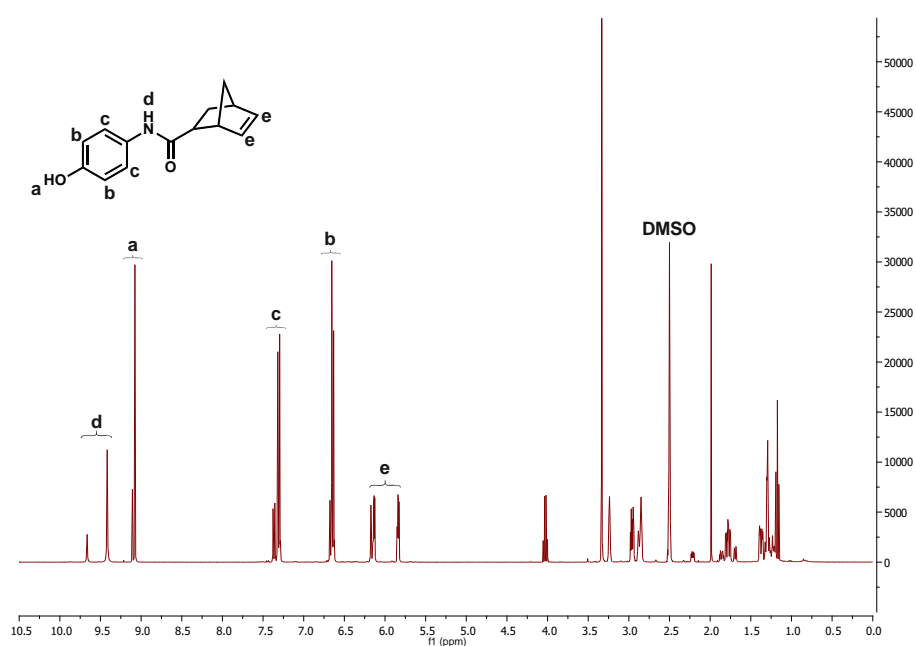
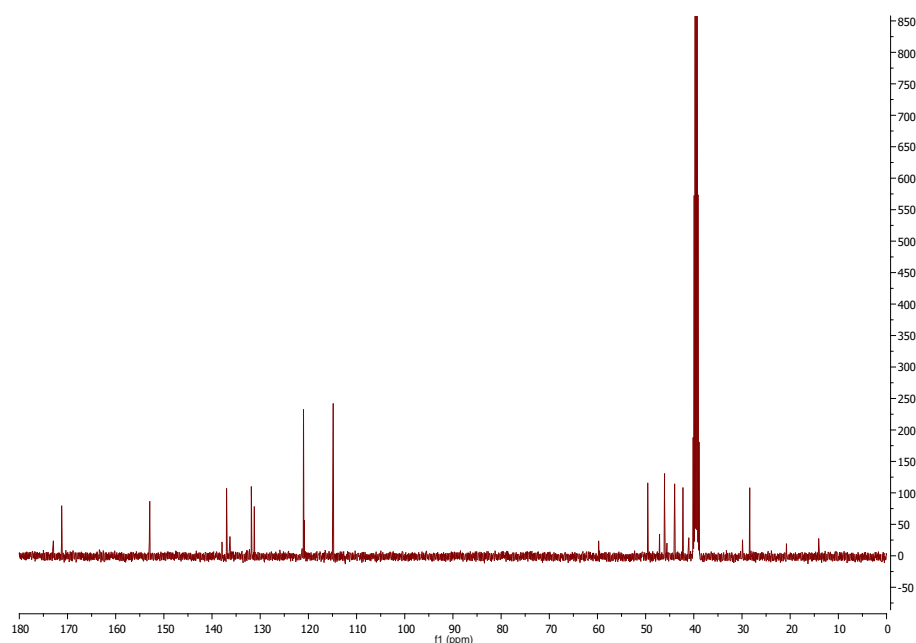


Figure S4: ¹H NMR spectrum of 8armPEG10k-ETPI-Nb

¹H NMR (CDCl₃, 400 MHz): δ (ppm) = 3.63 (s, -OCH₂CH₂-), 5.18 (d, 8H, -R₂CHOCHR-, *endo*) 5.21 (d, 8H, -R₂CHOCHR-, *exo*), 5.93 (m, 8H, -HC=CH-, *endo*), 6.05 (m, 16H, -HC=CH-, *exo*), 6.16 (m, 8H, -HC=CH-, *endo*), 6.24–6.50 (16H, -CH=CH-, *endo* and *exo*).

***N*-(4-hydroxyphenyl)bicyclo[2.2.1]hept-5-ene-2-carboxamide****Figure S5:** ^1H NMR spectrum of *N*-(4-hydroxyphenyl)bicyclo[2.2.1]hept-5-ene-2-carboxamide

^1H NMR (DMSO, 400 MHz): δ (ppm) = 5.83 (m, 1H, $-\text{HC}=\text{CH}-$, *endo*), 6.13 (m, 1H, $-\text{HC}=\text{CH}-$, *endo*), 6.17 (m, 2H, $-\text{HC}=\text{CH}-$, *exo*), 6.61–6.67 (m, 2H, Ar, *endo* and *exo*), 7.28–7.37 (m, 2H, Ar, *endo* and *exo*), 9.07 (s, 1H, HOAr, *endo*), 9.10 (s, 1H, HOAr, *exo*), 9.41 (s, 1H, $-\text{C}(\text{O})\text{NHAr}$, *endo*), 9.65 (s, 1H, $-\text{C}(\text{O})\text{NHAr}$, *exo*).

**Figure S6:** ^{13}C NMR spectrum of *N*-(4-hydroxyphenyl)bicyclo[2.2.1]hept-5-ene-2-carboxamide

^{13}C NMR (DMSO, 100 MHz): δ (ppm) = 28.39, 29.90, 41.05, 42.26, 43.88, 43.98, 45.57, 46.08, 47.11, 49.57, 114.86, 114.95, 120.83, 121.01, 131.23, 131.85, 136.28, 136.98, 137.92, 152.93, 171.22, 172.93

4-(bicyclo[2.2.1]hept-5-ene-2-carboxamido)phenyl (2,5-dioxopyrrolidin-1-yl) carbonate

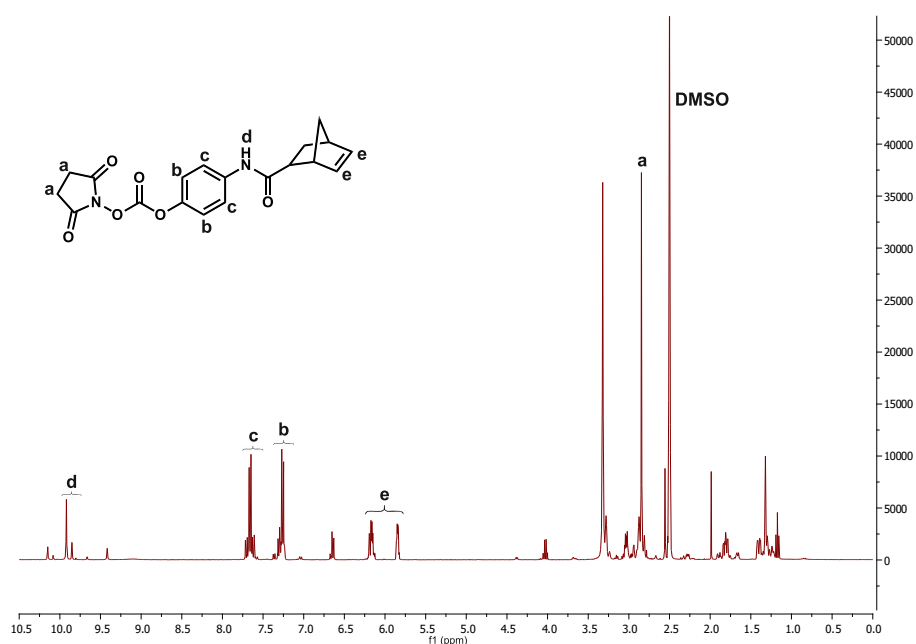


Figure S7: ¹H NMR spectrum of 4-(bicyclo[2.2.1]hept-5-ene-2-carboxamido)phenyl (2,5-dioxopyrrolidin-1-yl) carbonate

¹H NMR (DMSO, 400 MHz): δ (ppm) = 2.85 (s, 4H, (O)CCH₂CH₂C(O)), 5.85 (m, 1H, –HC=CH–, *endo*), 6.16 (m, 1H, –HC=CH–, *endo*), 6.19 (m, 2H, –HC=CH–, *exo*), 7.24–7.32 (m, 2H, Ar, *endo* and *exo*), 7.61–7.72 (m, 2H, Ar, *endo* and *exo*), 9.85 (s, 1H, (O)CNHAr), 9.92 (s, 1H, (O)CNHAr).

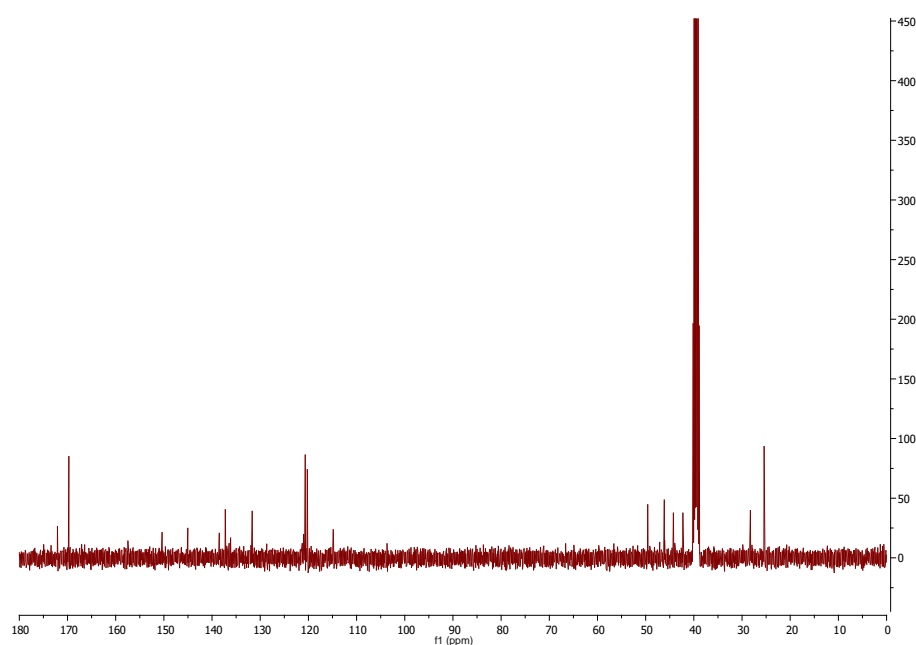
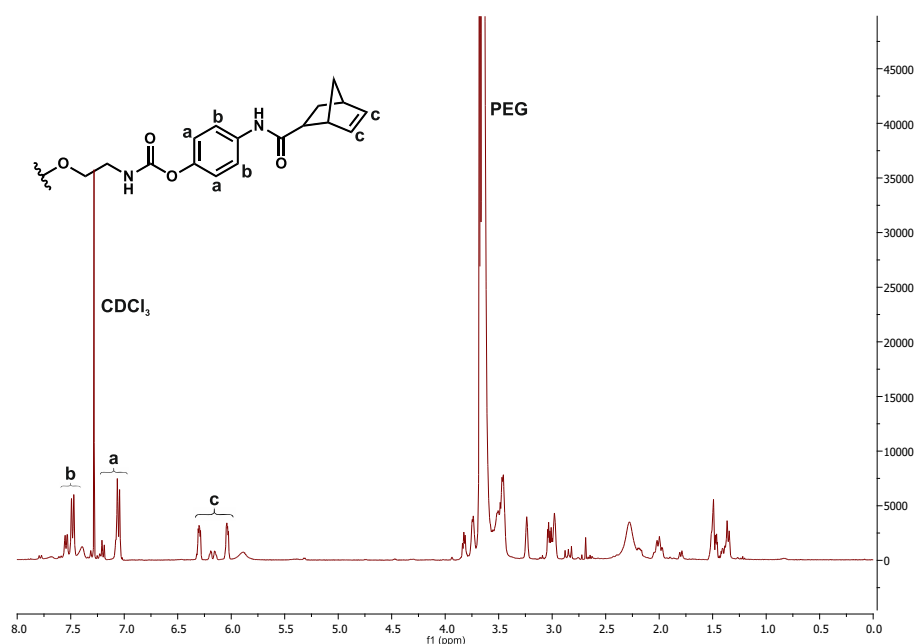
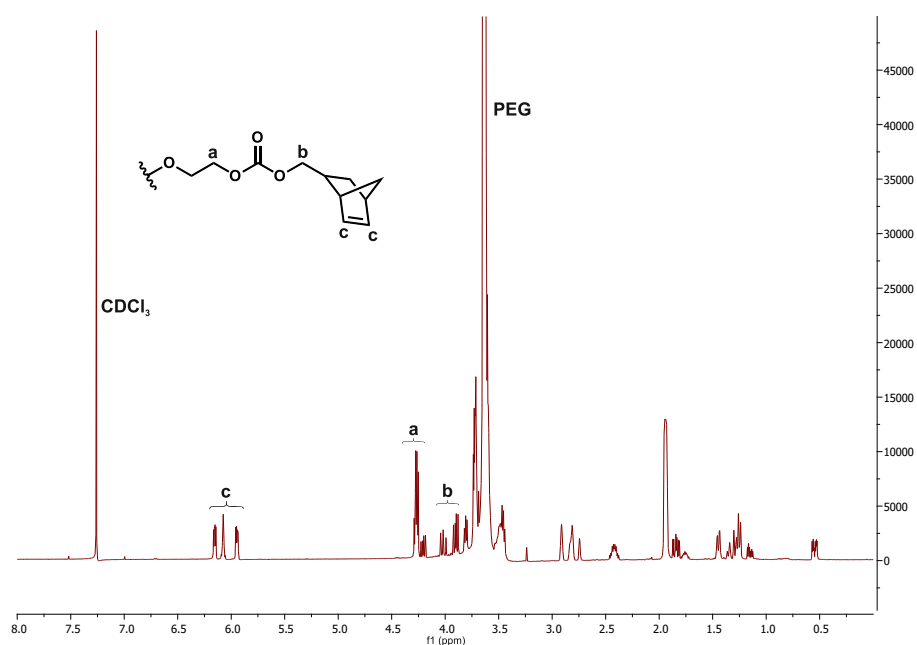


Figure S8: ¹³C NMR spectrum of N-(4-hydroxyphenyl)bicyclo[2.2.1]hept-5-ene-2-carboxamide

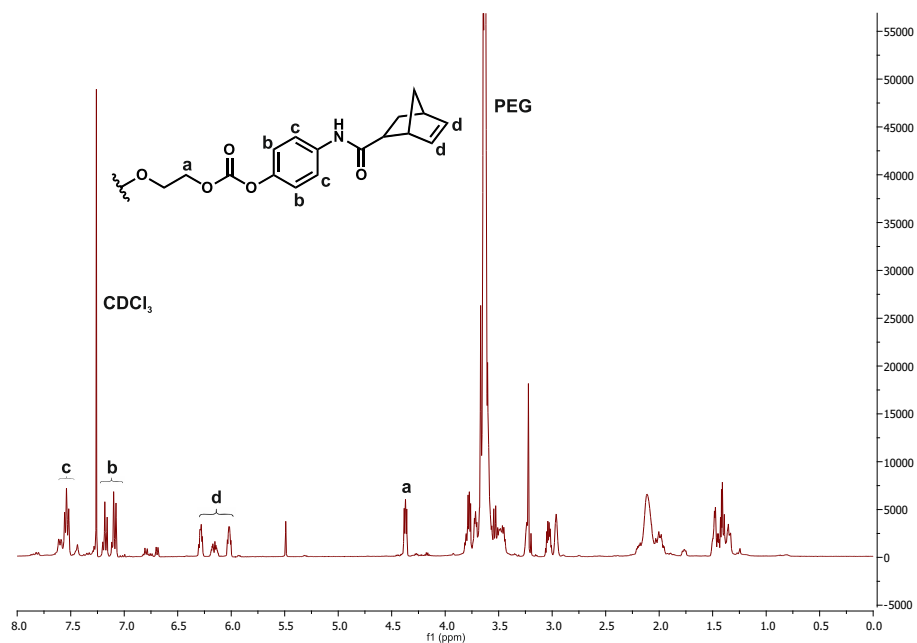
¹³C NMR (DMSO, 100 MHz): δ (ppm) = 25.42, 28.26, 42.28, 44.25, 46.13, 49.57, 114.85, 120.22, 120.66, 131.67, 137.24, 145.04, 150.36, 169.73, 172.08

8armPEG10k-carbamate-Nb**Figure S9:** ^1H NMR spectrum of 8armPEG10k-carbamate-Nb

^1H NMR (CDCl_3 , 400 MHz): δ (ppm) = 3.63 (s, $-\text{OCH}_2\text{CH}_2\text{O}-$), 6.01 (m, 8H, $-\text{HC}=\text{CH}-$, *endo*), 6.13 (m, 8H, $-\text{HC}=\text{CH}-$, *exo*), 6.16 (m, 8H, $-\text{HC}=\text{CH}-$, *exo*), 6.28 (m, 8H, $-\text{HC}=\text{CH}-$, *endo*), 7.02–7.19 (16H, Ar), 7.45–7.53 (16H, Ar).

8armPEG10k-carbonate-Nb**Figure S10:** ^1H NMR spectrum of 8armPEG10k-carbonate-Nb

^1H NMR (CDCl_3 , 400 MHz): δ (ppm) = 3.65 (s, $-\text{OCH}_2\text{CH}_2\text{O}-$), 3.88–4.04 (m, 16H, $-\text{OCH}_2\text{CHR}_2-$), 4.18–4.29 (16H, $-\text{OCH}_2\text{CH}_2\text{O}-$), 5.95 (m, 8H, $-\text{HC}=\text{CH}-$, *endo*), 6.07 (m, 16H, $-\text{HC}=\text{CH}-$, *exo*), 6.15 (m, 8H, $-\text{HC}=\text{CH}-$, *endo*).

8armPEG10k-phenyl carbonate-Nb**Figure S11:** ¹H NMR spectrum of 8armPEG10k-phenyl carbonate-Nb

¹H NMR (CDCl₃, 400 MHz): δ (ppm) = 3.63 (s, -OCH₂CH₂O-), 4.37 (m, 16H, -OCH₂CH₂O-), 6.02 (m, 8H, -HC=CH-, *endo*), 6.14 (m, 8H, -HC=CH-, *exo*), 6.17 (m, 8H, -HC=CH-, *exo*), 6.29 (m, 8H, -HC=CH-, *endo*), 7.08-7.20 (16H, Ar), 7.52-7.61 (16H, Ar).

Chapter 6

Injectable anhydrous PEG polymer liquids form protein depot for extended controlled release applications via rapid in situ gelation

To be submitted to a peer-reviewed journal

Abstract

Water-free preparation of protein delivery systems has the potential to overcome limitations of hydrogel depot systems such as off-target reactions, functional group hydrolysis, and limited loading capacity. However, a major roadblock in the development and use of these systems is administration as implantation is often required. In this study, we developed a biodegradable and water-free injectable protein delivery system via inverse electron demand Diels-Alder reaction between norbornene- and tetrazine-functionalized four-armed poly(ethylene glycol) macromonomers. 1:1 mixtures of these precursors gelled rapidly *in situ*, taking less than 11 s to reach their gelation point. Methyl substitution of tetrazine slowed the gelation time and increased the cross-linking density, whereas oxygen incorporation into norbornene changed the mechanical properties. Introduction of hydrolytically cleavable groups enabled biodegradability. Using carbamate and phenyl carbonate ester groups, we could tune the stability. Controlled release of the protein surrogate glucose oxidase was achieved over a period of 500 days. The novel preparation method presented here is a promising step towards the development of water-free injectable protein depots for controlled drug delivery.

1 Introduction

Hydrogels play a major role in the field of drug delivery. The large number of research papers published shows how much research effort has been devoted to the topic in recent years [1–3]. In this context, delivery over an extended time is possible primarily with hydrogels, which exert chemically covalent cross-links and, thus, exhibit higher stability [4,5]. However, polymerization in aqueous environments presents hurdles in the drug delivery system design process. For example, hydrolysis-prone functional groups, such as maleimide or tetrazine, degrade to form unreactive species, which negatively affect the cross-linking density and release kinetics [6,7]. In addition, water-based systems have limited drug loading capacity [8]. Increasing the amount of drug often leads to faster and less controlled release. Another issue is off-target reactions that can occur between precursor functional groups and the drug being loaded into the gel. This is particularly relevant when the drug is a protein, which can have many different reactive moieties [9,10]. Unintentional covalent tethering between the drug and the hydrogel matrix compromises chemical integrity and drug release [11].

Fortunately, these obstacles can be overcome using water-free hydrogel preparation [12]. For this approach, blends of furan- and maleimide-modified eight-armed poly(ethylene glycol) (PEG) precursors were heated above their respective melting points. The molten macromonomers gained sufficient mobility to undergo a Diels-Alder (DA) reaction and form a three-dimensional network. While these systems showed extremely promising results with regard to functional group stability, off-target interactions, drug loading capacity, and controlled protein release over 100 days, the *in vivo* administration represents a major drawback. Because the DA reaction is slow and the macromonomers used have melting points above body temperature, *in situ* gelation and, therefore, direct injection into the organism is precluded. Instead, the gels must be implanted.

To overcome this limitation, the inverse electron demand Diels-Alder (iEDDA) reaction between norbornene and tetrazine can be used. Besides high reaction kinetics, this cross-linking reaction excels in terms of efficiency, stability, and bioorthogonality without losing the benefits of the classical DA reaction such as not requiring a catalyst and avoiding the formation of toxic side products during polymerization [13–16]. Additionally, it has already been demonstrated that this reaction can be used for the preparation of water-based protein delivery systems to achieve controlled release [17,18]. However, we believe that this reaction can also benefit from water-free processing to prevent protein PEGylation via thiol-tetrazine interaction, which occurs in conventional hydrogels [19].

To avoid the issue of a melting point above body temperature, four-armed PEG macromonomers with a molecular weight of 2 kDa (4armPEG2k) instead of eight-armed PEG precursors with a molecular weight of 10 kDa (8armPEG10k) are used. These smaller macromonomers and their derivatives are liquid even at room temperature, which is a tremendous advantage for drug delivery systems since they allow for direct injection into the organism requiring only minimally invasive surgery [20]. Moreover, due to the absence of evaporating solvents, implants can also be prepared by 3D printing [21].

Kelmansky et al. have already shown that “neat biogels” can be prepared in a water-free manner through cross-linking with amine- and succinimidyl carbonate-functionalized 4armPEG2k precursors at 37 °C [22,23]. However, their material contained succinimidyl carbonate groups, that covalently bound to the tissue after injection. Such a material would also interact with amine groups from embedded protein drugs. Moreover, they did not achieve controlled protein release over long periods of time [23].

The goal of this study was to utilize our prior knowledge of melt polymerization, iEDDA reaction, and degrading linkers, to design a water-free system that forms immediately after combining two liquid polymers [12,19]. For this, norbornene- and tetrazine-functionalized 4armPEG2k macromonomers were used as polymer precursors. The cross-linking reaction was confirmed via FTIR and UV-VIS spectroscopy. Polymerization behavior was monitored using oscillatory rheology. The influence of chemical modifications of norbornene and tetrazine groups on the gelation time, complex shear modulus, and Young’s modulus of compression (compressive modulus) was analyzed. Additionally, we determined the stability of polymers containing different hydrolytically cleavable linkers. Scanning electron microscopy (SEM) was used to examine the structures of these polymers. Finally, protein delivery was assessed using the model protein glucose oxidase (GOx) to investigate the release behavior under physiological conditions.

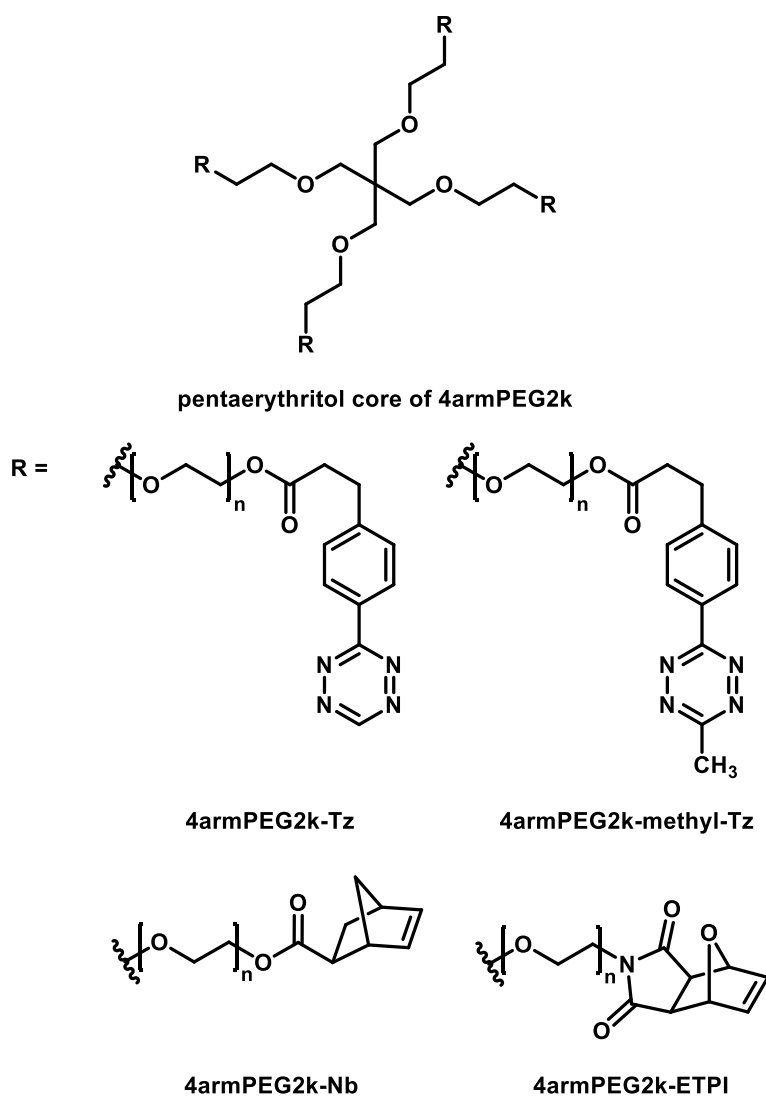
2 Materials and methods

2.1 Materials

4-Aminophenol, anhydrous acetonitrile, deuterated chloroform (CDCl₃), anhydrous dichloromethane (DCM), *N,N'*-dicyclohexylcarbodiimide, diisopropyl azodicarboxylate, anhydrous *N,N*-dimethylformamide (DMF), *N,N'*-disuccinimidyl carbonate, absolute ethanol, anhydrous ethyl acetate, glacial acetic acid, GOx (Type X-S, from *Aspergillus niger*), maleimide, hydrazine monohydrate, 5-norbornenecarboxylic acid (mixture of *endo* and *exo*), protein LoBind Eppendorf tubes, pyridine, QuantiPro™ BCA Assay Kit, sodium bicarbonate, sulfur, anhydrous tetrahydrofuran, triethylamine, and triphosgene were purchased from Sigma-Aldrich (Taufkirchen, Germany). 4armPEG2k was obtained from JenKem Technology (Allen, TX, USA). 4-Dimethylaminopyridine, phthalimide, and anhydrous sodium sulfate were received from Acros Organics (Geel, Belgium). Cyclohexane p.a., DCM p.a., and methanol p.a. were purchased from Fisher Chemical (Loughborough, UK). Diethyl ether (technical grade) was purchased from Jäcklechemie (Nuremberg, Germany). *O*-(Benzotriazol-1-yl)-*N,N,N',N'*-tetramethyluronium-hexafluorophosphat, citric acid monohydrate, hydrochloric acid, silica gel 60 (0.063–0.200 mm), sodium azide, sodium chloride, sodium dihydrogen phosphate monohydrate, sodium hydroxide, sodium nitrite, and triphenylphosphine were obtained from Merck KGaA (Darmstadt, Germany). 3-(4-Cyanophenyl)-propionic acid was obtained from abcr GmbH (Karlsruhe, Germany). 5-Norbornene-2-methanol was obtained from TCI Chemicals (Eschborn, Germany). Purified water was freshly prepared using a Milli-Q water purification system from Millipore (Schwalbach, Germany).

2.2 ^1H NMR spectroscopy

^1H NMR spectra were recorded in CDCl_3 using a Bruker Avance III 400 spectrometer (Bruker BioSpin GmbH, Rheinstetten, Germany). For calculation of end-group conversion, the integrated proton peak of the respective functional group was compared to the integrated PEG proton peak at $\delta 3.75\text{--}3.35$ ppm.



Scheme 1: Chemical structures of differently functionalized 4armPEG2k macromonomers. For simplification, 8armPEG-ETPI is only shown in *exo* position.

2.3 Synthesis of tetrazine-functionalized 4armPEG2k (4armPEG2k-Tz) (Scheme 1)

4armPEG2k-Tz was synthesized as previously described for 8armPEG10k-Tz [19]. The resulting product was purified using silica column chromatography with a mixture of methanol and DCM. The degree of end-group conversion was 90%, as determined by ^1H NMR spectroscopy.

2.4 Synthesis of methyl-tetrazine-functionalized 4armPEG2k (4armPEG2k-methyl-Tz) (Scheme 1)

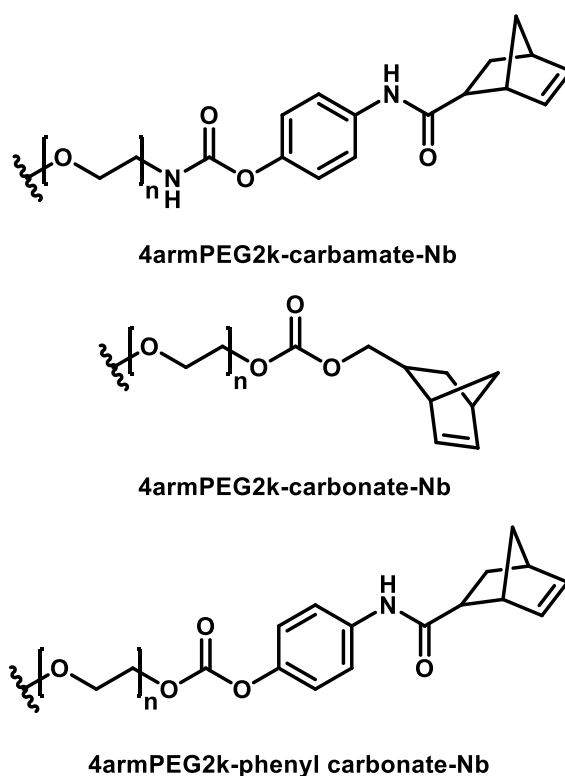
4armPEG2k-methyl-Tz was synthesized as previously described for 8armPEG10k-methyl-Tz [19]. The resulting product was purified using silica column chromatography with a mixture of methanol and DCM. The degree of end-group conversion was 95%, as determined by ^1H NMR spectroscopy.

2.5 Synthesis of norbornene-functionalized 4armPEG2k (4armPEG2k-Nb) (Scheme 1)

4armPEG2k-Nb was synthesized as previously described for 8armPEG10k-Nb [24]. The resulting product was purified using silica column chromatography with a mixture of methanol and DCM. The degree of end-group conversion was 98%, as determined by ^1H NMR spectroscopy.

2.6 Synthesis of 3,6-epoxy-1,2,3,6-tetrahydrophthalimide-substituted 4armPEG2k (4armPEG2k-ETPI) (Scheme 1)

4armPEG2k-ETPI was synthesized as previously described for 4armPEG10k-ETPI [25]. The degree of end-group conversion was 97%, as determined by ^1H NMR spectroscopy.



Scheme 2: Chemical structures of 4armPEG2k-Nb precursors containing different hydrolytically cleavable linkers.

2.7 Synthesis of 4armPEG2k-Nb precursors containing different hydrolytically cleavable linkers (Scheme 2)

4armPEG2k-amine (4armPEG2k-NH₂) was prepared according to a previously published procedure for 4armPEG10k-NH₂ [26]. 4armPEG2k-carbamate-Nb, 4armPEG2k-carbonate-Nb, and 4armPEG2k-phenyl carbonate-Nb were synthesized according to protocols for 8armPEG10k derivatives (**Chapter 5**). The degree of end-group conversion was 85% for 4armPEG2k-carbamate-Nb, 81% for 4armPEG2k-carbonate-Nb, and 71% for 4armPEG2k-phenyl carbonate-Nb, as determined by ¹H NMR spectroscopy.

2.8 Polymer preparation

For polymer preparation, equal volumes of the functionalized macromonomers were combined and stirred until a homogeneous mixture was obtained. For example, 10 μ l of 4armPEG2k-Nb and 10 μ l of 4armPEG2k-Tz were combined. Subsequently, the polymers were allowed to gel for 1 h at 37 °C. The gelation started immediately upon stirring and formed a 4armPEG2k-polymer.

2.9 Polymer characterization

Rheological experiments were performed on a Malvern Kinexus Lab+ rheometer (Malvern, Kassel, Germany) with an 8 mm parallel plate geometry, a shear strain of 1%, and an oscillation frequency of 1.0 Hz. After casting 10 μ l of each precursor liquid onto the lower plate, the mixture was stirred. Afterwards, the upper plate was lowered to a gap size of 500 μ m, and the experiment was started. Storage (G'), loss (G''), and complex shear modulus (G^*) were measured as a function of time at 37 °C. The cross-over point of G' and G'' was regarded as gel point. The absolute value of G^* ($|G^*|$) was determined after 1 h.

To determine the compressive modulus, 4armPEG2k-polymers were prepared in a cylindrical shape. For example, 10 μ l 4armPEG2k-Nb and 10 μ l 4armPEG2k-Tz were casted into a silicone mold with a diameter of 5 mm and mixed. Polymerization was carried out at 37 °C for 1 h. Afterwards, polymer diameter and height were measured using a caliper, and the polymer cylinders were placed onto the lower plate of an Instron 5542 materials testing machine (Norwood, MA, USA). The polymers were compressed uniaxially at a speed of 1 mm/min. Compressive force (N) and compressive strain (%) were recorded as a function of time. The compressive modulus was calculated from the linear part of the curve between 10 and 20% compression.

2.10 FTIR spectroscopy

FTIR-spectra of 4armPEG2k-Nb, 4armPEG2k-Tz, and 4armPEG2k-polymer were recorded using an Agilent Cary 630 FTIR (Agilent Technologies, Santa Clara, USA).

2.11 UV-VIS spectroscopy

Polymerization was monitored by UV-VIS spectroscopy. A mixture of 4armPEG2k-Nb and 4armPEG2k-methyl-Tz was placed on an LVis plate, and UV-VIS spectra were recorded over a time of 1 h on a microplate reader (all BMG Labtech, Ortenberg, Germany).

2.12 Scanning electron microscopy (SEM)

The structures of polymers prepared with 4armPEG2k-Nb and 4armPEG2k-Tz, 4armPEG2k-Nb and 4armPEG2k-methyl-Tz, and 4armPEG2k-ETPI and 4armPEG2k-Tz were imaged using a Zeiss SEM EVO MA 10 (Carl Zeiss Microscopy GmbH, Jena, Germany).

2.13 Swelling and degradation studies

Swelling and degradation studies were performed in 50 mM phosphate buffer (pH 7.4) with 0.02% sodium azide at 37 °C in a shaking water bath as previously described [12]. Polymers prepared with 10 µl 4armPEG2k-Nb and 10 µl 4armPEG2k-Tz were weighed after cross-linking to determine the exact mass. Subsequently, they were incubated in 5 ml buffer. At predetermined time points, the polymers were separated from the buffer, weighed, and incubated in 5 ml fresh buffer.

2.14 Release of GOx

For the GOx release experiment, 4armPEG2k-polymers containing approximately 1 mg GOx were prepared. For this, 4 mg GOx was mixed with 38 µl 4armPEG2k-Nb. Subsequently, 9.5 µl of this mixture was combined with 9.5 µl of 4armPEG2k-Tz and mixed again. Polymerization took place at 37 °C for 1 h. The polymers were transferred into 5 ml LoBind Eppendorf tubes and incubated in 5 ml 50 mM phosphate buffer (pH 7.4) with 0.02% sodium azide. The release experiments were performed in a shaking water bath at 37 °C. At regular time points, 300 µl samples were withdrawn and replaced with an equal volume of fresh buffer. The GOx concentration was quantified using a BCA assay.

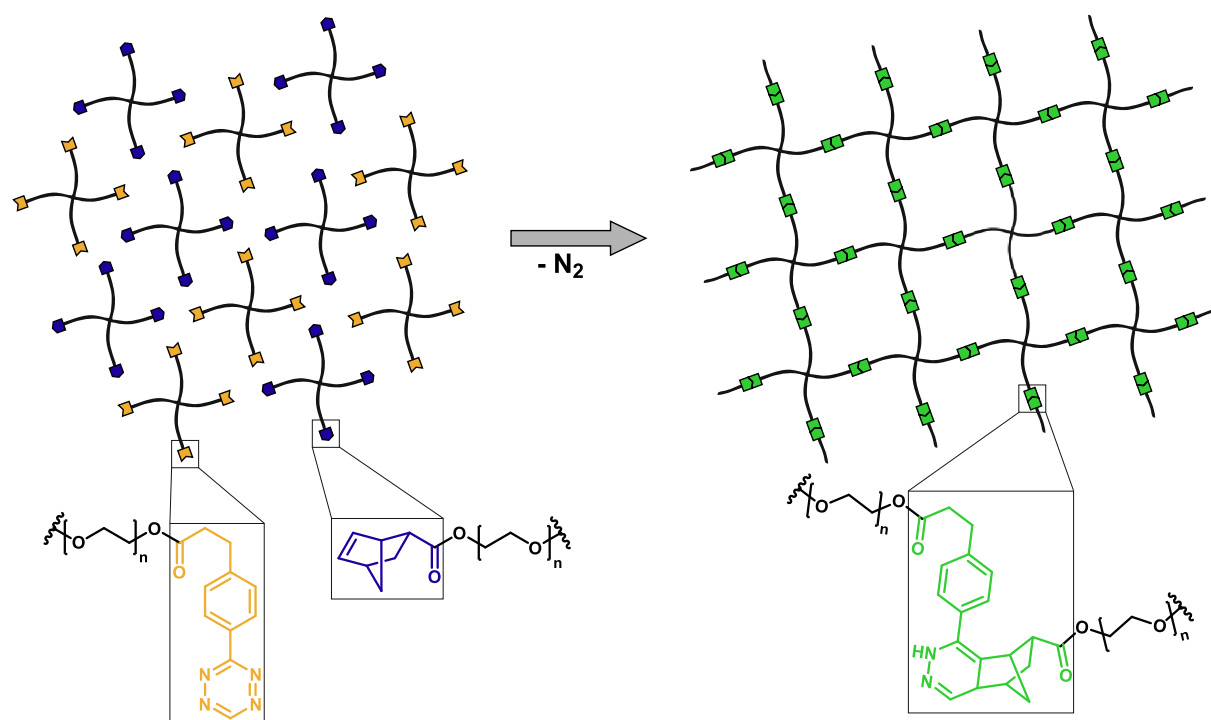
2.15 Statistical analysis

All experiments were performed with at least three samples, and the results are shown as

mean \pm standard deviation. Statistical significance was assessed using one-way ANOVA. Post hoc analysis was determined by Tukey's test (GraphPad Prism 6.0, GraphPad Software Inc., La Jolla, CA, USA).

3 Results and discussion

The goal of this study was to develop a water-free injectable hydrogel that forms a three-dimensional network via rapid *in situ* gelation for the controlled release of therapeutic proteins. We decided to introduce norbornene and tetrazine groups, which undergo rapid iEDDA reaction, into 4armPEG2k precursors, which are liquid even at room temperature, to create an injectable system. All polymer precursor syntheses had high end-group conversion, with values of at least 90% (Scheme 1), which is comparable to other multi-armed PEG modifications [27–29].



Scheme 3: Solvent-free polymerization via iEDDA reaction between 4armPEG2k-Nb and 4armPEG2k-Tz. For simplification, only one isoform of the iEDDA adduct is shown.

3.1 Cross-linking

Mixing 4armPEG2k-Nb and 4armPEG2k-Tz resulted in immediate formation of a three-dimensional polymer network (Scheme 3). To monitor the cross-linking process, FTIR spectra of 4armPEG2k-Nb, 4armPEG2k-Tz, and 4armPEG2k-polymer were recorded (Figure 1A). Both precursors showed peaks at 2866 and 1096 cm^{-1} corresponding to PEG [30]. Additionally, the carboxyl stretching of the ester groups was detectable at 1729 cm^{-1} , indicating the successful functionalization of the 4armPEG2k

macromonomers [31]. The band for the *cis* disubstituted alkene in norbornene appeared at 712 cm^{-1} (4armPEG2k-Nb) [32], and the band for the tetrazine ring was at 1349 cm^{-1} (4armPEG2k-Tz) [33]. Besides the characteristic bands of PEG and ester groups, the FTIR spectrum of the 4armPEG2k-polymer displayed decreases of the specific peaks attributed to norbornene and tetrazine, proving polymerization via iEDDA reaction.

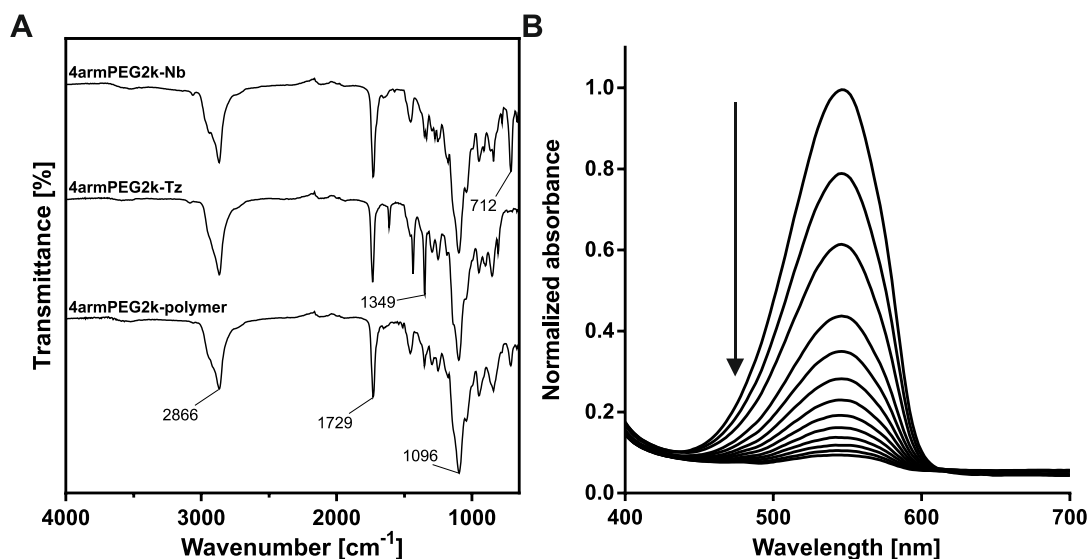


Figure 1: FTIR spectra of 4armPEG2k-Nb, 4armPEG2k-Tz, and 4armPEG2k-polymer, which was prepared via iEDDA reaction at $37\text{ }^{\circ}\text{C}$ for 1 h (A). UV-VIS spectra during the polymerization of 4armPEG2k-Nb and 4armPEG2k-methyl-Tz via iEDDA reaction (B). UV-VIS spectra were recorded in 5 min intervals for 1 h. The arrow indicates the reaction course.

Polymerization via iEDDA reaction can also be monitored by UV-VIS spectroscopy, since the pink color of the tetrazine disappears during the cross-linking reaction [34]. UV-VIS spectra of a mixture of 4armPEG2k-Nb and 4armPEG2k-methyl-Tz were recorded in the range of 350–800 nm (Figure 1B). Measurements were made in 5 min intervals for 1 h. Methyl-substituted tetrazine is known to react more slowly than unsubstituted tetrazine due to increased electron density and steric hindrance [7]. Therefore, 4armPEG2k-methyl-Tz was used as the precursor to capture the reaction progress more clearly. Initially, the mixture showed a peak at 546 nm, indicating the presence of tetrazine [35]. Over time, consumption of tetrazine via reaction with norbornene led to a gradual reduction in absorbance. After 1 h, the polymerization was considered complete as no further decrease was apparent. In summary, FTIR and UV-VIS spectroscopy confirmed the iEDDA reaction as the mechanism of cross-linking reaction for the 4armPEG2k-polymers.

3.2 Rheological characterization

Since our goal was to create an injectable, rapidly gelling, water-free protein depot system, the viscosity of 4armPEG macromonomer mixtures over time was of paramount significance. The desired viscosity profile has low viscosity initially to facilitate injection and then increased viscosity as the material

hardens and develops sufficient stiffness. To demonstrate this feature of our system, polymerization was monitored using oscillatory shear experiments.

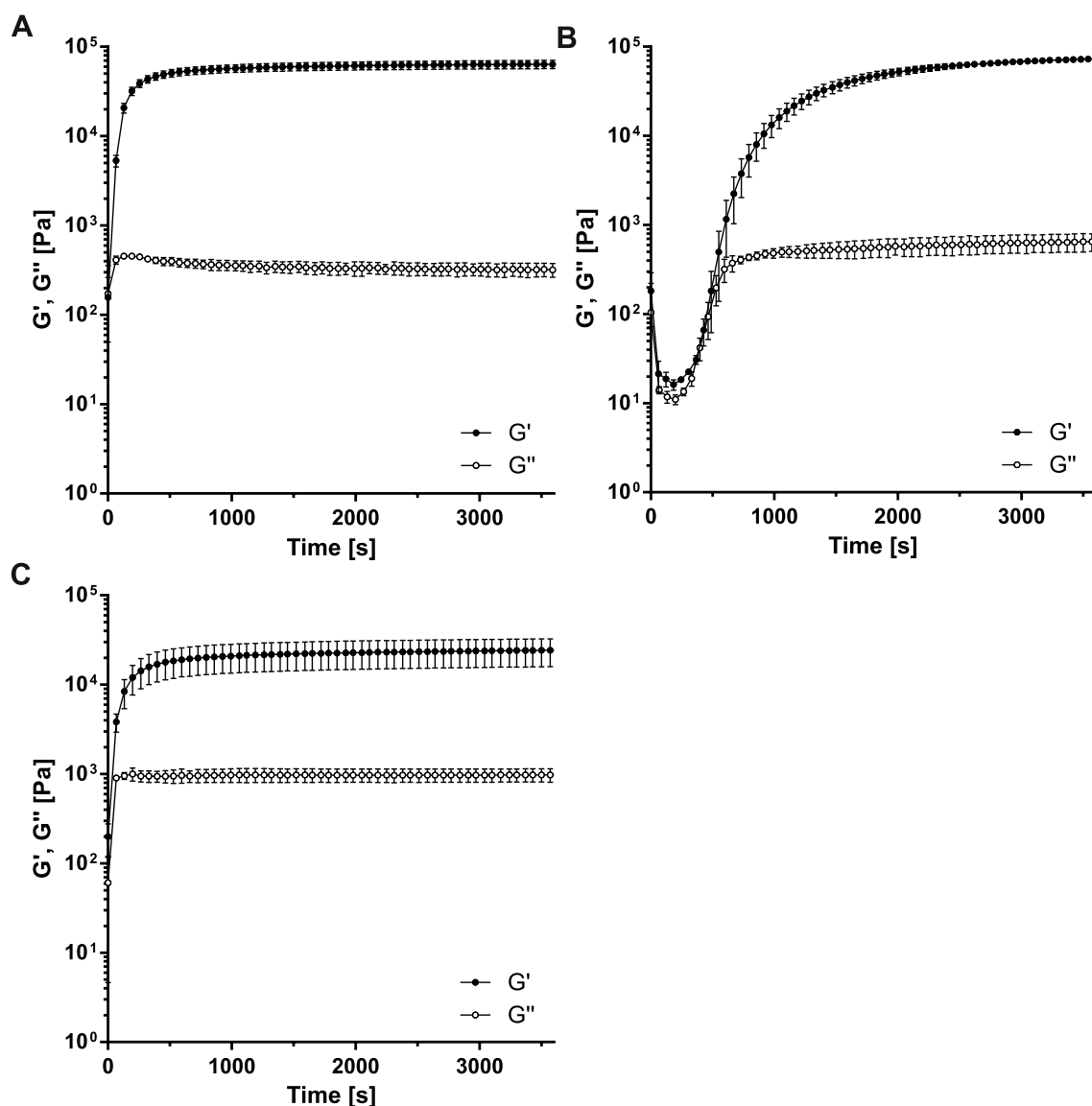


Figure 2: Rheograms of 1:1 mixtures of 4armPEG2k-Nb and 4armPEG2k-Tz (A), 4armPEG2k-Nb and 4armPEG2k-methyl-Tz (B), and 4armPEG2k-ETPI and 4armPEG2k-Tz (C). G' and G'' were measured as a function of time at 37 °C. An oscillation frequency of 1.0 Hz, an 8 mm parallel plate geometry, and a gap size of 500 μm were used for all experiments.

First, polymers consisting of 4armPEG2k-Nb and 4armPEG2k-Tz were analyzed (Figure 2A). After starting the experiment, the storage modulus (G'), which represents the elasticity of the system, immediately increased and reached a plateau after 500 s. The polymerization was considered complete at that point because only a marginal increase was observed thereafter. Next, the gel point, which is the cross-over point of G' and the loss modulus (G''), was measured to assess the time needed for *in situ* gelation. This point marks the transition from a liquid-like to a solid-like state [36]. The rapid gelation time of 10.6 ± 0.6 s (Figure 3) is sufficiently fast to assure instant embedding of proteins in a three-dimensional polymer network after injection into the organism, minimizing uncontrolled protein loss via diffusion into the surrounding tissue.

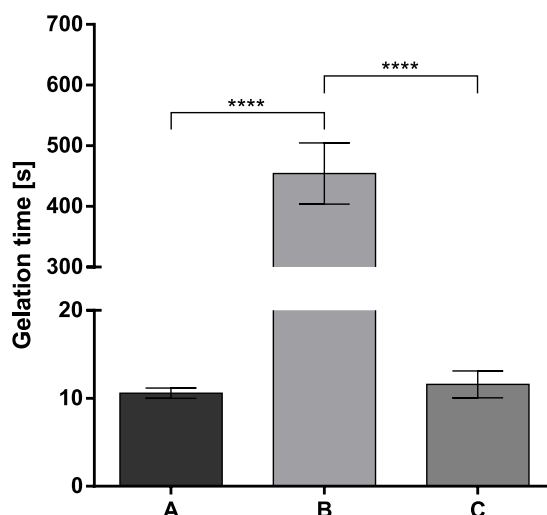


Figure 3: Gelation time of 4armPEG2k-polymers cross-linked via iEDDA reaction at 37 °C. Polymers consisting of 4armPEG2k-Nb and 4armPEG2k-Tz (A) were compared to polymers prepared with 4armPEG2k-Nb and 4armPEG2k-methyl-Tz (B) and polymers prepared with 4armPEG2k-ETPI and 4armPEG2k-Tz (C). Levels of statistical significance are indicated as **** $p \leq 0.0001$.

While rapid gelation is necessary for this application, a gelation time below 11 s presents a challenge for biomedical applications because the precursor mixture must be mixed and injected within that very short time frame. Exposure to shear forces once the system is beyond its gel point is undesirable because this affects the structural integrity of the polymer matrix, leading to changes in release kinetics and, in the worst case, dose dumping. Thus, we used chemical modifications of norbornene and tetrazine to reduce the gelation time as shown for conventional 5% (w/v) 8armPEG-hydrogels [19]. The reaction kinetics depend on the energy between the diene's (tetrazine) lowest unoccupied molecular orbital (LUMO) and the dienophile's (norbornene) highest occupied molecular orbital (HOMO). Adjusting the energy difference between these frontier molecular orbitals can be used to slow down the reaction rate [37,38]. The larger the $LUMO_{\text{diene}}-HOMO_{\text{dienophile}}$ energy gap, the slower the reaction [39]. Raising the LUMO via methyl substitution of tetrazine or decreasing the HOMO via oxygen incorporation of norbornene increases the $LUMO_{\text{diene}}-HOMO_{\text{dienophile}}$ energy gap [38]. For a polymer consisting of 4armPEG2k-Nb and 4armPEG2k-methyl-Tz, G' plateaued after 2500 s due to methyl substitution of tetrazine (Figure 2B). The gelation time was significantly increased to 454.2 ± 50.5 s (Figure 3). Interestingly, introducing oxygen into norbornene had no effect on the time to reach the plateau (Figure 2C) or the gelation time (11.6 ± 1.5 s). It is possible that the increase of the $LUMO_{\text{diene}}-HOMO_{\text{dienophile}}$ energy gap does not lead to a noticeable effect in the gelation time for a system consisting of 100% polymer. The very high number of functional groups and the absence of water in this system compared to conventional 5% (w/v) hydrogels, for which a significant effect on the gelation time was found, minimize the impact of the oxygen on the reaction time [19]. In contrast, the 4armPEG2k-methyl-Tz macromonomer reduced the reaction rate because the methyl substituent provided additional steric hindrance [7].

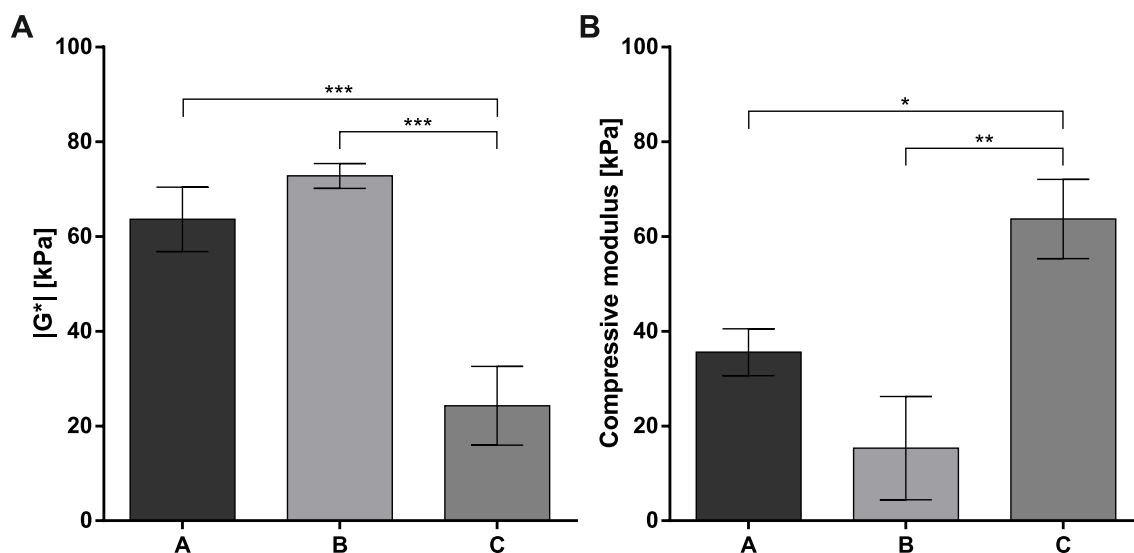


Figure 4: Absolute values of the complex shear modulus ($|G^*$) (A) and the compressive modulus (B) of 4armPEG2k-polymers consisting of 4armPEG2k-Nb and 4armPEG2k-Tz (A), 4armPEG2k-Nb and 4armPEG2k-methyl-Tz (B), and 4armPEG2k-ETPI and 4armPEG2k-Tz (C). Levels of statistical significance are indicated as * $p \leq 0.05$, ** $p \leq 0.01$, and *** $p \leq 0.001$.

Oscillatory rheology was also used to determine the stiffness of the different polymers, which is quantified by the absolute value of the complex shear modulus ($|G^*$) after 1 h (Figure 4A). Polymers prepared from 4armPEG2k-Nb and 4armPEG2k-methyl-Tz showed the highest stiffness (72.8 ± 2.6 kPa). Using 7-oxanorbornene modified macromonomers resulted in the significantly lowest stiffness (24.3 ± 8.3 kPa). In general, a higher cross-linking density and, therefore, a higher number of elastically active chains increases the stiffness of polymeric networks like hydrogels [25,40]. Hence, polymers consisting of 4armPEG2k-Nb and 4armPEG2k-methyl-Tz should have formed the densest network since they have the longest gelation time, which gives them more time to form elastically active chains than systems with faster gelation times. However, this could not be confirmed by the compressive modulus, which is the ratio of compressive stress to compressive strain and is used alongside stiffness to describe mechanical properties of three-dimensional networks [41]. The measured compressive moduli were found to be exactly the opposite of the stiffness (Figure 4B). Introduction of oxygen into norbornene gave the significantly highest compressive modulus (63.7 ± 8.4 kPa), and the methyl substitution of the tetrazine ring gave the lowest one (15.3 ± 10.9 kPa). This was surprising, as both the stiffness and the compressive modulus depend on elastically active chains and, hence, the cross-linking density of materials. We were able to explain this discrepancy by visualizing the different cross-linked materials using SEM imaging (Figure 5). For each polymer composition, we could see pores that were formed by nitrogen produced during the iEDDA reaction. The largest nitrogen bubbles were observed in the polymer prepared with 4armPEG2k-Nb and 4armPEG2k-methyl-Tz, which also had the longest gelation time. Apparently, the slower reaction rate led to coalescence of the nitrogen into larger bubbles, which are energetically preferred due to the reduced surface area. In contrast, faster gelation time resulted in smaller nitrogen bubbles. Interestingly, polymers containing the 7-oxanorbornene contained the smallest bubbles. These differences in network structure explain the seemingly contradictory results

from the measurements of stiffness and the compressive modulus. The polymers prepared with 4armPEG2k-Nb and 4armPEG2k-methyl-Tz had more time for gelation, leading to higher cross-linking density but larger nitrogen bubbles. The high cross-linking density increased the stiffness that is measured by applying low forces parallel to the material surface as during the oscillatory shear experiments. In contrast, compression of these polymers results in a rapid irreversible collapse of matrices containing large bubbles, leading to a decreased compressive modulus for the same material.

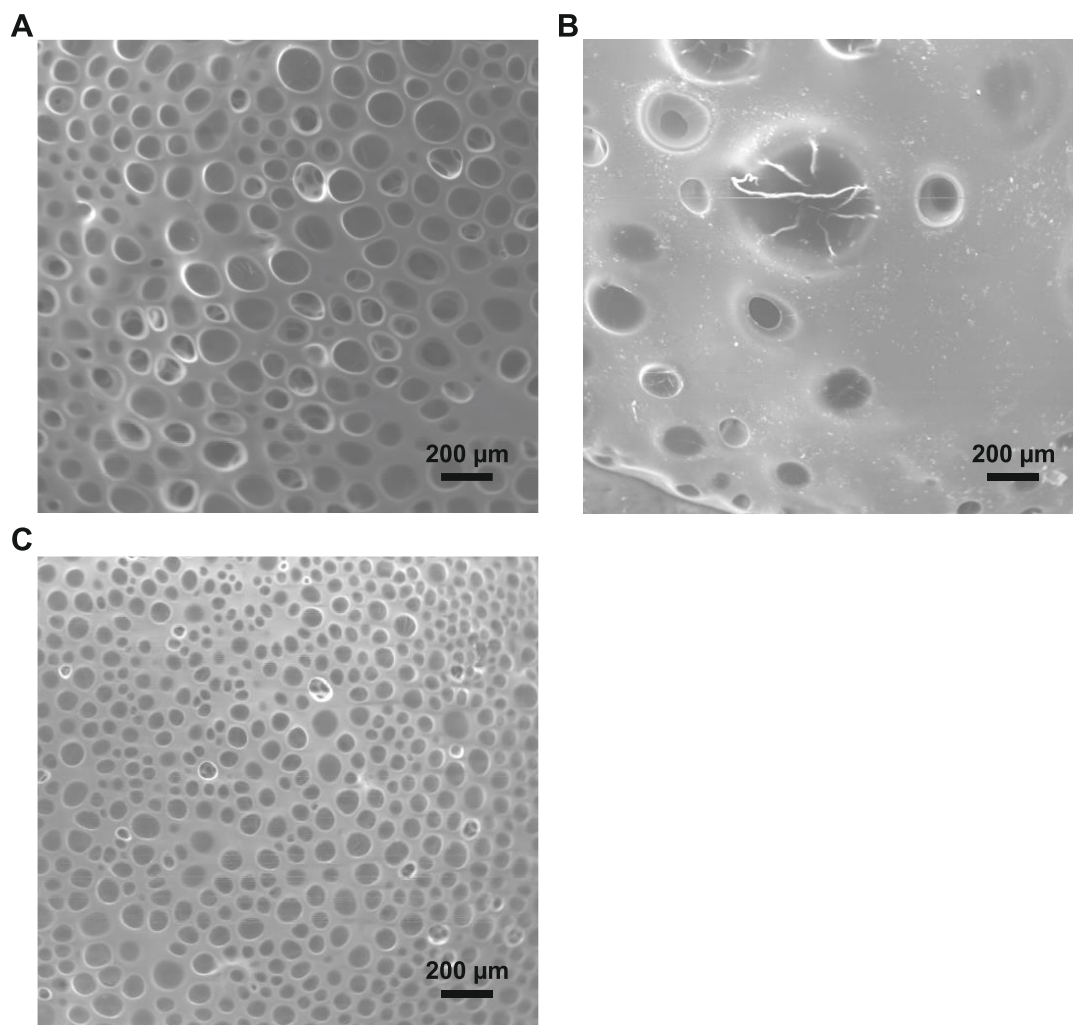


Figure 5: SEM images of the 4armPEG2k-polymers prepared with different precursors: 4armPEG2k-Nb and 4armPEG2k-Tz (A), 4armPEG2k-Nb and 4armPEG2k-methyl-Tz (B), and 4armPEG2k-ETPI and 4armPEG2k-Tz (C).

3.3 Swelling and degradation studies

In the previous sections, the cross-linking reaction and the mechanical properties were investigated. In the following experiments, we characterized the stability of the polymeric matrices, which is important for *in vivo* applications. To succeed as a controlled release system, a polymeric depot must remain sufficiently stable for the course of treatment, and ideally it would also biodegrade and negate the need for further surgeries to remove the material at the end of therapy. Stability and erosion of polymer

matrices prepared with 4armPEG2k-Nb and 4armPEG2k-Tz were investigated in 50 mM phosphate buffer (pH 7.4) at 37 °C. The polymers were weighed at specific time points, and the change in relative mass was calculated (Figure 6). While incubating in buffer, the mass of the polymers increased for 21 days, followed by a phase with negligible mass changes that lasted approximately 100 days. After that, the polymer swelled slowly for the next 300 days. After 450 days, the polymer mass started to decrease, signaling the beginning of complete dissolution. The experiment was stopped after 538 days. While the polymers did not completely dissolve in this time, these depot systems should completely erode due to the hydrolytically cleavable ester bonds [24,42].

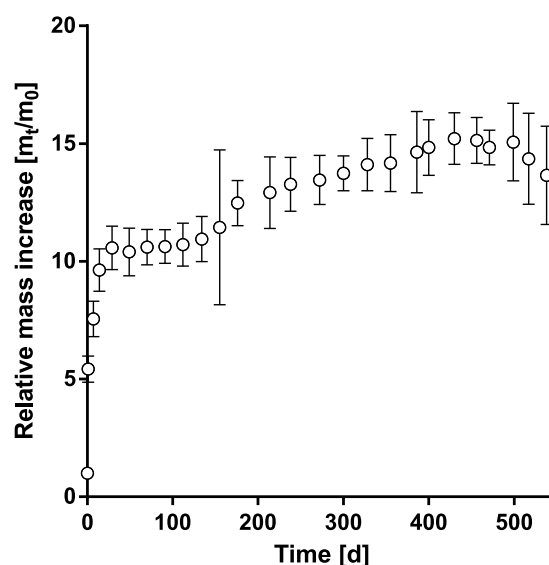


Figure 6: Swelling and degradation of polymers made with 4armPEG2k-Nb and 4armPEG2k-Tz. 4armPEG2k-polymers were incubated in 50 mM phosphate buffer (pH 7.4) at 37 °C. At predetermined time points, the masses of the polymers were measured.

In our previous work, we incorporated different hydrolytically cleavable linkers into the backbone of conventional hydrogels to accelerate degradation (**Chapter 5**). Carbamate, carbonate, and phenyl carbonate were used as designated breaking points. Incorporation of phenyl carbonate groups resulted in faster degradation, whereas carbonate and carbamate linkers did not reduce degradation time. Nevertheless, we tested all three groups in the 4armPEG2k-system because each linker had a different impact on the release kinetics of 8armPEG10k-hydrogels. Therefore, we wanted to show that incorporation of these groups is also possible for 4armPEG2k-macromonomers to increase the versatility of the new system. Since the water-free 4armPEG2k-system showed very high stability for over 500 days, only the first 200 days were compared to the classical polymers (Figure S1). Similar to the polymers containing two ester groups, all polymer types showed fast swelling at the beginning, followed by a reduced mass increase. For the carbamate and phenyl carbonate ester linkages, continuous swelling was observed to approximately 200 days. Since these polymers cross-linked without water, more elastically active chains are present, and the effects of the different linkers become noticeable much later than in the conventional hydrogels of our previous work. Therefore, further experiments over an extended timescale are needed. However, these swelling and degradation studies showed that it is

possible to prepare 4armPEG2k-polymers from hydrolyzable groups other than esters, which emphasizes the versatility of this novel delivery system.

3.4 GOx release

Controlled release is a critical feature of drug delivery systems. For successful medical applications, the drug should be continuously released over the course of therapy. Conventional hydrogels prepared in water are mainly used for short-term protein delivery. For extended protein release, modifications of the hydrogel backbone or the incorporation of additional excipients are usually required [43–46]. Also, conventional hydrogels have a limited capacity for protein loading because higher drug loading impacts the mesh sizes and ultimately leads to faster and less controlled release. Therefore, to achieve therapeutically relevant plasma levels of the therapeutic protein, a very high hydrogel volume is required [8]. To address this problem, we established the water-free preparation of 8armPEG10k-hydrogels via the DA reaction, with which we were able to achieve a drug content of at least 15% (w/w) [12]. However, these water-free hydrogels have to be prepared at temperatures above 40 °C and have polymerization times over 16 h and, hence, cannot be directly injected. The 4armPEG2k-system cross-linked via the rapid iEDDA reaction we present in this work solves these injection issues, but the question of protein loading and release remained.

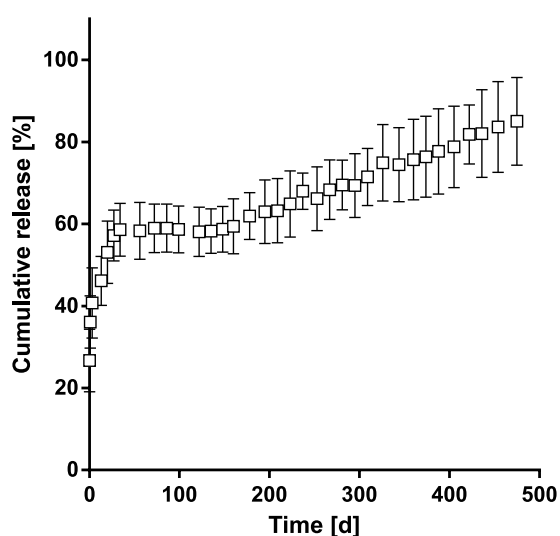


Figure 7: Release of GOx from polymers made with 4armPEG2k-Nb and 4armPEG2k-Tz in 50 mM phosphate buffer (pH 7.4) at 37 °C.

GOx was chosen as a model protein for these experiments because it has a hydrodynamic radius of 4.3 nm and a molecular weight of 160 kDa, which makes it an ideal surrogate for antibody drugs [47–49]. The release experiments were carried out in phosphate buffer (pH 7.4) at 37 °C to simulate physiological conditions (Figure 7). The release kinetics showed three distinct phases. Approximately 25% of the protein was released after 1 day of incubation in buffer. This burst release was followed by the continuous release of 35% of the protein over the next 50 days. In this phase, the protein was able to diffuse out via polymer meshes that were larger than its hydrodynamic diameter. However, the high

cross-linking density of the small 4armPEG2k-precursors also created meshes smaller than the protein, which contained the remaining enzyme and prevented any detectable release between 50 and 150 days. Only after 150 days, when the mesh sizes increased due to swelling and degradation, did the release start again. This is in accordance with the results found for the swelling and degradation studies (Figure 7), where the polymer mass increased after a long period without mass changes. Cleavage of the ester groups led to constant release over the following 300 days. After 475 days, the release experiment was stopped, and by this time, 85% of GOx was released. This release behavior shows that the 4armPEG2k macromonomers in combination with the iEDDA reaction between norbornene and tetrazine groups can be used for the preparation of water-free protein delivery systems that achieve long-term controlled release.

This system might be better suited to deliver proteins with smaller hydrodynamic diameters. They would be able to diffuse out of the mesh in the phase between 50 and 150 days, when the hydrogel meshes are static, leading to steady release. This could be useful for the delivery of endogenous hormones and their synthetic derivatives, which have hydrodynamic diameters smaller than GOx, because the constant release profile would produce stable hormone levels. However, more detailed experiments would be necessary to explore the full potential of our polymer system for protein and peptide delivery.

4 Conclusion

We successfully developed a water-free protein delivery system that is formed via rapid iEDDA reaction between norbornene and tetrazine groups. Liquid 4armPEG2k-precursors enable the direct injection of this system into the organism. The polymers were able to embed the model protein GOx into a three-dimensional network and release the enzyme over a period of 475 days in a controlled manner. Biodegradability was obtained by incorporating ester groups into the macromonomers. Additionally, carbamate and phenyl carbonate ester groups can be used to tune biodegradability for specific applications. Furthermore, the reaction rate and mechanical properties can be varied by methyl substitution of tetrazine groups or oxygen incorporation into norbornene to meet diverse application requirements.

References

- [1] J. Li, D.J. Mooney, Designing hydrogels for controlled drug delivery, *Nat. Rev. Mater.* 1 (2016).
- [2] A. Vashist, A. Kaushik, A. Vashist, R.D. Jayant, A. Tomitaka, S. Ahmad, Y.K. Gupta, M. Nair, Recent trends on hydrogel based drug delivery systems for infectious diseases, *Biomater. Sci.* 4 (2016) 1535–1553.
- [3] T. Vermonden, R. Censi, W.E. Hennink, Hydrogels for protein delivery, *Chem. Rev.* (Washington, DC, U. S.) 112 (2012) 2853–2888.
- [4] M.N. Collins, C. Birkinshaw, Physical properties of crosslinked hyaluronic acid hydrogels, *J. Mater. Sci.: Mater. Med.* 19 (2008) 3335–3343.
- [5] W. Hu, Z. Wang, Y. Xiao, S. Zhang, J. Wang, Advances in crosslinking strategies of biomedical hydrogels, *Biomater. Sci.* 7 (2019) 843–855.
- [6] S. Kirchhof, A. Strasser, H.-J. Wittmann, V. Messmann, N. Hammer, A.M. Goepferich, F.P. Brandl, New insights into the cross-linking and degradation mechanism of Diels–Alder hydrogels, *J. Mater. Chem. B* 3 (2015) 449–457.
- [7] M.R. Karver, R. Weissleder, S.A. Hilderbrand, Synthesis and evaluation of a series of 1,2,4,5-tetrazines for bioorthogonal conjugation, *Bioconjugate Chem.* 22 (2011) 2263–2270.
- [8] L.M. Ickenstein, P. Garidel, Hydrogel formulations for biologicals: current spotlight from a commercial perspective, *Ther. Delivery* 9 (2018) 221–230.
- [9] A.H. Zisch, M.P. Lutolf, M. Ehrbar, G.P. Raeber, S.C. Rizzi, N. Davies, H. Schmökel, D. Bezuidenhout, V. Djonov, P. Zilla, J.A. Hubbell, Cell-demanded release of VEGF from synthetic, biointeractive cell ingrowth matrices for vascularized tissue growth, *FASEB J.* 17 (2003) 2260–2262.
- [10] N. Hammer, F.P. Brandl, S. Kirchhof, V. Messmann, A.M. Goepferich, Protein compatibility of selected cross-linking reactions for hydrogels, *Macromol. Biosci.* 15 (2015) 405–413.
- [11] C.-C. Lin, K.S. Anseth, PEG hydrogels for the controlled release of biomolecules in regenerative medicine, *Pharm. Res.* 26 (2009) 631–643.
- [12] C.E. Ziegler, M. Graf, S. Beck, A.M. Goepferich, A novel anhydrous preparation of PEG hydrogels enables high drug loading with biologics for controlled release applications, *Eur. Polym. J.* 147 (2021) 110286.
- [13] H.-S. Han, N.K. Devaraj, J. Lee, S.A. Hilderbrand, R. Weissleder, M.G. Bawendi, Development of a bioorthogonal and highly efficient conjugation method for quantum dots using tetrazine-norbornene cycloaddition, *J. Am. Chem. Soc.* 132 (2010) 7838–7839.
- [14] A.-C. Knall, C. Slugovc, Inverse electron demand Diels–Alder (iEDDA)-initiated conjugation: a (high) potential click chemistry scheme, *Chem. Soc. Rev.* 42 (2013) 5131–5142.
- [15] B.L. Oliveira, Z. Guo, G.J.L. Bernardes, Inverse electron demand Diels–Alder reactions in chemical biology, *Chem. Soc. Rev.* 46 (2017) 4895–4950.

- [16] M. Gregoritza, F.P. Brandl, The Diels-Alder reaction: A powerful tool for the design of drug delivery systems and biomaterials, *Eur. J. Pharm. Biopharm.* 97 (2015) 438–453.
- [17] V. Delplace, A.J. Pickering, M.H. Hettiaratchi, S. Zhao, T. Kivijärvi, M.S. Shoichet, Inverse Electron-Demand Diels-Alder Methylcellulose Hydrogels Enable the Co-delivery of Chondroitinase ABC and Neural Progenitor Cells, *Biomacromolecules* 21 (2020) 2421–2431.
- [18] A. Famili, K. Rajagopal, Bio-Orthogonal Cross-Linking Chemistry Enables In Situ Protein Encapsulation and Provides Sustained Release from Hyaluronic Acid Based Hydrogels, *Mol. Pharmaceutics* 14 (2017) 1961–1968.
- [19] C.E. Ziegler, M. Graf, M. Nagaoka, H. Lehr, A.M. Goepferich, In Situ Forming iEDDA Hydrogels with Tunable Gelation Time Release High-Molecular Weight Proteins in a Controlled Manner over an Extended Time, *Biomacromolecules* (2021).
- [20] B. Mizrahi, S.A. Shankarappa, J.M. Hickey, J.C. Dohlman, B.P. Timko, K.A. Whitehead, J.-J. Lee, R. Langer, D.G. Anderson, D.S. Kohane, A Stiff Injectable Biodegradable Elastomer, *Adv. Funct. Mater.* 23 (2013) 1527–1533.
- [21] T. Croitoru-Sadger, S. Yogev, A. Shabtay-Orbach, B. Mizrahi, Two-component cross-linkable gels for fabrication of solid oral dosage forms, *J. Controlled Release* 303 (2019) 274–280.
- [22] R. Kelmansky, B.J. McAlvin, A. Nyska, J.C. Dohlman, H.H. Chiang, M. Hashimoto, D.S. Kohane, B. Mizrahi, Strong tissue glue with tunable elasticity, *Acta Biomater.* 53 (2017) 93–99.
- [23] R. Kelmansky, A. Shagan, B. Rozenblit, R. Omar, M. Lufton, B. Mizrahi, In Situ Dual Cross-Linking of Neat Biogel with Controlled Mechanical and Delivery Properties, *Mol. Pharmaceutics* 14 (2017) 3609–3616.
- [24] M. Gregoritza, K. Abstiens, M. Graf, A.M. Goepferich, Fabrication of antibody-loaded microgels using microfluidics and thiol-ene photoclick chemistry, *Eur. J. Pharm. Biopharm.* 127 (2018) 194–203.
- [25] S. Kirchhof, F.P. Brandl, N. Hammer, A.M. Goepferich, Investigation of the Diels–Alder reaction as a cross-linking mechanism for degradable poly(ethylene glycol) based hydrogels, *J. Mater. Chem. B* 1 (2013) 4855.
- [26] F. Brandl, M. Henke, S. Rothschenk, R. Gschwind, M. Breunig, T. Blunk, J. Tessmar, A. Göpferich, Poly(Ethylene Glycol) Based Hydrogels for Intraocular Applications, *Adv. Eng. Mater.* 9 (2007) 1141–1149.
- [27] K.A. Günay, T.L. Ceccato, J.S. Silver, K.L. Bannister, O.J. Bednarski, L.A. Leinwand, K.S. Anseth, PEG-Anthracene Hydrogels as an On-Demand Stiffening Matrix To Study Mechanobiology, *Angew. Chem., Int. Ed.* 58 (2019) 9912–9916.
- [28] V.X. Truong, I. Donderwinkel, J.E. Frith, Bioorthogonal hydrogels by thiol–halide click crosslinking with fast gelation time and tunable stability in aqueous media, *J. Polym. Sci., Part A: Polym. Chem.* 57 (2019) 1872–1876.

- [29] K. Vats, G. Marsh, K. Harding, I. Zampetakis, R.E. Waugh, D.S.W. Benoit, Nanoscale physicochemical properties of chain- and step-growth polymerized PEG hydrogels affect cell-material interactions, *J. Biomed. Mater. Res., Part A* 105 (2017) 1112–1122.
- [30] G. Bakirdogen, E.L. Sahkulubey Kahveci, M.U. Kahveci, Fast and efficient preparation of three-arm star block copolymers via tetrazine ligation, *Eur. Polym. J.* 140 (2020) 110027.
- [31] S.C. Edington, J.C. Flanagan, C.R. Baiz, An Empirical IR Frequency Map for Ester C=O Stretching Vibrations, *J. Phys. Chem. A* 120 (2016) 3888–3896.
- [32] D.S.B. Anugrah, M.P. Patil, X. Li, C.M.Q. Le, K. Ramesh, G.-D. Kim, K. Hyun, K.T. Lim, Click-cross-linked, doxorubicin-loaded hydrogels based on poly(styrene-alt-maleic anhydride), *eXPRESS Polym. Lett.* 14 (2020) 248–260.
- [33] K.-D. Topp, M. Grote, Synthesis and characterization of a 1,2,4,5-tetrazine-modified ion-exchange resin, *React. Funct. Polym.* 31 (1996) 117–136.
- [34] S.S. Kara, M.Y. Ateş, G. Deveci, A. Cetinkaya, M.U. Kahveci, Direct synthesis of tetrazine functionalities on polymer backbones, *J. Polym. Sci., Part A: Polym. Chem.* 57 (2019) 673–680.
- [35] C.F. Hansell, P. Espeel, M.M. Stamenović, I.A. Barker, A.P. Dove, F.E. Du Prez, R.K. O'Reilly, Additive-free clicking for polymer functionalization and coupling by tetrazine-norbornene chemistry, *J. Am. Chem. Soc.* 133 (2011) 13828–13831.
- [36] J.L. Dávila, M.A. d'Ávila, Laponite as a rheology modifier of alginate solutions: Physical gelation and aging evolution, *Carbohydr. Polym.* 157 (2017) 1–8.
- [37] Z.M. Png, H. Zeng, Q. Ye, J. Xu, Inverse-Electron-Demand Diels-Alder Reactions: Principles and Applications, *Chem. - Asian J.* 12 (2017) 2142–2159.
- [38] R.A.A. Foster, M.C. Willis, Tandem inverse-electron-demand hetero-/retro-Diels-Alder reactions for aromatic nitrogen heterocycle synthesis, *Chem. Soc. Rev.* 42 (2013) 63–76.
- [39] I. Fleming, *Frontier orbitals and organic chemical reactions*, Reprint ed., Wiley, London, 2007.
- [40] A. Metters, J. Hubbell, Network formation and degradation behavior of hydrogels formed by Michael-type addition reactions, *Biomacromolecules* 6 (2005) 290–301.
- [41] M. Gregoritz, V. Messmann, A.M. Goepferich, F.P. Brandl, Design of hydrogels for delayed antibody release utilizing hydrophobic association and Diels–Alder chemistry in tandem, *J. Mater. Chem. B* 4 (2016) 3398–3408.
- [42] M. Graf, C.E. Ziegler, M. Gregoritz, A.M. Goepferich, Hydrogel microspheres evading alveolar macrophages for sustained pulmonary protein delivery, *Int. J. Pharm. (Amsterdam, Neth.)* 566 (2019) 652–661.
- [43] V. Huynh, R.G. Wylie, Competitive Affinity Release for Long-Term Delivery of Antibodies from Hydrogels, *Angew. Chem., Int. Ed.* 57 (2018) 3406–3410.

-
- [44] U. Bhardwaj, R. Sura, F. Papadimitrakopoulos, D.J. Burgess, PLGA/PVA hydrogel composites for long-term inflammation control following s.c. implantation, *Int. J. Pharm.* (Amsterdam, Neth.) 384 (2010) 78–86.
- [45] K.W. Lee, J.J. Yoon, J.H. Lee, S.Y. Kim, H.J. Jung, S.J. Kim, J.W. Joh, H.H. Lee, D.S. Lee, S.K. Lee, Sustained release of vascular endothelial growth factor from calcium-induced alginate hydrogels reinforced by heparin and chitosan, *Transplant. Proc.* 36 (2004) 2464–2465.
- [46] Q. Peng, X. Sun, T. Gong, C.-Y. Wu, T. Zhang, J. Tan, Z.-R. Zhang, Injectable and biodegradable thermosensitive hydrogels loaded with PHBHHx nanoparticles for the sustained and controlled release of insulin, *Acta Biomater.* 9 (2013) 5063–5069.
- [47] S. Nakamura, S. Hayashi, K. Koga, Effect of periodate oxidation on the structure and properties of glucose oxidase, *Biochim. Biophys. Acta* 445 (1976) 294–308.
- [48] H. Tsuge, O. Natsuaki, K. Ohashi, Purification, properties, and molecular features of glucose oxidase from *Aspergillus niger*, *J. Biochem.* 78 (1975) 835–843.
- [49] S.K. Li, M.R. Liddell, H. Wen, Effective electrophoretic mobilities and charges of anti-VEGF proteins determined by capillary zone electrophoresis, *J. Pharm. Biomed. Anal.* 55 (2011) 603–607.

Chapter 6 – Supporting information

Injectable anhydrous PEG polymer liquids form protein depot for extended controlled release applications via rapid in situ gelation

1 Swelling and degradation studies

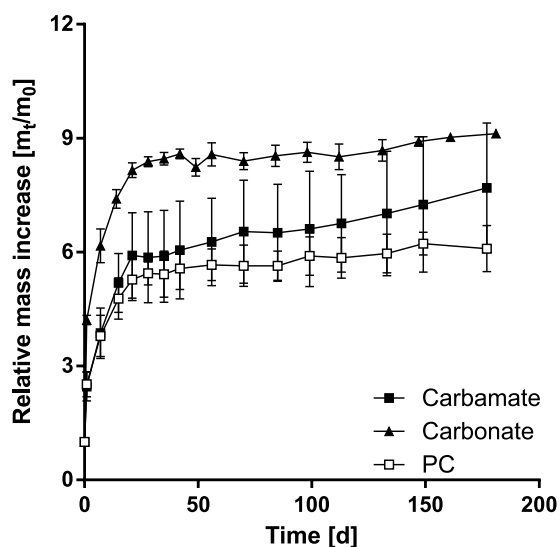


Figure S1: Swelling and degradation of 4armPEG2k-polymers containing carbamate, carbonate ester, and phenyl carbonate ester (PC) as hydrolytically cleavable groups in 50 mM phosphate buffer (pH 7.4) at 37 °C. At predetermined time points, the masses of the polymers were measured.

2 Spectroscopic data

4armPEG2k-Tz

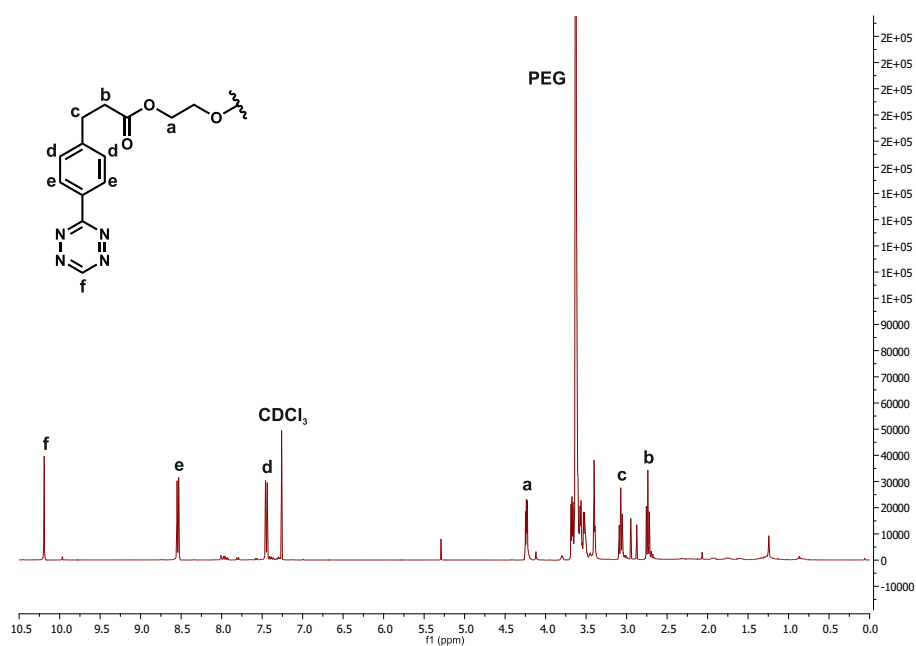


Figure S2: ^1H NMR spectrum of 4armPEG2k-Tz

^1H NMR (CDCl_3 , 400 MHz): δ (ppm) = 2.73 (t, 8H, $-\text{C}(\text{O})\text{CH}_2\text{CH}_2\text{Ar}$), 3.06 (t, 8H, $-\text{C}(\text{O})\text{CH}_2\text{CH}_2\text{Ar}$), 3.40 (s, 8H, $\text{R}_3\text{CCH}_2\text{O}-$), 3.63 (s, $-\text{OCH}_2\text{CH}_2\text{O}-$), 4.23 (t, 8H, $-\text{OCH}_2\text{CH}_2\text{O}-$), 7.44 (d, 8H, Ar), 8.54 (d, 8H, Ar), 10.19 (s, 4H, $-\text{N}=\text{CH}-\text{NH}-$).

4armPEG2k-methyl-Tz

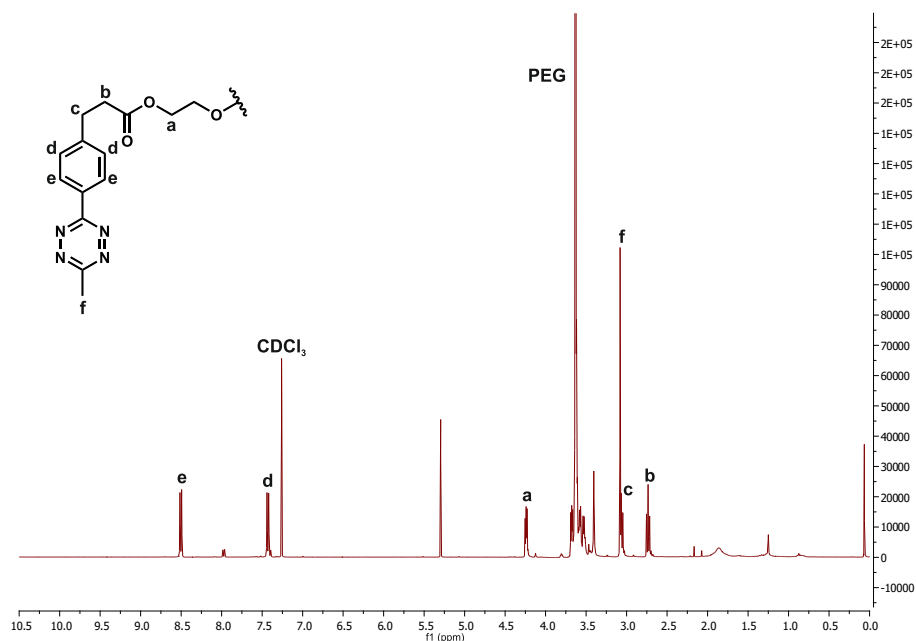


Figure S3: ^1H NMR spectrum of 4armPEG2k-methyl-Tz

^1H NMR (CDCl_3 , 400 MHz): δ (ppm) = 2.72 (t, 8H, $-\text{C}(\text{O})\text{CH}_2\text{CH}_2\text{Ar}$), 3.06 (t, 8H, $-\text{C}(\text{O})\text{CH}_2\text{CH}_2\text{Ar}$), 3.08 (s, 12H, CH_3Ar), 3.41 (s, 8H, $\text{R}_3\text{CCH}_2\text{O}-$), 3.63 (s, $-\text{OCH}_2\text{CH}_2\text{O}-$), 4.23 (t, 8H, $-\text{OCH}_2\text{CH}_2\text{O}-$), 7.43 (d, 8H, Ar), 8.50 (d, 8H, Ar).

4armPEG2k-Nb

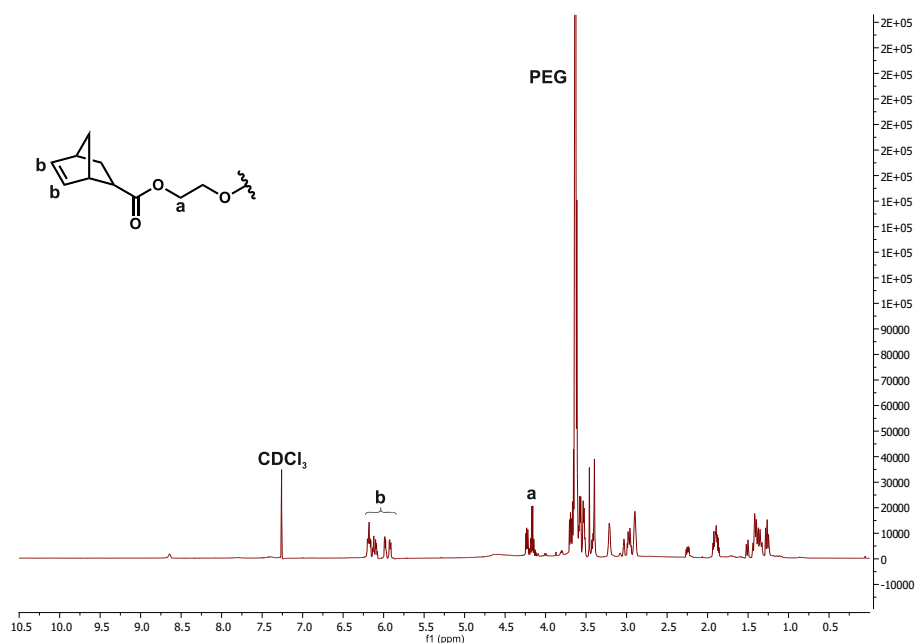


Figure S4: ^1H NMR spectrum of 4armPEG2k-Nb

^1H NMR (CDCl_3 , 400 MHz): δ (ppm) = 3.40 (s, 8H, $\text{R}_3\text{CCH}_2\text{O}-$), 3.63 (s, $-\text{OCH}_2\text{CH}_2\text{O}$), 4.24–4.12 (m, 8H, $-\text{OCH}_2\text{CH}_2\text{O}-$), 6.20–5.91 (m, 8H, $-\text{HC}=\text{CH}-$, *endo* and *exo*).

4armPEG2k-ETPI

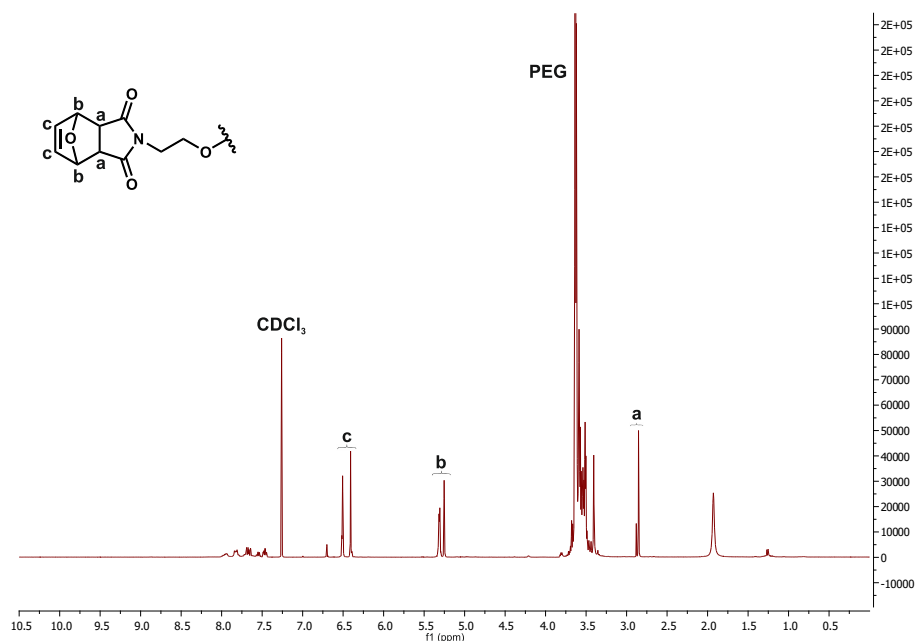


Figure S5: ^1H NMR spectrum of 4armPEG2k-ETPI

^1H NMR (CDCl_3 , 400 MHz): δ (ppm) = 2.85 (s, 4H, $-\text{C}(\text{O})\text{CHRCHRC}(\text{O})-$, *exo*), 2.88 (s, 4H, $-\text{C}(\text{O})\text{CHRCHRC}(\text{O})-$, *endo*), 3.41 (s, 8H, $\text{R}_3\text{CCH}_2\text{O}-$), 3.64 (s, $-\text{OCH}_2\text{CH}_2\text{O}-$), 5.25 (s, 8H, $\text{R}_2\text{CHOCHR}_2-$, *endo*), 5.31 (m, 4H, $-\text{R}_2\text{CHOCHR}_2-$, *exo*), 6.41 (s, 8H, $-\text{CH}=\text{CH}-$, *endo*), 6.51 (s, 8H, $-\text{CH}=\text{CH}-$, *exo*).

4armPEG2k-carbamate-Nb

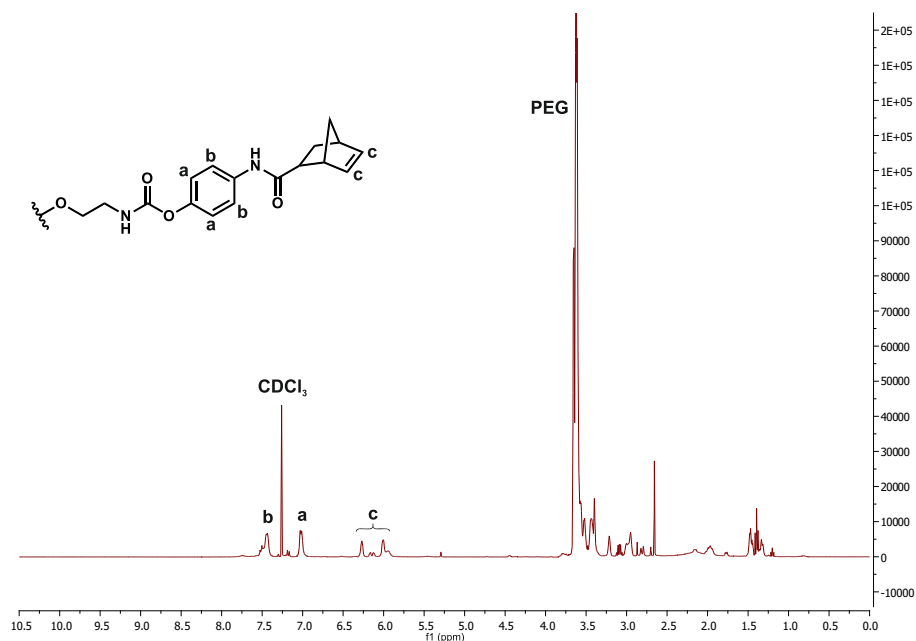


Figure S6: ^1H NMR spectrum of 4armPEG2k-carbamate-Nb

^1H NMR (CDCl_3 , 400 MHz): δ (ppm) = 3.61 (s, $-\text{OCH}_2\text{CH}_2\text{O}-$), 6.00 (m, 4H, $-\text{HC}=\text{CH}-$, *endo*), 6.14 (d, 8H, $-\text{HC}=\text{CH}-$, *exo*), 6.29 (m, 4H, $-\text{HC}=\text{CH}-$, *endo*), 7.02 (8H, Ar), 7.44 (8H, Ar).

4armPEG2k-carbonate-Nb

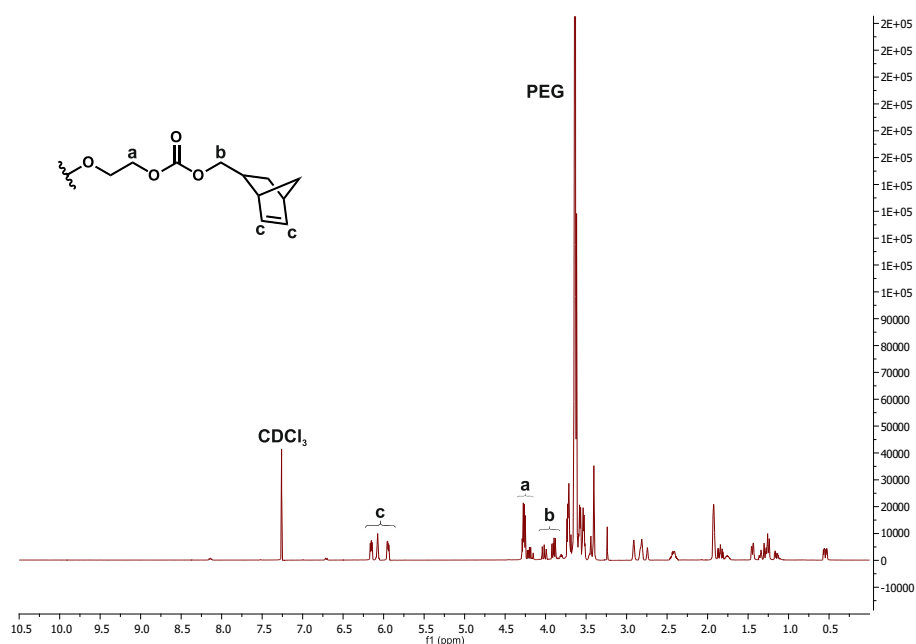


Figure S7: ¹H NMR spectrum of 4armPEG2k-carbonate-Nb

¹H NMR (CDCl₃, 400 MHz): δ (ppm) = 3.63 (s, -OCH₂CH₂O-), 4.15–4.29 (8H, -OCH₂CH₂O-), 5.94 (m, 4H, -HC=CH-, *endo*), 6.07 (m, 8H, -HC=CH-, *exo*), 6.15 (m, 4H, -HC=CH-, *endo*).

4armPEG2k-phenyl carbonate-Nb

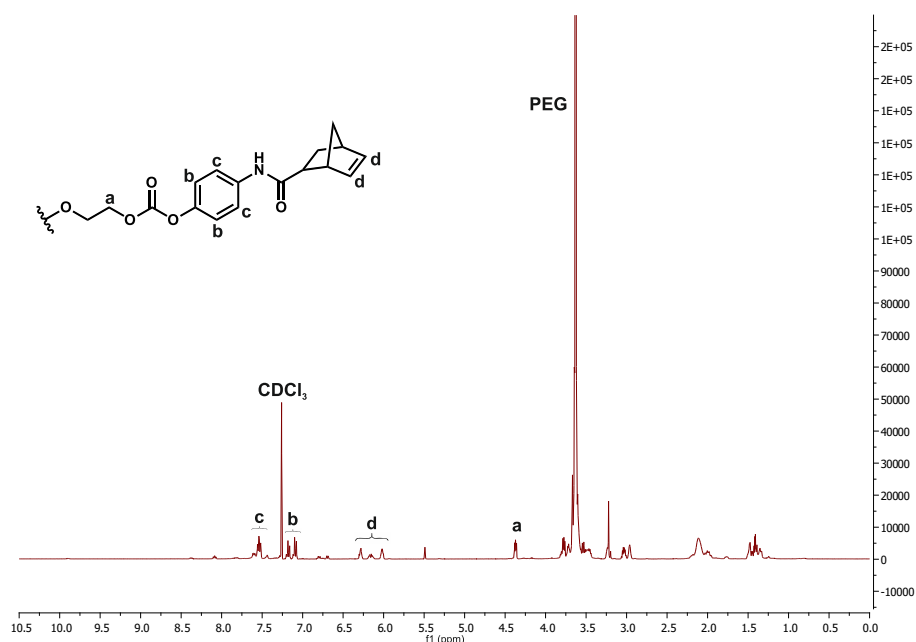


Figure S8: ¹H NMR spectrum of 4armPEG2k-phenyl carbonate-Nb

¹H NMR (CDCl₃, 400 MHz): δ (ppm) = 3.63 (s, -OCH₂CH₂O-), 4.37 (m, 8H, -OCH₂CH₂O-), 6.02 (m, 4H, -HC=CH-, *endo*), 6.14 (m, 4H, -HC=CH-, *exo*), 6.17 (m, 4H, -HC=CH-, *exo*), 6.29 (m, 4H, -HC=CH-, *endo*), 7.08–7.20 (8H, Ar), 7.52–7.61 (8H, Ar).

Chapter 7

Summary and conclusion

1 Summary

Since the first mention of the term hydrogel in 1960 [1], a lot of work has been put into research and development of this polymeric material. While the high versatility makes many different applications possible, the use as transport vehicle is particularly promising. The reason for this is the well-defined architecture of the three-dimensional structure that creates cavities, in which cargo can be embedded. After contact with an aqueous solution, hydrogels deliver the cargo with release kinetics depending on diffusion, degradation, or swelling. Used in the human organism, hydrogels can release encapsulated drugs to treat various diseases. Thereby, an extension of release time is primarily achieved via chemically cross-linked hydrogels due to their increased stability. For example, the monoclonal antibody bevacizumab embedded in chemically cross-linked hydrogels could be released in a controlled manner for the treatment of age-related macular degeneration over 100 days [2]. Such a drug depot would be ideal to avoid repeated antibody injections associated with high personnel costs and reduced patient compliance.

However, delivery of proteins by using chemically cross-linked hydrogels still has its limitations (**Chapter 1**). Off-target reactions between proteins and the functional groups of the hydrogel precursors can cause delay of release, activity changes of the protein, and even immunogenic reactions [3–5]. In addition, the number of embedded proteins is limited [5]. Usually, a loading capacity of below 1% (w/v) is common. The reason for these drawbacks is the use of water, which also poses a threat to the stability of hydrolysis-prone hydrogel precursors.

The goal of this thesis was to develop chemically cross-linked hydrogels for the extended release of proteins that circumvents the limitations caused by water and other solvents. For this, the polymerization had to be carried out in an anhydrous environment to obtain polymers that swell to hydrogels after absorption of water. Due to the definition that hydrogels are hydrophilic polymeric networks that are produced by any technique able to trigger polymeric cross-linking [6], these polymers can be considered anhydrous hydrogels.

To check if solvent-free cross-linking can be used to prepare hydrogels, furan- and maleimide-functionalized eight-armed poly(ethylene glycol) (PEG) macromonomers were homogeneously mixed. After heating above the melting point, rheology revealed polymerization in molten state. In addition, decreasing the molecular weight of the macromonomers resulted in lower melting points favorable for the embedding of thermolabile proteins. The absence of water prevented not only the hydrolysis of water-sensitive maleimide groups but also off-target reactions between maleimide and nucleophilic amine residues of proteins. In this way, proteins could be embedded unmodified in a denser hydrogel network. Incubation of these polymers in an aqueous solution showed a water uptake up to 35-fold of the polymer mass. Thereby, stability varied between 54 and 150 days depending on the molecular weight of the macromonomers. Additionally, the complete release of the low molecular weight protein lysozyme within 10 days without activity loss showed no interaction between protein and unreacted

polymer moieties after incubation in an aqueous environment. Finally, the model protein glucose oxidase (GOx), whose molecular weight and hydrodynamic diameter are similar to common antibodies, was released from anhydrous hydrogels over 100 days in biphasic behavior. Increasing the loading level from 5 to 15% (w/w) did not impact the release kinetics. Moreover, neither modification nor fragmentation were detected for the released protein, indicating the protective nature of these anhydrous protein depots (**Chapter 3**).

Despite prevention of off-target reactions and functional group hydrolysis and achieving protein release in a controlled manner, immediate anhydrous gelation in the organism is not possible with the Diels-Alder (DA) reaction between furan and maleimide. Therefore, the fast-proceeding inverse electron Diels-Alder (iEDDA) reaction between norbornene and tetrazine was introduced, which was not used to prepare hydrogels for the long-term release of proteins thus far. Besides the fast reaction rate, this reaction is bioorthogonal in an aqueous environment. Before the preparation of anhydrous hydrogels, conventional hydrogels were prepared to study the potential of the iEDDA reaction in combination with multi-armed PEGs. Aqueous mixtures of norbornene- and tetrazine-modified eight-armed PEGs showed gelation times below 1 min, complicating the injection due to premature gel formation. To facilitate handling, variations in polymer concentration, temperature, and chemical structure were applied. Additionally, a denser hydrogel network achieved by using a higher polymer concentration or smaller macromonomers resulted in increased mechanical properties. Then, lysozyme was used to examine off-target reactions in an aqueous environment. Modifications of only 11% of the model protein indicated the superiority of the iEDDA reaction over the DA reaction regarding unwanted side reactions. By incubation in 50 mM phosphate buffer (pH 7.4), hydrogel stability was found to be in the range of 186 and 530 days, depending on polymer concentration and molecular weight of the hydrogel precursors used. To assess the suitability of multi-armed PEG-hydrogels cross-linked via the iEDDA reaction for the application as a high molecular weight protein delivery system, GOx was embedded. The controlled *in vitro* release over more than 265 days proved the 15% (w/v) eight-armed PEG-hydrogels as highly promising injectable long-term protein delivery system (**Chapter 4**).

Although an extended release was achieved over more than 265 days, this long timeframe represents an obstacle regarding protein stability. For example, activity maintenance is not guaranteed for therapeutic proteins stored at 37 °C for a long time [7]. In addition, the material residues would remain in the organism beyond therapy time due to slow degrading ester groups. Therefore, hydrogels with an adjustable degradation time would be favorable. To this end, 3,6-epoxy-1,2,3,6-tetrahydrophthalimide (ETPI), carbamate, carbonate ester, and phenyl carbonate ester were introduced as hydrolyzable linkers into the PEG-norbornene precursor. First of all, the impact of the linkers on the *in situ* gelation was studied. Gel points of less than 20 s even at a low polymer concentration of 5% (w/v) for all hydrogels revealed immediate gelation. Additionally, the effect of the linkers on the mechanical properties was analyzed by rheology and compressive testing. The ETPI linker resulted in the highest hydrogel stiffness due to the formation of an increased number of cross-links, determined by NMR spectroscopy. In

contrast, the reduced stability of the phenyl carbonate ester linker led to hydrogels with the lowest mechanical properties. Since hydrogel precursor syntheses required toxic starting material, the hydrogel variants were examined considering cytocompatibility. All hydrogels passed the cytotoxicity assessment. Due to the goal of this chapter that was to shorten the erosion time of eight-armed PEG-hydrogels cross-linked via iEDDA reaction, the stabilities of 5% (w/v) hydrogels with different hydrolyzable linkers were determined. All hydrogels were stable at least 400 days except hydrogels containing the phenyl carbonate linkers, which showed complete erosion after 153 days. An increase in polymer concentration led to higher stability over more than 300 days for this hydrogel type, showing the potential of tuning the erosion time. The mesh sizes of the different hydrogels were found to be in the range of comparable hydrogels prepared with eight-armed PEGs, which were successfully used for protein delivery. In the final experiment, the release from all hydrogels was analyzed. A controlled release of 150 kDa fluorescein isothiocyanate-dextran over at least 150 days was achieved for all hydrogels (**Chapter 5**).

The iEDDA reaction was successfully introduced for the preparation of *in situ* forming delivery systems with varying degradation times. However, these drug depots were water-based, and off-target reactions, loading capacity, and functional group stability still limited the use of these hydrogels. To overcome these drawbacks and to achieve the goal of the thesis, the acquired knowledge regarding anhydrous hydrogel preparation, *in situ* gelation by using the iEDDA reaction, and tuning of erosion time was transferred to four-armed PEG macromonomers with a molecular weight of 2 kDa that are liquid at the operating temperature below 37 °C. For this, the macromonomers were functionalized with norbornene and tetrazine. Mixing of both precursors led to the formation of polymers, for which the iEDDA reaction was confirmed as cross-linking reaction by FTIR and UV-VIS spectroscopy. To prove the ability of *in situ* gelation, the liquid macromonomers were mixed and gelation time was determined. The polymers showed rapid gelation with gel points below 11 s. Chemical modification of norbornene and tetrazine groups led to changes in gelation time, stiffness, and three-dimensional structure. Despite the incorporation of various hydrolyzable groups, the polymers showed high stability of at least 200 days. In the final experiment, the suitability of this system for the delivery of proteins was investigated. For this, the protein GOx was embedded. The polymers were able to release the protein over a time of more than 475 days in a controlled manner, indicating the high potential of this polymeric material (**Chapter 6**).

2 Conclusion

In this thesis, anhydrous hydrogel preparation, rapid *in situ* gelation, and biodegradation were investigated and transferred to liquid multi-armed PEGs to accomplish the goal of developing an injectable anhydrous protein delivery system that exhibits instant gelation. Water-free polymerization via DA reaction was achieved by heating furan- and maleimide-modified eight-armed PEG

macromonomers above their melting points. The absence of water prevented detrimental off-target reactions of proteins and protected hydrolysis-prone maleimide groups from degradation. Moreover, in contrast to conventional hydrogels formed in water, the loading capacity could be increased by a multitude without affecting the release kinetics. Due to the ability of long-term protein release, these polymers could serve as protein delivery implants for the treatment of various diseases. To accelerate the gelation, the bioorthogonal iEDDA reaction between norbornene and tetrazine was introduced and conventional hydrogels were prepared. While immediate gelation was achieved, tuning the reaction kinetics via polymer concentration, temperature, and chemical modification facilitated the administration. Due to the long-term protein release, it is promising to further analyze this material for the delivery of biologics. In the next step, the hydrogel erosion time was modified by the incorporation of different hydrolyzable groups. Hydrogels with different stability and erosion behavior were prepared. In this way, hydrogel dissolution can be tuned depending on therapy time. Finally, the iEDDA reaction was transferred to liquid four-armed PEGs, and anhydrous protein delivery systems with instant gelation were realized. Thus, a protein depot was developed that can be injected into the organism for the extended controlled release without the disadvantages of water-based hydrogels. Summarized, these materials combined with techniques to tune gelation time, erosion time, and mechanical properties are major improvements for the delivery of high molecular weight proteins. All limitations of conventional water-based hydrogels could be overcome by anhydrous hydrogel preparation. As a next step, the delivery of suitable biologics for the treatment of a certain disease should be examined, and *in vivo* experiments regarding biocompatibility, stability, and release should be performed. Additionally, the results presented in this thesis could serve as the basis for further research not only in the field of protein delivery but also for vaccination or tissue engineering. For example, hydrogels with large mesh sizes could be used for the continuous delivery of cargo with a larger hydrodynamic diameter such as lipid nanoparticles or virus vectors used for the vaccination of SARS-CoV-2, reducing vaccine side effects and avoiding booster shots. In conclusion, the conventional and anhydrous hydrogels presented in this thesis represent highly promising materials for a multitude of biomedical applications

References

- [1] O. Wichterle, D. Lím, Hydrophilic Gels for Biological Use, *Nature* (London, U. K.) 185 (1960) 117–118.
- [2] M. Gregoritz, V. Messmann, K. Abstiens, F.P. Brandl, A.M. Goepferich, Controlled Antibody Release from Degradable Thermoresponsive Hydrogels Cross-Linked by Diels-Alder Chemistry, *Biomacromolecules* 18 (2017) 2410–2418.
- [3] N. Hammer, F.P. Brandl, S. Kirchhof, V. Messmann, A.M. Goepferich, Protein compatibility of selected cross-linking reactions for hydrogels, *Macromol. Biosci.* 15 (2015) 405–413.
- [4] C.-C. Lin, K.S. Anseth, PEG hydrogels for the controlled release of biomolecules in regenerative medicine, *Pharm. Res.* 26 (2009) 631–643.
- [5] L.M. Ickenstein, P. Garidel, Hydrogel formulations for biologicals: current spotlight from a commercial perspective, *Ther. Delivery* 9 (2018) 221–230.
- [6] E.M. Ahmed, Hydrogel: Preparation, characterization, and applications: A review, *J. Adv. Res.* 6 (2015) 105–121.
- [7] D.P. Chang, S. Burra, E.S. Day, J. Chan, L. Comps-Agrar, T. Nivaggioli, K. Rajagopal, Long-Term Stability of Anti-Vascular Endothelial Growth Factor (a-VEGF) Biologics Under Physiologically Relevant Conditions and Its Impact on the Development of Long-Acting Delivery Systems, *J. Pharm. Sci.* 110 (2021) 860–870.

Appendix

Abbreviations

3D	three-dimensional
ANOVA	analysis of variance
BCA	bicinchoninic acid
CuACC	Cu(I)-catalyzed azide-alkyne cycloaddition
DA	Diels-Alder
DCC	<i>N,N'</i> -dicyclohexylcarbodiimide
DCM	dichloromethane
DMAP	4-dimethylaminopyridine
DMF	<i>N,N</i> -dimethylformamide
DSC	differential scanning calorimetry
DSC	<i>N,N'</i> -disuccinimidyl carbonate
DSS	2,2-dimethyl-2-silapentane-5-sulfonate sodium salt
EMEM	Eagle's minimum essential medium
EtOAc	ethyl acetate
ETPI	3,6-epoxy-1,2,3,6-tetrahydrophthalimide
EWG	electron withdrawing group
FCS	fetal calf serum
FITC-dextran	fluorescein isothiocyanate-dextran
FTIR	fourier-transform infrared spectroscopy
GOx	glucose oxidase

HBTU	<i>O</i> -(benzotriazol-1-yl)- <i>N,N,N',N'</i> -tetramethyluronium-hexafluorophosphate
HOMO	highest occupied molecular orbital
HPLC	high-performance liquid chromatography
iEDDA	inverse electron demand Diels-Alder
IgG	immunoglobulin G
IPN	interpenetrating polymer network
ISO	International Organization for Standardization
LUMO	lowest unoccupied molecular orbital
Lys	lysine
LYS	lysozyme
MTT	3-(4,5-dimethylthiazol-2-yl)-2,5-diphenyltetrazolium bromide
MW	molecular weight marker
Nb	norbornene
NCL	native chemical ligation
NHS	<i>N</i> -hydroxysuccinimide
NMR	nuclear magnetic resonance
PAGE	polyacrylamide gel electrophoresis
PBS	phosphate buffered saline
PC	phenyl carbonate ester
PEG	poly(ethylene glycol)
4armPEG2k	four-armed PEG macromonomers with a molecular weight of 2 kDa
8armPEG10k	eight-armed poly(ethylene glycol) with a molecular mass of 10 kDa
8armPEG20k	eight-armed poly(ethylene glycol) with a molecular mass of 20 kDa
8armPEG40k	eight-armed poly(ethylene glycol) with a molecular mass of 40 kDa
mPEG5k	methoxy poly(ethylene glycol) with a molecular weight of 5 kDa
PHBHHx	poly(3-hydroxybutyrate-co-3-hydroxyhexanoate)

PLGA	poly(lactic-co-glycolic acid)
PVA	poly(vinyl alcohol)
PVP	poly(vinyl pyrrolidone)
rDA	retro-Diels-Alder
SDS	sodium dodecyl sulfate
SEC	size-exclusion chromatography
SEM	scanning electron microscopy
SIPN	semi-interpenetrating polymer network
SPAAC	strain-promoted azide-alkyne cycloaddition
SPOQC	strain-promoted oxidation-controlled cyclooctyne–1,2-quinone cycloaddition
TEA	triethylamine
THF	tetrahydrofuran
Tz	tetrazine
UV	ultraviolet
VCM	vacuum compression molding
VEGF	vascular endothelial growth factor
VIS	visible

Symbols

C_n	Flory characteristic ratio
χ_1	Flory-Huggins interaction parameter
D_g	diffusion coefficient in the hydrogel
D_0	diffusion coefficient in water
δ	phase angle
η	viscosity
f	branching factor of macromonomers
G^*	complex shear modulus
$ G^* $	absolute value of the complex shear modulus
G'	storage modulus
G''	loss modulus
γ^*	shear strain
k	Boltzmann constant
l	average bond length along the polymer backbone
m_p	total mass of polymer in the hydrogel
M_r	relative molecular mass
ω	angular frequency
r_H	hydrodynamic radius
σ^*	shear stress
T	temperature

t_{gel}	gel point
ν_e	number of moles of elastically active chains
ν_{2c}	polymer fraction of the hydrogel after cross-linking
ν_{2s}	polymer fraction of the hydrogel in swollen state
V_1	molar volume of solvent
V_{gc}	gel volume after cross-linking
V_{gs}	gel volume after swelling
V_p	dry polymer volume
ξ	average network mesh size
Y	ratio of the critical volume required for a successful translational movement of the solute molecule and the average free volume per solvent molecule

Curriculum Vitae

Name: Christian Erhard Ziegler

Date of birth: 18th of August 1990

Place of birth: Sulzbach-Rosenberg

Nationality: German

Scientific education and work experience

Since 08/2021 Compliance Officer, Boehringer Ingelheim Pharma GmbH & Co. KG,

Ingelheim am Rhein

05/2017 – 06/2021 PhD Candidate, Department of Pharmaceutical Technology,

University of Regensburg

12/2016 Licensure as Pharmacist

05/2016 – 10/2016 Practical training, Boehringer Ingelheim Pharma GmbH & Co. KG,

Ingelheim am Rhein

11/2015 – 04/2016 Practical training, Sonnen-Apotheke, Amberg

10/2011 – 10/2015 Study of Pharmacy, University of Regensburg

School education

11/2010 – 07/2011	Community service, Soziotherapeutische Suchthilfeeinrichtung, Königstein i.d.OPf.
09/2001 – 06/2010	Grammar school, Herzog-Christian-August Gymnasium, Sulzbach-Rosenberg
09/1997 – 08/2001	Primary school, Grundschule Königstein i.d.OPf.

List of publications

Peer-reviewed publications

1. Moritz Graf, **Christian E. Ziegler**, Manuel Gregoritzka, and Achim M. Göpferich; Hydrogel microspheres evading alveolar macrophages for sustained pulmonary protein delivery. *International Journal of Pharmaceutics* 2019, 566, 652-661.
2. **Christian E. Ziegler**, Moritz Graf, Sebastian Beck, and Achim M. Goeperich. A novel anhydrous preparation of PEG hydrogels enables high drug loading with biologics for controlled release applications. *European Polymer Journal* 2021, 147, 110286. (**Chapter 3**)
3. **Christian E. Ziegler**, Moritz Graf, Makoto Nagaoka, Heike Lehr, and Achim M. Goeperich. In Situ Forming iEDDA Hydrogels with Tunable Gelation Time Release High-Molecular Weight Proteins in a Controlled Manner over an Extended Time. *Biomacromolecules* 2021, 22, 8, 3223-3236. (**Chapter 4**)

To be submitted to peer-reviewed journals

1. **Christian E. Ziegler**, Moritz Graf, Makoto Nagaoka, and Achim M. Goeperich. Investigation of the impact of hydrolytically cleavable groups on the stability of PEG-based iEDDA hydrogels. (**Chapter 5**)
2. **Christian E. Ziegler**, Moritz Graf, Makoto Nagaoka, Jonas Groner, Miriam Breunig, and Achim M. Goeperich. Injectable anhydrous PEG polymer liquids form protein depot for extended controlled release applications via rapid in situ gelation. (**Chapter 6**)

Conference abstracts

1. **Christian E. Ziegler**, Moritz Graf, and Achim M. Goepferich. Water-free Preparation of Diels-Alder Hydrogels Maintains Protein Integrity and Enables Controlled Protein Release. *International PhD Student & Postdoc Meeting of the German Pharmaceutical Society, Virtual Meeting*, 2021.
2. **Christian E. Ziegler**, Moritz Graf, and Achim M. Goepferich. Tunable gelation time of in situ forming hydrogels cross-linked via bioorthogonal iEDDA reaction facilitates preparation of delivery systems for controlled protein release. *25th Anniversary of the German Chapter Inauguration of the BNLF Chapter Aachen, Virtual Meeting*, 2021.
3. Moritz Graf, **Christian E. Ziegler**, and Achim M. Goepferich. Hydrogel Particles for Pulmonary Protein Delivery. *Controlled Release Society German Chapter 23rd Annual Meeting*, Leipzig, 2019.

Acknowledgements

First and foremost, I would like to express my profound gratitude to Prof. Dr. Achim Göpferich, who gave me the opportunity to be part of his research group and entrusted me with this extremely exciting hydrogel project. I am deeply grateful for his scientific input in many discussions, which led me to look at things from a different angle. Above all, it was the freedom he gave me to bring my own ideas to this project that I enjoyed very much.

I also thank Prof. Dr. Miriam Breunig for the inspiring discussions, her valuable scientific advice, and the fruitful cooperation.

Furthermore, I want to express my deep gratitude to all former and present colleagues in the research group of the Department of Pharmaceutical Technology. They provided a friendly and enjoyable work atmosphere and made the four years in Regensburg so memorable. In particular, a special thanks goes out to the following colleagues:

Moritz Graf for his unmistakable calm and level-headed manner, with which he energetically (and eloquently) helped me in so many difficult scientific and gym-related questions. The development of the hydrogels would not have been possible in this way without him. Especially, I am grateful for his friendship.

My lab mate Dr. Marilena Bohley for the enjoyable atmosphere, the countless pleasant conversations, and the mutual encouragement during challenging situations.

Sebastian Beck for the unique conversations, his interesting opinion about football, and his friendship as a contribution to international understanding.

Jonas Groner for the entertaining everyday commute, digital game nights, completion of the last polymer experiments, and his friendship. The challenging exchange of opinions was always a pleasure.

Dr. Stefanie Thalhauser, Dr. Sara Maslanka Figueroa, and Heike Lehr for their advice and the great working atmosphere.

Dr. Raphael Mietzner for the HPLC support and continuation of the hydrogel project.

Oliver Zimmer for the exciting conversations during lunch.

Felix Baumann for the fruitful discussions on syntheses and his overwhelming enthusiasm in the field of hydrogels.

Further, I thank Eva Wrobel for her excellent organizational skills.

I am also deeply grateful for the outstanding technical assistants. In particular, I would like to thank Viktoria Eismann and Lukas Prock for their support with syntheses and hydrogel experiments. I thank Renate Liebl for the cell culture assistance and Stefan Kolb for the construction of several devices. Moreover, I would like to thank Andrea Blaimer for her support with the practical courses.

I thank Makoto Nagaoka for her great synthesis support during her research internship. The high number of syntheses would not have been possible without her.

A very special thanks goes to my roommates, who provided a wonderful everyday atmosphere away from science and made the lockdown enjoyable.

I thank my dear friends for their support and providing a beneficial distraction from science whenever needed.

The most important thanks goes to Jasmin for her unconditional support, always believing in me, and being my best friend. Thank you for your love!

And last but not least I would like to thank my family without whom this would not have been possible. Thank you for your constant support and always encouraging me to go my own way.

Declaration in lieu of an oath

I hereby declare that I have completed the dissertation presented without the impermissible help of third parties, without the use of resources other than those indicated, and that any data and concepts stemming directly or indirectly from other sources are indicated with citations to the literature.

No further persons were involved with the creation of the contents of the dissertation presented. In particular, I have not made use of the assistance of a doctoral consultant or other person in return for payment. No-one has received payment in kind either directly or indirectly for work which is associated with the content of the dissertation submitted.

The dissertation has not been submitted in the same or similar form to another examining authority, neither in Germany nor abroad.

Regensburg, 11.03.2022

(Christian Ziegler)